UNIVERSITÉ DE STRASBOURG

Thèse présentée pour obtenir le grade de Docteur

de l'Université de Strasbourg

DISCIPLINE : CHIMIE

ECOLE DOCTORALE : PHYSIQUE ET CHIMIE-PHYSIQUE

Présentée par

FREDERIC CHIVRAC

Nano-biocomposites : systèmes structurés à base d'amidon plastifié et d'argiles

Jury composé de :

Jean-François GÉRARD	Professeur, INSA de Lyon	Rapporteur Externe
Stéphane GUILBERT	Professeur, ENSA.M	Rapporteur Externe
Georges HADZIIOANNOU	Professeur, UdS Strasbourg	Rapporteur Interne
Patrice DOLE	Chargé de recherche, INRA Reims	Examinateur
Éric POLLET	Maître de Conférences, UdS Strasbourg	Examinateur
Luc AVÉROUS	Professeur UdS, Strasbourg	Directeur de thèse

Remerciements

Je tiens en premier lieu à exprimer ma profonde gratitude au Pr. Avérous qui m'a permis de réaliser cette thèse, qui m'a transmis au fur et à mesure ses différentes compétences et qui a toujours été là pour me conseiller et me soutenir. Son implication a grandement contribué à mon épanouissement et au succès de ce travail de recherche. Merci Luc !!!

Mes remerciements s'adressent également tout naturellement à Eric Pollet qui m'a suivi au quotidien, m'a guidé et qui ne s'est jamais lassé de devoir constamment corriger les différents papiers que je lui ai soumis depuis maintenant trois années. Je sais que ça n'a pas toujours été facile. Merci pour ta patience et ton implication.

Je souhaite aussi remercier le Pr. Hadziioannou qui a accepté il y a maintenant cinq années de m'intégrer à l'ECPM en 2e année Polymères et qui a donc été le point de départ de cette aventure. C'est donc pour moi un grand plaisir qu'il prenne part à la fin de ce voyage en étant dans mon jury de thèse.

Je tiens également à remercier Messieurs Jean-François Gérard (INSA de Lyon), Stéphane Guilbert (ENSA.M) et Patrice Dole (INRA, Reims) pour avoir accepté de juger ce travail de thèse.

Pour leurs collaborations, je remercie également l'équipe du professeur Saïd Ahzi (IMFS, Strasbourg), et tout particulièrement le Dr. Olivier Gueguen avec qui j'ai étroitement collaboré et avec qui j'ai passé de nombreuses soirées ces trois dernières années.

D'autres collaborations ont été essentielles pour mener à bien ce travail de recherche. Je remercie donc la société Roquette (France) pour nous avoir fourni gracieusement les différents réactifs utilisés pendant cette thèse. Je remercie également M. Léon Mentink (Roquette, France) pour sa gentillesse, son implication et ses différentes idées qui ont fait avancer ce projet. J'adresse également mes remerciements à Mme Pourroy, directrice du GMI (IPCMS, Strasbourg), pour nous avoir autorisé à utiliser les équipements de DRX et d'ATG et à M. Schmutz (ICS, Strasbourg) pour les différentes analyses TEM que j'ai effectuées dans son laboratoire.

Je souhaite également remercier toutes les personnes qui sont intervenues de prêt ou de loin sur ce projet de recherche : Fabien, Perrine, Christophe M., Christophe S., Thierry, Chheng, Catherine, Veronica. Je remercie également toutes les personnes qui ont cohabité avec moi dans le R1N2Bu1 : Perrine, Carine, Julie, Sébastien, Florence, Sandra et Marie. Je me remémorerais avec nostalgie les différents moments passés à écouter Ghinzu, les Fatals Picards (et notamment La Ferme et l'interprétation de Marie d'Eric le porc-épic), à manger des tartes à la banane et autres pâtisseries et tous les fous rire que nous avons eus.

Communications liées à l'étude

Articles publiés :

Chivrac, F.; Pollet, E.; Schmutz, M.; Averous, L., New Approach to Elaborate Exfoliated Starch-Based Nanobiocomposites. Biomacromolecules, 2008, 9, 896-900.

Chivrac, F.; Gueguen, O.; Pollet, E.; Ahzi, S.; Makradi, A.; Averous, L., Micromechanical Modeling and Characterization of the Effective Properties in Starch Based Nano-Biocomposites. Acta Biomaterialia, 2008, 4, 1707-1714.

Articles en cours de publication :

Chivrac, F.; Pollet, E.; Averous, L., Progress in Nano-Biocomposites Based on Polysaccharides and Nanoclays. Biomacromolecules, Submitted.

Chivrac, F.; Pollet, E.; Averous, L., Shear Induced Clay Organo-Modification: Application to Plasticized Starch Nano-biocomposites. Polymers for advanced technologies, Submitted.

Chivrac, F.; Pollet, E.; Dole, P.; Averous, L., Starch-Based Nano-Biocomposites: Plasticizer Impact on the Montmorillonite Exfoliation Process. Starch – Stärke, Submitted.

Chivrac, F.; Pollet, E.; Schmutz, M.; Averous, L., High performance starch nano-biocomposites based on needle-like sepiolite clays. Acta Biomaterialia, Submitted.

Chivrac, F.; Gueguen, O.; Pollet, E.; Ruch, D.; Ahzi, S.; Averous, L., Micromechanically-based formulation of the cooperative model for the yield behavior of starch-based nano-biocomposites. Journal of nanoscience and nanotechnology, Submitted.

Chapitre de livre :

Chivrac, F.; Pollet, E.; Avérous, L., Mechanical properties of starch-based nano-biocomposites. In Trends in Polymer Research, Zaikov, G. E.; Jimenez, A., Eds. Nova Publishers: 2009.

Présentations orales :

Averous, L.; Chivrac, F.; Pollet, E., Exfoliated starch-based nano-biocomposites: Elaboration and structure-property relationships. Biomacromolecules, Stockholm, Suède, 2008.

Gueguen, O.; <u>Chivrac, F.</u>; Ahzi, S.; Makradi, A.; Belouettar, S.; Pollet, E.; Averous, L.; Gracio., J., Micromechanical analysis of the properties of bio-polymer nanocomposites. 2nd International Conference on Advanced Nano Materials, Aveiro, Portugal, 2008.

Communications par affiches :

<u>Chivrac, F.</u>; Clauss, F.; Pollet, E.; Averous, L., Starch-based nano-biocomposites. In Chemistry contributing to the Society: Green Sustainable Chemistry - JSPS, Strasbourg, France, 2006.

<u>Chivrac, F.</u>; Clauss, F.; Pollet, E.; Averous, L., Starch nano-biocomposites: Elaboration and structural characterization. In Symposium ISIS-BASF, Strasbourg, France, 2006.

<u>Chivrac, F.</u>; Clauss, F.; Pollet, E.; Averous, L., Towards the improvement of "green plastic": starch-based nano-biocomposites. In Trends in Materials and Nanosciences, Strasbourg, France, 2006.

<u>Chivrac, F.</u>; Pollet, E.; Averous, L., Starch Nano-biocomposite: A new powerful approach to develop"green" plastics. In Biopolymer, Alicante, Espagne, 2007.

<u>Chivrac, F.</u>; Pollet, E.; Averous, L., New "green" compatibilizer for exfoliated starch nano-biocomposites. In European Polymer Congress - EPF, Portoroz, Slovénie, 2007.

<u>Chivrac, F.</u>; Pollet, E.; Averous, L., Starch nano-biocomposites: Towards the development of new environmentally friendly materials. In Polymer Processing Society Meeting - PPS23, Salvador, Brésil, 2007.

Abréviations

Techniques de caractérisation et données associées :

DRX/XRD		Diffraction des rayons-X
DRXPA/SAXD		Diffraction des rayons-X aux petits angles
WAXD		Diffraction des rayons-X aux grands angles
	2θ (°)	Angle de diffraction
	λ (Å ou nm)	Longueur d'onde
	d_{001} (Å ou nm)	Distance interfeuillets
MET/TEM		Microscopie électronique à transmission
DSC		Calorimétrie différentielle à balayage
	T_{gel} (°C)	Température de gélatinisation
	ΔH (cal/g)	Enthalpie de gélatinisation
	T_g (°C)	Température de transition vitreuse
DMTA		Analyse thermo-mécanique dynamique
	T_α (°C)	Température de relaxation associée à la température de transition vitreuse
	T_β (°C)	Température de relaxation associée à la température de transition sous-vitreuse
	$\tan \delta$	Tangente de l'angle de perte
TGA/ATG		Analyse thermo-gravimétrique
	TG	Courbe de perte de masse
	DTG	Dérivée de la perte de masse
RMN		Résonance magnétique nucléaire

Polymères

PLA	Poly(acide lactique) ou polylactide
PHA	Polyhydroxyalcanoate
PCL	Polycaprolactone
PEA	Polyesteramide
PBSA	Poly(butylene succinate-co-adipate)

PBAT	Poly(butylene succinate-co-butylene terephtalate)
PVAL	Polyvinyl alcohol / Alcool polyvinylique
WS	Wheat starch / Amidon de blé
PS	Pea starch / Amidon de pois
AS	Amylomaïs
CA	Acétate de cellulose

Nanocharges et composes et données associés

MMT	Montmorillonite
OMMT	Montmorillonite organomodifiée
MMT-Na	Montmorillonite sodique
OMMT-CS	Montmorillonite organomodifiée par de l'amidon cationique
OMMT-Alk1	Cloisite® 15A
OMMT-Alk2	Cloisite® 6A
OMMT-Alk3	Cloisite® 20A
OMMT-Alk4	Cloisite® 25A
OMMT-Alk5	Nanomer® I.30E
OMMT-Alk6	Montmorillonite organomodifiée par du trimethyldodecyl ammonium
OMMT-Alk7	Cloisite® 93A
OMMT-Bz	Cloisite® 10A
OMMT-OH1	Cloisite® 30B
OMMT-OH2	Nanofil® 804
OMMT-NH4	Bentone® 111
OMMT-EtA	Montmorillonite organomodifiée par de l'éthanolamine
OMMT-CitA	Montmorillonite organomodifiée par de l'acide citrique
SEP	Sépiolite
OSEP	Sépiolite organomodifiée
SEP-Na	Sépiolite sodique
OSEP-CS	Sépiolite organomodifiée par de l'amidon cationique

OSEP-1CS	Sépiolite organomodifiée par un équivalent d'amidon cationique
OSEP-2CS	Sépiolite organomodifiée par deux équivalents d'amidon cationique
OSEP-4CS	Sépiolite organomodifiée par trois équivalents d'amidon cationique
OSEP-6CS	Sépiolite organomodifiée par quatre équivalents d'amidon cationique
CEC	Capacité d'échange cationique
T	Tallow / suif
HT	Hydrogenated tallow / suif hydrogéné

Produits Chimiques

TEC	Triéthyle citrate
MA	Anhydride maleïque
CAB	Butyrate d'acetate de cellulose
CAB-g-MA	Butyrate d'acetate de cellulose greffé anhydride maleïque
Gly	Glycérol
Sorb	Sorbitol
DMSO	Diméthylsulfoxyde

Divers

SME (J/kg)	Energie mécanique spécifique
%RH	Pourcentage d'humidité relative
wt%	Pourcentage en poids
E (MPa)	Module d'Young ou module élastique
σ (MPa)	Contrainte vraie
ε_b (%)	Elongation à la rupture
S_0 (cm²)	Section initiale de l'éprouvette de traction
S (cm²)	Section de l'éprouvette de traction pendant l'essai
F (N)	Force appliquée

E_{MMT} (MPa)	Module d'Young de la montmorillonite
E_{MMT}^{eff} (MPa)	Module d'Young effectif de la montmorillonite
r_e	Rapport d'exfoliation
t_s (min)	Temps de séjour dans l'extrudeuse
SICO	Shear induced clay organo-modification
t_β (min)	Temps de séjour caractéristique du procédé SICO d'organomodification de la montmorillonite
EXAD	Exfoliation / adsorption
GMT	Generalized Mori Tanaka
vs.	versus

Sommaire

Index des Tables et Figures

Chapitre I – Publication I

Chapitre II – Publication III

Chapitre II – Publication IV

Chapitre III – PublicationV

Chapitre IV – PublicationVI

Chapitre IV – PublicationVII

Chapitre I – Publication I

Chapitre II – Publication II

Chapitre II – Publication III

Chapitre III – Publication IV

Chapitre III – Publication V

Chapitre IV – Publication VI

Chapitre IV – Publication VII

Introduction Générale

La prise de conscience de l'impact de l'activité humaine sur la dégradation de notre environnement est aujourd'hui devenue globale. L'attente sociétale qui en découle permet dès à présent la mise en place de nouvelles politiques de développement durables ambitieuses, soutenues à la fois par les pouvoirs publiques et les citoyens. Le récent « Grenelle de l'environnement », qui s'est tenu à Paris fin octobre 2007, est un parfait exemple de cette volonté d'instaurer une politique éco-responsable, visant au développement de solutions écologiques pérennes.

En parallèle, l'augmentation continue du prix des ressources fossiles ces dernières années (pétrole, gaz…), liée notamment à leur raréfaction, a rendu économiquement viable nombre de solutions alternatives, notamment dans les domaines de l'énergie et des matériaux. Même si la crise économique actuelle vient de diviser par trois le prix de ces ressources en seulement quelques mois, il paraît évident qu'une fois cette crise passée, le prix de ces matières repartira durablement à la hausse.

Dans ce contexte, les bioplastiques (plastiques biodégradables, voire biocompatibles), et principalement ceux issus de ressources renouvelables, apparaissent de plus en plus comme une alternative crédible aux plastiques synthétiques classiques (issus de la chimie du pétrole et du gaz), notamment pour des applications à faible durée de vie telles que l'emballage. En effet, en fin de vie, ces matières bio-sourcées se (bio)dégradent par réaction enzymatique et hydrolyse en milieu compost. Leurs sous-produits de dégradation permettent alors d'amender des sols et de favoriser la croissance d'une nouvelle génération de cultures, pouvant à leur tour produire de nouveaux bioplastiques dans un cycle vertueux durable.

Quoique la demande en « matériaux biodégradables » vienne aujourd'hui en second plan, au profit d'une demande en « matériaux issus de ressources renouvelables », ils représentent dès aujourd'hui une catégorie à part entière, en forte croissance, de l'industrie plastique. Pour illustrer cela, quelques chiffres : la part mondiale des polymères biodégradables dans l'environnement est passée de 0,03 % en 2000 à 0,3% en 2005. Leur capacité de production a été multipliée par un facteur 10 en moins de 7 ans et est actuellement proche de 500 000 tonnes/an (données European Bioplastics). En Europe, la consommation en polymères biodégradables était de 20 000 tonnes en 2000, elle a doublé en trois ans et elle représente déjà près de 1 % du tonnage d'emballages plastiques mis sur le marché. En plus de l'emballage, d'autres débouchés significatifs sont aussi trouvés à ces matériaux biodégradables dans les domaines de l'agriculture et de l'horticulture (films de paillage, clips, pots…). Ils peuvent également trouver des applications dans des domaines particuliers à haute

valeur ajoutée comme le biomédical, de par leur biocompatibilité et leur biorésorption au contact du tissu vivant.

Néanmoins, ces bioplastiques présentent un certain nombre de faiblesses intrinsèques (e.g. propriétés mécaniques insuffisantes) qu'il convient de limiter afin de favoriser leur développement. Il est possible de faire évoluer ces matériaux et leurs propriétés principalement au travers de deux approches : *(i)* la modification chimique et *(ii)* l'association physique du polymère avec d'autres composés par une démarche de type "formulation". Les nano-biocomposites s'inscrivent surtout dans cette deuxième stratégie. Il s'agit d'incorporer des nano-objets au sein d'une matrice biopolymère afin de concevoir des matériaux hybrides organiques/inorganiques présentant des propriétés améliorées (mécaniques, barrières, stabilité thermique, transparence…). Les nano-biocomposites s'inscrivent, par rapport aux nanocomposites « classiques » à base de matrices polymères non dégradables, comme une nouvelle étape technologique basée sur l'éco-conception de matériaux à forte valeur ajoutée.

Le développement de ces matériaux nanostructurés s'appuie principalement sur la très grande surface spécifique des nanocharges (plusieurs centaines de m^2/g) générant une interface importante et ceci à de faibles taux de charges, typiquement inférieurs à 5 % en masse. Cette interface contrôle en grande partie les propriétés globales du matériau. Toutefois, une bonne affinité polymère/nanocharge ainsi qu'une répartition homogène de la charge dans la matrice sont requises pour atteindre une amélioration significative des propriétés. Les nanocharges peuvent être classées en trois différentes catégories en fonction de leur facteur de forme : les feuillets (e.g. argiles lamellaires…), les tubes (e.g. nanotubes de carbone, argiles aciculaires, whiskers de cellulose…) et les sphères (e.g. billes de silice). Jusqu'à présent, les nanocharges les plus communément utilisées et étudiées sont les argiles lamellaires (e .g. montmorillonite) et les nanotubes de carbone. Toutefois, d'autres nanocharges d'origine naturelle, telles que la sépiolite (argile aciculaire), commencent à être employées.

Ce travail de thèse porte donc sur l'étude des relations « procédés-structures-propriétés » de matériaux nano-biocomposites amidon plastifié/argile. Le choix de l'amidon en tant que matrice s'est principalement fait en raison de sa biodégradabilité intrinsèque, de sa disponibilité (multiplicité des sources et des zones de production) et de son faible coût (environ 0,5 €/kg). De plus, de nombreuses résines bioplastiques à base d'amidon, telles que le Mater-Bi© (Novamont, Italie), le Biolice© (Livagrain, France) ou le Vegeplast© (Vegemat, France)… vont arriver ou sont déjà sur le marché. Par conséquent, ce travail de recherche s'inscrit dans une tendance globale tendant à favoriser l'émergence de matériaux à base de

matrices amylacées présentant des propriétés améliorées. De fait, l'incorporation de nanocharges paraît être une solution techniquement viable et efficace répondant aux principales faiblesses de l'amidon plastifié, à savoir, de faibles propriétés mécaniques et une forte sensibilité à l'humidité relative.

Par ailleurs, l'élaboration de tels nano-hybrides s'inscrit parfaitement dans la thématique *"Bioplastiques-Biopolymères"* du Laboratoire d'Ingénierie des Polymères pour les Hautes Technologies (LIPHT – UMR CNRS 7165) de Strasbourg et se positionne dans la continuité du travail de recherche effectué sur les matrices amidons plastifiés (mélanges, biocomposites …) et sur les matériaux nano-biocomposites (PHA/montmorillonite, …) du Pr. Avérous. Ce projet trouve également un écho dans l'ensemble des programmes de recherche visant à favoriser l'émergence de matériaux issus de ressources renouvelables. En France, l'ADEME finance nombre de ces projets valorisants des produits et coproduits d'origine agricole dans les domaines de l'énergie, de la chimie et des matériaux. Au niveau Européen, de nombreuses structures œuvrent afin d'encourager le développement de matériaux verts. Par exemple, l'ERRMA (European Renewable Ressources and Materials Association) est une structure européenne qui regroupe les agences française (ADEME), allemande (FNR), italienne (AIACE), britannique (ACTIN), belge (BELBIOM) … visant à la coordination des différents programmes de recherche sur la valorisation non alimentaire des agro-ressources. Enfin, ce travail de thèse se démarque par rapport à celui d'autres équipes internationales par son approche innovante visant à comprendre les interactions matrice amylacée/plastifiant/organo-modifiant/nanocharge et leurs influences sur les propriétés finales des nano-biocomposites.

Ce manuscrit, organisé autour d'articles scientifiques en anglais publiés ou soumis dans des journaux internationaux de référence, est structuré en quatre parties distinctes présentant chacune un aspect de ce travail de recherche.

Le – **Chapitre I** – présente un état de l'art sur les nano-biocomposites issus d'agro-polymères et de montmorillonite. Cette étude bibliographique s'est focalisée sur quelques matrices polysaccharides importantes, telles que l'amidon, la cellulose, le chitosane et la pectine. Comme cela a déjà été montré pour d'autres systèmes nanocomposites, ce travail a mis en évidence l'influence de trois facteurs sur la dispersion des nanocharges : l'affinité matrice/nanocharge, la concentration en nanocharges et le procédé d'élaboration de ces nano-biocomposites. Toutefois, il apparaît clairement qu'un autre paramètre modifie significativement la morphologie et donc les propriétés finales de ces matériaux. En effet, de

part leur grande sensibilité thermique, la mise en œuvre de ces polysaccharides doit souvent être réalisée avec ajout d'un plastifiant. Celui-ci influence directement le processus d'intercalation/exfoliation des nanocharges au travers d'interactions fortes (liaisons hydrogènes…) avec les feuillets d'argile. Par conséquent, la maîtrise de l'équation « matrice-plastifiant-nanocharge-procédé d'élaboration » est essentielle afin d'obtenir des argiles exfoliées au sein d'une matrice amidon plastifié.

Le – **Chapitre II** – présente les résultats des travaux menés sur l'élaboration des nano-biocomposites exfoliés à base d'amidon plastifié et de montmorillonite. Pour ce faire, cette étude s'est focalisée sur l'utilisation d'un nouveau compatibilisant, l'amidon cationique, permettant d'organo-modifier la surface de feuillets de montmorillonite et d'améliorer l'affinité matrice/nanocharge. Cette organo-modification a été effectuée selon deux approches distinctes : une approche conventionnelle nommée Exfoliation/Adsorption correspondant à la « voie solvant » et une approche plus novatrice nommée « Shear Induced clay organo-modification » correspondant à la « voie fondue ». Dans ce cas, le cisaillement sous contrainte thermomécanique est un paramètre clé de l'organo-modification. Par la suite, des nano-biocomposites d'amidon ont été élaborés avec cette montmorillonite organo-modifiée par de l'amidon cationique (OMMT-CS) au sein d'un mélangeur interne. Afin d'étudier l'influence de l'affinité matrice/nanocharge, des nano-biocomposites ont également été élaborés avec de la montmorillonite sodique (MMT-Na). La caractérisation de l'état de dispersion de ces nanocharges au sein des matrices amylacées a été effectuée à l'aide de la diffraction des rayons-X aux petits angles (DRXPA) et de la microscopie électronique à transmission (MET). L'influence des structures et morphologies obtenues sur les propriétés mécaniques de ces matériaux a ensuite été étudiée.

Le – **Chapitre III** – traite de différents paramètres influençant la morphologie, la nano-structuration et les propriétés finales de ces nano-biocomposites. Pour cela, la première partie de ce chapitre se focalise sur l'effet de la nature du plastifiant sur le processus d'intercalation-exfoliation de nano-biocomposites d'amidon plastifié élaborés avec de la MMT-Na et de l'OMMT-CS. Pour ce faire, trois plastifiants ont été incorporés dans la matrice amidon : du glycérol, du sorbitol et du Polysorb® (mélange de glycérol et de sorbitol). L'état de dispersion de la montmorillonite au sein de ces matériaux a été analysé par DRXPA. Ensuite, les différentes propriétés (thermiques, mécaniques…) ont été analysées en relation avec l'incorporation de ces nanocharges. La deuxième partie de ce chapitre traite de l'effet de l'adjonction d'une nanocharge argileuse aciculaire, la sépiolite, sur les propriétés finales des

nano-biocomposites d'amidon. Cette nanocharge a également été organo-modifiée avec de l'amidon cationique. L'état de dispersion de cette nanocharge a été caractérisé par MET et a été relié aux propriétés finales du matériau (thermiques, mécaniques…) lesquelles ont ensuite été comparées à celle des nano-biocomposites à base de montmorillonite.

Le – **Chapitre IV** – porte sur la modélisation des propriétés mécaniques, obtenues par traction uniaxiale, des nano-biocomposites d'amidon. Dans un premier temps, les propriétés d'élasticité de ces matériaux ont été modélisées en fonction de la concentration et du taux d'exfoliation de la montmorillonite au sein de la matrice amidon. Dans un second temps, les propriétés à la limite d'élasticité ont été modélisées en fonction du taux d'exfoliation, de la concentration en nanocharge, de la température ainsi que de l'intensité de la sollicitation.

Pour finir, une partie relative aux – **Conclusions générales** – permet de présenter de manière synthétique les résultats majeurs issus de cette étude et les – **Perspectives** – qui en découlent.

Chapitre I

-

Synthèse Bibliographique

Introduction

Les matériaux bio-sourcés, c'est-à-dire issus de ressources renouvelables, suscitent un intérêt grandissant. Ce phénomène s'est accéléré par la sensibilisation grandissante des citoyens et des pouvoirs publics, qui mettent en place des politiques de développement durable ayant pour objectif la limitation de l'impact de l'activité humaine sur l'environnement. Dans ce contexte, les biopolymères issus de ressources renouvelables apparaissent comme une alternative pleine de promesses aux polymères synthétiques classiques issus de la pétrochimie. Cette tendance s'incrit dans l'histoire. Celle qui a mené au développement de nouvelles matrices bio-sourcées, telles que l'acide polylactique (PLA), les polyhydroxyalcanoates (PHA)… ou à la valorisation non alimentaire d'agro-polymères, tels que les protéines ou les polysaccharides directement extraits des plantes, à des fins d'élaboration de matériaux. Cependant, même si l'intérêt de ces matériaux bio-sourcés n'est plus à prouver, leur développement est aujourd'hui limité par certaines faiblesses intrinsèques e.g., forte sensibilité à l'eau et propriétés mécaniques limitées. Jusqu'à présent, ces faiblesses étaient principalement résolues par modification chimique et par formulation au travers de l'élaboration de mélanges amidon/biopolyester ou par incorporation de charges, telles que des microfibrilles de cellulose.

Le développement relativement récent des matériaux nanocomposites ouvre également de nouvelles perspectives à ces biomatrices. Ces cinq dernières années ont en effet vu l'émergence de nombreuses études focalisées sur l'incorporation de nanocharges (principalement de la montmorillonite) dans des matrices polymères biodégradables afin d'élaborer des nano-biocomposites (nanocomposites biodégradables) présentant de nettes améliorations de leurs propriétés (mécaniques, barrières…). Ces nano-biocomposites sont une solution innovante et prometteuse, élargissant le champ de connaissance et d'application des matériaux bio-sourcés.

De ce fait, le travail de synthèse bibliographique, présenté dans ce chapitre au travers de la **Publication I** intitulée « Progress in nano-biocomposites based on polysaccharides and nanoclays », vise à rassembler les principaux résultats de recherche et les derniers développements publiés sur les matériaux nano-biocomposites produits à base de polysaccharides et de montmorillonite. Cette étude se focalisera plus particulièrement sur les nano-hybrides produits à base de matrices agro-sourcées, telles que l'amidon, le chitosane, la cellulose et la pectine.

Publication I – Progress in Nano-Biocomposites Based on Polysaccharides and Nanoclays

Frédéric Chivrac, Eric Pollet, Luc Avérous*

I. Abstract

The last decade has seen the development of an alternative chemistry, which intends to reduce the human impact on the environment. The polymers are obviously involved into this tendency and numerous bio-sourced plastics (bioplastics), such as polylatide, plasticized starch…, have been elaborated. However, even if a lot of commercial products are now available, their properties (mechanical properties, moisture sensitivity) have to be enhanced to be really competitive with the petroleum based plastics. One of the most promising answers to overcome these weaknesses is the elaboration of nano-biocomposites, namely the dispersion of nano-sized filler into a biopolymer matrix. This review reports the last developments in nano-biocomposites based on polysaccharides and nanoclays. The main elaboration strategies developed in starch, chitosan, cellulose acetate and pectin based nano-biocomposites elaborated with montmorillonite as the nanofiller are exposed herein. The corresponding dispersion state and properties are discussed.

KEYWORDS: Nano-biocomposites, review, polysaccharides, clay, exfoliation.

[*] Corresponding author: Luc Avérous.

Tel.: +33-3-90-242-707 - Fax: +33-3-90-242-716 - AverousL@ecpm.u-strasbg.fr

LIPHT-ECPM, UMR 7165, Université Louis Pasteur, 25 rue Becquerel, 67087 Strasbourg Cedex 2, France

II. Introduction

As a result of the increasing awareness concerning the human impact on the environment and the constant increase in the fossil resources price, the last decade has seen the development of efficient solutions to produce new environmentally friendly materials. Particular attention has been paid to the replacement of conventional petroleum-based plastics by materials based on biopolymers, such as biodegradable polyester (Gross, R.A., 2002, Reddy, C.S.K., 2003, Sinclair, R.G., 1996, Tsuji, H., 1998), proteins (Cuq, B., 1998, Guilbert, S., 1996, Redl, A., 1999) or polysaccharides (Averous, L., 2004a, Edgar, K.J., 2001, Neus Angles, M., 2000, Van Soest, J.J.G., 1996b).

Many biopolymer definitions exist and some of them are ambiguous, but it is now accepted that biopolymers are biodegradable materials capable of undergoing decomposition thanks to microorganisms and enzymatic degradation (*ASTM* standard *D-5488-94d*). Depending on the degradation conditions (aerobic vs. anaerobic) and the medium, the material is decomposed into water, inorganic compounds, carbon dioxide and/or methane, and biomass. The biopolymers can be classified in four different categories (Averous, L., 2004a):

(i)   Agro-polymers extracted from biomass, such as starch, cellulose, proteins, chitin...

(ii)   Polymers obtained by microbial production, such as the polyhydroxyalkanoates (PHA).

(iii)   Polymers conventionally and chemically synthesized and whose monomers are obtained from agro-resources, such as the polylactic acid (PLA).

(iv)   Polymers whose monomers are obtained from fossil resources, such as poly(ε-caprolactone) (PCL), polyesteramide (PEA), poly(butylene succinate-*co*-adipate) (PBSA), poly(butylene adipate-*co*-terephthalate) (PBAT)…

The biopolymers produced from renewable resources are an elegant and innovating answer to replace conventional petroleum-based products and fits with a real sustainable development approach. However, to obtain suitable and competitive materials, some of theirs properties have to be enhanced (brittleness, moisture sensitivity…). Consequently, even if the potential of these bio-based materials have been pointed out, until now, they are not widely used to replace non-degradable plastics. The common approach to tune their behaviors consists in the elaboration of multiphase materials e.g., blends (Averous, L., 2000a, Averous,

L., 2001, Buchanan, C.M., 1992) or composites (Averous, L., 2004b, Curvelo, A.A.S., 2001, Mohanty, A.K., 2002, Wollerdorfer, M., 1998).

A new class of composite materials based on the incorporation of nanosized fillers (nanofillers) has been investigated (Alexandre, M., 2000, Cho, J.W., 2001, Giannelis, E.P., 1996, Krishnamoorti, R., 1996, Lebaron, P.C., 1999, Sinha Ray, S., 2003, Thostenson, E.T., 2001, Vaia, R.A., 1997). Depending on the nanofiller, nanocomposites could exhibit drastic modifications in their properties, as improved mechanical properties, transparency, barrier properties (Chivrac, F., 2007, Gain, O., 2005, Gorrasi, G., 2004, Peprnicek, T., 2006, Picard, E., 2007, Picard, E., 2008, Sinha Ray, S., 2003)… Such properties enhancements rely both on the nanofiller geometry and on the nanofiller surface area (from 600 to 800 m^2/g when the nanofiller is homogeneously dispersed and exfoliated for the montmorillonite). The different nanofillers can be classified depending on their aspect ratio and geometry, such as (i) layered particles (e.g., clay), (ii) spherical (e.g., silica) or (iii) acicular ones (e.g., whiskers, carbon nanotubes). At the present, the most intensive researches are focused on layered silicates, such as montmorillonite (MMT), due to their availability, versatility and respectability towards the environment and health. A wide range of nano-biocomposites (nanocomposites based on biopolymers) (Chivrac, F., 2006) have been elaborated with different matrices, such as, PCL (Gorrasi, G., 2004, Jimenez, G., 1997, Lepoittevin, B., 2002a, Lepoittevin, B., 2002b, Lepoittevin, B., 2003, Messersmith, P.B., 1993), PLA (Ogata, N., 1997, Paul, M.A., 2002, Paul, M.A., 2003, Paul, M.A., 2005, Pluta, M., 2002, Sinha Ray, S., 2002) or PHA (Bordes, P., 2008, Maiti, P., 2007, Sanchez-Garcia, M.D., 2008) or agro-polymers (Chiou, B.S., 2004, Fischer, S., 2001, Park, H.M., 2002, Park, H.M., 2003), such as starch or chitosan… and have demonstrated that nano-biocomposites elaboration could be a powerful strategy to overcome the conventional drawbacks of agro-based polymers.

The following paper presents an overview of the major developments in polysaccharides nano-biocomposites based on nanoclays. The main nanofillers and nano-biocomposites elaboration processes will be discussed. The major systems will be extensively described and compared.

III. From the Nanoclay to the Nanocomposite

The following section will be focused on nanoclay, and more especially on phyllosilicate nano-particles, and on the nanocomposites elaboration protocols.

1. Phyllosilicates: Structure, Properties and Organo-Modification

Phyllosilicates are a wide family in which clays with different structure, texture or morphology can be found. For instance, the montmorillonite (MMT) and the synthetic laponite clay are anisotropic particles with a thickness of one nanometer but a width of hundreds and tens nanometers, respectively.

1.1 Multi-Scale Structure

The phyllosilicates present different, mainly three organization levels depending on the observation scale, *(i)* the layer, *(ii)* the primary particle and *(iii)* the aggregate (Figure I.1).

(i)   The layer is equivalent to a disc or a platelet having a width varying from 10 nm to 1 µm and a thickness of 1 nm. These layers, and more especially the widest, are flexible and deformable.

(ii)   The primary particle is composed of five to ten stacked platelets. The cohesion of the structure is assured by Van der Waals and electrostatic attraction forces between the cations and the platelets. The stacking of these particles is perpendicular to the z direction and is disordered in the plan (x, y). The structure thickness is around 10 nm.

(iii)   The aggregate is the association of primary particles orientated in all the directions. The size of the aggregates varies from 0.1 to 10 µm.
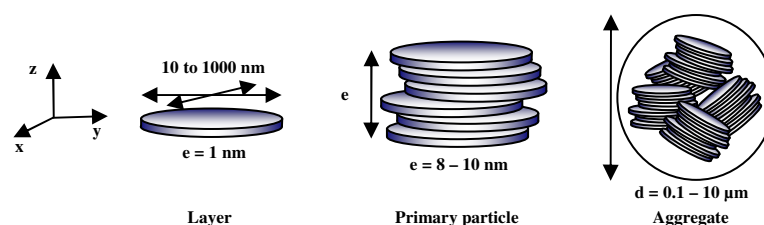
Figure I.1. Phyllosilicate multi-scale structure.

1.2 Nanoclays Structure

The phyllosilicate crystal structure is based on the pyrophyllite structure $Si_4Al_2O_{10}(OH)_2$ and can be described as a crystalline 2:1 layered clay mineral with a central alumina octahedral sheet sandwiched between two silica tetrahedral sheets corresponding to seven atomic layers superposed (Figure I.2) (Hendricks, S.B., 1942). This structure becomes $(Si_8)(Al_{4-y}Mg_y)O_{20}(OH)_4, M_y^+$ for the montmorillonite or $(Si_8)(Al_{6-y}Li_y)O_{20}(OH)_4, M_y^+$ for the hectorite… These differentiations are mainly due to the isomorphic substitutions that take place inside the aluminum oxide layer. These substitutions induce a negative charge inside the

clay platelet, which is naturally counter balanced by inorganic cations (Li^+, Na^+, Ca^{2+}, K^+, Mg^{2+}…) located into the inter-layer spacing, The global charge varies depending on the phyllosilicates. For the smectite and the mica families, this charge varies from 0.4 to 1.2 and from 2 to 4 per unit cell, respectively (Table I.1). The charge amount is characterized by the cationic exchange capacity (CEC) and corresponds to the amount of monovalent cations necessary to compensate the platelets negative charge, which is usually given in milliequivalent per 100 grams (meq/100g). For instance, the montmorillonite CEC varies from 70 to 120 meq/100g depending on their extraction site (Thomas, F., 1999).
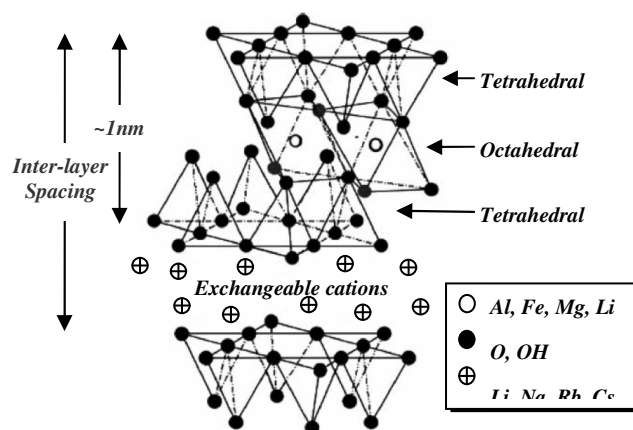
Figure I.2. Structure of 2:1 phyllosilicates.

The distance observed between two platelets of the primary particle, named inter-layer spacing or d-spacing (d_{001}), depends on the silicate type. This value does not entirely depend on the layer crystal structure, but also on the type of the counter-cation and on the hydration state of the silicate. For instance, $d_{001} = 9.6$ Å for anhydrous montmorillonite with sodium as counter ion, but $d_{001} = 12$ Å in usual conditions. This increase is linked to the adsorption of one layer of water molecule into the clay platelets (Alexandre, M., 2000).

Table I.1. Classification of 2:1 Phyllosilicates (Jozja, N., 2003).

Charge per unit cell	Di-octahedral Phyllosilicate	Tri-octahedral Phyllosilicate
	Smectites	
	Montmorillonite	Hectorite
	$(Si_8)(Al_{4-y}Mg_y)O_{20}(OH)_4, M_y^+$	$(Si_8)(Al_{6-y}Li_y)O_{20}(OH)_4, M_y^+$
0.4 to 1.2	Beidellite	Saponite
	$(Si_{8-x}Al_x)Al_4O_{20}(OH)_4, M_x^+$	$(Si_{8-x}Al_x)(Mg_6)O_{20}(OH)_4, M_x^+$
	Illites	Vermiculite
1.2 to 1.8	$(Si_{8-x}Al_x)(Al_{4-y}M_y^{2+}O_{20}(OH)_4, K_{x+y}^+$	$(Si_{8-x}Al_x)(Mg_{6-y}M_y^{3+})O_{20}(OH)_4, K_{x-y}^+$
	Micas	
	Muscovite	Phlogopites
2	$(Si_6Al_2)(Al_4)O_{20}(OH)_2, K_2^+$	$(Si_6Al_2)(Mg_6)O_{20}(OH)_2, K_2^+$
	Margarite	Clintonite
4	$(Si_4Al_4)(Al_4)O_{20}(OH)_2, Ca_2^{2+}$	$(Si_4Al_4)(Mg_6)O_{20}(OH)_2, Ca_2^{2+}$

1.3 Phyllosilicate Swelling Properties

The phyllosilicate multi-scale structure has different porosity levels, which drive its swelling properties. The water absorption occurs thanks to the intercalated cation hydration, which lowers the attractive forces between the clay layers (Sposito, G., 1999), and also thanks to the water capillarity phenomena, which take place into the inter-particle and inter-aggregate porosities (Luckham, P.F., 1999, Méring, J., 1946). For a given pressure, this swelling is characterized by a d_{001} increase until an equilibrium distance (Cases, J.M., 1992). In general, the smaller is the cations and the lower is its charge, the higher the clay swelling is. For MMT, the swelling decreases depending on the cation chemical type according to the following trend: $Li^+ > Na^+ > Ca^{2+} > Fe^{2+} > K^+$ (Powell, D.H., 1998a, Powell, D.H., 1998b, Tettenhorst, R., 1962). The potassium is a specific case because its size is equal to the dimension of the platelet surface cavity. Thus, the potassium is trapped into these cavities, leading to a lowering of its hydration ability.

1.4 Phyllosilicate Organo-Modification

To enhance the intercalation/exfoliation process, a chemical modification of the clay surface, with the aim to match the polymer matrix polarity, is often carried out (Alexandre, M., 2000, Sinha Ray, S., 2003). The cationic exchange is the most common technique, but other original techniques as the organosilane grafting (Dai, J.C., 1999, Ke, Y., 2000), the use

of ionomers (Lagaly, G., 1999, Shen, Z., 2002) or block copolymers adsorption (Fischer, H.R., 1999) are also used.

The cationic exchange consists in the inorganic cations substitution by organic ones. These surfactants are often alkylammonium cations having at least one long alkyl chain. Phosphonium salts are also interesting clay modifiers, thanks to their higher thermal stability, but they are not often used (Wilkie, C.A., 2001). The ionic substitution is performed into water because of the clay swelling, which facilitates the organic cations insertion between the platelets. Then, the solution is filtered, washed with distilled water (to remove the salt formed during the surfactant adsorption and the surfactant excess) and lyophilized to obtain the organo-modified clay. In addition to the modification of the clay surface polarity, organo-modification increases the d_{001}, which will also further facilitate the polymer chains intercalation (Lagaly, G., 1986). Various commercially available organo-modified montmorillonites (OMMT), which mainly differ from the nature of their counter-cation and their CEC, are produced with this technique (e.g. Cloisite® 15A, 20A, 30B… or Nanofil® 804…).

2. Nanocomposites Eboration Protocol

The nanofiller incorporation into the polymer matrix can be carried out with three main techniques (Alexandre, M., 2000), (i) the in-situ polymerization, (ii) the solvent intercalation or (iii) the melt intercalation process.

Depending on the process conditions and on the polymer/nanofiller affinity, different morphologies can be obtained. These morphologies can be divided in three distinct categories, (i) microcomposites, (ii) intercalated nanocomposites or (iii) exfoliated nanocomposites (Alexandre, M., 2000, Sinha Ray, S., 2003, Vaia, R.A., 1997). For microcomposites, the polymer chains have not penetrated into the inter-layer spacing and the clay particles are aggregated. In this case, the designation as nanocomposite is abusive. In the intercalated structures, the polymer chains have diffused into the platelets leading to a d_{001} increase. In the exfoliated state, the clay layers are individually delaminated and homogeneously dispersed into the polymer matrix. Intermediate dispersion states are often achieved, such as intercalated-exfoliated structures. This classification does not take into account the dispersion multi-scale structure, such as percolation phenomenon, preferential orientation of the clay layers...

2.1 In-Situ Polymerization Process

In this method, layered silicates are swollen into a monomer solution. Then, the monomer polymerization is initiated and propagated. The macromolecules molecular weight increases, leading to a d_{001} increase and to an exfoliated morphology in the most studied systems (Sinha Ray, S., 2003). However, since polysaccharides chains are synthesized during the plant growth and then extracted from the vegetal, this technique cannot be used to prepare polysaccharides nano-biocomposites.

2.2 Solvent Intercalation Process

This elaboration process is based on a solvent system in which the polymer is soluble and the silicate layers are swellable. The polymer is first dissolved in an appropriate solvent. In parallel, the clay (organo-modified or not) is swollen and dispersed into the same solvent or another one to obtain a miscible solution. Both systems are pooled together leading to a polymer chains intercalation. Then, the solvent is evaporated to obtain nanocomposite materials. Nevertheless, for non water-soluble polymers, this process involves the use of large amount of organic solvents, which is environmentally unfriendly and cost prohibitive. Moreover, a small amount of solvent remains in the final product at the polymer/clay interface creating lower interfacial interaction between the polymer and the clay surfaces (Jin, Y.H., 2002). Thus, this technique is mainly used in academic studies. Since some polysaccharides, such as chitosane or pectin, cannot be melt processed due to high thermal or thermomechanical degradations, the solvent process has been extensively used to produce polysaccharide hybrid materials.

2.3 Melt Intercalation Process

Both the polymer and the clay are introduced simultaneously into a melt mixing device (extruder, internal mixer…). According to Denis et al. (Dennis, H.R., 2001), in addition to the polymer/nanofiller affinity, two main process parameters favor the nano-dispersion of the nanoclay. These parameters, which are the driving force of the intercalation-exfoliation process into the matrix, are (i) the residence time and (ii) the shearing. The shearing is necessary to induce the platelets delamination from the clay tactoïds. The extended residence time is needed to allow the polymer chains diffusion into the inter-layer gallery and then to obtain an exfoliated morphology (Figure I.3).

This simple process has extensively been used to prepare polysaccharide nano-biocomposite materials. Nevertheless, the thermal or thermomechanical inputs lead to a partial

chains degradation. Moreover, the high residence needed to enhance the clay exfoliation process favor the matrix degradation. Therefore, it is necessary to balance the process parameters to minimize the chains degradation and to obtain a well exfoliated morphology.

Phyllosilicate   Shear Induced Dislocation
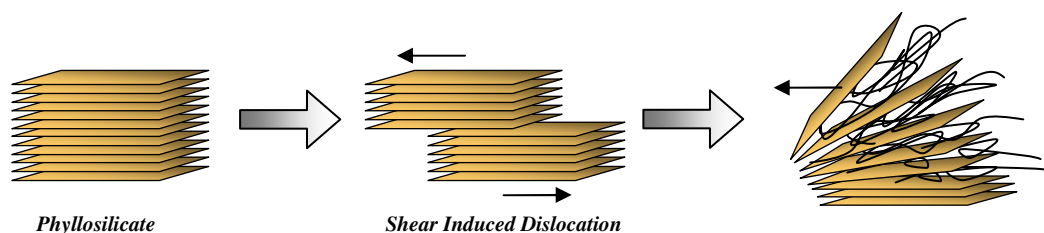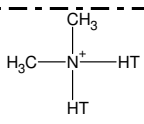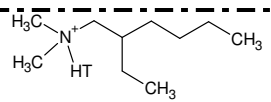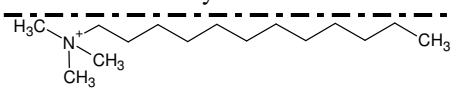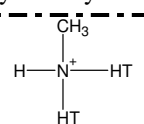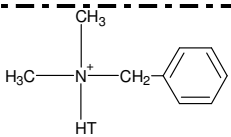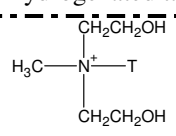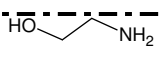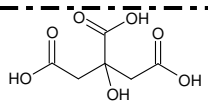
Figure I.3. Mechanism leading to clay exfoliation under shearing (Dennis, H.R., 2001).

IV. Polysaccharides-Based Nano-Biocomposites

Polysaccharides are the most abundant macromolecules in the biosphere. These complex carbohydrates constituted of monosaccharides joined together by glycosidic bonds are often one of the main structural elements of plants and animals exoskeleton (e.g. cellulose, carrageenan, chitin…) or have a key role in the plant energy storage (e.g. starch, paramylon…).

The following chapter is focused on the main studied nano-biocomposite based on nanoclay and polysaccharides, namely starch and its derivatives, cellulose, chitosan and pectin. Throughout this paper, the nanofillers used to produce nano-hybrid materials are designated according to the abbreviations given in Table I.2.

Table I.2. Nanofiller types (trade-name and code) and their corresponding counter-ion chemical structure.

Code	Name	Counter-Cation
MMT-Na	Natural sodium montmorillonite	Na+
OMMT-Alk1	Cloisite® 15A – Southern Clay	
OMMT-Alk2	Cloisite® 6A – Southern Clay	
OMMT-Alk3	Cloisite® 20A – Southern Clay	Dimethyl-dihydrogenated tallow ammonium
OMMT-Alk4	Cloisite® 25A – Southern Clay	Dimethyl-hydrogenated tallow-2-ethylhexyl ammonium
OMMT-Alk5	Nanomer® I.30E – Nanocor	$H_{35}C_{18}-NH_3^+$ Octadecyl ammonium
OMMT-Alk6	/	Trimethyldodecyl ammonium
OMMT-Alk7	Cloisite® 93A – Southern Clay	Methyl-dihydrogenated tallow ternary ammonium hydrogen sulfate
OMMT-Bz	Cloisite® 10A – Southern Clay	Dimethyl-benzyl-hydrogenated tallow ammonium
OMMT-OH1	Cloisite® 30B – Southern Clay	
OMMT-OH2	Nanofil® 804 – Süd Chemie	Methyl-tallow-bis-2-hydroxyethyl ammonium
OMMT-NH₄	Bentone® 111 - Elementis Specialties	NH_4^+
OMMT-EtA	/	Ethalonamine
OMMT-CitA	/	Citric acid
T = Tallow (~65% C18; ~30% C16; ~5% C14) - HT = Hydrogenated Tallow		

1. Starch

Starch is mainly extracted from cereals (wheat, corn, rice…) and from tubers (potatoes, manioc…). It is stocked into seeds or roots and represents the main plant energy reserve.

1.1 Native Starch Structure

Depending on the botanical origin of the plant, starch granules can have very different shapes (sphere, platelet, polygon…) and size (from 0.5 to 175 µm). These granules are composed of two α-D-glucopyranose homopolymers, the amylose and the amylopectin. Their proportions into the granules depend directly on the botanical source. In addition, starch contains also in smaller proportion other compounds, such as proteins, lipids and minerals (Table I.3), which can interfere with starch, e.g. by the formation of lipid complexes or with the proteins by "Maillard reaction" during the process.

Table I.3. Composition and physical chemical characteristics of different starches (Guilbot, A., 1985).

Starch	Amylose[*] (%)	Lipids[*] (%)	Proteins[*] (%)	Minerals[*] (%)	Crystallinity (%)	Water content[†] (%)
Wheat	26-27	0.63	0.30	0.10	36	13
Corn	26-28	0.63	0.30	0.10	39	12-13
Waxy Maize	<1	0.23	0.10	0.10	39	/
Amylocorn	52-80	1.11	0.50	0.20	19	/
Potato	20-24	0.03	0.05	0.30	25	18-19

[*] Dry-basis proportion

[†] Water content after stabilization at 65 %RH and 20 °C

a. Amylose

The amylose is mainly a linear polysaccharide composed of D-glucose units linked by α(1→4) linkages (Figure I.4). These chains are partially ramified with some α(1→6) linkages. Their number is directly proportional to the amylose molecular weight (from 10^5 to 10^6 g.mol^{-1}) (Della Valle, G., 1998). The amylose polydispersity index varies from 1.3 to 2.1 depending on the botanical source and the extraction process (Colonna, P., 1984).

The average number of glucose units into the amylose varies from 500 to 5,000. Comprised between 1 and 20 per macromolecule, each branch has an average polymerization degree of 500 (Hizukuri, S., 1981). The amylose chains show a single or double helix conformation with a rotation on the α(1→4) linkage (Hayashi, A., 1981). The helix is composed of six glucose units per turn with a 4.5 Å diameter.
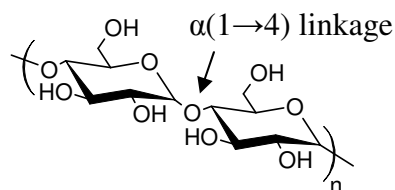
Figure I.4. Amylose chemical structure.

b. **Amylopectin**

The amylopectin is the main starch component and has the same monomeric unit as amylose. It shows 95 % of α(1→4) and 5 % of α(1→6) linkages. These latter are found every 24 to 79 glucose units (Zobel, H.F., 1988) and brought to the amylopectin a highly branched structure. Depending on the botanical source, the molecular weight varies from 10^7 to 10^8 g.mol^{-1}. Consequently, the amylopectin structure and organization, which have been elucidated for the first time by Hizuruki (Hizukuri, S., 1986), can be seen as a grape with pending chains (Figure I.5).
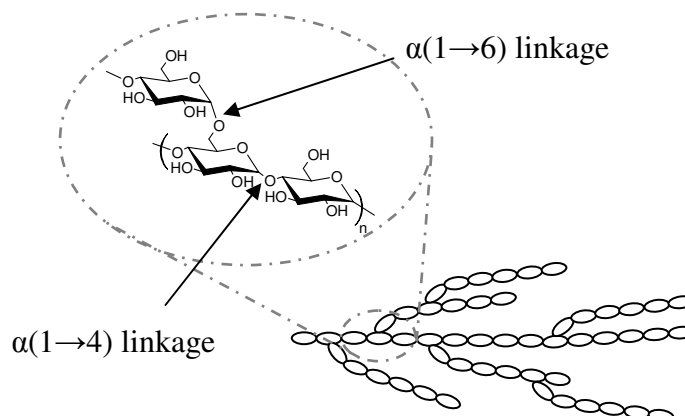
Figure I.5. Amylopectin chemical and grape structure (Hizukuri, S., 1986).

c. **Starch Granule**

The starch granule organization consists in an alternation of crystalline and amorphous areas leading to a concentric structure (Jenkins, P.J., 1995). The amorphous areas are constituted of the amylose chains and the amylopectin branching points. The semi-crystalline areas are mainly composed of the amylopectin side chains. Some co-crystalline structures with the amylose chains have been also identified (Van Soest, J.J.G., 1996a, Van Soest, J.J.G., 1997a). Depending on the botanical origin, starch granules present a crystallinity varying from 20 to 45 %. Four starch allomorphic structures exist (Van Soest, J.J.G., 1996a):

(i)   A-type: This structure is synthesized in cereals in dry and warm conditions. The chains are organized in a double helix conformation with 6 glucose units per turn. These helixes are organized into a monoclinic structure containing 8 water molecules per unit cell.

(ii)   B-type: This structure is synthesized in tuber and into starch with high amylose content. It is also organized in a double left helix with 6 glucose units per turn into a hexagonal system containing 36 water molecules per unit cell.

(iii)   C-type: Mainly synthesized into vegetables, this structure is a mix of the two previous structures.

(iv)   V-type: This structure is synthesized in presence of small molecules like iodine or fatty acids. This crystalline form is characterized by a simple left helix with 6 glucose units per turn.

1.2 Plasticized Starch

Because of the numerous intermolecular hydrogen bonds existing between the chains, starch melting temperature is higher than its degradation temperature (Jang, J.K., 1986, Shogren, R.L., 1992a). Consequently, to elaborate a plastic-like material with conventional plastic processing techniques, it is necessary to introduce high water content or/and some unvolatile plasticizers (glycerol, sorbitol…), which will increase the free volume and thus decrease the glass transition and the melting temperature (Swanson, C.L., 1993, Tomka, I., 1991). These plasticized materials are currently named « thermoplastic starch » or « plasticized starch ».

a.   Plasticized Starch Elaboration Process

To be transformed, the starch granule structure has to be disrupted. The disruption is obtained by two different processes, (i) the casting process where the starch granules are introduced in a large amount of solvent under thermal treatment and (ii) the melting process. The starch granules and the plasticizers are mixed under thermomechanical treatment.

Casting Process

At ambient temperature, starch remains insoluble in water and keeps its granular structure. Water temperature increase induces an irreversible swelling named "gelatinization". This phenomenon occurs at a given temperature defined as "gelatinization temperature" (T_{gel}).

During this gelatinization, the amylose is rather solubilized, the granule semi-crystalline structure disappears and the granules swell rapidly. T_{gel}, commonly determined by DSC (Cooke, D., 1992), does not depend on the granule crystalline structure but on the starch botanical origin (corn, rice…) (Table I.4) (Stevens, D.J., 1971). This dependence has been recently highlighted and explained by the starch granule crystal lattice defects, which depend on the starch botanical origin (Genkina, N.K., 2007). To obtain a quite full starch solubilization hot DMSO is often used as solvent. Then, this solvent is volatilized under vacuum and heat.

Table I.4. Gelatinization temperatures and enthalpies vs. the starch botanical source (Stevens, D.J., 1971).

Starch	ΔH (cal/g)	T_{gel} (°C)
Wheat	2.4	69
Corn	3.7	78
Potato	5.5	71
Rice	3.4	82

ii.   Melting Process

The granules' melting is often carried out in association with plasticizers using e.g. extrusion, a common thermomechanical mixing process, to obtain a homogeneous molten phase. During this transformation, different and successive phenomena can occurs such as (i) the fragmentation of the starch granules, (ii) the disruption and the plasticization of the destructured granules, (iii) the material melting and (iv) a partial chains degradation, under the thermomechanical input (Figure I.6) (Averous, L., 2004a).
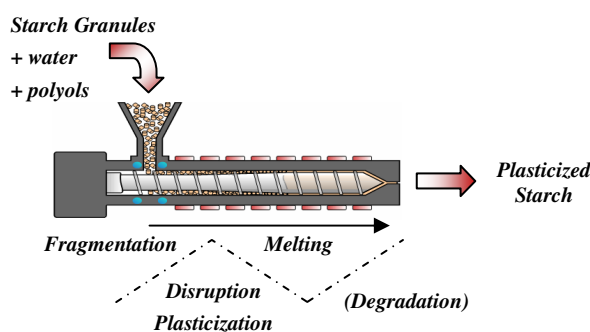
Figure I.6. Schematic representation of the starch extrusion process.

The mechanical energy of this process can be evaluated according to the specific mechanical energy (SME, Equation I.1):

$$SME(J / kg) = \frac{Screw\,Rotation\,Speed\ (rpm) * Screw\,Torque(N.m)}{Incorporation\,Flow\,Rate\ (kg / min)} \qquad (I.1)$$

SME variations directly influence the starch granules disruption. According to Ollett et al. (Ollett, A.L., 1990), an energy of 400 J/g is required to disrupt the granular structure. Because of its high SME sensitivity, this material could be described as a "thermo-mechanical-plastic" material (Martin, O., 2003).

The amylose and amylopectin degradation mechanisms have been highlighted thanks to intrinsic viscosity measurements (Della Valle, G., 1995, Vergnes, B., 1987) and size exclusion chromatography (Orford, P.D., 1993, Sagar, A.D., 1995). The pending chains of amylopectin are the most sensitive to this mechanism of chain scissions (Baud, B., 1999). This phenomenon is obviously dependent on the thermal and mechanical energy brought to the system, but the contribution of each parameter is not fully understood. Wang et al. (Wang, S.S., 1989) have demonstrated that the activation energy of the shearing degradation is lower than the thermal degradation one, suggesting that the main contribution on the degradation is induced by shearing. According to Davidson et al. (Davidson, V.J., 1984a, Davidson, V.J., 1984b), the mechanical energy contribution to the global degradation is prevailing at low temperature. However, at higher temperature, the thermal energy contribution becomes preponderant.

b. Plasticized Starch Behavior and Properties

i. *Plasticizer Influence*

Since starch is a hydrophilic material, water is the best plasticizer (Kalichevsky, M.T., 1992, Tomka, I., 1991, Van Soest, J.J.G., 1997c, Zeleznak, K.J., 1987). Nevertheless, the water content and thus the plasticized starch properties are strongly dependent on the storage conditions (temperature and atmosphere relative humidity) through sorption-desorption exchanges. This drawback is partially solved with the use of less volatile plasticizers, which present lower plasticization efficiency. These compounds based on hydroxyl groups (polyols) can interact with the starch chains through hydrogen bonds. Glycerol is the most common plasticizer (Forssell, P., 1996, Hulleman, S.H.D., 1999, Lourdin, D., 1997c, Van Soest, J.J.G., 1994), but numerous other polyols, such as sorbitol (Gaudin, S., 2000), xylitol (Lourdin, D., 1995), fructose (Kalichevsky, M.T., 1993), glucose, (Ollett, A.L., 1991) glycols (Shogren,

R.L., 1992b)... or plasticizer with amino groups, like urea, can be used (Shogren, R.L., 1992b). Nevertheless, these plasticizers are more hydrophilic than starch and are also sensitive to the relative humidity.

The plasticized starch T_g is sometimes difficult to determine by DSC analyses, because the heat capacity change is often quite low at the glass transition then DMTA determination is preferably used. Depending on the glycerol content, the thermograms obtained display one or two relaxation peaks, corresponding to a homogeneous or multiphasic material. Lourdin et al. (Lourdin, D., 1997c, Lourdin, D., 1998) have demonstrated that this phase separation occurs for glycerol content higher than 27 wt% dry-basis. The main relaxation (named α), associated to an important decrease of the storage modulus, is attributed to the plasticized starch T_g. The second relaxation (named β) is consistent with the glycerol glass transition and occurs around -50 to -70 °C. Several authors have shown that this secondary transition is dependent on the glycerol concentration and more particularly on the 'free' glycerol (Averous, L., 2000a, Lourdin, D., 1997a).

According to Lourdin et al. (Lourdin, D., 1997b), when the glycerol content varies from 0 to 25 wt%, the plasticized starch T_g decreases from 90 °C to -10 °C, respectively (samples stored 48 h at 57 %RH). In the same way, Avérous et al. (Averous, L., 2000a) have determined the influence of the glycerol content on the starch T_g by DSC and DMTA. According to these authors, the starch T_g is decreased from 43 °C to -20 °C with 13.5 and 58.8 wt% of glycerol, respectively (samples stored 2 weeks at 65 %RH).

The influence on the water content at equilibrium for a define glycerol concentration has been determined by Lourdin et al. (Lourdin, D., 1997c). They have studied the T_g variation of potato starch vs. the water content for different glycerol concentration (Figure I.7) and have concluded that the higher the water content, the lower the plasticized starch T_g.
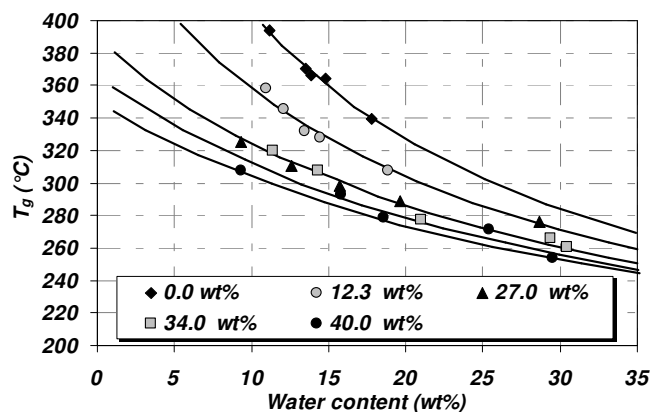
Figure I.7. Potato starch T_g variation at different glycerol concentration vs. water content (Lourdin, D., 1997c).

To better understand these systems, Godbillot et al. (Godbillot, L., 2006) have recently proposed a phase diagram for the water/glycerol/starch system, as a function of the plasticizer content, which highlights the different interactions taking place in these multiphasic systems. Depending on the glycerol content and the relative humidity, the plasticizer can be more or less linked with the polysaccharide chains. It could occupy specific sorption sites when the water and plasticizer content are low, or free when the carbohydrate chains sorption sites are filled, at high relative humidity and glycerol content. Between these two limit cases, complex interactions between the different components could be established.

ii. *Plasticization and Anti-Plasticization Effect*

As for the traditional synthetic polymers, the plasticizer incorporation leads to an increase in the strain at break and a decrease in both, the Young's modulus and the stress at break. Actually, these phenomena are directly linked to the increase in the free volume, which leads to an increase in the chain mobility. A study from Lourdin et al. (Lourdin, D., 1997b) have highlighted this common evolution for glycerol content higher than 12 wt%. Nevertheless, below this concentration, a remarkable behavior is observed. A decrease in the stress and the strain at break correlated to a rise in plasticizer content is shown (Figure I.8). The same trend has also been observed in sorbitol plasticized systems and has been attributed to an antiplasticization effect. To explain this phenomenon, Gaudin et al. (Gaudin, S., 2000) concluded to the formation of a physical network stabilized by the hydrogen bonds established between the plasticizer and the starch chains, leading to a hardening of the material below a critical plasticizer concentration.
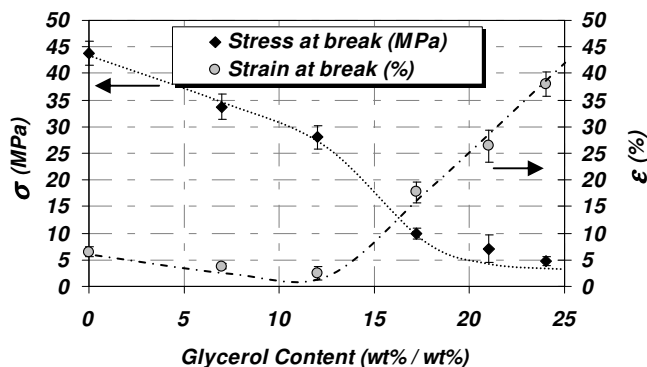
Figure I.8. Stress and strain at break variations against glycerol content for potato starch stored at 57 %RH (Lourdin, D., 1997b).

iii. Post Processing Ageing

During processing, the starch granules lose their crystalline structure and become an amorphous material. This physical state is non-stable and the material will evoluate with time. This evolution corresponds to molecular reorganization, which are dependent on the process protocol and the storage conditions. When the samples are stored below the T_g, the samples will undergo physical ageing with a material densification (Thiewes, H.J., 1997). When $T > T_g$, the samples will retrogradate with a crystallinity increase (Lu, T.J., 1997).

The physical ageing is only observed for materials with low plasticizer content. According to Shogren et al. (Shogren, R.L., 1992a) and Appelqvist et al. (Appelqvist, I.A.M., 1993), this phenomenon occurs for materials having plasticizer content lower than 25 wt%. This molecular reorganization corresponds to an evolution of the material to a more stable energetic state, characterized by a material volume decrease. This physical ageing induces a hardening and a lowering of the strain at break.

The retrogradation takes place after the amylose crystallization and concerns the amylopectin crystallization. This phenomenon is slow and lasts for more than a month (Averous, L., 2000a, Averous, L., 2000b). This crystallization is limited by the branching points of the amylopectin and is induced by the crystallization of the amylopectin pending chains. The retrogradation induces a strong variation of the mechanical properties (Van Soest, J.J.G., 1996c, Van Soest, J.J.G., 1996d, Van Soest, J.J.G., 1997a, Van Soest, J.J.G., 1997b).

Thus, even if these two ageing processes are very different in their mechanisms, both of them induce the creation of internal stress into the material, which leads to an

embrittlement of the materials characterized by a stiffness increase correlated to a strain at break decrease (Table I.5).

Table I.5. Wheat starch - Tensile test parameters vs. storage time and glycerol content (Averous, L., 2000a).

Ratio Glycerol/Starch	2 weeks of ageing			6 weeks of ageing		
	Young's Modulus (MPa)	Stress at break (MPa)	Strain at break (%)	Young's Modulus (MPa)	Stress at break (MPa)	Strain at break (%)
0.135	997 (59)	21.4 (1.0)	3.8 (0.3)	1,144 (42)	21.4 (1.7)	3.4 (0.4)
0.257	52 (9)	3.3 (0.1)	126.0 (2.0)	116 (11)	4.0 (0.1)	104.0 (4.7)
0.358	26 (4)	2.6 (0.1)	110.0 (11.1)	45 (5)	3.3 (0.1)	98.2 (5.2)
0.538	2 (1)	0.6 (0.2)	90.7 (4.8)	11 (1)	1.4 (0.1)	60.4 (5.2)

Samples stored at 23 °C and 50 %RH

iv. *Botanical Source Influence*

The mechanical properties are directly influence by the amylose/amylopectin ratio, which vary with the botanical origin. The materials rich in amylopectin, like waxy corn starch, are ductile (Van Soest, J.J.G., 1996c) and show a Young's modulus between 10 MPa and 20 MPa and a strain at break of 500 %. On the opposite, the materials rich in amylose, like amylocorn starch, have a higher modulus and a lower strain at break, between 5 % and 35 % (Van Soest, J.J.G., 1997b). According to Lourdin et al. (Lourdin, D., 1995), the Young's modulus increases linearly with the amylose content until 40 wt% and then reaches a threshold. Since the amylopectin mainly stays in an amorphous state after processing, this trend is a consequence of the amylose crystallization (Van Soest, J.J.G., 1997b).

1.3 Starch-Based Nano-Biocomposites

Starch has been the most studied polysaccharide in nano-biocomposite systems, mainly into its plasticized state (Avella, M., 2005, Bagdi, K., 2006, Chaudhary, D.S., 2008, Chen, B., 2005, Chen, M., 2005, Chiou, B.-S., 2005, Chiou, B.-S., 2006, Chiou, B.S., 2004, Chiou, B.S., 2007, Cyras, V.P., 2008a, Dean, K., 2007, Dean, K.M., 2008, Huang, M., 2005, Huang, M., 2006a, Huang, M., 2006b, Huang, M.F., 2004, Huang, M.F., 2005a, Huang, M.F., 2005b, Kampeerapappun, P., 2007, Lilichenko, N., 2008, Ma, X., 2007, Mondragon, M., 2008, Pandey, J.K., 2005, Park, H.M., 2002, Park, H.M., 2003, Tang, X., 2008a, Tang, X., 2008b, Wilhelm, H.-M., 2003a, Zhang, Q.X., 2007), but also with blends elaborated with PLA (Lee, S.Y., 2007, Lee, S.Y., 2008a, Lee, S.Y., 2008b, Lee, S.Y., 2008c), PCL (Kalambur, S., 2005, Kalambur, S.B., 2004, McGlashan, S.A., 2003, Perez, C.J., 2007a, Perez, C.J., 2007b, Perez, C.J., 2008a, Perez, C.J., 2008b, Perez, C.J., 2008c) or poly(vinyl

alcohol) (PVAL) (Dean, K.M., 2008) or with chemically modified (e.g. acetylated) starch matrices (Qiao, X., 2005, Xu, Y., 2005).

a. Plasticized Starch-Based Nano-Biocomposites

To reach exfoliation for plasticized starch-based nano-biocomposites, different nanofillers and elaboration protocols were developed. First, from 1 to 9 wt% of rather hydrophobic nanofillers were incorporated into starch plasticized with glycerol by melt blending (Chiou, B.-S., 2005, Chiou, B.-S., 2006, Park, H.M., 2002, Park, H.M., 2003, Zhang, Q.X., 2007) (internal batch mixer or into a twin screw extruder) or solvent process (Tang, X., 2008a). It was clearly demonstrated that the incorporation of OMMT-Alk1 (Chiou, B.-S., 2005), OMMT-Alk2 (Park, H.M., 2002) or OMMT-Bz (Chiou, B.-S., 2005, Park, H.M., 2002) led to the formation of conventional micro-biocomposites. This structure has been evidenced by the constant values of the basal d_{001} from X-ray diffraction experiments. Better results were obtained with OMMT-Alk5 (Tang, X., 2008a) and OMMT-Alk7 (Zhang, Q.X., 2007), the corresponding nano-biocomposites displaying a slight shift in d_{001} towards lower angles. The dispersion of the more hydrophilic OMMT-OH1 led to higher dispersion state with a shift in the d_{001} value to lower angle and a strong decrease in the diffraction peak intensity (Chiou, B.-S., 2005, Chiou, B.-S., 2006, Park, H.M., 2002, Park, H.M., 2003). This morphology was likely achieved thanks to the hydrogen bonds established between the hydroxyl groups brought by the carbohydrate chains and the clay surfactant (Park, H.M., 2003).

Besides, nano-biocomposites based on plasticized starch with glycerol were elaborated with MMT-Na. Thanks to the hydrophilic nature of both starch and MMT-Na, this nanofiller was supposed to lead to an enhanced nano-dispersion state. These materials were prepared with solvent (Cyras, V.P., 2008a, Kampeerapappun, P., 2007, Lilichenko, N., 2008, Mondragon, M., 2008, Pandey, J.K., 2005, Tang, X., 2008b, Wilhelm, H.-M., 2003a) or melt blending process (Avella, M., 2005, Bagdi, K., 2006, Chen, B., 2005, Chiou, B.-S., 2005, Chiou, B.-S., 2006, Chiou, B.S., 2004, Chiou, B.S., 2007, Huang, M.F., 2004, Park, H.M., 2002, Park, H.M., 2003, Zhang, Q.X., 2007). It was highlighted that for glycerol content higher than 10 wt%, such systems led to the formation of an intercalated structure with d_{001} increased from 12 to 18 Å. This d_{001} value is already well reported into the literature and generally attributed to glycerol intercalation (Pandey, J.K., 2005, Park, H.M., 2003, Tang, X., 2008b). Similar morphology was obtained with sorbitol as the plasticizer (Ma, X., 2007) However, for glycerol content lower than 10 wt%, Tang et al. (Tang, X., 2008b) have

obtained an intercalated/exfoliated structure, meaning that the clay exfoliation process is likely perturbed by the polyol plasticizer content. On this way, Dean et al. have elaborated amylocorn starch nano-biocomposites by solvent (Dean, K., 2007) and melt (Dean, K.M., 2008) processes, with water as the unic plasticizer, to obtain a homogeneous dispersion with an intercalated or exfoliated structure. In addition, Chaudhary (Chaudhary, D.S., 2008) has obtained an intercalated/exfoliated morphology with the melt dispersion of a hydrophobic nanofiller, OMMT-Alk4, without polyol plasticizer. These results confirm the strong influence of the polyol plasticizer on the exfoliation process and thus on the resulting morphology. This trend is likely related to the hydrogen bonds established between glycerol and MMT platelets, which could disturb the clay exfoliation process (Huang, M.F., 2004, Pandey, J.K., 2005, Wilhelm, H.-M., 2003a).

To overcome these limitations induced by polyol plasticizers, some authors replaced these plasticizers by urea (Chen, M., 2005, Tang, X., 2008b), urea/ethanolamine (Huang, M., 2006b), formamide (Tang, X., 2008b), formamide/ethanolamine (Huang, M.F., 2005a, Huang, M.F., 2005b) or urea/formamide (Huang, M., 2005, Huang, M., 2006a). MMT-Na dispersion into these urea or formamide plasticized starch matrices by solvent (Tang, X., 2008b) or melt (Chen, M., 2005) process led to the formation of intercalated structures. Thus, to increase the clay/matrix affinity, different organo-modified MMT have been incorporated namely, OMMT-EtA (Huang, M., 2006b, Huang, M.F., 2005a, Huang, M.F., 2005b), OMMT-CitA (Huang, M., 2005, Huang, M., 2006a) and OMMT-NH$_4$ (Chen, M., 2005). These OMMT were incorporated into the urea, urea/ethanolamine, formamide/ethanolamine or urea/formamide plasticized starch by melt process. The incorporation of OMMT-EtA into formamide/ethanolamine or urea/ethanolamine plasticized matrices led to intercalated structures with d_{001} = 26 Å (Huang, M.F., 2005a, Huang, M.F., 2005b) and exfoliation (Huang, M., 2006b), respectively. In the same way, exfoliated nano-biocomposites have been obtained with the dispersion of OMMT-CitA (Huang, M., 2005, Huang, M., 2006a) and OMMT-NH$_4$ (Chen, M., 2005) into urea/formamide and urea plasticized starch, respectively. Such an exfoliated structure has been obtained even for clay content higher than 5 wt%. Thus, it has been demonstrated that with the modification of the plasticizer and clay polarity, exfoliation can be reached. Nevertheless, these compounds are eco-toxic and cannot be used to elaborate safe biodegradable "green" materials.

On this way, Kampeerappun et al. (Kampeerapappun, P., 2007) have focused their attention on the use of a new eco-friendly compatibilizer, chitosan, to promote the MMT

platelets exfoliation. Thus, they have prepared cassava starch/chitosan/MMT-Na nano-biocomposites by casting. The nano-biocomposites were prepared with the mixing of starch with chitosan powder (varied from 0 to 15 wt% of starch) and MMT-Na (varied from 0 to 15 wt% of starch). Only a small increase in the clay d_{001} from 12 to 14-15 Å was achieved since the molecular mass of the chitosan used was too high to be easily intercalated into the MMT inter-layer spacing. However, these authors assumed that this polycation can act as a compatibilizing agent leading to few clay aggregates and improved mechanical properties. The different morphologies obtained with these plasticized starch matrices are summarized in Tables I.6 and I.7.

Table I.6. Morphology of the plasticized starch nano-biocomposites elaborated by solvent process.

Plasticizer	Nanofillers	Morphology	References
Only water	MMT-Na	Intercalated	(Dean, K., 2007)
		Exfoliated	(Dean, K., 2007)
Glycerol content < 10 wt%	MMT-Na	Intercalated/Exfoliated	(Tang, X., 2008b)
	OMMT-Alk5	Intercalated	(Tang, X., 2008a)
Glycerol content > 10 wt%	MMT-Na	Intercalated - d_{001} ~ 18 Å	(Cyras, V.P., 2008a, Kampeerapappun, P., 2007, Lilichenko, N., 2008, Mondragon, M., 2008, Pandey, J.K., 2005, Tang, X., 2008b, Wilhelm, H.-M., 2003a)
	MMT-Na/Chitosan	Intercalated - d_{001} ~ 15 Å	(Kampeerapappun, P., 2007)
Urea	MMT-Na	Intercalated - d_{001} ~ 23 Å	(Tang, X., 2008b)
Formamide	MMT-Na	Intercalated - d_{001} ~ 23 Å	(Tang, X., 2008b)

Table I.7. Morphology of the plasticized starch nano-biocomposites elaborated by melt process.

Plasticizer	Nanofillers	Morphology	References
Only water	MMT-Na	Exfoliated	(Dean, K.M., 2008)
	OMMT-Alk4	Intercalated – Exfoliated	(Chaudhary, D.S., 2008)
Glycerol content > 10 wt%	OMMT-Bz	Microcomposite	(Chiou, B.-S., 2005, Park, H.M., 2002)
	OMMT-Alk1	Microcomposite	(Chiou, B.-S., 2005)
	OMMT-Alk2	Microcomposite	(Park, H.M., 2002)
	OMMT-Alk7	Intercalated - d_{001} ~ 34 Å	(Zhang, Q.X., 2007)
	OMMT-OH1	Intercalated - d_{001} ~ 20 Å	(Chiou, B.-S., 2005, Chiou, B.-S., 2006, Park, H.M., 2002, Park, H.M., 2003)
	MMT-Na	Intercalated - d_{001} ~ 18 Å	(Avella, M., 2005, Bagdi, K., 2006, Chen, B., 2005, Chiou, B.-S., 2005, Chiou, B.-S., 2006, Chiou, B.S., 2004, Chiou, B.S., 2007, Huang, M.F., 2004, Park, H.M., 2002, Park, H.M., 2003, Zhang, Q.X., 2007)
Sorbitol	MMT-Na	Intercalated - d_{001} ~ 18 Å	(Ma, X., 2007)
Urea	MMT-Na	Intercalated - d_{001} ~ 18 Å	(Chen, M., 2005)
	OMMT-NH$_4$	Exfoliated	(Chen, M., 2005)
Urea/Ethanolamine	OMMT-EtA	Exfoliated	(Huang, M., 2006b)
Formamide/Ethanolamine	OMMT-EtA	Intercalated - d_{001} ~ 26 Å	(Huang, M.F., 2005a, Huang, M.F., 2005b)
Urea/Formamide	OMMT-CitA	Exfoliated	(Huang, M., 2005, Huang, M., 2006a)

Park et al. (Park, H.M., 2002, Park, H.M., 2003) have shown with DMTA analyses that potato starch/OMMT-OH1 nano-biocomposites displayed higher elastic modulus compared to those elaborated with OMMT-Bz or OMMT-Alk2. This behavior was explained by the poor nanofiller dispersion and the lack of compatibility between the plasticized starch and these more hydrophobic organo-clays. Surprisingly, these hybrid materials displayed lower elastic modulus compared to the virgin matrix. Such a result was unexpected since the nanoplatelets generally induce a stiffness increase. This behavior was explained by a shift to lower temperatures of the relaxation peaks, observed on tan δ, suggesting a matrix plasticization. This assumption is consistent with the nanofiller excess of surfactants, which may diffuse into the matrix and plasticize it. The highest elastic moduli were obtained with MMT-Na. This behavior is linked to the reinforcing effect of the clay and to a shift of the tan δ peaks toward higher temperatures, which indicates that layered clays strongly influence the starch chain mobility (Figure I.9). This tendency was attributed to the MMT-Na higher affinity with the starch chains. The same trends were observed by DSC (Huang, M., 2006a), meaning that starch/clay hybrids were strongly affected by the clay surface polarity and the clay/matrix interactions. Besides, Chiou et al. (Chiou, B.-S., 2005) analyzed the thermo-mechanical properties of wheat starch/MMT-Na nano-biocomposites and observed that elastic modulus did not depend on the high frequency solicitations. This behavior indicates that these samples formed a gel-like structure and had a better dispersion state than the more hydrophobic nanofillers (Chiou, B.-S., 2005, Pogodina, N.V., 2008).

The Young's modulus of wheat and corn starch-based nano-biocomposites elaborated with MMT-Na has been studied by uniaxial tensile tests. These materials displayed substantial improvement in mechanical properties correlated to the clay loading for MMT-Na (Lilichenko, N., 2008, Zhang, Q.X., 2007) (with corn and wheat starch). These stiffness increases were linked to the nanofiller rigidity and dispersion state and to the specific interactions established between the nanofiller surface and the matrix.
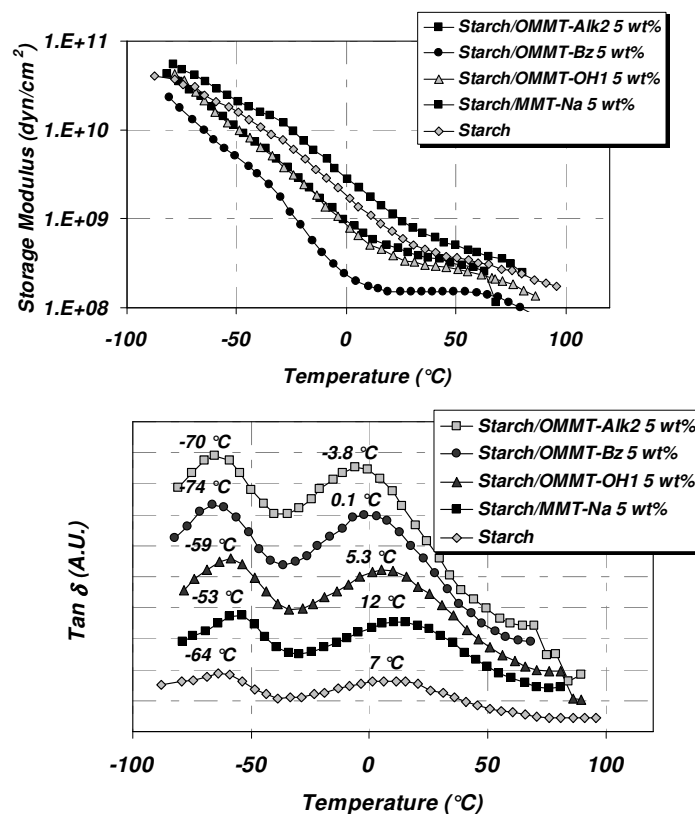
Figure I.9. Storage modulus and tan δ vs. temperature of potato starch/clay nano-biocomposites with different kind of clays (Park, H.M., 2002).

Park et al. (Park, H.M., 2002) have determined the mechanical behavior of potato starch nano-biocomposites elaborated with OMMT-Alk2, OMMT-Bz, OMMT-OH1 and MMT-Na. It was clearly seen that the most hydrophobic nanofillers (OMMT-Alk2, OMMT-Bz) displayed lower tensile strength and strain at break compared to the neat matrix. This behavior was induced by the huge clay aggregates, which generate internal stress at the clay/matrix interface and thus enhanced the material embrittlement. For OMMT-OH1, higher tensile strength properties were obtained thanks to its higher dispersion state. The MMT-Na hybrids showed the highest tensile strength and strain at break, higher than the neat matrix ones (Table I.8). These results were partially contradicted by those of Lilichenko et al. (Lilichenko, N., 2008) and Mondragon et al. (Mondragon, M., 2008). These different authors have seen a decrease in the strain at break of starch/MMT-Na nano-biocomposites. These differences were not explained but could be linked to the differences in the starch botanical origin and/or to the plasticizer content. However, it seems that with well exfoliated nanofillers, it is possible to harden the plasticized starch materials without affecting their strain at break.

Table I.8. Tensile test results of potato starch/(O)MMT 5 wt% nano-biocomposites (Park, H.M., 2002).

Samples	Tensile strength (MPa)	Strain at break (%)
Plasticized starch	2.6	47.0
Plasticized starch/MMT-Na	3.3	57.2
Plasticized starch/OMMT-OH1	2.8	44.5
Plasticized starch/OMMT-Bz	2.1	34.9
Plasticized starch/OMMT-Alk2	2.5	38.0

Some authors studied in details the thermal stability of starch-based nano-biocomposites. Park et al. (Park, H.M., 2003) showed by TGA that the potato starch/MMT-Na and OMMT-OH1 hybrids had a higher degradation temperature in comparison to the neat matrix. This increase in the thermal stability was significant up to 5 wt% of clay for either MMT-Na or OMMT-OH1, while this increase was leveled off with further increases in clay content. Moreover, the potato starch/MMT-Na thermal stability was higher than the OMMT-OH1 nano-biocomposites one. Such results highlighted some relationships between the MMT dispersion and the thermal stability. The same tendency was observed with other studies based on various starches and nanofillers (Cyras, V.P., 2008a, Ma, X., 2007, Park, H.M., 2003). These results assessed for an enhancement of the material thermal stability induced by the MMT. This behavior is commonly observed in nanocomposite systems and is linked to the clay aspect ratio and dispersion state. The exfoliation of the MMT nano-platelets into the matrix increases the tortuosity of the combustion gas diffusion pathway and favors the formation of a char at the material surface (Alexandre, M., 2000).

The nanofiller is also known to greatly influence the water vapor permeability of the nano-biocomposite materials. Park et al. (Park, H.M., 2002) examined the potato starch nano-biocomposite water vapor permeabilities with different clays (Figure I.10). According to the presented results, all the hybrid films showed lower water vapor permeability compared to the pristine matrix. For instance, the MMT-Na hybrid water vapor permeability has been reduced by nearly a half compared to the pristine matrix with 5 wt% of clay loading. The same trends are observed into other plasticized starch nano-biocomposites (Huang, M., 2006b, Park, H.M., 2003). This behavior is induced by two distinct phenomena, namely (i) the dispersion of the silicate layers and (ii) the solubility of the penetrant gas into the nano-biocomposite films (Alexandre, M., 2000). Thus, for the micro-biocomposites based on OMMT-Bz, OMMT-Alk2 or OMMT-OH1 the barrier properties enhancements were linked to decreases in the water solubility due to the surfactant hydrophobic character. On the contrary, for MMT-

Na, the permeability decrease likely resulted from the higher nano-dispersion. Finally, Cyras et al. (Cyras, V.P., 2008a) and Mondragon et al. (Mondragon, M., 2008) have highlighted the clay influence on the water content, at equilibrium. According to these authors, the higher is the clay content, the lower the water content is. This behavior was likely induced by the nanofiller, which modified the water solubility thanks to its dispersion state.

To conclude, these different studies have clearly demonstrated the possibility to exfoliate MMT nanofillers into plasticized starch matrices with solvent and melt processes. The resulting properties (mechanical, barrier, thermal stability…) of the corresponding nano-biocomposites are largely enhanced and point out the great potential of these innovative materials. However, the negative impact of the starch plasticizers on the clay intercalation/exfoliation process has also been clearly highlighted. Thus, to fully describe and understand the starch nano-biocomposite materials, studies should be focused on the analyses of the clay/plasticizer/matrix interactions, species mobilities and local nanostructures with advances characterization techniques.
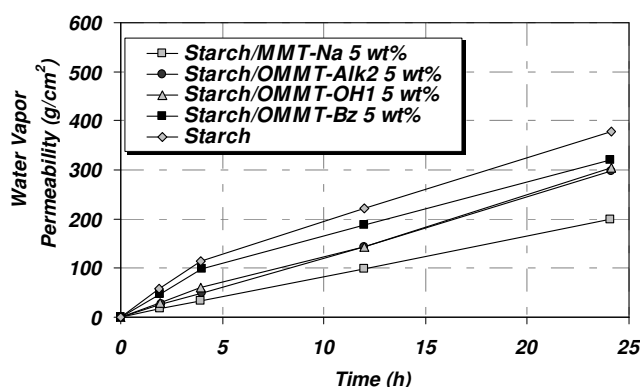
Figure I.10. Water vapor permeability vs. Time of potato starch/clay nano-biocomposites with different clays, at 25 °C (Park, H.M., 2002).

b. Starch Blends-Based Nano-Biocomposites

An usual answer to the water sensitivity and poor mechanical properties of the starch-based materials is the development of multiphase materials such as starch/polymer blends (Martin, O., 2001). Tapioca starch/PLA nano-biocomposites (90/10 wt%/wt%) have been elaborated by Lee et al. (Lee, S.Y., 2007, Lee, S.Y., 2008a, Lee, S.Y., 2008b, Lee, S.Y., 2008c) by melt process. The dispersion of hydrophobic nanofillers, namely, OMMT-Bz, OMMT-Alk1, OMMT-Alk3, OMMT-Alk4 and OMMT-Alk7 led to intercalated nano-biocomposites with $29 < d_{001} < 34$ Å. Intercalated morphologies have also been obtained with the more hydrophilic OMMT-OH1. These intercalated morphologies are related to the high

starch content of these blends, which is known to hinder the clay exfoliation process of the hydrophobic clays (Park, H.M., 2002, Park, H.M., 2003).

After MMT-Na incorporation, nano-biocomposites displayed an intercalated structure with d_{001} ~ 23 Å. Similar results were obtained with amylocorn starch/PVAL nano-biocomposites elaborated by melt process (Dean, K.M., 2008). High intensity and sharp diffraction peak (d_{001} ~ 18 Å) was obtained with the inclusion of PVAL leading to a highly ordered-intercalated and non exfoliated structure, as pointed out by TEM analyses (Figure I.11). Since Dean et al. (Dean, K., 2007, Dean, K.M., 2008) have reported the formation of well exfoliated structure for amylocorn starch/MMT-Na nano-biocomposites elaborated without non-volatile plasticizer, these results may indicate a restriction of the MMT-Na intercalation/exfoliation process induced by PLA and PVAL. For PLA, the lack of compatibility with MMT-Na explains this trend (Maiti, P., 2002). For PVAL, infrared spectroscopy analyses have shown hydrogen bonds between MMT-Na and PVAL chains, which likely maintain the tactoïds organization (Dean, K.M., 2008).
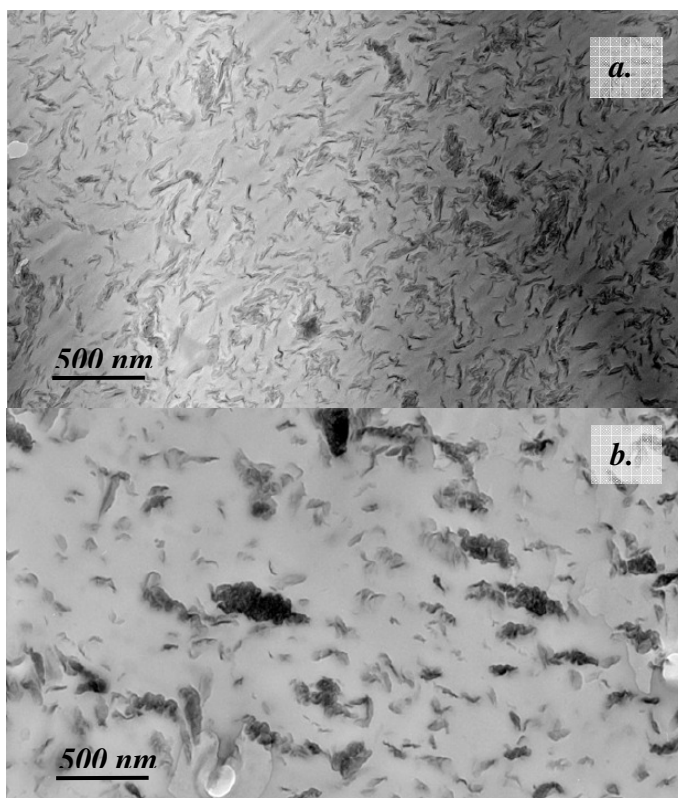
Figure I.11. TEM micrographs of (a.) amylocorn starch nanocomposite with 2.5 wt% of MMT-Na content and (b.) amylocorn starch/PVAL nanocomposite with 5 wt% of PVAL and 2.5 wt% of MMT-Na content (Dean, K.M., 2008).

Starch/PCL nano-biocomposites have also been elaborated by melt blending process. McGlashan et al. (McGlashan, S.A., 2003) demonstrated that depending on the PCL/starch ratio, the OMMT-OH1 incorporation led to intercalated or exfoliated nano-biocomposites (McGlashan, S.A., 2003). For PCL content higher than 70 wt%, a clay exfoliated state was obtained. Then, with a starch content increase, a diffraction peak corresponding to an intercalated structure appeared with a d_{001} ~ 40 Å and with an intensity correlated to the starch content. Since OMMT-OH1 is easily exfoliated into PCL and mainly intercalated into plasticized starch, one may suppose that these nanofillers were mainly dispersed into the PCL domains. These results have been confirmed by Perez et al. (Perez, C.J., 2007b, Perez, C.J., 2008a, Perez, C.J., 2008c), who reached exfoliation for high PCL content with OMMT-OH1. The same dispersion state has been achieved with OMMT-Bz has the nanofiller for high PCL content. According to Perez et al. (Perez, C.J., 2007b, Perez, C.J., 2008a, Perez, C.J., 2008b, Perez, C.J., 2008c), such morphology is favored by the good nanofiller/PCL affinity, which promote the clay exfoliation. Besides, Kalambur et al. (Kalambur, S., 2005, Kalambur, S.B., 2004) obtained microcomposites with the dispersion of OMMT-Alk5 into starch/PCL blends plasticized with glycerol. This morphology was related to the low matrix/nanofiller affinity and to the glycerol which is known to restrict the clay platelets delamination (Tang, X., 2008b).

Finally, the MMT-Na dispersion led to an intercalated structure with a $d_{001} = 18$ Å. According to Perez et al. (Perez, C.J., 2007a, Perez, C.J., 2007b, Perez, C.J., 2008a, Perez, C.J., 2008c), since the diffraction peak intensity was low, the existence of intercalated/exfoliated structure is possible but not fully proved. The different clay morphologies obtained with these blends are summarized in Table I.9.

Table I.9. Morphology of the starch-blends nano-biocomposites elaborated by melt process.

Polymer into the starch blend	Nanofillers	Morphology	References
PLA content = 10 wt%	MMT-Na	Intercalated - $d_{001} \sim 23$ Å	(Lee, S.Y., 2007, Lee, S.Y., 2008b)
	OMMT-OH1	Intercalated	(Lee, S.Y., 2007, Lee, S.Y., 2008c)
	OMMT-Bz	Intercalated - $d_{001} \sim 34$ Å	(Lee, S.Y., 2008a)
	OMMT-Alk1	Intercalated - $d_{001} \sim 32$ Å	(Lee, S.Y., 2008a)
	OMMT-Alk3	Intercalated	(Lee, S.Y., 2007)
	OMMT-Alk4	Intercalated - $d_{001} \sim 29$ Å	(Lee, S.Y., 2008a)
	OMMT-Alk7	Intercalated - $d_{001} \sim 32$ Å	(Lee, S.Y., 2008a)
PVAL content < 7 wt%	MMT-Na	Intercalated - $d_{001} \sim 18$ Å	(Dean, K.M., 2008)
PCL content > 70 wt%	MMT-Na	Intercalated - $d_{001} \sim 18$ Å	(Perez, C.J., 2007a, Perez, C.J., 2007b, Perez, C.J., 2008a, Perez, C.J., 2008c)
	OMMT-Bz	Exfoliated	(Perez, C.J., 2007b, Perez, C.J., 2008a, Perez, C.J., 2008b, Perez, C.J., 2008c)
	OMMT-OH1	Exfoliated	(McGlashan, S.A., 2003, Perez, C.J., 2007b, Perez, C.J., 2008a, Perez, C.J., 2008c)
PCL content < 70 wt%	OMMT-OH1	Intercalated - $d_{001} \sim 40$ Å	(McGlashan, S.A., 2003)
PCL & Glycerol	OMMT-Alk5	Microcomposite	(Kalambur, S., 2005, Kalambur, S.B., 2004)

The uniaxial tensile properties of starch/PCL nano-biocomposites have been characterized and have shown that, whatever the clay type, the incorporation of the nanoclays led to an increase in the material rigidity, related to the clay modulus and clay/matrix interactions (McGlashan, S.A., 2003, Perez, C.J., 2007b). Perez et al. (Perez, C.J., 2007b, Perez, C.J., 2008a) have demonstrated that the most significant stiffness enhancements were obtained with OMMT-Bz. This result was attributed to the high compatibility OMMT-Bz/PCL, which led to an exfoliated morphology. In the same way, McGlashan et al. (McGlashan, S.A., 2003) reported significant stiffness improvement with OMMT-OH1 correlated to the clay dispersion state. The highest mechanical reinforcing efficiencies were obtained with the exfoliated blends obtained with high PCL content. Then, starch content increase led to a lower stiffness increase. Starch blends elaborated with PLA (Lee, S.Y.,

2008a, Lee, S.Y., 2008b) or PVAL (Dean, K.M., 2008) also shown an increase in the Young's modulus related to the clay content. As usual, these increases are linked to the clay stiffness and dispersion state (Table I.10).

The nanoclay effect on the strain at break properties was very significant. For PCL (McGlashan, S.A., 2003, Perez, C.J., 2008a) or PVAL (Dean, K.M., 2008) blends, a huge increase correlated to the clay introduction into the matrix was reported. Dean et al. showed that, the strains at break of starch nano-biocomposites filled with 2 wt% of PVAL were generally lower than those without. However, with 5 wt% of PVAL, the strain at break increased (Table I.10). These trends were linked to the clay/PVAL interactions. At 2 wt%, the PVAL chains were tightly bound to the MMT-Na generating aggregations. At higher PVAL content, 'free' PVAL chains results in material plasticization.

The effects of these nanofillers on the thermal properties were studied by DSC. Perez et al. (Perez, C.J., 2007a, Perez, C.J., 2008c) have shown a significant effect of MMT-Na, OMMT-OH1 and OMMT-Bz on the PCL crystallization process, these nanofillers acting like nucleating agents. As the blend was cooled from the molten state, the platelets have generated nucleation sites leading to a crystallization temperature increase. However, restrictions in chain mobility with the association of exfoliated platelets have reduced the degree of crystallinity and have altered the crystallization mechanism. The same trends were also reported by McGlashan et al. (McGlashan, S.A., 2003) and Kalambur et al. (Kalambur, S., 2005) with, respectively, OMMT-OH1 and OMMT-Alk5. Finally, for Starch/PCL blends, Perez et al. (Perez, C.J., 2008a) have clearly highlighted a decrease in the water uptake and water diffusion coefficient linked to the clay content and dispersion state.

To conclude, well exfoliated starch/PCL nano-biocomposites displaying enhanced properties have been elaborated with high PCL content. However, with the increase in the starch content, the nano-hybrid materials become more and more intercalated. This trend is likely related to the nanofiller polarity, which led to a poor starch/MMT affinity. The dispersion of a mix of hydrophilic and hydrophobic nanofillers, which can respectively be exfoliated both into the carbohydrate phase and into a more hydrophobic biopolymer matrix, could be a powerful answer to obtain a more homogeneous MMT nano-dispersion even at high starch content.

Table I.10. Uniaxial Tensile parameters of starch blends (Dean, K.M., 2008, McGlashan, S.A., 2003).

Biopolymers	Nanofillers	Samples composition per weight (starch/biopolymer/MMT)	Young's Modulus (MPa)	Strain at break (%)*
PCL	OMMT-OH1	30/70/0	17	1086
		30/70/1.5	58	1500+
		30/70/5	64	1500+
		50/50/0	22	184
		50/50/1.5	52	615
		50/50/5	38	1500+
		70/30/0	15	260
		70/30/1.5	14	310
		70/30/5	24	860
PVAL	MMT-Na	100/0/0	3085	8.7
		100/0/2.5	4212	6.0
		100/0/5	4612	4.2
		100/2/0	2808	8.3
		100/2/2.5	4947	5.8
		100/2/5	5429	4.2
		100/5/0	2955	10.0
		100/5/2.5	5429	9.4
		100/5/5	5250	8.6
		100/7/0	3176	10.3
		100/7/2.5	4008	9.2
		100/7/5	4677	8.7

* 1500+ = tensile bar not broken

c. Modified Starch-Based Nano-Biocomposites

To decrease the starch-based material water sensitivity, another approach consists in the chemical modification of the starch chains. The objective of this chemical modification is the substitution of hydroxyl groups by less hydrophilic functions, such as acetate groups (Fringant, C., 1996). Qiao et al. (Qiao, X., 2005) have developed acetylated starch nano-biocomposites with glycerol as plasticizer and with 5 wt% of MMT-Na and OMMT-Alk6 into an internal batch mixer. Besides, Xu et al. (Xu, Y., 2005) have elaborated acetylated starch nano-biocomposite foams by melt extrusion techniques with 5 wt% of OMMT-OH1, OMMT-Bz, OMMT-Alk3 or OMMT-Alk4.

The morphological analyses carried out on these nano-biocomposites have demonstrated that the MMT-Na incorporation into this more hydrophobic matrix (compared to unmodified starch) led to an intercalated structure displaying an intense and sharp diffraction peak. This peak, corresponding to a d_{001} of 18 Å, was assigned to glycerol

intercalation (Chiou, B.-S., 2006, Wilhelm, H.-M., 2003b). The morphological analyses carried out on samples prepared with the rather hydrophobic nanofillers have highlighted that the intercalation extent follows the sequence, OMMT-OH1 > OMMT-Bz ~ OMMT-Alk3 > OMMT-Alk4 > OMMT-Alk6 (Table I.11) (Qiao, X., 2005, Xu, Y., 2005).

Table I.11. Morphology of the acetylated starch nano-biocomposites elaborated by melt process (Qiao, X., 2005, Xu, Y., 2005).

Nanofiller	Morphology	References
MMT-Na	Intercalated - d_{001} ~ 18 Å	(Qiao, X., 2005)
OMMT-Alk6	Intercalated - d_{001} ~ 31 Å	(Qiao, X., 2005)
OMMT-Alk4	Intercalated - d_{001} ~ 35 Å	(Xu, Y., 2005)
OMMT-Alk3	Intercalated - d_{001} ~ 38 Å	(Xu, Y., 2005)
OMMT-Bz	Intercalated - d_{001} ~ 38 Å	(Xu, Y., 2005)
OMMT-OH1	Intercalated - d_{001} ~ 40 Å	(Xu, Y., 2005)

The effect of MMT on uniaxial tensile properties of acetylated starch nano-biocomposites was investigated by Qiao et al. (Qiao, X., 2005) They reported an increase in the tensile strength after the addition of 5 wt% of MMT-Na or OMMT-Alk6. On the contrary, the strain at break properties of these nano-biocomposites were depressed, the lower strain at break values being obtained with OMMT-Alk6 (Table I.12). This trend was linked to the corresponding highly intercalated structure.

Table I.12. Tensile properties of acetylated starch nano-biocomposites (Qiao, X., 2005).

Samples	Tensile strength (MPa)	Strain at break (%)
Acetylated starch	5.5	49.6
Acetylated starch/MMT-Na 5 wt%	8.8	38.4
Acetylated starch/OMMT-Alk6 5 wt%	10.4	28.0

The nanofiller effect on the thermal behavior was analyzed by Qiao et al. (Qiao, X., 2005) by DMTA. The different samples exhibited a relaxation transition at 50 °C, corresponding to the glassy state transition of the starch-rich phase (Figure I.12). The relaxation of acetylated starch/clay nano-biocomposites shifted towards higher temperature, compared to the neat matrix. Thus, it has been concluded that the presence of clay reduced the chain mobility and increased the T_g of the starch-rich phase. Moreover, these authors assume that the shift temperature of the acetylated starch/OMMT-Alk6 samples was still higher than with MMT-Na because of the easier intercalation into OMMT-Alk6 layers.
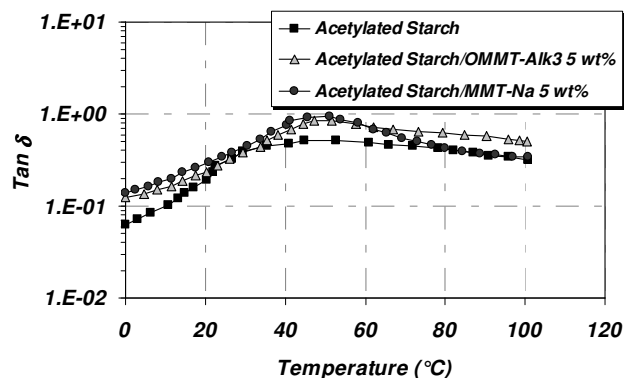
Figure I.12. Tan δ vs. temperature for acetylated starch and acetylated starch nano-biocomposites, at 1 Hz (Qiao, X., 2005).

Such behavior was confirmed by Xu et al. (Xu, Y., 2005) who analyzed the T_g of the acetylated nano-biocomposites by DSC. According to these authors, the T_g of starch acetate was increased by the addition of organo-clay. The greatest increase was shown with the incorporation of OMMT-OH1, whereas the smallest increase was observed for OMMT-Alk4. The authors attributed this T_g increase to the formation of an intercalated structure, which restricted the movement of starch acetate chains. Moreover, the different increases in T_g observed with the addition of various organo-clays were due to the level of compatibility between starch acetate and organo-clays.

The study of the nanofiller influence on the starch acetate nano-biocomposites thermal stability has shown an enhancement of this property linked to the increase in the tortuosity of the combustion gas diffusion pathway (Xu, Y., 2005). However, the best thermal stability was not achieved with the most homogeneously nano-dispersed nanofiller, namely OMMT-OH1, but with OMMT-Alk4. According to the authors, a possible reason for this difference was the higher thermal stability of the organic modifiers in OMMT-Alk4 compared to OMMT-OH1.

To conclude, these studies have highlighted that the higher nano-dispersion are achieved with OMMT-OH1. These results are linked to the rather hydrophobic behavior of this matrix in comparison to unmodified starch, which leads to a lack of compatibility with more hydrophilic nanofillers, such as MMT-Na. Nevertheless, even if a good nano-dispersion is obtained with OMMT-OH1, the corresponding nano-biocomposites only displayed an intercalated structure. Consequently, to obtain an exfoliated state, new organo-modified nanofillers have to be prepared. In addition, until now, studies have only been focused on the use of acetylated matrices. Other modified starch matrices could also be used, such as methylated or carboxymethyled starch.

2. Cellulose

Cellulose is the most abundant biopolymer in the biosphere. Often associated with lignins (ligno-cellulose products), this carbohydrate polymer is the main constituent of wood, flax, ramie, hemp or cotton (Table I.13).

2.1 Cellulose Structure

This biopolymer is a linear macromolecule constituted of D-glucose units (cellobiose) linked by β(1→4) linkages and show a semi-crystalline structure. The glucose monomers units in cellulose form both intra- and inter-molecular hydrogen bonds generating cellulose microfibrils. These hydrogen bonds lead to formation of a linear crystalline structure with a high theoretical tensile strength (Lilholt, H., 2000). Four principal allomorph structures have been identified for cellulose (Atalla, R.H., 1984, Heiner, A.P., 1997, Nishiyama, Y., 2002, Van der Hart, D.L., 1984):

(i)   Cellulose *I* crystal structure, which is the natural form of the cellulose, is the result of the co-existence of two distinct crystalline forms named cellulose I_α and I_β, which have respectively a triclinic and a monoclinic unit cell.

(ii)   Cellulose *II* is generally obtained by regeneration of cellulose *I* from solution. This allomorph is known by the term "regenerated" cellulose. The transition from cellulose *I* to *II* is not reversible.

(iii)   Cellulose *III* is prepared from celluloses *I* and *II* with liquid ammonia or ethylene diamine treatment. These two celluloses are named cellulose III_I and III_{II}, respectively.

(iv)   Cellulose *IV* is prepared with glycerol at high temperature from Cellulose *III*. Here again two types exist: cellulose IV_I and IV_{II} obtained from cellulose III_I and III_{II}, respectively.

Table I.13. Composition of ligno-cellulosic fibers, from various botanical sources (Bledzki, A.K., 1999).

Fibers	Cellulose content (%)	Lignin content (%)	Hemicellulose content (%)	Ash (silica, ...) (%)
Straw fibers:				
Wheat	29–35	16-21	27	5-9
Rice	28-36	12-16	23-28	15-20
Rye	33-35	16-19	27-30	2-5
Wood fibers:				
Conifers	40-45	36-34	7-14	< 1
Leafwood	38-49	23-30	19-26	< 1
Others:				
Flax	43-47	21-23	16	5
Jute	45-53	21-26	15	0.5-2
Cotton linters	90-85	/	1-3	0.8-2

Depending on their origin, cellulose microfibrils have diameters from 20-200 Å while their length can achieve several tens of microns (Chanzy, H., 1990). The microfibrils cellulose chains are aligned in parallel in an almost perfect crystalline array. Some imperfections arose from dislocations at the interface of microcrystalline domains along the microfibril length (Revol, J.F., 1985). These imperfections were used to advantage by treatment with acid to produce rod-like mono-crystals called whiskers having the same diameter as the starting microfibrils but shorter length. These cellulose whiskers possessed a mechanical modulus of about 130 GPa (Sakurada, L., 1962). Thanks to these characteristics (microscopic dimensions, form and exceptional mechanical properties), these fillers whiskers are incorporated as a reinforcing component into polymer matrices to produce nanocomposite materials with enhances properties for a wide range of applications (Dufresne, A., 1998).

To produce plastic materials from cellulose, a chemical modification has to be performed. This modification often consists in the replacement of the cellulose hydroxyl functions, which create a physical network, by acetate or methyl functions. The objective of this modification is the decrease in the hydrogen bonds intensity, which makes the material non fusible (Gomes, M.E., 2001).

2.2 Modified Cellulose-Based Nano-Biocomposites

Only few cellulose acetate (CA) nano-biocomposites have been elaborated, studied and reported in the litterature (Park, H.M., 2004a, Park, H.M., 2004b, Park, H.M., 2006, Wibowo, A.C., 2006, Yoshioka, M., 2006). Park et al. (Park, H.M., 2004a) and Wibowo et

al. (Wibowo, A.C., 2006) have elaborated CA/OMMT-OH1 nano-biocomposites with various triethyl citrate (TEC) plasticizer content by melt blending process. Different morphological analyses, such as XRD experiments, have been performed. According to the results, nano-biocomposites with 20 wt% of TEC plasticizer and 5 wt% of OMMT-OH1 displayed an exfoliated structure. In comparison, nano-biocomposites having 30-40 wt% of plasticizers displayed an intercalated structure with a $d_{001} = 40$ Å. Moreover, the higher the TEC content, the higher the diffraction peak intensity. This tendency is related to the hydrogen bonds established between the -OH groups of the TEC plasticizer and those of the organo-modifier in OMMT-OH1, which disturb the intercalation/exfoliation process. Thus, OMMT-OH1 seems suitable to achieve exfoliation in CA nano-biocomposites but only at low TEC content.

To enhance the clay exfoliation process, even for high plasticizer content, Park et al. (Park, H.M., 2004b, Park, H.M., 2006) have elaborated CA-based nano-biocomposites with a carbohydrate compatibilizer, cellulose acetate butyrate grafted maleic anhydride (CAB-*g*-MA). This compatibilizer was synthesized by radical graft polymerization of maleic anhydride (MA) monomers onto cellulose acetate butyrate (CAB). This grafting was conducted by melt process compounder with (2,5-dimethyl-2,5-di(tert-butylperoxy)hexane). The same blends as those previously presented (Park, H.M., 2004a, Wibowo, A.C., 2006) were elaborated with a CA/TEC ratio of 75/25 wt%/wt%. The mixtures were mixed with 5 wt% of OMMT-OH1 and between 0 to 7.5 wt% of CAB-*g*-MA and melt compounded. Without CAB-*g*-MA, the nano-biocomposites displayed an intercalated structure with a $d_{001} = 40$ Å. On the contrary, an exfoliated state was achieved with this compatibilizer, the best exfoliated state being obtained with 5 wt% of CAB-*g*-MA.

To achieve exfoliation into CA-based nano-biocomposites, Yoshioka et al. (Yoshioka, M., 2006) developed a different approach. These authors used a hybrid elaboration protocol between the in-situ polymerization and the solvent intercalation process. Their objective was the use of poly(ε-caprolactone) (PCL) to facilitate the clay delamination process. According to the presented results, a well exfoliated nano-biocomposite is obtained. Nevertheless, these materials were composed of 80 wt% of PCL and then, the CA content is rather low. The different morphologies obtained with these nano-hybrid materials are summarized in Table I.14.

Table I.14. Morphology of the CA/OMMT-OH1 nano-biocomposites.

CA nano-biocomposites with:	Elaboration process	Morphology	References
TEC content < 20 wt%	Melt Process	Exfoliated	(Park, H.M., 2004a, Wibowo, A.C., 2006)
TEC content > 20 wt%	Melt Process	Intercalated - d_{001} ~ 40 Å	(Park, H.M., 2004a, Wibowo, A.C., 2006)
TEC Plasticized = 25 wt% & CAB-*g*-MA 5 wt%	Melt Process	Exfoliated	(Park, H.M., 2004b, Park, H.M., 2006)
PCL content = 80 wt%	In-situ & Solvent Process	Exfoliated	(Yoshioka, M., 2006)

The effect of the clay dispersion state on the main nano-biocomposites properties has been studied with various techniques. Park et al. (Park, H.M., 2004a) observed a sharp increase in the notched izod impact strength and the tensile strain at break of the CA/OMMT-OH1 hybrid materials correlated to the increase in plasticizer content. As expected, the clay nanoplatelets incorporation increased the tensile modulus of the CA hybrids (compared to pristine matrix - Figure I.13). Park et al. also studied the tensile and flexural properties of the plasticized CA/OMMT-OH1 hybrids with various MA-g-CAB contents (Park, H.M., 2004b, Park, H.M., 2006). According to the presented results, the best mechanical properties enhancements are obtained with the exfoliated morphology, with 5 wt% of MA-*g*-CAB. At higher compatibilizer content, the mechanical properties decreased. Since, it has been clearly demonstrated in different nanocomposite systems, that the better the dispersion, the better the resulting mechanical properties improvement (Alexandre, M., 2000, Sinha Ray, S., 2003, Vaia, R.A., 1997), these mechanical properties variations are linked to the MMT dispersion state.
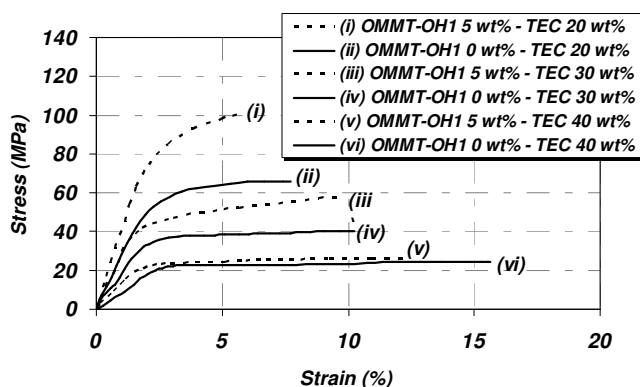
Figure I.13. Cellulose acetate nano-biocomposite tensile curves with increasing TEC plasticizer, with different clay contents (Park, H.M., 2004a).

The nanofiller dispersion effect on T_g has also been studied by DMTA. Park et al. (Park, H.M., 2004a) have shown that the higher the plasticizer content, the lower the T_g (130 and 86 °C for CA/TEC ratio of 80/20 and 60/40 wt%/wt%, respectively). An increase in the nano-biocomposite T_g was observed after incorporation of the nanoplatelets (Park, H.M., 2004a, Park, H.M., 2004b). This trend is likely related to the clay dispersion state, which can hinder the material chain mobility. Another possible explanation is linked to the hydrogen bonds, which could be established between the –OH groups of the organo-modifier and those of the carbohydrate chains and which could reduce the CA mobility.

Besides, water vapor permeabilities were examined in a controlled temperature and relative humidity chamber (Park, H.M., 2004a). A strong decrease in permeability, reaching 2-fold at the highest organo-clay content, was observed. This decrease was due to the well-ordered and dispersed silicate layers having a large aspect ratio, which leads to a more tortuous path for the diffusion of gas molecules through the film (Gorrasi, G., 2003).

To conclude, these studies have shown that exfoliation can be reached in CA nano-biocomposite materials. Nevertheless, a negative effect of the CA plasticizer on the MMT exfoliation process has been highlighted. This limitation has been overcame thanks to the use of a carbohydrate compatibilizer, which modifies the clay/matrix interface. However only OMMT-OH1 has been tested into CA matrices. To reach a full exfoliation, new OMMTs prepared with carbohydrate surfactants should also be tested Exfoliation has been achieved with CA/PCL blends. However, the morphology is mainly achieved thanks to the high PCL content.

3. Chitin and Chitosan

Chitin is the second agro-polymer produced in the nature after cellulose. It appears in nature as ordered crystalline microfibrils forming structural components in the exoskeleton of arthropods or in the cell walls of fungi and yeast (Campbell, N.A., 1999, Rinaudo, M., 2006). It is an acetylated polysugar composed of N-acetyl-D-glucosamine groups linked by β(1→4) linkages (Figure I.14). From chitin, chitosan is obtained by deatecylation.
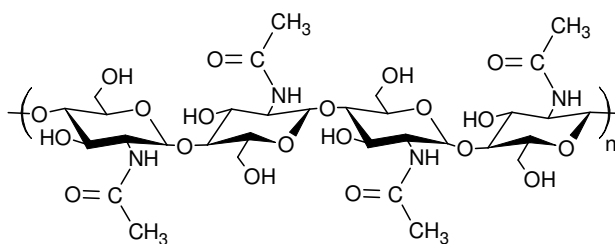
Figure I.14. Chitin chemical structure.

3.1 Chitin and Chitosan Structures

Depending on the source, chitin occurs as two allomorphs forms named α et β (Rudall, K.M., 1973). A third allomorph structure chitin γ has also been reported, but is seems that it is a variant of the α form (Atkins, E.D.T., 1985). These two structures are organized in crystalline sheets where numbers of intra-sheet hydrogen bonds tightly holds them. The α form presents some inter-sheets hydrogen bonds. Such a feature is not found for the β form, which is consequently more prone than the α form to water swelling (Gardner, K.H., 1975, Minke, R., 1978). Like cellulose, the semi-crystalline structure of chitin microfibrils can be treated with acid to produce whisker-shaped nanofillers that can be incorporated into polymer as a nanofiller to elaborate nano-hybrid mlaterials (Lu, Y., 2004, Paillet, M., 2001).

Contrary to chitin, chitosan is not widespread in the nature. It is found in some mushrooms (zygote fungi) and into the termite queen's abdominal wall. It is industrially obtained by partial chitin deacetylation (Peter, M.G.P.I., 2002). Its chemical structure, represented in Figure I.15, is a random linear chaining of N-acetyl-D-glucosamine units (acetylated unit) and D-glucosamine (deacetylated unit) linked by β(1→4) linkages.
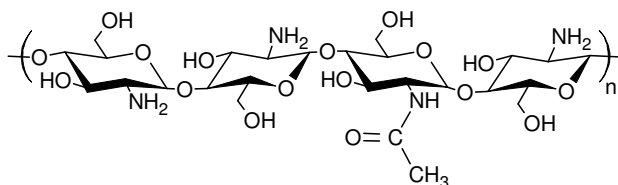
Figure I.15. Chitosan chemical structure.

Thanks to its amino group and compared to chitin, chitosan shows some particular properties. In acid conditions, when the amino groups are protonated, it becomes a water soluble polycation. Some polysaccharides can have a polyelectrolyte behavior, like carrageenan, but these agro-polymers are mainly polyanions (Shahidi, F., 1999). The chitosan is characterized by its acetylation degree and by its molecular weight. These last parameters influence its viscosity and solubility. According to the bioresource, industrial chitosans have molecular weights varying from 5,000 to 1,000,000 g.mol^{-1} and acetylation degrees from 2 to 60 %.

In solid state, chitosan is a semi-crystalline polymer. Its morphology has been investigated and many allomorphs have been described, depending on its acetylation degree, on the distribution of the acetyl groups along the carbohydrate chain, on the chitosan preparation procedure (Ogawa, K., 1991, Ogawa, K., 1992)…

3.2 Chitosan-Based Nano-Biocomposites

Compared to the cellulose based-nano-biocomposites, a great number of chitosan-based nano-hybrids have been elaborated, studied and reported in the literature (Darder, M., 2003, Darder, M., 2005, Günister, E., 2007, Kampeerapappun, P., 2007, Lin, K.-F., 2005, Wang, S., 2006, Wang, S.F., 2005, Wang, X., 2006, Xu, Y., 2006). Chitosan/OMMT-OH1 nano-hybrid materials have been prepared into water by solvent process but led to the formation of highly flocculated systems. This morphology is obtained because OMMT-OH1 can not be dispersed into water (Xu, Y., 2006). Besides, since chitosan is a polycation in acid conditions, it can be easily adsorbed on the MMT-Na surface. This property has been extensively used to elaborate chitosan/MMT-Na hybrid materials by solvent route. Solutions were prepared by chitosan addition into 1 or 2 % v/v of acetic acid solution. MMT-Na was dispersed into water to obtain a 2 wt% clay suspension. To avoid any structural alteration of the phyllosilicate structure, the polysaccharide solution was adjusted with NaOH to pH=4.9 and then was slowly added to the clay suspension at ambient temperature. This mixture was stirred and finally washed with purified water to remove acetate and then casted (Darder, M., 2003, Darder, M., 2005, Günister, E., 2007, Wang, S.F., 2005, Xu, Y., 2006). According to recent XRD experiments performed by Kampeerapappun et al. (Kampeerapappun, P., 2007), it has been shown that chitosan did not diffuse into the clay inter-layers spacing. However, these results were contradicted by those of Darder et al. (Darder, M., 2003), which concluded to chitosan intercalation thanks to a shift of the MMT-Na diffraction peak to lower angles. Moreover, a broadening and intensity decrease in the diffraction peak was observed, indicating a disordered intercalated/exfoliated structure (Darder, M., 2005, Wang, S.F., 2005). Günister et al. (Günister, E., 2007) have studied the interactions between MMT-Na and chitosan by zeta potential measurements and have shown a chitosan ionic adsorption on the clay surface and an effective intercalation.

This inter-layer chitosan structure was studied by infrared spectroscopy (Darder, M., 2003, Darder, M., 2005), evidencing the adsorption of two chitosan layers on the clay surface and even inside the inter-layer spacing (Figure I.16). The first chitosan layer was mainly adsorbed thanks to electrostatic interactions between the chitosan -NH$_3^+$ groups and the MMT negative charges. The second layer adsorption was promoted by hydrogen bonds established between the chitosan amino and -OH groups and the clay substrate. At low MMT content, several authors have even shown the formation of an exfoliated nanostructure (Lin, K.-F.,

2005, Wang, S.F., 2005, Wang, X., 2006, Xu, Y., 2006). At higher MMT content, more than 5 wt%, the formation of intercalated/flocculated structure was observed (Wang, S.F., 2005).
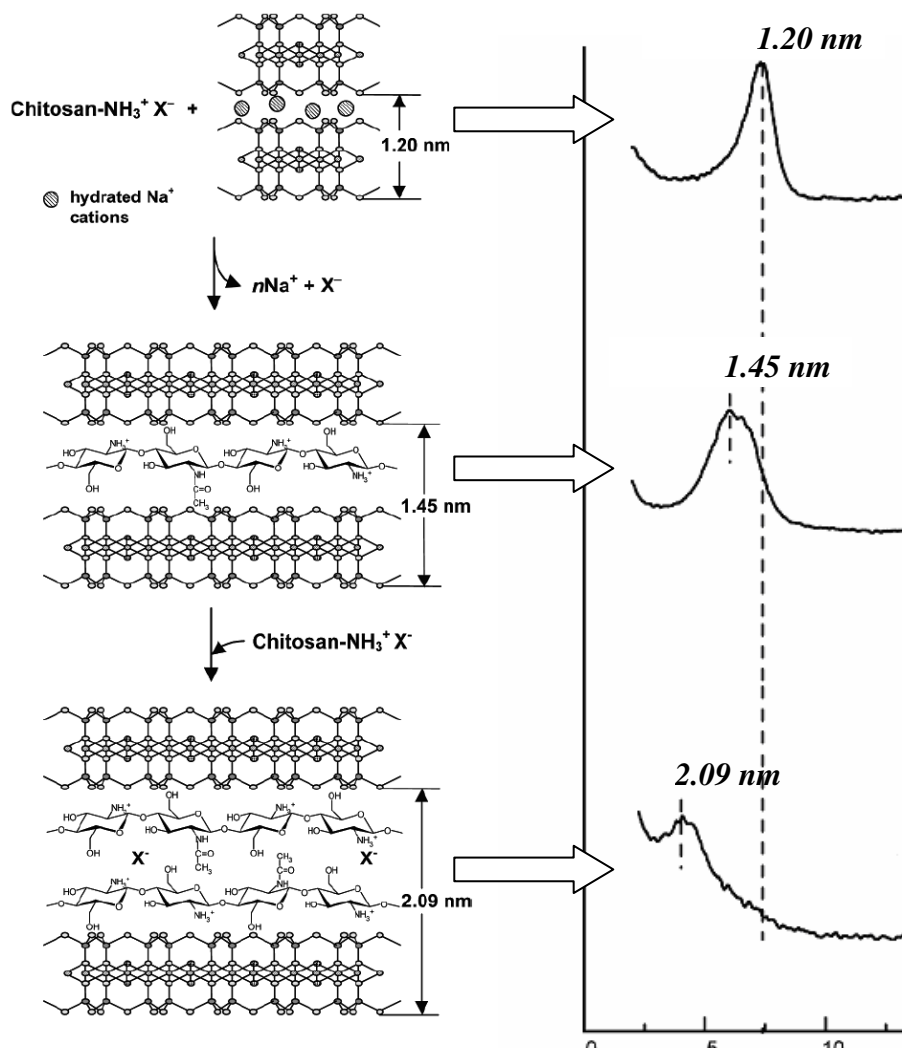
Figure I.16. Intercalation of the chitosan layers into clay inter-layer spacing and the corresponding XRD patterns for MMT-Na (a.) and chitosan nano-biocomposites prepared from chitosan/clay ratios of 0.5/1 (b.) and 10/1 (c.) (Darder, M., 2003).

Recently, Wang et al. (Wang, S., 2006) have introduced carboxymethyl groups into chitosan to enhance the hydrogen-bonding reaction between the matrix and -OH group located at the edges of MMT-Na. The corresponding nano-biocomposites were elaborated with a conventional solvent elaboration process, the MMT-Na being exfoliated into a large excess of water and then mixed with a solution of carboxymethylated chitosan. Nevertheless, this strategy has led to the formation of highly flocculated systems. According to the authors, this flocculated structure has been favored by the hydroxylated edge-edge interaction of the silicate layers. The different morphologies obtained in these systems are summarized in the Table I.15.

Table I.15. Morphology of the Chitosan nano-biocomposites elaborated by solvent process.

Matrices	Nanofillers	Morphology	References
Chitosan	OMMT-OH1	Microcomposite	(Xu, Y., 2006)
	MMT-Na	Intercalated *14* Å $< d_{001} <$ 21 Å	(Darder, M., 2003, Darder, M., 2005, Günister, E., 2007, Wang, S., 2006, Wang, S.F., 2005, Xu, Y., 2006)
		Exfoliated	(Lin, K.-F., 2005, Wang, S.F., 2005, Wang, X., 2006, Xu, Y., 2006)
Carboxymethyl Chitosan	MMT-Na	Microcomposite	(Wang, S., 2006)

The thermal transitions of these nano-biocomposites were investigated and related to the material dispersion state. Günister et al. (Günister, E., 2007) have measured the effect of the nanofiller addition on the T_g (by DSC) and observed an increase directly linked to the ionic interactions established between the chitosan and nanofiller, which reduced the chains mobility.

As usual, increases in the tensile strength correlated to a small decrease in the strain at break were observed in the different chitosan nano-biocomposite (Xu, Y., 2006). These raises were induced by the nanofillers/chitosan interactions, which enhance the stress transfer at the interface. The strain at break decrease was related to the morphology of the chitosan/MMT hybrid materials, which displayed in the best case an intercalated/exfoliated structure. Such a stiffness increase is already well reported into the literature and is correlated to the clay rigidity and dispersion state (Luo, J.J., 2003).

In addition, in vitro antimicrobial tests showed that chitosan/layered silicate nanocomposites had higher antimicrobial activity than pure chitosan. Thus, Wang et al. (Wang, X., 2006) and Lin et al. (Lin, K.-F., 2005) concluded that these materials could be an interesting solution to develop new materials for biomedical applications as surgery.

To conclude, exfoliated chitosan nano-biocomposites displaying extended properties have been elaborated with MMT-Na. However, such nano-hybrids have only been prepared by solvent process. The elaboration of chitosan/polyester blends could be an interesting option to produce melt processable chitosan nano-biocomposites. Besides, to better understand the chitosan intercalation process, nano-biocomposites should be prepared with various chitosans

having different molecular weight, acetylation degree and distribution of the acetyl groups along the carbohydrate chain.

4. Pectin

Pectin is a linear macromolecule constituted of α(1→4) linkages D-galacturonic acid (Figure I.17). This monomer unit could be partially replaced by α(1→2)-linked L-rhamnose leading to a new structure named rhamnogalacturonan I. A third pectin structural type is rhamnogalacturonan II, which is a less frequent, complex and highly branched polysaccharide (Thakur, B.R., 1997).

4.1 Pectin Structure

In nature, around 80 % of the galacturonic acid carboxyl groups are esterified with methanol. This proportion depends on the extraction conditions. Since, the ratio of esterified/non-esterified galacturonic acid determines the behavior of pectin in food applications, pectins are classified as high- or low-ester pectins (May, C.D., 1990). The non-esterified galacturonic acid units can be either free acid or salts, with sodium, potassium or calcium as the counter ion. The partially esterified pectin salts are named pectinates. If the degree of esterification is below 5 %, the salts are called pectates.
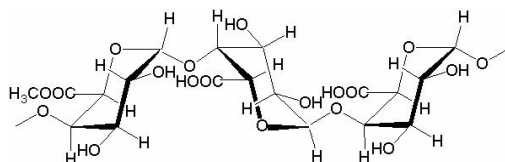
Figure I.17. Pectin chemical structure.

4.2 Pectin-Based Nano-Biocomposites

Only few systems based on pectin nano-biocomposites have been elaborated, studied and reported in the literature with MMT-Na or OMMT-OH2 (Mangiacapra, P., 2006). The elaboration protocol was a two steps procedure, ball milling followed by classical solvent elaboration process. First, the MMT and the pectin powders were mixed in the proper weight ratio in a stainless steel vial filled with tungsten carbide balls. The energy supplied during each impact of these tungsten carbide balls was used to decrease the polymer particles and the clay agglomerates size and to enhance the clay dispersion into the polymeric powder (Magini, M., 1998). This pectin/clay powder was milled. Then, sample films were prepared by dissolving milled pectin/clay in distilled water. The solutions were stirred and casted.

With OMMT-OH2, the results pointed out the major effect of the residence milling time on the resulting clay dispersion, a complete destructuration of the clay lamellar morphology being observed for high residence time. In similar condition, exfoliation state was also obtained with MMT-Na. The different dispersion states reached in these systems are summarized in the Table I.16.

Table I.16. Morphology of pectin nano-biocomposites.

Elaboration Technique	Nanofillers	Morphology	References
Ball Milling & Solvent Process	MMT-Na	Exfoliated	(Mangiacapra, P., 2006)
	OMMT-OH2	Exfoliated	(Mangiacapra, P., 2006)

Contrary to pectin/OMMT-Na systems, tensile tests did not display a stiffness increase for pectin/OMMT-OH2 samples. According to Mangiacapra et al. (Mangiacapra, P., 2006), this behavior could be due to the higher affinity of the pectin with the MMT-Na platelets and a corresponding chain mobility decrease. Water and oxygen diffusion coefficients were determined for unfilled and nano-biocomposite materials. Decreases in these diffusion coefficients were pointed out for all the nano-biocomposites, whatever the nanoclay type. Moreover, the diffusion coefficients obtained for MMT-Na samples were lower than those of OMMT-OH2 ones (Figure I.18) (Mangiacapra, P., 2006). Such results show that the unmodified clay had a higher dispersion than OMMT-OH2, leading to an increase in the tortuosity of the diffusion pathway. No variation in the nano-hybrid degradation temperature measured by TGA was observed whatever the nanofiller and the experimental conditions (air or nitrogen).
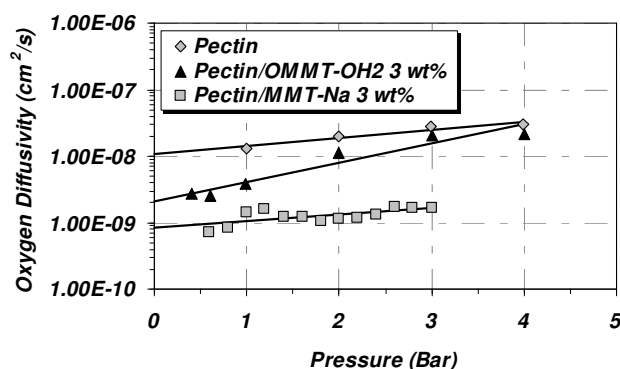
Figure I.18. Diffusion coefficients of oxygen in Pectin samples at 25 °C from kinetic gravimetric sorption experiments (Mangiacapra, P., 2006).

To conclude, this study has demonstrated the interest in the ball milling process to obtain the MMT exfoliation with a pectin matrix. However, such elaboration is time and cost prohibitive. Consequently a melt approach should be developed to validate the potential of these nano-hybrid materials, e.g. with the elaboration of blends. In the same way, other nanofillers should be tested to understand better the effect of the nanofiller/matrix interface on the resulting properties.

V. Conclusions

This review presented the state of the art of polysaccharides/nanoclay nano-biocomposites. These nano-hybrid materials mainly differ from conventional nanocomposites due to their hydrophilic character. Consequently, only microcomposite morphologies are reached with the dispersion of the common hydrophobic commercially available organo-modified nanoclays, such as Cloisite®-based MMT. On the opposite, exfoliated structures are often obtained with more hydrophilic nanofillers, such as natural MMT.

Because of the high thermal sensitivity of the carbohydrate chains, solvent intercalation process is often required for the nano-biocomposites elaboration. Such efficient strategy allows the nanoclay exfoliation in various matrices, e.g. starch and chitosan. Nevertheless, since this process is cost and time prohibitive, it may be not adapted for an industrial scale-up. Besides, the melt elaboration process appears as a rising option to produce polysaccharide-based nano-biocomposites. However, plasticizer incorporation is often needed to melt the carbohydrate-based matrix and to limit its thermal degradation. These plasticizers greatly affect the nano-hybrid morphology with the establishment of strong hydrogen interactions with the nanofillers, which perturb the clay platelets intercalation/exfoliation process. Consequently, these nano-hybrids display mainly intercalated structures at high plasticizer content. To overcome this limitation and reach exfoliation, an organo-modification of the clay surface with hydrophilic surfactants, such as carbohydrate surfactants, is required to modify the nanofiller polarity and thus the clay/matrix affinity. Such nano-hybrid materials display improved mechanical reinforcement, higher thermal stability and barrier properties, and lower moisture sensitivity.

However, although a significant amount of work has already been performed on various aspects of polysaccharide nano-biocomposites, most researches still remain to understand the complex plasticizer/matrix/nanofiller interactions and their influence on the resulting morphology and properties. In addition, it is known that high plasticizer content

leads to inhomogeneous materials (e.g. plasticized starch with high glycerol content). Until now, no attention has been paid to the nanofiller influence on such phase separation and on the resulting nanostructuration. These investigations could be performed with advances characterization techniques. Besides, new nanocomposites have been recently elaborated from needle-shaped nanofillers (e.g. sepiolite, palygorskite…) (Bilotti, E., 2008, Bokobza, L., 2004, Duquesne, E., 2007). Compared to more conventional layered silicates, they present substantial differences, namely their aspect ratio and their surface properties (silanol groups located at the nanofiller surface) and thus could permit the elaboration of innovative polysaccharide-based nano-hybrid materials with extended properties.

To conclude, these materials are a valid answer to produce low cost highly competitive and pioneering environmentally friendly materials. Moreover, since the citizens are more and more concerned about sustainable development and since the global need and the price of the fossil resources increase, such agro-based materials will yet represent an interesting option to replace conventional fossil resources based-plastic. They present a wide range of applications, such as packaging, agriculture devices, or even for biomedical applications with some developments based on the biocompatility of these materials.

Conclusion de la partie bibliographique

Ce chapitre a présenté l'état de l'art dans le domaine des nano-biocomposites polysaccharide/montmorillonite. Il a clairement été démontré que dans de tels systèmes, la nano-dispersion est affectée par l'affinité matrice/argile, mais également par la concentration en nanocharge et la voie d'élaboration choisie. L'influence clé du taux et de la nature des plastifiants utilisés dans ces matériaux a également été mise en évidence, ceux-ci pouvant moduler de manière significative la qualité de la nano-dispersion. Ces différents nano-biocomposites présentent une stabilité thermique ainsi que des propriétés barrières et mécaniques améliorées. De telles améliorations sont liées à l'état de dispersion de la nanocharge au sein de la matrice. Les meilleurs résultats sont obtenus avec les nanocharges exfoliées pour un taux d'inorganique généralement inférieur à 5 % en masse.

Comme ces nano-biocomposites peuvent être élaborés par des techniques classiques de mise en œuvre (e.g. extrusion, casting …) et parce qu'ils présentent de nettes améliorations des propriétés intrinsèques du matériau, ils sont dès à présent une solution innovante permettant de produire de nouveaux matériaux compétitifs respectueux de l'environnement. La raréfaction des ressources fossiles combinée à la volonté générale de mettre en place des produits éco-responsables favorisera le développement de ces matériaux bio-sourcés et abaissera leur coût relatif de production. Ils représenteront donc à terme une alternative crédible aux plastiques conventionnels issus de ressources fossiles dans une gamme d'applications pouvant aller de l'emballage aux implants médicaux biorésorbables.

Les études développées dans les chapitres suivants seront focalisées sur l'élaboration de nano-biocomposites exfoliés dans des matrices amidon surplastifiées. Pour ce faire, une attention particulière sera portée à l'organo-modification de la montmorillonite afin d'améliorer l'interface matrice/nanocharge et la nano-structuration de ces matériaux.

Références de la partie bibliographique

Alexandre, M.; Dubois, P., Polymer-layered silicate nanocomposites: Preparation, properties and uses of a new class of materials. Mater. Sci. Eng. R-Rep. 2000, 28, 1-63.

Appelqvist, I. A. M.; Cooke, D.; Gidley, M. J.; Lane, S. J., Thermal properties of polysaccharides at low moisture: 1 - An endothermic melting process and water-carbohydrate interactions. Carbohydr. Polym. 1993, 20, 291-299.

Atalla, R. H.; Van der Hart, D. L., Native cellulose: a composite of two distinct crystalline forms. Science 1984, 223, 283-285.

Atkins, E. D. T., Conformation in polysaccharides and complex carbohydrates. J. Biosci. 1985, 8, 375-387.

Avella, M.; De Vlieger, J. J.; Errico, M. E.; Fischer, S.; Vacca, P.; Volpe, M. G., Biodegradable starch/clay nanocomposite films for food packaging applications. Food Chem. 2005, 93, 467-474.

Averous, L.; Moro, L.; Dole, P.; Fringant, C., Properties of thermoplastic blends: Starch-polycaprolactone. Polymer 2000a, 41, 4157-4167.

Averous, L.; Fauconnier, N.; Moro, L.; Fringant, C., Blends of Thermoplastic Starch and Polyesteramide: Processing and Properties. J. Appl. Polym. Sci. 2000b, 76, 1117-1128.

Averous, L.; Fringant, C., Association between plasticized starch and polyesters: Processing and performances of injected biodegradable systems. Polym. Eng. Sci. 2001, 41, 727-734.

Averous, L., Biodegradable multiphase systems based on plasticized starch: A review. J. Macromol. Sci. Part C-Polym. Rev. 2004a, 44, 231-274.

Averous, L.; Boquillon, N., Biocomposites based on plasticized starch: Thermal and mechanical behaviours. Carbohydr. Polym. 2004b, 56, 111-122.

Bagdi, K.; Muller, P.; Pukanszky, B., Thermoplastic starch/layered silicate composites: Structure, interaction, properties. Compos. Interfaces 2006, 13, 1-17.

Baud, B.; Colonna, P.; Della Valle, G.; Roger, P., Macromolecular degradation of extruded starches measured by HPSEC-MALLS. . In *Biopolymer Science: Food and Non Food Applications/Les Colloques de l'INRA*, Colonna, P.; Guilbert, S., Eds. Paris, 1999; pp 217-221.

Bilotti, E.; Fischer, H. R.; Peijs, T., Polymer nanocomposites based on needle-like sepiolite clays: Effect of functionalized polymers on the dispersion of nanofiller, crystallinity, and mechanical properties. J. Appl. Polym. Sci. 2008, 107, 1116-1123.

Bledzki, A. K.; Gassan, J., Composites reinforced with cellulose based fibres. Prog. Polym. Sci. 1999, 24, 221-274.

Bokobza, L.; Burr, A.; Garnaud, G.; Perrin, M. Y.; Pagnotta, S., Fibre reinforcement of elastomers: Nanocomposites based on sepiolite and poly(hydroxyethyl acrylate). Polym. Int. 2004, 53, 1060-1065.

Bordes, P.; Pollet, E.; Bourbigot, S.; Averous, L., Structure and properties of PHA/clay nano-biocomposites prepared by melt intercalation. Macromol. Chem. Phys. 2008, 209, 1473-1484.

Buchanan, C. M.; Gedon, S. C.; White, A. W.; Wood, M. D., Cellulose acetate butyrate and poly(hydroxybutyrate-co-valerate) copolymer blends. Macromolecules 1992, 25, 7373-7381.

Campbell, N. A.; Reece, J. B.; Mitchell, L. G., Biology. 5th ed.; Menlo Park CA: New Work, 1999.

Cases, J. M.; Brend, I.; Besson, G.; François, M.; Uriot, J. P.; Thomas, F.; Poirier, J. E., Mechanism of adsorption and desorption of water vapor by homoionic montmorillonite. 1. The sodium-exchanged form. Langmuir 1992, 8, 2730-2739.

Chanzy, H., Aspects of Cellulose Structure. In *Cellulose Sources and Exploitation*, Kennedy, J. F.; Phillips, G. O.; Williams, P. A., Eds. Ellis Horwood Ltd.: New York, 1990; pp 3-12.

Chaudhary, D. S., Understanding amylose crystallinity in starch-clay nanocomposites. J. Polym. Sci. Pt. B-Polym. Phys. 2008, 46, 979-987.

Chen, B.; Evans, J. R. G., Thermoplastic starch-clay nanocomposites and their characteristics. Carbohydr. Polym. 2005, 61, 455-463.

Chen, M.; Chen, B.; Evans, J. R. G., Novel thermoplastic starch-clay nanocomposite foams. Nanotechnology 2005, 16, 2334-2337.

Chiou, B.-S.; Yee, E.; Glenn, G. M.; Orts, W. J., Rheology of starch-clay nanocomposites. Carbohydr. Polym. 2005, 59, 467-475.

Chiou, B.-S.; Yee, E.; Wood, D.; Shey, J.; Glenn, G.; Orts, W., Effects of processing conditions on nanoclay dispersion in starch-clay nanocomposites. Cereal Chem. 2006, 83, 300-305.

Chiou, B. S.; Yee, E.; Glenn, G. M.; Orts, W. J.; Wood, D. F.; Imam, S. H. In *Biopolymer nanocomposites containing native wheat starch and nanoclays*, ACS National Meeting Book of Abstracts, 2004///, 2004; 2004.

Chiou, B. S.; Wood, D.; Yee, E.; Imam, S. H.; Glenn, G. M.; Orts, W. J., Extruded starch-nanoclay nanocomposites: Effects of glycerol and nanoclay concentration. Polym. Eng. Sci. 2007, 47, 1898-1904.

Chivrac, F.; Kadlecova, Z.; Pollet, E.; Averous, L., Aromatic copolyester-based nano-biocomposites: Elaboration, structural characterization and properties. J. Polym. Environ. 2006, 14, 393-401.

Chivrac, F.; Pollet, E.; Averous, L., Nonisothermal crystallization behavior of poly(butylene adipate-co-terephthalate)/clay nano-biocomposites. J. Polym. Sci. Pt. B-Polym. Phys. 2007, 45, 1503-1510.

Cho, J. W.; Paul, D. R., Nylon 6 nanocomposites by melt compounding. Polymer 2001, 42, 1083-1094.

Colonna, P.; Mercier, C., Macromolecular structure of wrinkled- and smooth-pea starch components. Carbohydr. Res. 1984, 126, 233-247.

Cooke, D.; Gidley, M. J., Loss of crystalline and molecular order during starch gelatinisation: Origin of the enthalpic transition. Carbohydr. Res. 1992, 227, 103-112.

Cuq, B.; Gontard, N.; Guilbert, S., Proteins as agricultural polymers for packaging production. Cereal Chem. 1998, 75, 1-9.

Curvelo, A. A. S.; De Carvalho, A. J. F.; Agnelli, J. A. M., Thermoplastic starch-cellulosic fibers composites: Preliminary results. Carbohydr. Polym. 2001, 45, 183-188.

Cyras, V. P.; Manfredi, L. B.; Ton-That, M. T.; Vazquez, A., Physical and mechanical properties of thermoplastic starch/montmorillonite nanocomposite films. Carbohydr. Polym. 2008, 73, 55-63.

Dai, J. C.; Huang, J. T., Surface modification of clays and clay-rubber composite. Appl. Clay Sci. 1999, 15, 51-65.

Darder, M.; Colilla, M.; Ruiz-Hitzky, E., Biopolymer-clay nanocomposites based on chitosan intercalated in montmorillonite. Chem. Mater. 2003, 15, 3774-3780.

Darder, M.; Colilla, M.; Ruiz-Hitzky, E., Chitosan-clay nanocomposites: Application as electrochemical sensors. Appl. Clay Sci. 2005, 28, 199-208.

Davidson, V. J.; Paton, D.; Diosady, L. L.; Larocque, G., Degradation of Wheat Starch in a Single Screw Extruder: Characteristics of Extruded Starch Polymers J. Food Sci. 1984a, 49, 453-458.

Davidson, V. J.; Parker, R.; Diosady, L. L.; Rubin, L. T., A Model for Mechanical Degradation of Wheat Starch in a Single-Screw Extruder J. Food Sci. 1984b, 49, 1154-1169.

Dean, K.; Yu, L.; Wu, D. Y., Preparation and characterization of melt-extruded thermoplastic starch/clay nanocomposites. Compos. Sci. Technol. 2007, 67, 413-421.

Dean, K. M.; Do, M. D.; Petinakis, E.; Yu, L., Key interactions in biodegradable thermoplastic starch/poly(vinyl alcohol)/montmorillonite micro- and nanocomposites. Compos. Sci. Technol. 2008, 68, 1453-1462.

Della Valle, G.; Boche, Y.; Colonna, P.; Vergnes, B., The extrusion behaviour of potato starch. Carbohydr. Polym. 1995, 28, 255-264.

Della Valle, G.; Buleon, A.; Carreau, P. J.; Lavoie, P. A.; Vergnes, B., Relationship between structure and viscoelastic behavior of plasticized starch. J. Rheol. 1998, 42, 507-525.

Dennis, H. R.; Hunter, D. L.; Chang, D.; Kim, S.; White, J. L.; Cho, J. W.; Paul, D. R., Effect of melt processing conditions on the extent of exfoliation in organoclay-based nanocomposites. Polymer 2001, 42, 9513-9522.

Dufresne, A.; Vignon, M. R., Improvement of starch film performances using cellulose microfibrils. Macromolecules 1998, 31, 2693-2696.

Duquesne, E.; Moins, S.; Alexandre, M.; Dubois, P., How can nanohybrids enhance polyester/sepiolite nanocomposite properties? Macromol. Chem. Phys. 2007, 208, 2542-2550.

Edgar, K. J.; Buchanan, C. M.; Debenham, J. S.; Rundquist, P. A.; Seiler, B. D.; Shelton, M. C.; Tindall, D., Advances in cellulose ester performance and application. Prog. Polym. Sci. 2001, 26, 1605-1688.

Fischer, H. R.; Gielgens, L. H.; Koster, T. P. M., Nanocomposites from polymers and layered minerals. Acta polym. 1999, 50, 122-126.

Fischer, S.; De Vlieger, J.; Kock, T.; Batenburg, L.; Fischer, H. In *"Green" nanocomposite materials - New possibilities for bioplastics*, Materials Research Society Symposium - Proceedings, 2001, 2001; 2001; pp 628-661.

Forssell, P.; Mikkila, J.; Suortti, T.; Seppala, J.; Poutanen, K., Plasticization of barley starch with glycerol and water. J. Macromol. Sci. Part A-Pure Appl. Chem. 1996, 33, 703-715.

Fringant, C.; Desbrieres, J.; Rinaudo, M., Physical properties of acetylated starch-based materials: Relation with their molecular characteristics. Polymer 1996, 37, 2663-2673.

Gain, O.; Espuche, E.; Pollet, E.; Alexandre, M.; Dubois, P., Gas barrier properties of poly(ε-caprolactone)/clay nanocomposites: Influence of the morphology and polymer/clay interactions. J. Polym. Sci. Pt. B-Polym. Phys. 2005, 43, 205-214.

Gardner, K. H.; Blackwell, J., Refinement of the structure of β-chitin. Biopolymers 1975, 14, 1581-1595.

Gaudin, S.; Lourdin, D.; Forssell, P. M.; Colonna, P., Antiplasticisation and oxygen permeability of starch-sorbitol films. Carbohydr. Polym. 2000, 43, 33-37.

Genkina, N. K.; Wikman, J.; Bertoft, E.; Yuryev, V. P., Effects of structural imperfection on gelatinization characteristics of amylopectin starches with A- and B-type crystallinity. Biomacromolecules 2007, 8, 2329-2335.

Giannelis, E. P., Polymer layered silicate nanocomposites. Adv. Mater. 1996, 8, 29-35.

Godbillot, L.; Dole, P.; Joly, C.; Roge, B.; Mathlouthi, M., Analysis of water binding in starch plasticized films. Food Chem. 2006, 96, 380-386.

Gomes, M. E.; Ribeiro, A. S.; Malafaya, P. B.; Reis, R. L.; Cunha, A. M., A new approach based on injection moulding to produce biodegradable starch-based polymeric scaffolds: Morphology, mechanical and degradation behaviour. Biomaterials 2001, 22, 883-889.

Gorrasi, G.; Tortora, M.; Vittoria, V.; Pollet, E.; Lepoittevin, B.; Alexandre, M.; Dubois, P., Vapor barrier properties of polycaprolactone montmorillonite nanocomposites: Effect of clay dispersion. Polymer 2003, 44, 2271-2279.

Gorrasi, G.; Tortora, M.; Vittoria, V.; Pollet, E.; Alexandre, M.; Dubois, P., Physical Properties of Poly(ε-caprolactone) Layered Silicate Nanocomposites Prepared by Controlled Grafting Polymerization. J. Polym. Sci. Pt. B-Polym. Phys. 2004, 42, 1466-1475.

Gross, R. A.; Kalra, B., Biodegradable polymers for the environment. Science 2002, 297, 803-807.

Günister, E.; Pestreli, D.; Unlu, C. H.; Atici, O.; Gungor, N., Synthesis and characterization of chitosan-MMT biocomposite systems. Carbohydr. Polym. 2007, 67, 358-365.

Guilbert, S.; Gontard, N.; Gorris, L. G. M., Prolongation of the shelf-life of perishable food products using biodegradable films and coatings. LWT-Food Sci. Technol. 1996, 29, 10-17.

Guilbot, A.; Mercier, C., The Polysaccharides. In *Molecular Biology*, Aspinall, G. O., Ed. Academic Press Incorporation: New-York, 1985; Vol. 3, pp 209-282.

Hayashi, A.; Kinoshita, K.; Miyake, Y.; Cho, C. H., Conformation of amylose in solution. Polym. J. 1981, 13, 537-541.

Heiner, A. P.; Teleman, O., Interface between monoclinic crystalline cellulose and water: Breakdown of the odd/even duplicity. Langmuir 1997, 13, 511-518.

Hendricks, S. B., Lattice Structure of Clay Minerals and Some Properties of Clay. J. Geol. 1942, 50, 276-293.

Hizukuri, S.; Takeda, Y.; Yasuda, M., Multibranched nature of amylose and the action of debranching enzymes. Carbohydr. Res. 1981, 94, 205-213.

Hizukuri, S., Polymodal distribution of the chain lengths of amylopectins, and its significance. Carbohydr. Res. 1986, 147, 342-347.

Huang, M.; Yu, J.; Ma, X., Studies on properties of the thermoplastic starch/montmorillonite composites. Acta Polym. Sin. 2005, 862-867.

Huang, M.; Yu, J.; Ma, X., High mechanical performance MMT-urea and formamide-plasticized thermoplastic cornstarch biodegradable nanocomposites. Carbohydr. Polym. 2006a, 63, 393-399.

Huang, M.; Yu, J., Structure and properties of thermoplastic corn starch/montmorillonite biodegradable composites. J. Appl. Polym. Sci. 2006b, 99, 170-176.

Huang, M. F.; Yu, J. G.; Ma, X. F., Studies on the properties of Montmorillonite-reinforced thermoplastic starch composites. Polymer 2004, 45, 7017-7023.

Huang, M. F.; Yu, J. G.; Ma, X. F.; Jin, P., High performance biodegradable thermoplastic starch - EMMT nanoplastics. Polymer 2005a, 46, 3157-3162.

Huang, M. F.; Yu, J. G.; Ma, X. F., Preparation of the thermoplastic starch/montmorillonite nanocomposites by melt-intercalation. Chin. Chem. Lett. 2005b, 16, 561-564.

Hulleman, S. H. D.; Kalisvaart, M. G.; Janssen, F. H. P.; Feil, H.; Vliegenthart, J. F. G., Origins of B-type crystallinity in glycerol-plasticised, compression-moulded potato starches. Carbohydr. Polym. 1999, 39, 351-360.

Jang, J. K.; Pyun, Y. R., Effect of Moisture Content on the Melting of Wheat Starch. Starch-Starke 1986, 48, 48-51.

Jenkins, P. J.; Donald, A. M., The influence of amylose on starch granule structure. Int. J. Biol. Macromol. 1995, 17, 315-321.

Jimenez, G.; Ogata, N.; Kawai, H.; Ogihara, T., Structure and thermal/mechanical properties of poly(ε-caprolactone)-clay blend. J. Appl. Polym. Sci. 1997, 64, 2211-2220.

Jin, Y. H.; Park, H. J.; Im, S. S.; Kwak, S. Y.; Kwak, S., Polyethylene/clay nanocomposite by in-situ exfoliation of montmorillonite during Ziegler-Natta polymerization of ethylene. Macromol. Rapid Commun. 2002, 23, 135-140.

Jozja, N. Étude de matériaux argileux Albanais. Caractérisation "multi-échelle" d'une bentonite magnésienne. Impact de l'interaction avec le nitrate de plomb sur la perméabilité. Université d'Orléans, Orléans, 2003.

Kalambur, S.; Rizvi, S. S. H., Biodegradable and functionally superior starch-polyester nanocomposites from reactive extrusion. J. Appl. Polym. Sci. 2005, 96, 1072-1082.

Kalambur, S. B.; Rizvi, S. S., Starch-based nanocomposites by reactive extrusion processing. Polym. Int. 2004, 53, 1413-1416.

Kalichevsky, M. T.; Jaroszkiewicz, E. M.; Ablett, S.; Blanshard, J. M. V.; Lillford, P. J., The glass transition of amylopectin measured by DSC, DMTA and NMR. Carbohydr. Polym. 1992, 18, 77-88.

Kalichevsky, M. T.; Blanshard, J. M. V., The effect of fructose and water on the glass transition of amylopectin. Carbohydr. Polym. 1993, 20, 107-113.

Kampeerapappun, P.; Aht-ong, D.; Pentrakoon, D.; Srikulkit, K., Preparation of cassava starch/montmorillonite composite film. Carbohydr. Polym. 2007, 67, 155-163.

Ke, Y.; Lü, J.; Yi, X.; Zhao, J.; Qi, Z., The effects of promoter and curing process on exfoliation behavior of epoxy/clay nanocomposites. J. Appl. Polym. Sci. 2000, 78, 808-815.

Krishnamoorti, R.; Vaia, R. A.; Giannelis, E. P., Structure and dynamics of polymer-layered silicate nanocomposites. Chem. Mater. 1996, 8, 1728-1734.

Lagaly, G., Interaction of alkylamines with different types of layered compounds. Solid State Ion. 1986, 22, 43-51.

Lagaly, G., Introduction: from clay mineral-polymer interactions to clay mineral-polymer nanocomposites. Appl. Clay Sci. 1999, 15, 1-9.

Lebaron, P. C.; Wang, Z.; Pinnavaia, T. J., Polymer-layered silicate nanocomposites: An overview. Appl. Clay Sci. 1999, 15, 11-29.

Lee, S. Y.; Xu, Y. X.; Hanna, M. A., Tapioca starch-poly (lactic acid)-based nanocomposite foams as affected by type of nanoclay. Int. Polym. Process. 2007, 22, 429-435.

Lee, S. Y.; Chen, H.; Hanna, M. A., Preparation and characterization of tapioca starch-poly(lactic acid) nanocomposite foams by melt intercalation based on clay type. Ind. Crop. Prod. 2008a, 28, 95-106.

Lee, S. Y.; Hanna, M. A., Preparation and characterization of tapioca starch-poly(lactic acid)-Cloisite NA$^+$ nanocomposite foams. J. Appl. Polym. Sci. 2008b, 110, 2337-2344.

Lee, S. Y.; Hanna, M. A.; Jones, D. D., An adaptive neuro-fuzzy inference system for modeling mechanical properties of tapioca starch-poly(lactic acid) nanocomposite foams. Starch/Staerke 2008c, 60, 159-164.

Lepoittevin, B.; Pantoustier, N.; Devalckenaere, M.; Alexandre, M.; Kubies, D.; Calberg, C.; Jerome, R.; Dubois, P., Poly(ε-caprolactone)/clay nanocomposites by in-situ intercalative polymerization catalyzed by dibutyltin dimethoxide. Macromolecules 2002a, 35, 8385-8390.

Lepoittevin, B.; Devalckenaere, M.; Pantoustier, N.; Alexandre, M.; Kubies, D.; Calberg, C.; Jerome, R.; Dubois, P., Poly (ε-caprolactone)/clay nanocomposites prepared by melt intercalation: mechanical, thermal and rheological properties. Polymer 2002b, 43, 4017-4023.

Lepoittevin, B.; Pantoustier, N.; Devalckenaere, M.; Alexandre, M.; Calberg, C.; Jerome, R.; Henrist, C.; Rulmont, A.; Dubois, P., Polymer/layered silicate nanocomposites by combined intercalative polymerization and melt intercalation: A masterbatch process. Polymer 2003, 44, 2033-2040.

Lilholt, H.; Lawther, J. M., Natural organic fibres. In *Comprehensive composite materials*, Kelly, A.; Zweben, C., Eds. Elsevier: 2000; Vol. 1, pp 303-325.

Lilichenko, N.; Maksimov, R. D.; Zicans, J.; Merijs Meri, R.; Plume, E., A biodegradable polymer nanocomposite: Mechanical and barrier properties. Mech. Compos. Mater. 2008, 44, 45-56.

Lin, K.-F.; Hsu, C.-Y.; Huang, T.-S.; Chiu, W.-Y.; Lee, Y.-H.; Young, T.-H., A novel method to prepare chitosan/montmorillonite nanocomposites. J. Appl. Polym. Sci. 2005, 98, 2042-2047.

Lourdin, D.; Della Valle, G.; Colonna, P., Influence of amylose content on starch films and foams. Carbohydr. Polym. 1995, 27, 261-270.

Lourdin, D.; Bizot, H.; Colonna, P., Correlation between static mechanical properties of starch-glycerol materials and low-temperature relaxation. Macromol. Symp. 1997a, 114, 179-185.

Lourdin, D.; Bizot, H.; Colonna, P., "Antiplasticization" in starch-glycerol films? J. Appl. Polym. Sci. 1997b, 63, 1047-1053.

Lourdin, D.; Coignard, L.; Bizot, H.; Colonna, P., Influence of equilibrium relative humidity and plasticizer concentration on the water content and glass transition of starch materials. Polymer 1997c, 38, 5401-5406.

Lourdin, D.; Ring, S. G.; Colonna, P., Study of plasticizer-oligomer and plasticizer-polymer interactions by dielectric analysis: maltose-glycerol and amylose-glycerol-water systems. Carbohydr. Res. 1998, 306, 551-558.

Lu, T. J.; Jane, J. L.; Keeling, P. L., Temperature effect on retrogradation rate and crystalline structure of amylose. Carbohydr. Polym. 1997, 33, 19-26.

Lu, Y.; Weng, L.; Zhang, L., Morphology and properties of soy protein isolate thermoplastics reinforced with chitin whiskers. Biomacromolecules 2004, 5, 1046-1051.

Luckham, P. F.; Rossi, S., The colloid and rhelogical properties of bentonite suspensions, Advances in Colloid and Interface Science. Adv. Colloid Interface Sci. 1999, 82, 43-92.

Luo, J. J.; Daniel, I. M., Characterization and modeling of mechanical behavior of polymer/clay nanocomposites. Compos. Sci. Technol. 2003, 63, 1607-16.

Ma, X.; Yu, J.; Wang, N., Production of thermoplastic starch/ MMT-sorbitol nanocomposites by dual-melt extrusion processing. Macromol. Mater. Eng. 2007, 292, 723-728.

Magini, M.; Colella, C.; Iasonna, A.; Padella, F., Power measurements during mechanical milling - II. The case of "single path cumulative" solid state reaction. Acta Mater. 1998, 46, 2841-2850.

Maiti, P.; Yamada, K.; Okamoto, M.; Ueda, K.; Okamoto, K., New polylactide/layered silicate nanocomposites: Role of organoclays. Chem. Mater. 2002, 14, 4654-4661.

Maiti, P.; Batt, C. A.; Giannelis, E. P., New biodegradable polyhydroxybutyrate/layered silicate nanocomposites. Biomacromolecules 2007, 8, 3393-3400.

Mangiacapra, P.; Gorrasi, G.; Sorrentino, A.; Vittoria, V., Biodegradable nanocomposites obtained by ball milling of pectin and montmorillonites. Carbohydr. Polym. 2006, 64, 516-523.

Martin, O.; Averous, L., Poly(lactic acid): Plasticization and properties of biodegradable multiphase systems. Polymer 2001, 42, 6209-6219.

Martin, O.; Averous, L.; Della Valle, G., In-line determination of plasticized wheat starch viscoelastic behavior: Impact of processing. Carbohydr. Polym. 2003, 53, 169-182.

May, C. D., Industrial pectins: Sources, production and applications. Carbohydr. Polym. 1990, 12, 79-99.

McGlashan, S. A.; Halley, P. J., Preparation and characterisation of biodegradable starch-based nanocomposite materials. Polym. Int. 2003, 52, 1767-1773.

Méring, J., The hydration of montmorillonite. Trans. Faraday Soc. 1946, 42B, 205-219.

Messersmith, P. B.; Giannelis, E. P., Polymer-layered silicate nanocomposites: In situ intercalative polymerization of ε-Caprolactone in layered silicates. Chem. Mat. 1993, 5, 1064-1066.

Minke, R.; Blackwell, J., The structure of α-chitin. J. Mol. Biol. 1978, 120, 167-181.

Mohanty, A. K.; Misra, M.; Drzal, L. T., Sustainable Bio-Composites from renewable resources: Opportunities and challenges in the green materials world. J. Polym. Environ. 2002, 10, 19-26.

Mondragon, M.; Mancilla, J. E.; Rodriguez-Gonzalez, F. J., Nanocomposites from plasticized high-amylopectin, normal and high-amylose maize starches. Polym. Eng. Sci. 2008, 48, 1261-1267.

Neus Angles, M.; Dufresne, A., Plasticized starch/tuniein whiskers nanocomposites. 1. Structural analysis. Macromolecules 2000, 33, 8344-8353.

Nishiyama, Y.; Langan, P.; Chanzy, H., Crystal structure and hydrogen-bonding system in cellulose 1 beta from synchrotron X-ray and neutron fiber diffraction. J. Am. Chem. Soc. 2002, 124, 9074-9082.

Ogata, N.; Jimenez, G.; Kawai, H.; Ogihara, T., Structure and thermal/mechanical properties of poly(L-lactide)-clay blend. J. Polym. Sci. Pt. B-Polym. Phys. 1997, 35, 389-396.

Ogawa, K., Effect of heating an aqueous suspension of chitosan on the crystalliity and polymorph. Agric. Biol. Chem. 1991, 55, 2375-2379.

Ogawa, K.; Yui, T.; Miya, M., Dependence on the preparation procedure of the polymorphism and crystallinity of chitosan membranes. Biosci. Biotech. Biochem. 1992, 56, 858-862.

Ollett, A. L.; Parker, R.; Smith, A. C.; Miles, M. J.; Morris, V. J., Microstructural changes during the twin-screw extrusion cooking of maize grits. Carbohydr. Polym. 1990, 13, 69-84.

Ollett, A. L.; Parker, R.; Smith, A. C., Deformation and fracture behaviour of wheat starch plasticized with glucose and water. J. Mater.Sci. 1991, 26, 1351-1356.

Orford, P. D.; Parker, R.; Ring, S. G., The Functional Properties of Extrusion-cooked Waxy-maize Starch. J. Cereal Sci. 1993, 18, 277-286.

Paillet, M.; Dufresne, A., Chitin whisker reinforced thermoplastic nanocomposites [1]. Macromolecules 2001, 34, 6527-6530.

Pandey, J. K.; Singh, R. P., Green nanocomposites from renewable resources: Effect of plasticizer on the structure and material properties of clay-filled starch. Starch-Starke 2005, 57, 8-15.

Park, H. M.; Li, X.; Jin, C. Z.; Park, C. Y.; Cho, W. J.; Ha, C. S., Preparation and properties of biodegradable thermoplastic starch/clay hybrids. Macromol. Mater. Eng. 2002, 287, 553-558.

Park, H. M.; Lee, W. K.; Park, C. Y.; Cho, W. J.; Ha, C. S., Environmentally friendly polymer hybrids Part I mechanical, thermal, and barrier properties of thermoplastic starch/clay nanocomposites. J. Mater. Sci. 2003, 38, 909-915.

Park, H. M.; Misra, M.; Drzal, L. T.; Mohanty, A. K., "Green" nanocomposites from cellulose acetate bioplastic and clay: Effect of eco-friendly triethyl citrate plasticizer. Biomacromolecules 2004a, 5, 2281-2288.

Park, H. M.; Liang, X.; Mohanty, A. K.; Misra, M.; Drzal, L. T., Effect of compatibilizer on nanostructure of the biodegradable cellulose acetate/organoclay nanocomposites. Macromolecules 2004b, 37, 9076-9082.

Park, H. M.; Mohanty, A. K.; Drzal, L. T.; Lee, E.; Mielewski, D. F.; Misra, M., Effect of sequential mixing and compounding conditions on cellulose acetate/layered silicate nanocomposites. J. Polym. Environ. 2006, 14, 27-35.

Paul, M. A.; Alexandre, M.; Degee, P.; Henrist, C.; Rulmont, A.; Dubois, P., New nanocomposite materials based on plasticized poly(L-lactide) and organo-modified montmorillonites: Thermal and morphological study. Polymer 2002, 44, 443-450.

Paul, M. A.; Alexandre, M.; Degee, P.; Calberg, C.; Jerome, R.; Dubois, P., Exfoliated polylactide/clay nanocomposites by in-situ coordination-insertion polymerization. Macromol. Rapid Commun. 2003, 24, 561-566.

Paul, M. A.; Delcourt, C.; Alexandre, M.; Degee, P.; Monteverde, F.; Rulmont, A.; Dubois, P., (Plasticized) polylactide/(organo-)clay nanocomposites by in situ intercalative polymerization. Macromol. Chem. Phys. 2005, 206, 484-498.

Peprnicek, T.; Kalendova, A.; Pavlova, E.; Simonik, J.; Duchet, J.; Gerard, J. F., Poly(vinyl chloride)-paste/clay nanocomposites: Investigation of thermal and morphological characteristics. Polym. Degrad. Stabil. 2006, 91, 3322-3329.

Perez, C. J.; Alvarez, V. A.; Mondragon, I.; Vazquez, A., Mechanical properties of layered silicate/starch polycaprolactone blend nanocomposites. Polym. Int. 2007a, 56, 686-693.

Perez, C. J.; Alvarez, V. A.; Stefani, P. M.; Vazquez, A., Non-isothermal crystallization of MaterBi-Z/clay nanocomposites. J. Therm. Anal. Calorim. 2007b, 88, 825-832.

Perez, C. J.; Vazquez, A.; Alvarez, V. A., Isothermal crystallization of layered silicate/starch-polycaprolactone blend nanocomposites. J. Therm. Anal. Calorim. 2008a, 91, 749-757.

Perez, C. J.; Alvarez, V. A.; Vazquez, A., Creep behaviour of layered silicate/starch-polycaprolactone blends nanocomposites. Mater. Sci. Eng. A-Struct. 2008b, 480, 259-265.

Perez, C. J.; Alvarez, V. A.; Mondragon, I.; Vazquez, A., Water uptake behavior of layered silicate/starch-polycaprolactone blend nanocomposites. Polym. Int. 2008c, 57, 247-253.

Peter, M. G. P. I., Chitin and Chitosan from Fungi. In *Biopolymers, Vol. 6: Polysaccharides II*, Steinbüchel, A., Ed. Wiley-VCH: Weinheim, 2002; pp 123 - 157.

Picard, E.; Vermogen, A.; Gerard, J. F.; Espuche, E., Barrier properties of nylon 6-montmorillonite nanocomposite membranes prepared by melt blending: Influence of the clay content and dispersion state. Consequences on modelling. J. Membr. Sci. 2007, 292, 133-144.

Picard, E.; Gerard, J. F.; Espuche, E., Water transport properties of polyamide 6 based nanocomposites prepared by melt blending: On the importance of the clay dispersion state on the water transport properties at high water activity. J. Membr. Sci. 2008, 313, 284-295.

Pluta, M.; Galeski, A.; Alexandre, M.; Paul, M. A.; Dubois, P., Polylactide/montmorillonite nanocomposites and microcomposites prepared by melt blending: Structure and some physical properties. J. Appl. Polym. Sci. 2002, 86, 1497-1506.

Pogodina, N. V.; Cerclé, C.; Averous, L.; Thomann, R.; Bouquey, M.; Muller, R., Processing and characterization of biodegradable polymer nanocomposites: detection of dispersion state. Rheol. Acta 2008, 47, 543-553.

Powell, D. H.; Fischer, H. E.; Skipper, N. T., The structure of interlayer water in Li-montmorillonite studied by neutron diffraction with isotopic substitution. J. Phys. Chem. B 1998a, 102, 10899-10905.

Powell, D. H.; Tongkhao, K.; Kennedy, S. J.; Slade, P. G., Interlayer water structure in Na- and Li-montmorillonite clays. Physica B 1998b, 241-243, 387-389.

Qiao, X.; Jiang, W.; Sun, K., Reinforced thermoplastic acetylated starch with layered silicates. Starch-Starke 2005, 57, 581-586.

Reddy, C. S. K.; Ghai, R.; Rashmi; Kalia, V. C., Polyhydroxyalkanoates: An overview. Bioresour. Technol. 2003, 87, 137-146.

Redl, A.; Morel, M. H.; Bonicel, J.; Vergnes, B.; Guilbert, S., Extrusion of wheat gluten plasticized with glycerol: Influence of process conditions on flow behavior, rheological properties, and molecular size distribution. Cereal Chem. 1999, 76, 361-370.

Revol, J. F., Change of the d spacing in cellulose crystals during lattice imaging. J. Mat. Sci. Letters 1985, 4, 1347-1349.

Rinaudo, M., Chitin and chitosan: Properties and applications. Prog. Polym. Sci. 2006, 31, 603-632.

Rudall, K. M.; Kenchington, W., The chitin system. Biol. Rev. 1973, 40, 597-636.

Sagar, A. D.; Merrill, E. W., Starch fragmentation during extrusion processing. Polymer 1995, 36, 1883-1886.

Sakurada, L.; Nukushina, Y.; Ito, T., Experimental determination of the elastic modulus of crystalline regions in oriented polymers. J. Polym. Sci. 1962, 57, 651-660.

Sanchez-Garcia, M. D.; Gimenez, E.; Lagaron, J. M., Morphology and barrier properties of nanobiocomposites of poly(3-hydroxybutyrate) and layered silicates. J. Appl. Polym. Sci. 2008, 108, 2787-2801.

Shahidi, F.; Arachchi, J. K. V.; Jeon, Y. J., Food applications of chitin and chitosan. Trends Food Sci. Technol. 1999, 10, 37-51.

Shen, Z.; Simon, G. P.; Cheng, Y. B., Comparison of solution intercalation and melt intercalation of polymer-clay nanocomposites. Polymer 2002, 43, 4251-4260.

Shogren, R. L., Effect of moisture content on the melting and subsequent physical aging of cornstarch. Carbohydr. Polym. 1992a, 19, 83-90.

Shogren, R. L.; Swanson, C. L.; Thompson, A. R., Extrudates of Cornstarch with Urea and Glycols: Structure/Mechanical Property Relations. Starch-Starke 1992b, 44, 335-338.

Sinclair, R. G., The case for polylactic acid as a commodity packaging plastic. J. Macromol. Sci. Part A-Pure Appl. Chem. 1996, 33, 585-597.

Sinha Ray, S.; Maiti, P.; Okamoto, M.; Yamada, K.; Ueda, K., New polylactide/layered silicate nanocomposites. 1. Preparation, characterization, and properties. Macromolecules 2002, 35, 3104-3110.

Sinha Ray, S.; Okamoto, M., Polymer/layered silicate nanocomposites: A review from preparation to processing. Prog. Polym. Sci. 2003, 28, 1539-1641.

Sposito, G.; Grasso, D., Electrical Double Layer Structure, Forces, and Fields at the Clay Water Interface. Surfactant Sci. Ser. 1999, 85, 107-249.

Stevens, D. J.; Elton, G. A. H., Thermal Properties of the Starch/Water System Part I. Measurement of Heat of Gelatinisation by Differential Scanning Calorimetry. Starch-Starke 1971, 23, 8-11.

Swanson, C. L.; Shogren, R. L.; Fanta, G. F.; Imam, S. H., Starch-plastic materials-Preparation, physical properties, and biodegradability (a review of recent USDA research). J. Environ. Polym. Deg. 1993, 1, 155-166.

Tang, X.; Alavi, S.; Herald, T. J., Barrier and mechanical properties of starch-clay nanocomposite films. Cereal Chem. 2008a, 85, 433-439.

Tang, X.; Alavi, S.; Herald, T. J., Effects of plasticizers on the structure and properties of starch-clay nanocomposite films. Carbohydr. Polym. 2008b, 74, 552-558.

Tettenhorst, R., Cation migration in montmorillonites. Am. Miner. 1962, 47, 769-773.

Thakur, B. R.; Singh, R. K.; Handa, A. K., Chemistry and uses of pectin--a review. Crit. Rev. Food Sci. Nutr. 1997, 37, 47-73.

Thiewes, H. J.; Steeneken, P. A. M., The glass transition and the sub-Tg endotherm of amorphous and native potato starch at low moisture content. Carbohydr. Polym. 1997, 32, 123-130.

Thomas, F.; Michot, L. J.; Vantelon, D.; Montarges, E.; Prelot, B.; Cruchaudet, M.; Delon, J. F., Layer charge and electrophoretic mobility of smectites. Colloid Surf. A-Physicochem. Eng. Asp. 1999, 159, 351-358.

Thostenson, E. T.; Ren, Z.; Chou, T. W., Advances in the science and technology of carbon nanotubes and their composites: A review. Compos. Sci. Technol. 2001, 61, 1899-1912.

Tomka, I., Thermoplastic starch. Adv. Exp. Med. Biol. 1991, 302, 627-637.

Tsuji, H.; Ikada, Y., Blends of aliphatic polyesters. II. Hydrolysis of solution-cast blends from poly(L-lactide) and poly (ε-caprolactone) in phosphate-buffered solution. J. Appl. Polym. Sci. 1998, 67, 405-415.

Vaia, R. A.; Giannelis, E. P., Polymer melt intercalation in organically-modified layered silicates: Model predictions and experiment. Macromolecules 1997, 30, 8000-8009.

Van der Hart, D. L.; Atalla, R. H., Studies of microstructure in native celluloses using solid state 13C NMR. Macromolecules 1984, 17, 1465-1472.

Van Soest, J. J. G.; De Wit, D.; Tournois, H.; Vliegenthart, J. F. G., The influence of glycerol on structural changes in waxy maize starch as studied by Fourier transform infra-red spectroscopy. Polymer 1994, 35, 4722-4727.

Van Soest, J. J. G.; Hulleman, S. H. D.; De Wit, D.; Vliegenthart, J. F. G., Crystallinity in starch bioplastics. Ind. Crop. Prod. 1996a, 5, 11-22.

Van Soest, J. J. G.; De Wit, D.; Vliegenthart, J. F. G., Mechanical properties of thermoplastic waxy maize starch. J. Appl. Polym. Sci. 1996b, 61, 1927-1937.

Van Soest, J. J. G.; Hulleman, S. H. D.; De Wit, D.; Vliegenthart, J. F. G., Changes in the mechanical properties of thermoplastic potato starch in relation with changes in B-type crystallinity. Carbohydr. Polym. 1996c, 29, 225-232.

Van Soest, J. J. G.; Benes, K.; De Wit, D.; Vliegenthart, J. F. G., The influence of starch molecular mass on the properties of extruded thermoplastic starch. Polymer 1996d, 37, 3543-3552.

Van Soest, J. J. G.; Essers, P., Influence of amylose-amylopectin ratio on properties of extruded starch plastic sheets. J. Macromol. Sci. Part A-Pure Appl. Chem. 1997a, 34, 1665-1689.

Van Soest, J. J. G.; Borger, D. B., Structure and properties of compression-molded thermoplastic starch materials from normal and high-amylose maize starches. J. Appl. Polym. Sci. 1997b, 64, 631-644.

Van Soest, J. J. G.; Knooren, N., Influence of glycerol and water content on the structure and properties of extruded starch plastic sheets during aging. J. Appl. Polym. Sci. 1997c, 64, 1411-1422.

Vergnes, B.; Villemaire, J. P.; Colonna, P.; Tayeb, J., Interrelationships between thermomechanical treatment and macromolecular degradation of maize starch in a novel rheometer with preshearing. J. Cereal Sci. 1987, 5, 189.

Wang, S.; Chen, L.; Tong, Y., Structure-property relationship in chitosan-based biopolymer/montmorillonite nanocomposites. J. Polym. Sci. Pt. A-Polym. Chem. 2006, 44, 686-696.

Wang, S. F.; Shen, L.; Tong, Y. J.; Chen, L.; Phang, I. Y.; Lim, P. Q.; Liu, T. X., Biopolymer chitosan/montmorillonite nanocomposites: Preparation and characterization. Polym. Degrad. Stabil. 2005, 90, 123-131.

Wang, S. S.; Chiang, W. C.; Yeh, A. I.; Zhao, B.; KIM, I. H., Kinetics of Phase Transition of Waxy Corn Starch at Extrusion Temperatures and Moisture Contents. J. Food Sci. 1989, 54, 1298–1301.

Wang, X.; Du, Y.; Yang, J.; X., W.; Shi, X.; Hu, Y., Preparation, characterization and antimicrobial activity of chitosan/layered silicate nanocomposites. Polymer 2006, 47, 6738-6744.

Wibowo, A. C.; Misra, M.; Park, H. M.; Drzal, L. T.; Schalek, R.; Mohanty, A. K., Biodegradable nanocomposites from cellulose acetate: Mechanical, morphological, and thermal properties. Compos. Pt. A-Appl. Sci. Manuf. 2006, 37, 1428-1433.

Wilhelm, H.-M.; Sierakowski, M.-R.; Souza, G. P.; Wypych, F., Starch films reinforced with mineral clay. Carbohydr. Polym. 2003a, 52, 101-110.

Wilhelm, H.-M.; Sierakowski, M.-R.; Souza, G. P.; Wypych, F., The influence of layered compounds on the properties of starch/layered compound composites. Polym. Int. 2003b, 52, 1035-1044.

Wilkie, C. A.; Zhu, J.; Uhl, F., How Do Nanocomposites Enhance the Thermal. Stability of Polymers? Polymer Preprints 2001, 42, 392.

Wollerdorfer, M.; Bader, H., Influence of natural fibres on the mechanical properties of biodegradable polymers. Ind. Crop. Prod. 1998, 8, 105-112.

Xu, Y.; Zhou, J.; Hanna, M. A., Melt-intercalated starch acetate nanocomposite foams as affected by type of organoclay. Cereal Chem. 2005, 82, 105-110.

Xu, Y.; Ren, X.; Hanna, M. A., Chitosan/clay nanocomposite film preparation and characterization. J. Appl. Polym. Sci. 2006, 99, 1684-1691.

Yoshioka, M.; Takabe, K.; Sugiyama, J.; Nishio, Y., Newly developed nanocomposites from cellulose acetate/layered silicate/poly(ε-caprolactone): Synthesis and morphological characterization. J. Wood Sci. 2006, 52, 121-127.

Zeleznak, K. J.; Hoseney, R. C., The glass transition in starch. Cereal Chem. 1987, 64, 121-124.

Zhang, Q. X.; Yu, Z. Z.; Xie, X. L.; Naito, K.; Kagawa, Y., Preparation and crystalline morphology of biodegradable starch/clay nanocomposites. Polymer 2007, 48, 7193-7200.

Zobel, H. F., Molecules to granules: a comprehensive starch review. Starch-Starke 1988, 40, 44-50.

Chapitre II

-

Nano-biocomposites à base d'amidon et de montmorillonite

Introduction

La synthèse bibliographique réalisée dans le chapitre précédent a clairement mis en évidence les limites induites par la dispersion d'argiles dans une matrice amidon plastifiée par une concentration importante en glycérol (> 20 % en masse). En effet, au-delà d'une concentration de 10 % en masse de glycérol, les nano-biocomposites élaborés avec de la montmorillonite sodique (MMT-Na) présentent une morphologie intercalée. Par conséquent, l'étude que nous avons réalisée s'est focalisée sur l'organo-modification de la MMT-Na afin de changer la nature de l'interface matrice/nanocharge et donc de favoriser l'obtention de morphologies exfoliées. Cette partie se présente sous la forme de deux publications. La première publication traite de l'organo-modification de la montmorillonite par la « voie solvant ». La deuxième publication examinera plus particulièrement une nouvelle technique d'organo-modification des nanocharges par « voie fondue ».

La **Publication II** étudie l'influence de l'amidon cationique comme compatibilisant matrice/nanocharge sur le processus d'intercalation/exfoliation de la montmorillonite. Pour ce faire, la montmorillonite a été organo-modifiée par « voie solvant », c'est-à-dire par exfoliation/adsorption dans l'eau. L'OMMT-CS ainsi que la MMT-Na ont été dispersées dans une matrice amidon de blé au moyen d'un mélangeur interne. La nano-structuration des différents hybrides obtenus est analysée conjointement par DRXPA et MET. Par la suite, les propriétés mécaniques des nano-biocomposites ont été déterminées à l'aide de tests de traction uniaxiale puis reliées aux morphologies des nano-biocomposites d'amidon obtenus.

La **Publication III** se focalise plus particulièrement sur le développement et la description d'un nouveau procédé appelé « shear induced clay organo-modification ». Cette approche rend possible l'organo-modification simple et rapide des feuillets de montmorillonite par « voie fondue ». L'intérêt de ce protocole est étudié par la préparation conjointe d'OMMT-CS par « voie fondue » et par la « voie solvant ». Ces nanocharges sont ensuite introduites dans des matrices amidon plastifié (blé, pois et amylomaïs) par malaxage au sein d'un mélangeur interne. Les matériaux ainsi obtenus ont été caractérisés par DRXPA et des tests de traction uniaxiale afin de comparer les deux protocoles d'organo-modification.

New Approach to Elaborate Exfoliated Starch-Based Nanobiocomposites

Frédéric CHIVRAC, Eric POLLET, Marc SCHMUTZ and Luc AVEROUS

Biomacromolecules, 2008, vol. 9 , n° 3, pages 896–900

Publication II : pages 117-129 :

UNIVERSITÉ DE STRASBOURG

Publication II : Discussion et commentaires

Cette étude a porté sur l'obtention de nano-biocomposites exfoliés dans des matrices amidons surplastifiées en glycérol. Pour ce faire, un nouveau compatibilisant, l'amidon cationique, a été utilisé afin de modifier l'interface matrice/nanocharge. L'organo-modification des feuillets de montmorillonite par l'amidon cationique a été effectuée selon une approche « voie solvant » par un processus d'exfoliation/adsorption dans l'eau.

Afin de montrer l'intérêt de cette organo-modification, des nano-biocomposites d'amidon ont été élaborés avec de l'OMMT-CS et de la MMT-Na. Les nano-hybrides élaborés avec la MMT-Na présentent une structure faiblement intercalée avec essentiellement intercalation du glycérol dans l'espace inter-feuillets. A l'opposé, les nano-biocomposites préparés avec l'OMMT-CS présentent une morphologie exfoliée, sans orientation préférentielle des feuillets de montmorillonite. Par ailleurs, les analyses de MET ont mis en évidence une séparation de phase entre des domaines riches et pauvres en glycérol. L'origine de cette hétérogénéité est traitée dans la **Publication IV**.

L'influence de la nano-structuration (intercalée vs. exfoliée) sur la viscosité à l'état fondu et les propriétés mécaniques a ensuite été étudiée. Ces analyses ont montré que la MMT-Na entraine une augmentation de la viscosité à l'état fondu et une fragilisation des nano-biocomposites. A l'inverse, l'obtention d'une structure exfoliée n'augmente pas la viscosité à l'état fondu, les feuillets individualisés de montmorillonite pouvant être plus aisément orientés par le cisaillement lors de la mise en œuvre. En outre, il a clairement été démontré que l'obtention d'une morphologie exfoliée améliore de manière significative les propriétés mécaniques de ces matériaux nano-biocomposites d'amidon avec une augmentation du module d'Young sans diminution de l'allongement à la rupture.

Ces analyses ont donc mis en évidence la possibilité d'obtenir un matériau à la structure exfoliée présentant des propriétés améliorées en utilisant l'amidon cationique comme compatibilisant amidon/montmorillonite. Cependant, l'organo-modification des feuillets de montmorillonite par « voie solvant » est un procédé long, coûteux et peu respectueux de l'environnement. C'est pourquoi nous nous sommes intéressés dans la **Publication III** à la possibilité d'organo-modifier cette nanocharge par la « voie fondue », cette approche ayant l'avantage d'être beaucoup plus simple, directe et rapide.

Shear induced clay organo-modification: application to plasticized starch nano-biocomposites

Frédéric CHIVRAC, Eric POLLET and Luc AVEROUS

Polymers for Advanced Technologies, 2009 published online : 28 may 2009

Publication III : pages 133-147 :

La publication présentée ici dans la thèse est soumise à des droits détenus par un éditeur commercial.

Les utilisateurs de l'UdS peuvent consulter cette publication sur le site de l'éditeur :
http://dx.doi.org/10.1002/pat.1468

La version imprimée de cette thèse peut être consultée à la bibliothèque ou dans un autre établissement via une demande de prêt entre bibliothèques (PEB) auprès de nos services :
http://www-sicd.u-strasbg.fr/services/peb/

UNIVERSITÉ DE STRASBOURG

Publication III : Discussion et commentaires

Cette étude nous a permis de développer un nouveau procédé simple et rapide d'organo-modification des argiles par « voie fondue » sous traitement thermomécanique, nommé « shear induced clay organo-modification ».

Cette organo-modification est rendue possible à la fois par le gonflement de la montmorillonite dans l'eau et par le cisaillement lors du mélangeage . Ces deux phénomènes modifient la structure tactoïdique de la nanocharge et permettent la diffusion de l'amidon cationique dans l'espace inter-feuillets, cette diffusion diminuant les forces d'attraction inter-feuillets. Lorsque les conditions (temps, énergie) le permettent, les interactions feuillets/feuillets sont suffisamment faibles pour permettre la délamination de la montmorillonite et l'obtention d'une nanocharge à la fois organo-modifiée et pré-exfoliée.

Afin de démontrer le potentiel important de ce procédé, des montmorillonites organo-modifiées en « voie fondue » et en « voie solvant » ont été incorporées dans une matrice d'amidon plastifié. Les matériaux obtenus ont été étudiés par DRXPA et par traction uniaxiale. D'après ces analyses, ces deux protocoles d'organo-modification permettent, de manière équivalente, l'obtention de nanocharges exfoliées, les nano-biocomposites obtenus présentant les mêmes propriétés mécaniques. L'intérêt de la « voie fondue » par rapport à la « voie solvant » a ainsi été clairement démontré.

Ce procédé doit maintenant être testé avec d'autres approches ; notamment des techniques d'élaboration en continu de type extrusion. Celles-ci permettraient d'organomodifier les nanocharges et d'élaborer les nano-biocomposites en deux étapes successives sur une même ligne de production ; et donc de réduire le coût de ces matériaux nano-hybrides. Ces études doivent également s'orienter vers d'autres types d'argiles (hectorite, laponite…), d'organo-modifiants et une large gamme de matrices polymères afin d'élargir au maximum le champ d'application de ce procédé.

Chapitre II : Conclusions et perspectives

Ce chapitre, au travers de ces deux études, aura permis de montrer les différentes possibilités d'obtention de nano-biocomposites exfoliés avec des matrices amidon surplastifiées par du glycérol. Pour cela, nous avons utilisé un « nouveau compatibilisant » original pour l'élaboration de nanocomposites, l'amidon cationique. Cette modification de la surface des feuillets de montmorillonite a été effectuée selon deux protocoles distincts correspondant respectivement à une approche classique par « voie solvant » et une approche novatrice rapide et efficace qu'est la « voie fondue ». Dans les deux cas, cette organo-modification a conduit à une morphologie exfoliée améliorant de manière significative les propriétés de ces nanomatériaux.

Afin de réaffirmer l'intérêt de l'amidon cationique en tant que compatibilisant amidon/nanocharge, les études réalisées dans le – **Chapitre III** – vont s'attarder sur l'élaboration de nano-biocomposites d'amidon en modifiant la nature d'éléments de la formulation : le plastifiant et la nanocharge.

Références du Chapitre II

Alexandre, M.; Dubois, P., Polymer-layered silicate nanocomposites: Preparation, properties and uses of a new class of materials. Mater. Sci. Eng. R-Rep. 2000, 28, 1-63.

Averous, L.; Moro, L.; Dole, P.; Fringant, C., Properties of thermoplastic blends: Starch-polycaprolactone. Polymer 2000, 41, 4157-4167.

Averous, L., Biodegradable multiphase systems based on plasticized starch: A review. J. Macromol. Sci. Part C-Polym. Rev. 2004a, 44, 231-274.

Averous, L.; Boquillon, N., Biocomposites based on plasticized starch: Thermal and mechanical behaviours. Carbohydr. Polym. 2004b, 56, 111-122.

Bagdi, K.; Muller, P.; Pukanszky, B., Thermoplastic starch/layered silicate composites: Structure, interaction, properties. Compos. Interfaces 2006, 13, 1-17.

Chiou, B.-S.; Yee, E.; Wood, D.; Shey, J.; Glenn, G.; Orts, W., Effects of processing conditions on nanoclay dispersion in starch-clay nanocomposites. Cereal Chem. 2006, 83, 300-305.

Chivrac, F.; Kadlecova, Z.; Pollet, E.; Averous, L., Aromatic copolyester-based nano-biocomposites: Elaboration, structural characterization and properties. J. Polym. Environ. 2006, 14, 393-401.

Chivrac, F.; Pollet, E.; Averous, L., Nonisothermal crystallization behavior of poly(butylene adipate-co-terephthalate)/clay nano-biocomposites. J. Polym. Sci. Pt. B-Polym. Phys. 2007, 45, 1503-1510.

Chivrac, F.; Pollet, E.; Schmutz, M.; Averous, L., New Approach to Elaborate Exfoliated Starch-Based Nanobiocomposites. Biomacromolecules 2008, 9, 896-900.

Dean, K.; Yu, L.; Wu, D. Y., Preparation and characterization of melt-extruded thermoplastic starch/clay nanocomposites. Compos. Sci. Technol. 2007, 67, 413-421.

Dennis, H. R.; Hunter, D. L.; Chang, D.; Kim, S.; White, J. L.; Cho, J. W.; Paul, D. R., Effect of melt processing conditions on the extent of exfoliation in organoclay-based nanocomposites. Polymer 2001, 42, 9513-9522.

Fornes, T. D.; Yoon, P. J.; Keskkula, H.; Paul, D. R., Nylon 6 nanocomposites: The effect of matrix molecular weight. Polymer 2001, 42, 9929-9940.

Fornes, T. D.; Paul, D. R., Modeling properties of nylon 6/clay nanocomposites using composite theories. Polymer 2003, 44, 4993-5013.

Gain, O.; Espuche, E.; Pollet, E.; Alexandre, M.; Dubois, P., Gas barrier properties of poly(ε-caprolactone)/clay nanocomposites: Influence of the morphology and polymer/clay interactions. J. Polym. Sci. Pt. B-Polym. Phys. 2005, 43, 205-214.

Gorrasi, G.; Tortora, M.; Vittoria, V.; Pollet, E.; Lepoittevin, B.; Alexandre, M.; Dubois, P., Vapor barrier properties of polycaprolactone montmorillonite nanocomposites: Effect of clay dispersion. Polymer 2003, 44, 2271-2279.

Gorrasi, G.; Tortora, M.; Vittoria, V.; Pollet, E.; Alexandre, M.; Dubois, P., Physical Properties of Poly(ε-caprolactone) Layered Silicate Nanocomposites Prepared by Controlled Grafting Polymerization. J. Polym. Sci. Pt. B-Polym. Phys. 2004, 42, 1466-1475.

Huang, M. F.; Yu, J. G.; Ma, X. F.; Jin, P., High performance biodegradable thermoplastic starch - EMMT nanoplastics. Polymer 2005, 46, 3157-3162.

Kampeerapappun, P.; Aht-ong, D.; Pentrakoon, D.; Srikulkit, K., Preparation of cassava starch/montmorillonite composite film. Carbohydr. Polym. 2007, 67, 155-163.

Lepoittevin, B.; Devalckenaere, M.; Pantoustier, N.; Alexandre, M.; Kubies, D.; Calberg, C.; Jerome, R.; Dubois, P., Poly (ε-caprolactone)/clay nanocomposites prepared by melt intercalation: mechanical, thermal and rheological properties. Polymer 2002, 43, 4017-4023.

Luo, J. J.; Daniel, I. M., Characterization and modeling of mechanical behavior of polymer/clay nanocomposites. Compos. Sci. Technol. 2003, 63, 1607-16.

Martin, O.; Averous, L., Poly(lactic acid): Plasticization and properties of biodegradable multiphase systems. Polymer 2001, 42, 6209-6219.

Park, H. M.; Li, X.; Jin, C. Z.; Park, C. Y.; Cho, W. J.; Ha, C. S., Preparation and properties of biodegradable thermoplastic starch/clay hybrids. Macromol. Mater. Eng. 2002, 287, 553-558.

Park, H. M.; Lee, W. K.; Park, C. Y.; Cho, W. J.; Ha, C. S., Environmentally friendly polymer hybrids Part I mechanical, thermal, and barrier properties of thermoplastic starch/clay nanocomposites. J. Mater. Sci. 2003, 38, 909-915.

Pollet, E.; Delcourt, C.; Alexandre, M.; Dubois, P., Organic-inorganic nanohybrids obtained by sequential copolymerization of ε-caprolactone and L,L-lactide from activated clay surface. Macromol. Chem. Phys. 2004, 205, 2235-2244.

Sinha Ray, S.; Okamoto, M., Polymer/layered silicate nanocomposites: A review from preparation to processing. Prog. Polym. Sci. 2003, 28, 1539-1641.

Swanson, C. L.; Shogren, R. L.; Fanta, G. F.; Imam, S. H., Starch-plastic materials-Preparation, physical properties, and biodegradability (a review of recent USDA research). J. Environ. Polym. Deg. 1993, 1, 155-166.

Tomka, I., Thermoplastic starch. Adv. Exp. Med. Biol. 1991, 302, 627-637.

Vaia, R. A.; Ishii, H.; Giannelis, E. P., Synthesis and properties of two-dimensional nanostructures by direct intercalation of polymer melts in layered silicates. Chem. Mat. 1993, 5, 1694-1696.

Vaia, R. A.; Giannelis, E. P., Polymer melt intercalation in organically-modified layered silicates: Model predictions and experiment. Macromolecules 1997, 30, 8000-8009.

Wilhelm, H.-M.; Sierakowski, M.-R.; Souza, G. P.; Wypych, F., The influence of layered compounds on the properties of starch/layered compound composites. Polym. Int. 2003a, 52, 1035-1044.

Wilhelm, H.-M.; Sierakowski, M.-R.; Souza, G. P.; Wypych, F., Starch films reinforced with mineral clay. Carbohydr. Polym. 2003b, 52, 101-110.

Xu, W.; Ge, M.; He, P., Nonisothermal crystallization kinetics of polypropylene/montmorillonite nanocomposites. J. Polym. Sci. Pt. B-Polym. Phys. 2002, 40, 408-414.

Zhang, X.; Do, M. D.; Dean, K.; Hoobin, P.; Burgar, I. M., Wheat-gluten-based natural polymer nanoparticle composites. Biomacromolecules 2007, 8, 345-353.

Chapitre III

-

Nano-biocomposites d'amidon : Étude de l'influence du type de plastifiant *(glycérol vs. sorbitol)* et de nanocharge *(montmorillonite vs. sépiolite)*

Introduction

Dans cette partie, nous allons faire varier les différents éléments de la formulation de base des nano-biocomposites, à savoir le plastifiant et la nanocharge, et étudier leur impact sur les nano-hybrides. Cette partie se présente sous la forme de deux publications. La première publication étudie l'influence du plastifiant utilisé sur les nano-hybrides amidon de blé/montmorillonite. La deuxième publication traite de l'élaboration de nano-biocomposites amidon à partir d'une nanocharge argileuse aciculaire originale et peu utilisée, la sépiolite.

La **Publication IV** fait état de l'influence de la nature du plastifiant (glycérol, sorbitol et un mélange des deux : le Polysorb®), sur le processus d'intercalation/exfoliation de montmorillonites sodique et organo-modifiée par de l'amidon cationique. Pour cela, différents nano-hybrides ont été élaborés par voie fondue au sein d'un mélangeur interne, puis analysés par DRXPA, afin de caractériser la structuration des feuillets de montmorillonite au sein de la matrice. Ces différentes morphologies ont ensuite été corrélées aux propriétés macroscopique (mécanique, thermique, teneur en eau) du matériau.

La **Publication V** rapporte pour la première fois l'incorporation au sein d'une matrice amylacée d'une nanocharge argileuse de structure aciculaire et jusqu'ici très peu utilisée : la sépiolite. Cette nanocharge a été dispersée sous deux formes différentes, sépiolite sodique ou organo-modifiée avec de l'amidon cationique. Les nano-hybrides amidon/sépiolite ont été élaborés par voie fondue dans un mélangeur interne. La structuration de ces aiguilles de sépiolite dans la matrice amidon de blé plastifié est mise en évidence par MET. Par la suite, l'influence de l'état de dispersion de ces nanocharges sur les propriétés finales (cristallinité, stabilité thermique et mécaniques) a été étudiée et comparée à celles des nano-biocomposites amidon/montmorillonite.

Publication IV – Starch-Based Nano-Biocomposites: Plasticizer Impact on the Montmorillonite Exfoliation Process

Frédéric Chivrac[1], Eric Pollet[1], Patrice Dole[2], Luc Avérous[1]*

I. Abstract

The present paper analyzes the effects of the plasticizer nature on the clay exfoliation process into starch-based nano-biocomposites. The nano-hybrids have been elaborated by melt blending starch with different plasticizers, such as glycerol, sorbitol and Polysorb[®], which is a mix of both previous plasticizers. In addition two types of nanofillers, namely, natural montmorillonite (MMT-Na) and montmorillonite organo-modified with cationic starch (OMMT-CS) have been tested. Intercalated/aggregated and exfoliated morphologies were obtained with, respectively, MMT-Na and OMMT-CS as the nanofillers and glycerol as the plasticizer. Morphological analyses combined with uniaxial tensile tests have shown the negative effect of the sorbitol on the exfoliation extent into such nano-materials. Besides, thermo-mechanical analyses revealed the occurrence of a phase separation between domains rich and without nanofillers induced by the high plasticizer content of the starch formulations.

KEYWORDS: Nano-biocomposites, starch, montmorillonite, plasticizer, clay, exfoliation.

* Corresponding author: Luc Avérous.

Tel.: +33-3-90-242-707 - Fax: +33-3-90-242-716 - AverousL@ecpm.u-strasbg.fr

[1]LIPHT-ECPM, UMR 7165, Université Louis Pasteur, 25 rue Becquerel, 67087 Strasbourg Cedex 2, France

[2]INRA Reims, Bat. Europol'Agro – Moulin de la Housse, 51100 Reims, France

II. Introduction

Nano-biocomposites are a new class of hybrid materials composed of nano-sized filler (nanofiller) incorporated into a bio-based matrix (Chivrac, F., 2006). Such an association between eco-friendly biopolymers and nano-objects, with the aim to obtain synergic effects, is one of the most innovating routes to enhance the properties of these bio-matrices (Alexandre, M., 2000).

Depending on the geometry and the nature of the nanofiller, new and/or improved properties (gas barrier, mechanical stiffness, transparency, thermal stability…) can be obtained (Gain, O., 2005, Gorrasi, G., 2003, Sinha Ray, S., 2003). Such properties enhancements rely both on the nanofiller geometry and on its surface area, which is directly linked to the nanofiller dispersion state.

In the case of layered silicates (e.g. montmorillonite), depending on the process conditions and on the matrix/nanofiller affinity, the clay platelets can either be intercalated by macromolecules and/or exfoliated, leading different behaviors. Intercalated structures show regularly alternating silicate layers and polymer chains compared to exfoliated structures in which the clay platelets are individually delaminated and fully dispersed into the polymer matrix. The best performances are commonly observed with the latter structure (Alexandre, M., 2000, Sinha Ray, S., 2003).

At the present, it is well known that starch, which is an inherently biodegradable and renewable material, is a promising answer to develop new environmentally friendly materials especially for packaging and disposable applications. Several authors have already demonstrated the possibility to transform native starch into thermoplastic resin-like products under destructuring and plasticization conditions with small water contents and, often, higher polyols concentration (Swanson, C.L., 1993, Tomka, I., 1991). Nevertheless, the water sensitivity and the brittleness of these materials have to be overcame to obtain suitable "green" plastics (Averous, L., 2004a). To reduce these weaknesses, the elaboration of plasticized starch-based nano-biocomposites appears as a rising option (Park, H.M., 2002, Park, H.M., 2003). Since plasticized starch is hydrophilic, most of the first studies were focused on the dispersion of natural and non organo-modified montmorillonite (MMT-Na), to achieve an exfoliated morphology (Chiou, B.-S., 2006, Chiou, B.S., 2007, Cyras, V.P., 2008a, Dean, K., 2007, Lilichenko, N., 2008, Mondragon, M., 2008, Park, H.M., 2002, Park, H.M., 2003, Tang, X., 2008b). However, it has been shown that for glycerol content higher than 10

wt%, such systems leads to the formation of an intercalated structure with a clay inter-layer spacing (d_{001}) of 18 Å corresponding mainly to glycerol intercalation (Pandey, J.K., 2005, Park, H.M., 2003, Tang, X., 2008b). The same behavior has been reported by Ma et al. (Ma, X., 2007) with sorbitol as the nano-biocomposite plasticizer. Consequently, these results have highlighted the great influence of the plasticizers on the clay intercalation/exfoliation process and thus on the resulting properties.

To overcome the limit of the plasticizer preferential intercalation, some authors have focused their attention on the organo-modification of the clay surface. The use of cationic starch is, up to now, the most efficient strategy to obtain an exfoliated morphology with highly glycerol plasticized systems (Chivrac, F., 2008b). However, even if this strategy is well adapted for glycerol plasticized systems, its efficiency has not been proved for other types of polyol plasticizers. Therefore, the aim of this work is the study of the montmorillonite exfoliation process into starch nano-biocomposites plasticized with sorbitol and a mixture of glycerol/sorbitol commercially named Polysorb®. The influence of these plasticizers on the exfoliation process will be highlighted thanks to morphological, water desorption, thermal and mechanical analyses.

III. Experimental part

1. Materials

Wheat starch (WS) was supplied by Roquette (France). The amylose and amylopectin contents are 23 and 77%, respectively. Residual protein content is less than 1 %. The glycerol, Polysorb® and sorbitol used as non-volatile plasticizers were supplied by Roquette (France). Glycerol was a 99.5% purity product. The sorbitol was a water/sorbitol solution (79.2/20.8 by weight). Supplied by Roquette (France), the Polysorb® was a glycerol/sorbitol mixture (59/41 by weight). The cationic starch has also been supplied by Roquette (France). Its charge density is 944 µequiv.g^{-1}. The cationic functions are quaternary ammonium with chloride as counter-anion. The Dellite® LVF sodium montmorillonite (MMT-Na) was supplied by Laviosa Chimica Mineraria S.p.A. (Italy) and has a cationic exchange capacity (CEC) of 1050 µequiv.g^{-1}.

2. Samples preparation

STARCH DRY-BLENDS PREPARATION. The formulation used in this study contained 54 wt% of native starch, 23 wt% of polyol plasticizer and 23 wt% of water. The water was

introduced with the clay during the nano-biocomposites elaboration, as described below. Granules of plasticized starch were prepared according to the following procedure. Native wheat starch was first dried overnight at 70 °C in a ventilated oven. Then, the starch powder was introduced into a turbo-mixer and the plasticizer (glycerol, Polysorb® or sorbitol), was slowly added under stirring. After complete addition of the plasticizer, the mixture was mixed at high speed (1700 rpm) to obtain a homogeneous dispersion. The mixture was then placed in a ventilated oven at 170 °C for 40 min and occasionally stirred, allowing vaporization of water and diffusion of the plasticizers into the starch granules. The powder was then stored in polyethylene bag.

ORGANO-MODIFIED MONTMORILLONITE PREPARATION. The MMT-Na organo-modification has been carried out with a Shear Induced Clay Organo-modification process (SICO). In this organo-modification process, 11.0 g of MMT-Na, 12.3 g of cationic starch and 52 ml of distilled water were first premixed to obtain a "gel". The cationic starch and MMT-Na proportions match the charge equivalence between these two compounds. Then, this mixture was introduced into an internal batch mixer, Rheocord 9000 (Haake, USA), at 70 °C for 40 min with a rotor speed of 100 rpm. After processing, the OMMT-CS was obtained in a swollen state as a paste. The amounts of the different compounds correspond to the nano-biocomposite formulation filled with 6 wt% of clay. To elaborate nano-biocomposites filled with 3 wt% of clay, 56.0 g of water are added to this OMMT-CS/water paste to obtain a diluted paste.

NANO-BIOCOMPOSITES ELABORATION. In this protocol, the nano-clay was introduced into the dry-blend in a swollen state to elaborate nano-biocomposite hybrid materials filled with 3 to 6 wt% of inorganic clay content (compared to the weight of starch and glycerol). For nano-hybrids elaborated with non-modified montmorillonite (MMT-Na), from 1.38 g to 2.86 g of MMT-Na have been introduced into 13.5 ml of water and dispersed with an ultra-sonic bath at 60 °C for 4 h to obtain the swollen clay. Then this swollen clay is introduced into the dry-blend. For the nano-hybrid based on OMMT-CS, the nanoclay is already obtained into a swollen state after the SICO process. Thus, to elaborate the nano-biocomposites field with 6 wt% of clay, 19.52 g of the OMMT-CS/water mixture is added to the dry-blend. For the nano-biocomposites field with 3 wt% of clay, 16.37 g of the diluted OMMT-CS/water mixture are introduced into the dry-blend. Then, the dry blend and the swollen clay were introduced together into a counter-rotating internal batch mixer. The starch nano-biocomposites were prepared by mechanical kneading with a residence time of 20 min and with a rotor speed of

150 rpm. After melt processing, molded specimens and films were obtained by hot-pressing at 110 °C, applying 20 MPa pressure for 15 min. The samples of starch-based nano-biocomposites were then equilibrated at 23 °C and 33, 57 or 75 %RH (relative humidity percentage) during 1 month before characterization.

Throughout this paper, the samples are designated WS/ZZZ/XXX y% where WS stands for wheat starch, ZZZ for the type of plasticizer (Gly for glycerol, Polysorb for Polysorb® or Sorb for sorbitol), XXX for the type of (organo)clay (MMT-Na or OMMT-CS) and y for the weight percentage of clay inorganic fraction.

3. Characterization

SAXD. The small angle X-Ray diffraction (SAXD) morphological analyses were performed on a powder diffractometer Siemens D5000 (Germany) using Cu (Kα) radiation (λ = 1.5406 Å) at room temperature in the range of 2θ = 1.5 to 10° by step of 0.01° of 4 s, each. The clay inter-layer spacing values (d_{001}) were calculated from the MMT diffraction peak using the Bragg's law (Equation IV.1).

$$2d_{001} \sin \theta = n\lambda \qquad\qquad\qquad\qquad (IV.1)$$

WATER DESORPTION ANALYSES. The water contents of the samples were estimated on a MB45 moisture analyzer (Ohaus corporation, USA) on films of 1.2 mm thickness considering the weight loss measured after 8h of drying at 95 °C.

TGA CHARACTERIZATION. The thermogravimetric analyses (TGA) were performed on a Hi-Res TGA 2950 apparatus from TA Instruments (USA). For all starch/clay nano-biocomposites, the analyses were carried out under "synthetic air", which is a mixture of 75% N_2 and 25% O_2. The clay content in inorganics (in wt%) of each composite was assessed by the combustion residue left at 600 °C.

DMTA. Thermo-mechanical properties of the different nano-biocomposites were determined using tensile geometry with a dynamic thermo-mechanical analyzer (TA instrument DMA 2980, USA). Samples were cut to get specimens with dimensions 0.9 x 9.5 x 24.5 mm^3. The displacement amplitude was set to 15 µm. The measurements were performed at a frequency of 1 Hz. The range of temperature was from -70 °C to 70 °C at the scanning rate of 3 °C/min.

TENSILE TESTS. Tensile tests were carried out with an Instron tensile testing machine (model 4204, USA), on dumbbell-shaped specimens; at 25 °C with a constant deformation rate of 5 mm/min. For each formulation five samples were tested.

IV. Results and discussion

1. Morphology

Figure IV.1 displays the typical SAXD curves recorded for MMT-Na and WS/MMT-Na 6 wt% nano-biocomposites plasticized with glycerol, Polysorb® and sorbitol. The MMT-Na diffraction pattern displays an intense diffraction peak at 2θ angle of 7.3° corresponding to a clay interlayer spacing value (d_{001}) of 12 Å. As expected, all the nano-biocomposites samples display a diffraction peak located at 4.9° corresponding to a d_{001} value of 18 Å. The presence of this diffraction peak reveals that these materials are mainly intercalated, whatever the type of plasticizer, and that only few starch chains have been incorporated into the clay inter-layer spacing. This result is in agreement with the literature in which it is mentioned that both glycerol and sorbitol, by their preferential intercalation, lead to the formation of intercalated structures in highly plasticized starch nano-biocomposite hybrid materials (Ma, X., 2007, Pandey, J.K., 2005, Park, H.M., 2003, Tang, X., 2008b).
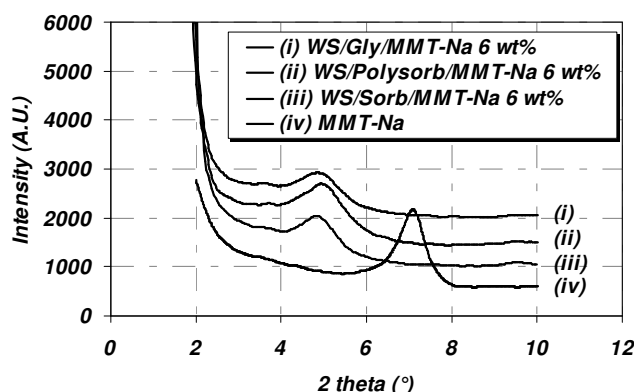
Figure IV.1. SAXD patterns for MMT-Na and WS/MMT-Na 6 wt% nano-biocomposites plasticized with glycerol, Polysorb® or sorbitol.

Figure IV.2 displays the typical SAXD curves recorded for OMMT-CS and WS/OMMT-CS 6 wt% nano-biocomposites plasticized with glycerol, Polysorb® and sorbitol. The diffraction pattern of OMMT-CS displays an intense peak at 3.6° corresponding to a d_{001} value of 24.5 Å. It can be shown from these experiments that the WS/Gly/OMMT-CS 6 wt% diffractogram displays no diffraction peak suggesting a completely exfoliated morphology. On the contrary, diffractograms of both the WS/Polysorb/OMMT-CS and WS/Sorb/OMMT-CS nano-biocomposites with 6 wt% of clay display a wide and low intensity diffraction peak corresponding to a $d_{001} = 25$ Å. This value almost directly corresponds to the initial OMMT-CS clay interlayer spacing before incorporation into the starch matrix. According to these

experiments, one may suppose that intercalated/exfoliated structures, with small clay tactoïds remaining, are obtained with either Polysorb® or sorbitol.
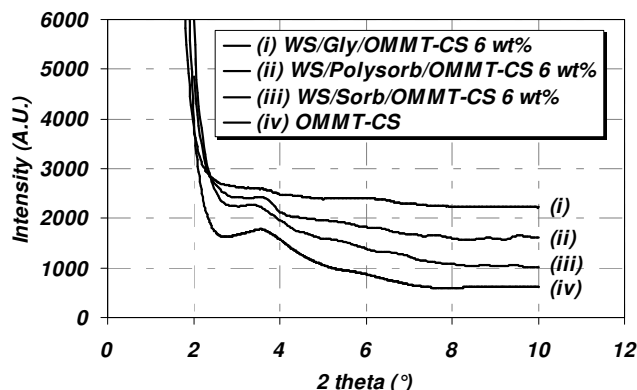
Figure IV.2. SAXD patterns for OMMT-CS and WS/OMMT-CS 6 wt% nano-biocomposites plasticized with glycerol, Polysorb® or sorbitol.

2. Water content

The water content of the different unfilled matrices and nano-biocomposite hybrid materials have been determined by desorption measurements, after one month equilibration. Water content is determined from the mass decrease. The unfilled matrices water content variations determined at different storage relative humidity are presented in Figure IV.3. It is seen from this graph that whatever the storage relative humidity, the water content of the glycerol plasticized nano-biocomposites is higher than those of the other plasticizers in agreement with previous results on plasticized starch (Gaudin, S., 1999, Lourdin, D., 2003). The lower water content is obtained with the sorbitol-based materials. These results are explained by the higher hydrophilic character of the glycerol compared to sorbitol.
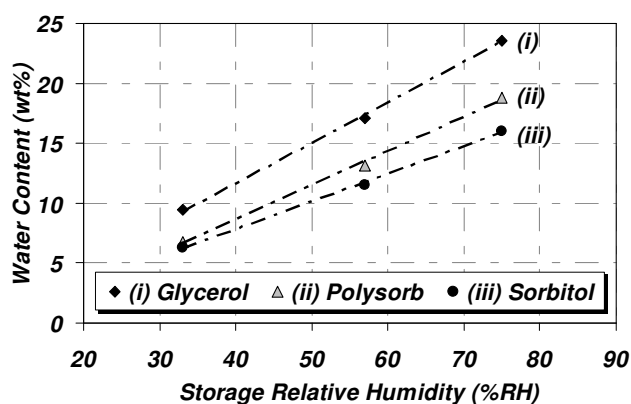
Figure IV.3. Water content of wheat starch plasticized with glycerol, Polysorb® or sorbitol against storage relative humidity.

These desorption experiments have been performed on nano-biocomposite materials to understand the influence of the nanofiller content and dispersion state on the water content after equilibrium. The water contents obtained for the different starch nano-biocomposites are summarized in the Table IV.1. According to these data, the introduction of the nanofiller induces only small modifications of the water content without clear and interpretable trends. This is likely linked to the hydrophilic nature of the nanofillers that do not vary the overall hydrophilicity of the plasticized starch matrices. Nevertheless, as already mentioned, the water contents measured for glycerol-plasticized materials are higher than those recorded for Polysorb[®] or sorbitol due to higher hydrophilicity of this plasticizer.

Table IV.1. Water content of starch nano-biocomposite plasticized with glycerol, Polysorb[®] or sorbitol at different relative humidities (%RH).

	33 %RH			57 %RH			75 %RH		
	Gly	Polysorb[®]	Sorb	Gly	Polysorb[®]	Sorb	Gly	Polysorb[®]	Sorb
WS/MMT-Na 3 wt%	7.8	7.0	6.0	16.4	13.1	11.5	24.2	18.8	16.7
WS/MMT-Na 6 wt%	8.4	7.5	6.8	16.8	13.3	11.8	25.0	19.0	16.9
WS/OMMT-CS 3 wt%	8.9	6.9	6.4	18.5	13.1	11.8	24.4	19.1	17.1
WS/OMMT-CS 6 wt%	9.1	6.7	6.2	19.6	14.7	12.6	24.7	19.0	17.1

3. Thermo-mechanical properties

Thermo-mechanical measurements have been performed on starch nano-biocomposites to analyze the plasticizer and nanofiller impact on their thermal properties. Figure IV.4 displays the tan δ curves recorded for the unfilled plasticized starch matrices. For each plasticizer, two relaxations peaks are observed. Such behavior is associated to the high plasticizer content of the starch formulation which leads to a phase separation between domains rich in carbohydrate chains and domains rich in plasticizer (Lourdin, D., 1997c, Lourdin, D., 1998). The main relaxation (named α) is attributed to the plasticized starch T_g. The second relaxation (named β) is consistent with the plasticizer glass transition and occurs at lower temperature. A shift of both the α and β transition is observed and correlated to the ratio sorbitol/plasticizer. Such a behavior is related to the higher plasticizing efficiency of glycerol compared to sorbitol and to the higher water uptake at equilibrium with glycerol.

Table IV.2 displays the T_α and T_β variations vs. clay content for starch nano-biocomposites plasticized with glycerol, Polysorb[®] and sorbitol. For T_β, only small variations, which are not significant, are observed. Such trend may suggest that the clay nano-platelets have no effect on the T_g of the domains rich in plasticizer. On the opposite, an increase in the

T_α versus clay content is observed with all the plasticizers. At 3 wt% of clay loading, the nano-biocomposites prepared with both OMMT-CS and MMT-Na display the same T_α. For higher clay content, the T_α recorded with MMT-Na as the nanofiller are slightly higher than for those elaborated with OMMT-CS. Since the better the dispersion, the higher the clay/matrix interface, a higher T_α was expected for the WS/OMMT-CS samples. This unexpected behavior could be explained by the morphology of the WS/MMT-Na nano-hybrid. It has been demonstrated that such nano-biocomposites display an intercalated structure with preferential plasticizer intercalation. Consequently, a part of these plasticizers is immobilized into the galleries of clay platelets and cannot plasticize the starch matrix, explaining the higher T_α obtained for the WS/MMT-Na 6 wt% nano-biocomposites.
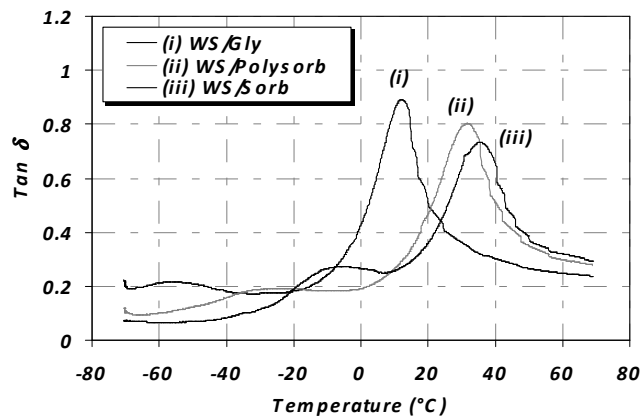
Figure IV.4. Tan δ vs. temperature for WS plasticized with glycerol, Polysorb$^\circledR$ or sorbitol.

Table IV.2. T_α and T_β vs. clay inorganic content for starch nano-biocomposites plasticized with (a.) glycerol, (b) Polysorb$^\circledR$ or (c) sorbitol.

	T_α (°C)			T_β (°C)		
	Gly	Polysorb$^\circledR$	Sorb	Gly	Polysorb$^\circledR$	Sorb
WS	11.7	31.7	35.3	-54.6	-23.6	-6.1
WS/MMT-Na 3 wt%	15.7	36.5	41.7	-54.9	-22.9	-6.0
WS/MMT-Na 6 wt%	23.9	38.5	49.8	-50.56	-21.1	-6.0
WS/OMMT-CS 3 wt%	14.9	35.2	41.8	-53.56	-22.9	-6.7
WS/OMMT-CS 6 wt%	21.7	38.4	47.1	-51.6	-22.2	-4.9

These results also have to be related to our previous observations from TEM analyses (Chivrac, F., 2008b) where a phase separation was observed between domains rich in clay platelets and domains without nanofiller. We supposed that this phase separation was induced by the high glycerol content of the formulation and that the nanofillers were dispersed

into the glycerol-rich domains. Such assumption was based on the high affinity between the clay platelets and the polyol plasticizers. According to the thermo-mechanical analyses performed here, only T_α is influenced by the addition of clay and shifted to higher temperature. However, this shift alone is not sufficient to localize the clays into the material. Complementary experiments, such as nanoindentation and dielectrical analyses are currently performed to better understand the mechanism of this phase separation.

4   Mechanical properties

Figure IV.5 displays the Young's modulus variations of plasticized starch nano-biocomposites filled with 3 to 6 wt% of (O)MMT and stabilized at 57 %RH. It is shown that the plasticizer nature greatly influences the plasticized starch stiffness. The Young's modulus of starch plasticized with Polysorb® is higher than that of the glycerol plasticized one, the highest stiffness properties being obtained with sorbitol as the plasticizer. This trend seems to be related to the sorbitol/plasticizer ratio. Since the water content of these matrices is also linked to this ratio, most of these variations are correlated to the water content of the materials which affects the starch stiffness properties.

For all the plasticized starch nano-biocomposites, whatever the type of plasticizer, an increase in the matrix stiffness is observed and correlated to the clay content. This increase in stiffness is commonly observed in nano-biocomposite materials and is related to the clay hardness, its dispersion state and to the nanofiller/matrix interface (Luo, J.J., 2003). As expected, the WS/Gly/OMMT-CS nano-biocomposites display higher stiffness values compared to those of the WS/Gly/MMT-Na nano-biocomposites (Chivrac, F., 2008b). Such behavior is linked to the well exfoliated structure of the samples based on OMMT-CS compared to the intercalated/aggregated structure obtained with MMT-Na as the nanofiller. However, this relation between better dispersion and higher stiffness properties, is not observed for the sorbitol and Polysorb® plasticized materials. In both cases, the increase in stiffness of the MMT-Na nano-biocomposites is higher than the OMMT-CS one. As for the T_α variations recorded by DMTA, this trend may be linked to the morphology of the nano-biocomposites elaborated with MMT-Na. In these materials, a part of the plasticizer is intercalated and immobilized between the clay platelets and thus no longer acts as a plasticizer leading to slightly higher materials rigidity compared to the WS/OMMT-CS nano-hybrids.

Figure IV.5. Young's modulus vs. clay inorganic content for starch nano-biocomposites plasticized with glycerol, Polysorb® or sorbitol.

Figure IV.6.6 displays the strains at break of plasticized starch nano-biocomposites filled from 3 to 6 wt% of (O)MMT, and stabilized at 57 %RH. Like for the Young's modulus variations, the plasticizer impact on the unfilled plasticized starch matrices is significant. The strain at break properties of the glycerol plasticized starch are lower than the Polysorb® or sorbitol ones. As for the modulus, this trend is likely linked to the water content of the plasticized starch matrices. Indeed, the formulation used in this study is highly plasticized with plasticizer content (polyol + water) which vary from 40 to 50 wt% and consequently, the polysaccharides chains are "swollen" and dispersed into the plasticizer. Thus, a lower water content implies a decrease in the overall plasticizer content (increase in starch content) and leads to a more "cohesive" material with higher strain at break properties.

The strains at break of the plasticized starch-based nano-biocomposites materials greatly depend on the plasticizer nature. For starch nano-biocomposites plasticized with glycerol, Polysorb® or sorbitol a decrease in the strain at break properties is shown with MMT-Na as the nanofiller, this decrease being more pronounced for the sorbitol plasticized samples. At 6 wt% of MMT-Na incorporation, the strain at break properties of these different materials are almost equivalent, suggesting that the macroscopic properties mainly depends on the nanofiller dispersion state. This trend is explained thanks to the intercalated/aggregated structure of the WS/MMT-Na nano-hybrids which creates internal stress at the filler/matrix interface and thus embrittles the nano-biocomposite materials.

The strain at break properties of the nano-biocomposites based on OMMT-CS are more dependent on the plasticizer nature. For glycerol plasticized nano-biocomposites, no variation with the OMMT-CS content is seen. This is related to the highly exfoliated structure of these materials. However, the strain at break properties of the sorbitol and Polysorb®

plasticized nano-biocomposites slightly decrease with the increase in the OMMT-CS content. This trend is likely linked to the nanofiller dispersion state into the starch matrix. According to the morphological analyses performed on these materials, it was highlighted that a low intensity and wide diffraction peak remained after OMMT-CS incorporation into the matrix, such results suggesting an intercalated/exfoliated structure. Thus, the observed decreases in strain at break values are likely due to the remaining small clay tactoïds which slightly embrittle the plasticized starch matrices.
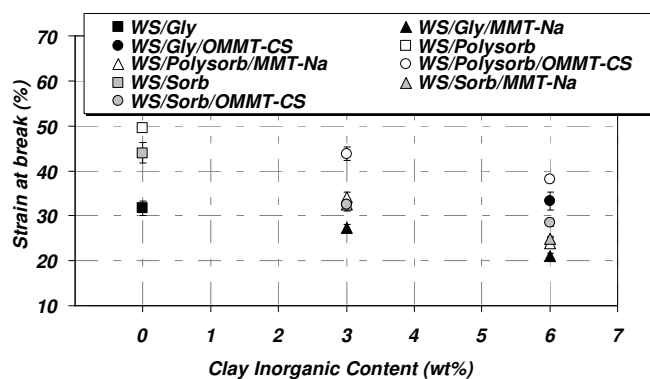
Figure IV.6. Strain at break vs. clay inorganic content for starch nano-biocomposites plasticized with glycerol, Polysorb® or sorbitol.

Finally, Figure IV.7 displays the energy at break variations of plasticized starch nano-biocomposites filled with 3 to 6 wt% of (O)MMT and stabilized at 57 %RH. This property estimated from the area of the tensile curve is a global parameter which depends on the stiffness, yield and break properties and thus which represents well the global mechanical properties of the materials. In direct correlation with the previous results obtained on the stiffness and strain at break properties, the energy at break properties of the different unfilled plasticized starch matrices increases with the increase in the sorbitol/glycerol ratio.

For the nano-biocomposites elaborated with MMT-Na, a decrease in the energy at break corresponding to an embrittlement of the nano-biocomposite is observed with all the plasticizers. This decrease is more pronounced for the sorbitol-plasticized materials. As for the strain at break properties, the OMMT-CS incorporation into the plasticized starch matrix leads to different trends depending on the plasticizer. For glycerol-plasticized nano-biocomposites, an overall increase in the energy at break properties related to the well exfoliated morphology of these nano-hybrid materials is observed. On the contrary, no significant variations of the energy at break are observed for the Polysorb®-plasticized materials and a decrease is observed with the sorbitol-plasticized samples. Such tendencies are

related to the intercalated/exfoliated morphology, which has been previously highlighted with SAXD analyses. Thus, all these experiments have demonstrated that sorbitol perturbs the exfoliation process and then decreases the exfoliation extent into the starch matrix. This perturbation may be related to great interactions (through hydrogen bonds) taking place between the sorbitol and the nanofillers, generating a kind of 3D network.

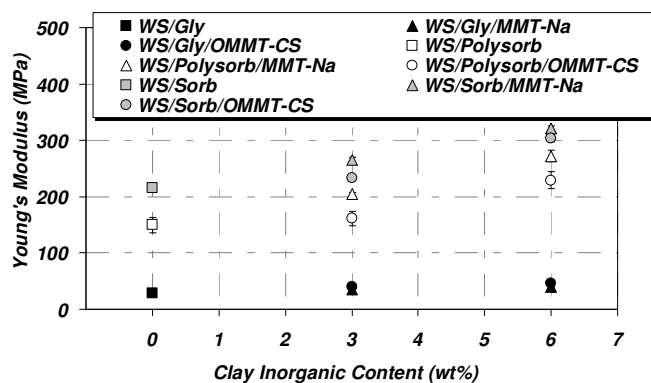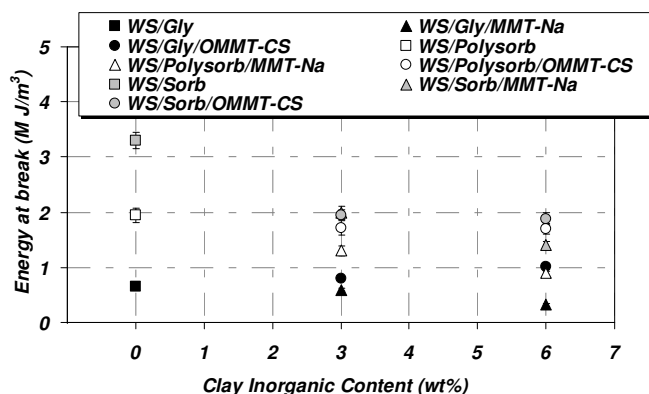**Figure IV.7. Energy at break vs. clay inorganic content for starch nano-biocomposites plasticized with glycerol, Polysorb® or sorbitol.**

V. Conclusion

This study analyzed the impact of three kinds of polyol plasticizers (glycerol, Polysorb® and sorbitol) on the plasticized starch material properties and on the montmorillonite intercalation/exfoliation process into starch nano-hybrids. It has clearly demonstrated that from a mechanical point of view, the sorbitol is the best raw starch plasticizer, the resulting properties being higher than those obtained with the Polysorb® and the glycerol.

For the starch nano-biocomposite materials, morphological analyses performed on WS/MMT-Na materials revealed an intercalated structure with preferential plasticizer intercalation whatever the plasticizer type. Such materials can be considered as conventional micro-biocomposites, since a huge decrease in the tensile properties, corresponding to an embrittlement of the material, has been shown.

The addition of OMMT-CS led to different dispersion state depending on the plasticizer nature. Exfoliated morphologies are obtained with glycerol as the starch nano-hybrids plasticizer. For Polysorb® and sorbitol, SAXD analyses showed an intercalated/exfoliated structure. These morphologies have been confirmed with the results of uniaxial tensile tests. An overall enhancement of the WS/Gly/OMMT-CS nano-biocomposites

tensile properties, characteristic of an exfoliated morphology, is observed. On the opposite, WS/Sorb/OMMT-CS materials display a slight decrease in these properties corresponding to a more aggregated structure. Thus, these results clearly highlight a disruption of the clay intercalation/exfoliation process induced by the sorbitol, likely because of the sorbitol/montmorillonite strong interactions. To overcome this limitation, further studies should be focused on the clay organo-modifier, namely the cationic starch. Special attention must be paid to the impact of the charge density and the cationic starch content adsorbed on the nano-platelets surface.

Besides, for WS/Gly/(O)MMT, we previously reported a phase separation between domains rich and without nanofillers. Thermo-mechanical analyses confirmed that these heterogeneities are induced by the high plasticizer content of the starch formulations which leads to a phase separation between domains rich in carbohydrate chains and rich in plasticizer. Further experiments, such as nanoindentation and dielectric analyses have to be performed to better understand and describe the mechanism of this phase separation. Finally, since these heterogeneities are induced by the high plasticizer content of the matrix, they could be used as a marker of the different plasticized starch phases.

VI. Acknowledgment

Publication IV : Discussion et commentaires

Cette étude avait pour but d'améliorer la compréhension du rôle du plastifiant sur le processus d'intercalation/exfoliation de nano-biocomposites amidon/montmorillonite. Pour cela, trois types de plastifiants ont été utilisés : du glycérol, du sorbitol et du Polysorb® (mélange glycérol/sorbitol). Il a clairement été montré que la nature du plastifiant influence significativement les propriétés des amidons plastifiés, les meilleures propriétés mécaniques ayant été obtenues avec le sorbitol.

Les analyses morphologiques effectuées sur les nano-hybrides à base de MMT-Na ont clairement montré que l'on obtenait une structure intercalée quelle que soit la nature du plastifiant. Dans le cas des nano-biocomposites à base de OMMT-CS, les résultats sont plus contrastés. Avec du glycérol comme plastifiant, une structure exfoliée est obtenue. En revanche, l'incorporation de Polysorb® ou de sorbitol induit la formation d'une structure intermédiaire intercalée/exfoliée sans que l'on puisse, à ce stade, expliquer totalement la cause de cette différence de comportement entre plastifiants.

Cependant, il semble qu'il y ait une corrélation entre la diminution de la qualité de la dispersion de l'OMMT-CS et l'augmentation du ratio sorbitol/plastifiant total. Cette tendance a été confirmée par les tests de traction uniaxiale. Il apparaît donc que le sorbitol perturbe le processus d'intercalation/exfoliation de la montmorillonite, probablement au travers d'interactions fortes (liaisons hydrogènes) entre le plastifiant et l'amidon cationique. Aussi, afin d'obtenir une structure totalement exfoliée pour ce type de matériaux à base de sorbitol, les futurs travaux devront se focaliser sur la compréhension des interactions plastifiants/organo-modifiants/nanocharges.

Cette étude aura également permis de mettre en évidence l'origine de la séparation de phase observée précédemment entre des zones riches et pauvres en nanocharges. Cette hétérogénéité est induite par le taux élevé de plastifiant de la formulation qui engendre une démixtion entre des domaines riches et pauvres en plastifiant. Afin de mieux comprendre et d'approcher le mécanisme de cette séparation de phases, des expériences de nano-indentation et des analyses dielectriques sont actuellement en cours de réalisation. Enfin, la répartition inhomogène des nanocharges dans le matériau pourrait servir de marqueur permettant d'observer la séparation de phase et d'identifier les domaines riches et pauvres en plastifiant.

Publication V – High performance starch nano-biocomposites based on needle-like sepiolite clays

Frédéric Chivrac[1], Eric Pollet[1], Marc Schmutz[2], Luc Avérous[1]*

I. Abstract

The present paper reports the successful elaboration and study of an innovative and high performance class of plasticized starch nano-biocomposites based on needle-like sepiolite clays. Sepiolite with and without surfactant i.e., natural sepiolite (SEP-Na) and sepiolite organo-modified with cationic starch (OSEP-CS), have been incorporated into plasticized starch. The transmission electronic microscopy has highlighted a well-nanodispersed morphology with almost individual sepiolite strands, with and without filler organo-modification. Different micro/nano-structurations are obtained varying the surfactant content. Moreover, an increase in the thermal stability of the plasticized starch has been demonstrated with SEP-Na, linked with the sepiolite dehydration phenomenon. Finally, uniaxial tensile tests have clearly evidenced the great interest in using sepiolite nanofillers, and more especially OSEP-CS, to tune the plasticized starch properties. Thanks to this needle-shaped nanofiller the material rigidity is increased without decreasing its properties at break.

KEYWORDS: Nano-biocomposites, plasticized starch, sepiolite, montmorillonite, organo-modification, cationic starch, clay.

* Corresponding author: Luc Avérous.

Tel.: +33-3-90-242-707 - Fax: +33-3-90-242-716 - AverousL@ecpm.u-strasbg.fr

[1] LIPHT-ECPM, UMR 7165, Université Louis Pasteur, 25 rue Becquerel, 67087 Strasbourg Cedex 2, France

[2] ICS, UPR 22, Université Louis Pasteur, 23 rue Becquerel, 67034 Strasbourg Cedex, France

II. Introduction

The new sustainable development policies combined with the increasing environmental concern imply the development of environmentally friendly materials. Bio-based plastics, produced from wheat, corn, vegetable oil…, could be a powerful answer to replace conventional petroleum-based plastics, at least for disposable applications. Since starch is a low cost eco-friendly biopolymer, it appears as an interesting option to produce green plastics. Several authors have already demonstrated the possibility to transform native starch granules into thermoplastic-like material under destructuring and plasticizing conditions (Swanson, C.L., 1993, Tomka, I., 1991). Nevertheless, the water sensitivity and the brittleness of this promising material have to be reduced to obtain suitable materials (Averous, L., 2004a).

Nanofiller (nano-sized filler) incorporation into bio-based matrix to produce nano-biocomposites is an innovating solution to answer these drawbacks (Chivrac, F., 2006). Depending on the nature and the geometry of the nanofiller, new and/or improved properties (gas barrier, mechanical stiffness, transparency, thermal stability…) could be obtained (Alexandre, M., 2000, Gain, O., 2005, Gorrasi, G., 2003, Luo, J.J., 2003, Sinha Ray, S., 2003). Compared to conventional composites, the main reason for such improvement relies on the large interface area resulting in high interactions between the polymer matrix and the nanofillers (Alexandre, M., 2000, Dennis, H.R., 2001, Sinha Ray, S., 2003).

Up to now, the most intensive researches have been focused on layered silicates, and especially on montmorillonites (MMT), as the reinforcing phase. Many authors tried to disperse "natural" sodium MMT into starch since both of these compounds are hydrophilic (Bagdi, K., 2006, Cyras, V.P., 2008b, Dean, K., 2007, Ma, X., 2007, Pandey, J.K., 2005, Park, H.M., 2002, Park, H.M., 2003, Wilhelm, H.-M., 2003a, Wilhelm, H.-M., 2003b, Zhang, Q.X., 2007). Nevertheless, it has been demonstrated that the non-volatile plasticizer (glycerol, sorbitol…) induces a restriction of the nanoclay dispersion leading to intercalated structures (Cyras, V.P., 2008b, Dean, K., 2007, Ma, X., 2007, Pandey, J.K., 2005). Thus, authors have tried to modify the clay/matrix affinity with different compatibilizer or surfactant (Dean, K.M., 2008, Huang, M., 2006a, Huang, M.F., 2004, Kampeerapappun, P., 2007). Very recently, Chivrac et al. (Chivrac, F., 2008b) have described the use of cationic starch as a new and very powerful strategy to organo-modify MMT nanoclay and to obtain exfoliated morphologies with enhanced properties.

MMT is not the only type of nanoclay that can be incorporated into polymer matrices. Recently, some studies have been focused on the use of sepiolite (SEP), a nanofiller with a needle-like structure, to elaborate nanocomposites (Bilotti, E., 2008, Chen, H., 2007, Darder, M., 2006, Duquesne, E., 2007, Ma, J., 2007, Zheng, Y., 2006). This nanofiller is a microcrystalline hydrated magnesium silicate of theoretical unit cell formula $Mg_8Si_{12}O_{30}(OH)_4.(H_2O)_4.8H_2O$. It shows an alternation of blocks and channels that grow up in the fiber direction. The blocks are basically constituted by two layers of tetrahedral silica sandwiching a central octahedral magnesium oxide-hydroxide layer (Figure V.1). Some isomorphic substitutions occur inside these central layers creating a negative charge naturally counterbalanced by the presence of inorganic cations (Na^+, Ca^{2+}…). The SEP channels are filled both with the coordinated water molecules, which are bonded to the Mg^{2+} ions located at the edges of octahedral sheets, and with the zeolitic water, which is associated to the structure by hydrogen bonding. The discontinuity of the silica sheets gives rise to the presence of silanol groups (Si-OH) at the edges of the external surface of the SEP nanoparticles.
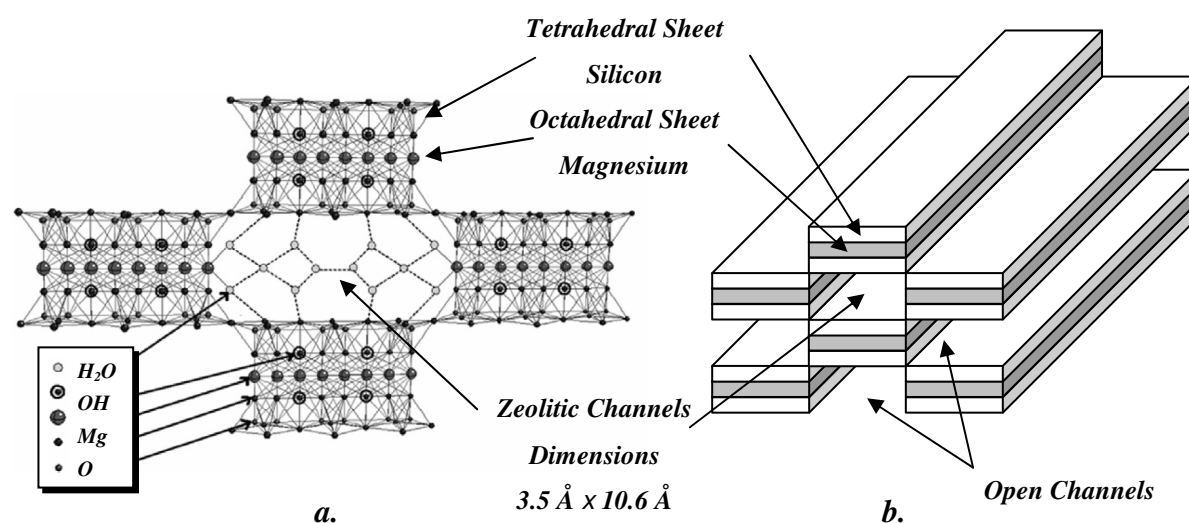
Figure V.1. Sepiolite - (*a.*) projection onto the (001) plane, (*b.*) fibrous structure.

The aim of this study is the use of such innovative nanofillers, namely natural sepiolite (SEP-Na) or sepiolite organo-modified with cationic starch (OSEP-CS), to elaborate a new class of starch-based nano-biocomposites. The relationship between the nanofiller nature, its nano-structuration and the resulting properties (thermal stability, mechanical properties) will be investigated. Finally, these new nano-biocomposites materials will be compared to more conventional starch/montmorillonite nano-biocomposites to assess the interest of these needle-shaped nanofillers.

III. Experimental part

1. Materials

Wheat starch (WS) was supplied by Roquette (France). The amylose and amylopectin contents are 23 and 77 %, respectively. Residual protein content is less than 1 %. The glycerol used as non-volatile plasticizer was supplied by the Société Française des Savons (France) and is a 99.5 % purity product. The cationic starch has been supplied by Roquette (France). Its charge density is 944 µequiv.g^{-1}. The cationic functions are quaternary ammonium with chloride as counter-anion. The Pangel$^{®}$ S9 natural sepiolite (SEP-Na) was supplied by Tolsa (Spain) and has a cationic exchange capacity (CEC) of 15 meq/100 g.

2. Samples preparation

ORGANO-MODIFIED SEPIOLITE PREPARATION. The SEP-Na organo-modification was carried out with cationic starch by dispersion/adsorption technique (Figure V.2). Four different types of organo-modified sepiolite, OSEP-1CS, OSEP-2CS, OSEP-4CS and OSEP-6CS corresponding respectively to one, two, four and six charge equivalence between the SEP and the cationic starch, have been prepared. First, 5 g of SEP-Na were introduced into 250 mL of distilled water and dispersed in an ultrasonic bath at 60 °C for 4 h. In parallel, from 0.79 to 4.77 g of cationic starch were introduced in 30 mL of distilled water and solubilized in an ultrasonic bath at 60 °C for 1 h. Then, the two solutions were pooled together and placed for 1 day at 60 °C in ultrasonic bath. The solution was filtered and washed with 1 L of distilled water at 60 °C to remove the salt formed (NaCl) during the cationic starch adsorption. Then, the filtrate was lyophilized to obtain the cationic starch organo-modified sepiolite (OSEP-CS).
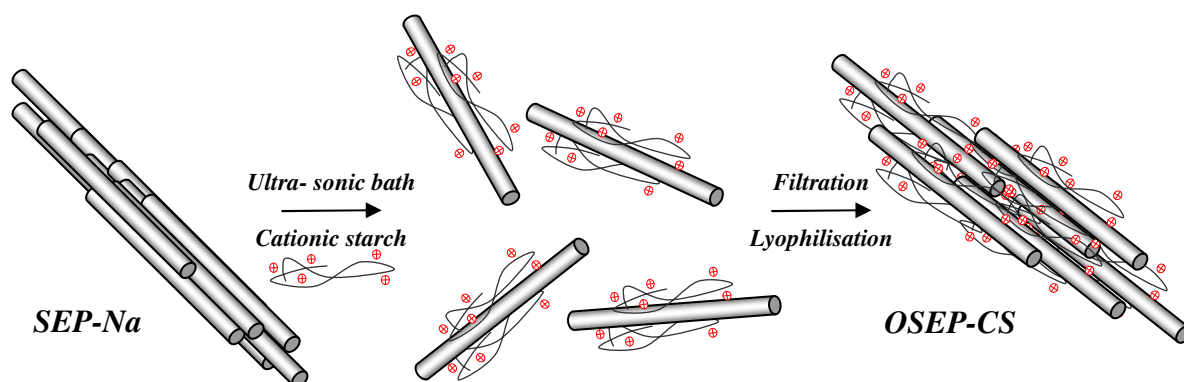
Figure V.2. Schematic representation of the SEP-Na organo-modification by dispersion/adsorption technique.

STARCH DRY-BLENDS PREPARATION. The formulation used in this study contained 54 wt% of native starch, 23 wt% of glycerol and 23 wt% of water. The water was introduced with the SEP during the nano-biocomposites elaboration, as described below. Granules of plasticized starch were prepared according to the following procedure. Native wheat starch was first dried overnight at 70 °C in a ventilated oven. Then, the starch powder was introduced into a turbo-mixer and the glycerol was slowly added under stirring. After complete addition of glycerol, the mixture was mixed at high speed (1700 rpm) to obtain a homogeneous dispersion. The mixture was then placed in a ventilated oven at 170 °C for 40 min and occasionally stirred, allowing vaporization of water and diffusion of glycerol into the starch granules. The dry-blend (powder) was then stored in polyethylene bag.

NANO-BIOCOMPOSITES ELABORATION. To obtain nano-biocomposites, from 3 to 6 wt% of SEP inorganic matter (compared to the weight of starch and glycerol) have been added into the dry-blend. A pre-weighted amount of (O)SEP (1.38 to 2.86 g of clay inorganic fraction, depending on the formulation) was first dispersed in 13.5 ml of distilled water to obtain a dispersed clay and processed according to the protocol presented hereafter. Then, the dry blend and the (O)SEP/water dispersion were introduced together into the mixing chamber. The starch nano-biocomposites were prepared by mechanical kneading with a counter-rotating internal batch mixer, Rheocord 9000 (Haake, USA), at 70 °C for 20 min with a rotor speed of 150 rpm. After melt processing, molded specimens and films were obtained by hot-pressing at 110 °C applying 20 MPa pressure for 15 min. The nano-biocomposite samples were then allowed to equilibrate at 57 %RH (relative humidity percentage) for 1 month in a controlled humidity chamber before characterization. Throughout this paper, the samples are designated WS/ XXX y% where XXX stands for the type of (organo)clay and y for the weight percentage of clay inorganic fraction.

3 Characterization

TEM CHARACTERIZATION. For transmission electronic microscopy (TEM) observation, the samples were microtomed at low temperature (-80 °C) using a Diatome AG-microtome (Switzerland) equipped with a diamond knife. The ultra thin sections (nominal thickness 60 nm) were examined using a Philips CM 12 (Netherlands) transmission electron microscope using an acceleration voltage of 120 kV.

XRD CHARACTERIZATION. The X-Ray diffraction (XRD) morphological analyses were performed on a powder diffractometer Siemens D5000 (Germany) using Cu (Kα) radiation (λ= 1.5406 Å) at room temperature in the range of 2θ = 3 to 40° by step of 0.01° of 4 s each.

TGA CHARACTERIZATION. The thermogravimetric analyses (TGA) were performed on a Hi-Res TGA 2950 apparatus from TA Instruments (USA). For all starch/SEP nano-biocomposites, the analyses were carried out under "synthetic air" which is a mixture of 75 % N_2 and 25 % O_2. The clay content in inorganics (in wt%) of each composite was assessed by the combustion residue left at 600 °C. The degradation temperature was determined from the peak temperature of the derivative weight loss curve.

MECHANICAL TESTS. Uniaxial tensile tests were carried out with an Instron tensile testing machine (model 4204, USA), on dumbbell-shaped specimens; at 25 °C with a constant deformation rate of 5 mm/min. For each formulation five samples were tested. The non linear mechanical behavior of the different samples was determined through different parameters. The true strain (ε) is given by Equation V.1 where L and L_0 are the test piece length during the experiment and at zero time, respectively.

$$\varepsilon = \ln(\frac{L}{L_0}) \tag{V.1}$$

The nominal stress ($<\sigma>$) and the true stress (σ) were determined by Equations V.2 and V.3, respectively, where F is the applied load, S_0 is the initial cross-sectional area and S is the cross-sectional area. S was estimated by assuming that the total volume of the sample remained constant, according to Equation V.4.

$$<\sigma> = \frac{F}{S_0} \tag{V.2}$$

$$\sigma = \frac{F}{S} \tag{V.3}$$

$$S = S_0 * \frac{L_0}{L} \tag{V.4}$$

Young's modulus (E) was determined and calculated from the slope of the low strain region of the tensile curve ($\sigma = \varepsilon = 0$). The energy at break values were calculated from the area of the tensile curves obtained for each sample.

IV. Results and discussion

1. Morphological characterization

Figure V.3 displays the optical microscopy micrographs obtained from WS/SEP-Na, WS/OSEP-1CS, WS/OSEP-2CS and WS/OSEP-4CS 6 wt%. From these observations, it is seen that no aggregates are observed for WS/SEP-Na nano-biocomposites (Figure V.3a). This result is in agreement with the assumption that hydrogen bonds can be established between the SEP silanol groups and the starch chains, which could facilitate the nanofiller dispersion. Surprisingly, large clay aggregates with a mean diameter around 200 – 300 µm are observed when the nanofiller is organo-modified with one equivalent of cationic starch (Figure V.3b). This result is unexpected since cationic starch is assumed to act as a compatibilizer. To explain these SEP aggregates, one may suppose that, for OSEP-1CS, cationic starch surfactant establishes "bridges" between the nanofiller strands leading to flocculated structure, as represented in Figure V.4. This assumption is supported by the low CEC of the SEP, which leads to a low charge density. Thus, when a cationic starch polyelectrolyte is adsorbed on the SEP strand surface, the probability for this macromolecular surfactant to be adsorbed on another SEP strand (to compensate its excess of positive charge) is not negligible and may lead to the formation of aggregates.

As seen in Figures V.3c and V.3d, at this magnification no more aggregates are observed for nano-biocomposites based on OSEP-2CS and OSEP-4CS. Thus, with the increase in the cationic starch content, OSEP has lost is highly aggregated structure. To explain such a behavior, we have to notice that an excess of positive charge (compared to the CEC of the SEP) which generates nanoparticles repulsion has been added into the system. Moreover, when cationic starch chains are adsorbed on the SEP strand surface, they are much less prone to create a bridge with another strand because the other SEP negative charges have already been counterbalanced by other cationic starch macromolecules.
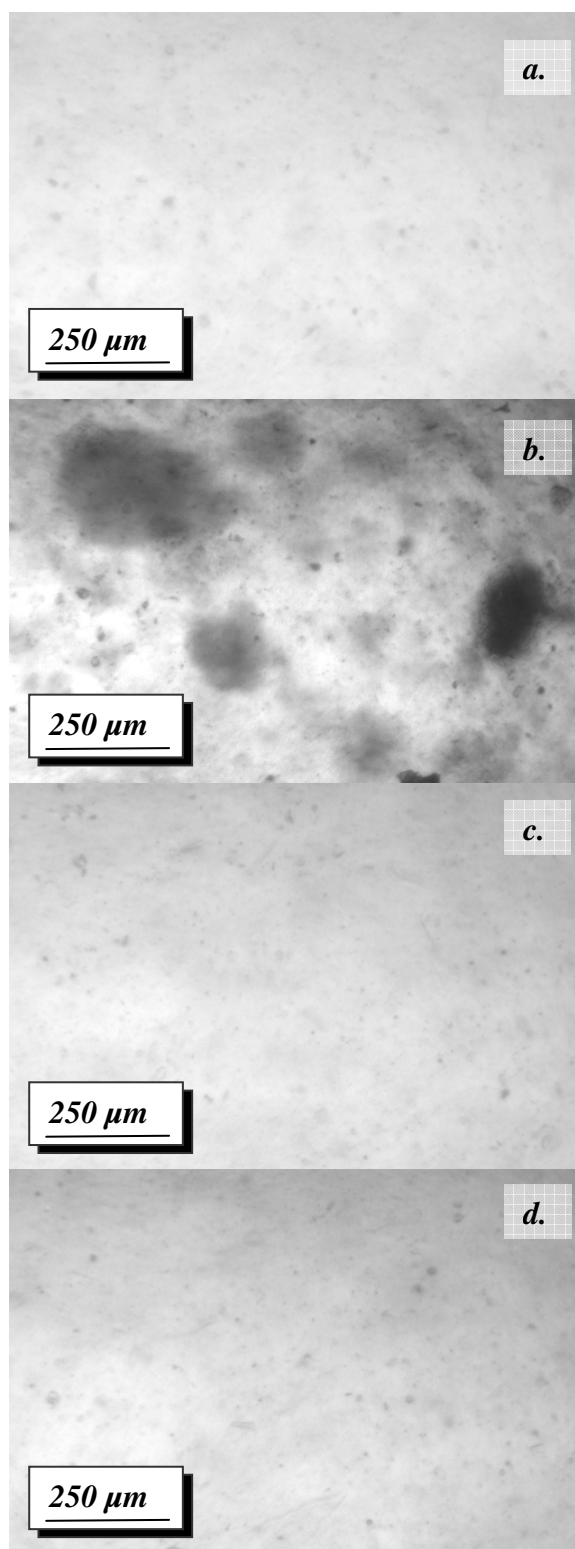
Figure V.3. Optical microscopy micrographs of (*a.*) WS/SEP-Na 6 wt%, (*b.*) WS/OSEP-1CS 6 wt%, (*c.*) WS/OSEP-2CS 6 wt% and (*d.*) WS/OSEP-4CS 6 wt%.
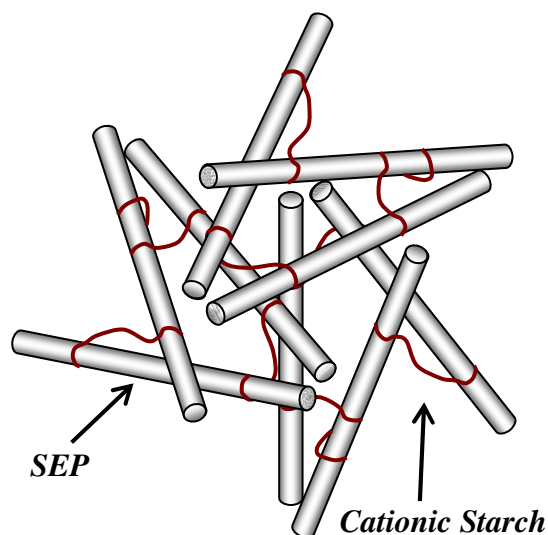
Figure V.4. Oversimplified representations of SEP nanoparticles being aggregated by bridging flocculation into WS/OSEP-1CS nano-biocomposites.

Figures V.5 and V.6 show typical TEM micrographs of WS/SEP-Na 3 wt% and WS/OSEP-4CS 3 wt%, respectively. At low magnification scale (Figures V.5a and V.6a), a heterogeneous structuration is observed with domains rich in SEP nanofiller and some regions without clay.
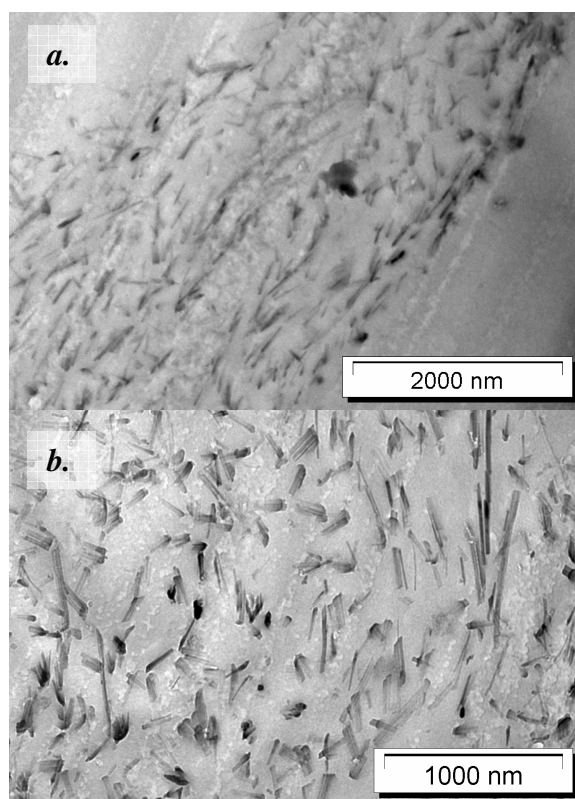
Figure V.5. TEM pictures of WS/SEP-Na 3 wt% nano-biocomposites at (a) low magnification and (b) high magnification level.
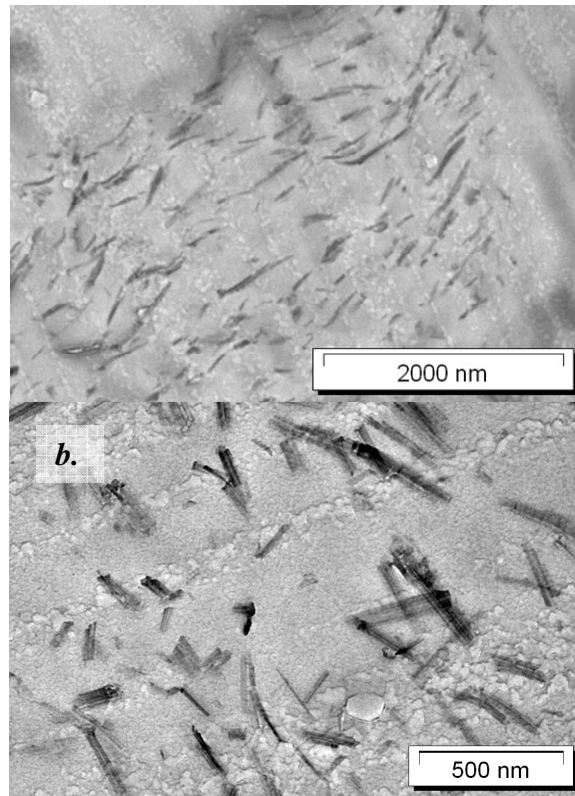
Figure V.6. TEM pictures of WS/OSEP-4CS 3wt% nano-biocomposites at (a) low magnification and (b) high magnification level.

This heterogeneity has been previously reported with plasticized starch/montmorillonite nano-biocomposites (Chivrac, F., 2008b). This structuration state is linked to the high glycerol content of these materials, which is known to induce a phase separation and create glycerol-rich domains (Averous, L., 2004a). In a previous article, Zhang et al. (Zhang, X., 2007) have reported the preferential MMT dispersion into these domains for plasticized wheat gluten nano-biocomposites. Besides, Chivrac et al. (Chivrac, F., 2008b) have assumed that for plasticized wheat starch nano-biocomposites, the MMT platelets were mainly dispersed into the glycerol-rich domains, due to the high glycerol/MMT affinity. Since SEP and MMT have equivalent chemical structures, one may suppose that the SEP is also preferentially dispersed into high glycerol content domains. In these regions, at high magnification level (Figures V.5b and V.6b), the TEM micrographs show only small clay aggregates and almost individuals SEP strands with a random dispersion without preferential orientation. Thus, even if the OSEP-1CS leads to an aggregated structure, a true nano-dispersion of the OSEP strands is achieved with cationic starch increasing content.

Figure V.7 displays the typical XRD curves recorded for SEP-Na, WS, WS/SEP-Na 3 and 6 wt%, WS/OSEP-1CS and WS/OSEP-4CS 6 wt%. The diffractogram of the SEP-Na displays an intense peak at 7.5° corresponding to the internal channel reflections of the SEP

needle-like structure (Darder, M., 2006). The other diffraction peaks correspond to the SEP structure. After dispersion in the starch matrix, the SEP internal channel diffraction peak is not shifted, attesting that the channel structure of the primary particles remains unchanged. The diffractogram obtained for the neat matrix displays B-Type crystallization peak at $2\theta = 17.2°$, corresponding to the amylopectine recrystallization. V_H-type crystallization peaks are also observed at $2\theta = 19.9°$ and $22.5°$ and correspond to the process induced amylose crystallization into single helical structure (Van Soest, J.J.G., 1996d). No significant evolution of these B-Type and V_H-Type crystallization peaks are observed for the nano-biocomposites samples. However, the diffractograms display a new diffraction peak located at $26.4°$, corresponding to a crystal lattice structure of 3.4 Å (calculated from the Bragg's law). From Table V.1, it is seen that this peak intensity seems to be correlated with the nanofiller content. Moreover, its intensity is clearly higher for SEP-Na than for OSEP-CS. In addition, no influence of CS content is observed, the intensity of this diffraction peak being almost equivalent for the nano-biocomposites prepared with OSEP-1CS and OSEP-4CS. Such a new diffraction peak has been previously reported into starch/tunicin whiskers composites. It is attributed to amylopectine recrystallization at the filler interface, and is favored by hydrogen bonds established between the filler and the macromolecules (Neus Angles, M., 2000). Thus, these results suggest the occurrence of a transcrystallization phenomenon taking place at the plasticized starch/SEP interface. This new crystalline structure is likely induced by the hydrogen bonds that could be established between the silanol groups located at the edge of the SEP needles and the hydroxyl groups of the polysaccharide chains.
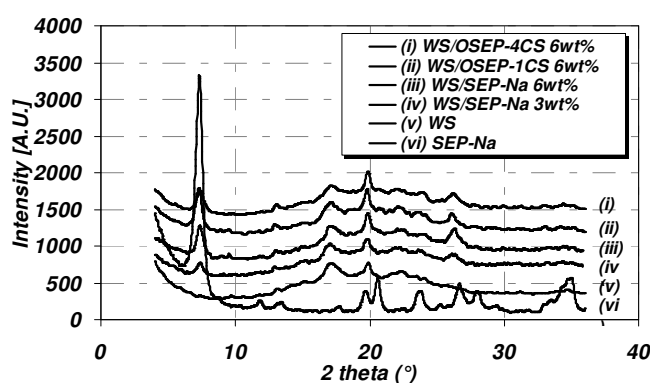
Figure V.7. XRD patterns for SEP-Na, WS and WS/(O)SEP nano-biocomposites.

Table V.1. WS/(O)SEP transcrystalline diffraction peak intensity ($2\theta = 26.4°$).

Samples	Diffraction peak intensity (Counts)
WS/SEP-Na 3 wt%	110
WS/SEP-Na 6 wt%	200
WS/OSEP-1CS 6 wt%	119
WS/OSEP-4CS 6 wt%	110

2. Thermal stability

The thermal stability of the plasticized starch based nano-biocomposites has been assessed by thermogravimetric analysis (TGA). Figure V.8 displays the typical thermogram obtained for pristine plasticized wheat starch, three different steps of weight loss being detected at 292, 317 and 526 °C. Since the first weight loss matches the glycerol content of the formulation and since it is not observed for non-plasticized starch matrix (not shown here), this first degradation step corresponds to the glycerol plasticizer volatilization. The two others weight losses correspond to the starch amylose and amylopectin thermal degradation.
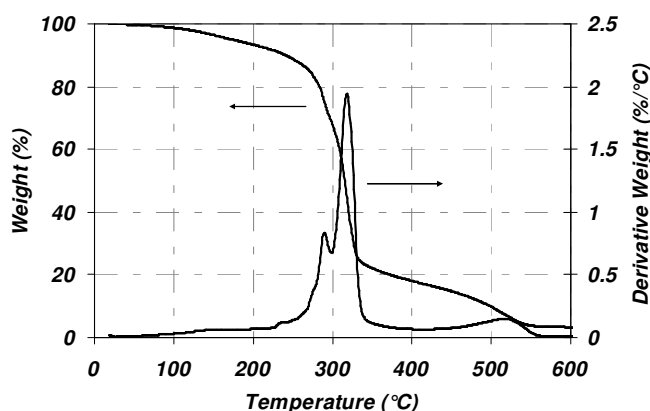
Figure V.8. TG and DTG curves obtained for plasticized WS.

Figure V.9 displays the thermogram recorded for unmodified sepiolite (SEP-Na). A three steps weight loss is clearly highlighted in this experiment. According to the literature (Kuang, W., 2003, Sandi, G., 2002, Tartaglione, G., 2008, Weir, M.R., 2002), these weight losses are linked to the SEP multi-step dehydration process. This first dehydration step occurs at 100 °C and is attributed to the loss of water physically bonded to SEP i.e., adsorbed on the external surface and in the structural channels. The loss of this hydration water is complete at 150 °C. The second step located at 270 °C is attributed to the loss of two of the four coordinated water molecules of the SEP crystal structure. The third step, observed at 530 °C, is a result of the elimination of the two other coordinated water molecules. A fourth

degradation step located around 800 °C is also mentioned into the literature and is linked to the dehydroxylation of the SEP magnesium silicate itself that loses its structure. This multistep dehydration/degradation process is summarized hereafter:

1st step: $Mg_8Si_{12}O_{30}(OH)_4.(H_2O)_4.8H_2O \rightarrow Mg_8Si_{12}O_{30}(OH)_4.(H_2O)_4 + 8H_2O$

2nd step: $Mg_8Si_{12}O_{30}(OH)_4.(H_2O)_4 \rightarrow Mg_8Si_{12}O_{30}(OH)_4.(H_2O)_2 + 2H_2O$

3rd step: $Mg_8Si_{12}O_{30}(OH)_4.(H_2O)_2 \rightarrow Mg_8Si_{12}O_{30}(OH)_4 + 2H_2O$

4th step: $Mg_8Si_{12}O_{30}(OH)_4 \rightarrow 8MgSiO_3 + 4SiO_2 + 2H_2O$
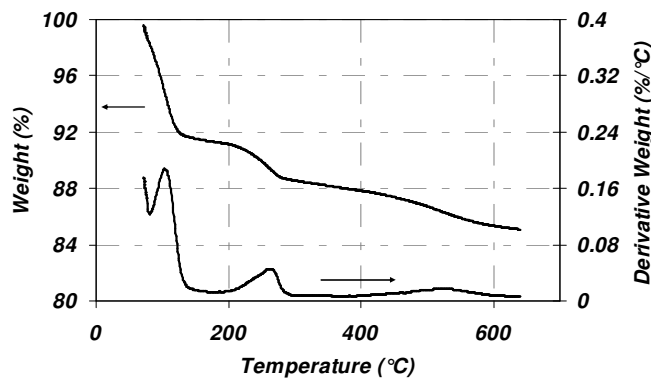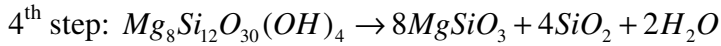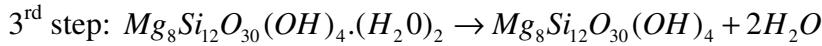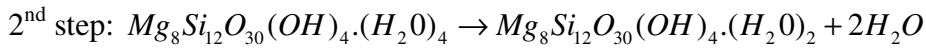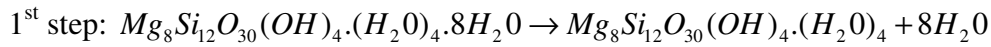
Figure V.9. TG and DTG curves obtained for SEP-Na

Figure V.10 displays the thermograms recorded for the pristine plasticized wheat starch matrix and the nano-biocomposites filled with 3 and 6 wt% of SEP-Na. Regarding the derivative weight loss curves (DTG), a decrease in the first peak intensity, corresponding to the glycerol volatilization, is observed with the incorporation of the SEP-Na nanofiller, this decrease being linked with the clay content. This tendency is likely related to the SEP/glycerol strong interactions which increase the glycerol volatilization temperature. Moreover, the starch maximum degradation temperature, observed at 318 °C in the neat matrix, is shifted towards higher temperatures (321 and 326 °C for a SEP-Na content of 3 and 6 wt%, respectively) and is correlated with the SEP-Na content. This increase in the degradation temperature is commonly observed in MMT-based nanocomposites. It is mainly attributed to an increase in the tortuosity of the diffusion pathway induced by the clay dispersion, which limits the diffusion of the combustion gas to the material surface (Alexandre, M., 2000, Sinha Ray, S., 2003). According to the needle-like structure of the SEP-Na, an increase in the tortuosity of the diffusion pathway is less plausible. This increase in degradation temperature is likely induced by the SEP-Na dehydration phenomenon, which occurs at 270 °C. This

dehydration absorbs thermal energy and decreases the sample temperature, and then could limit the amylose and amylopectin degradation.
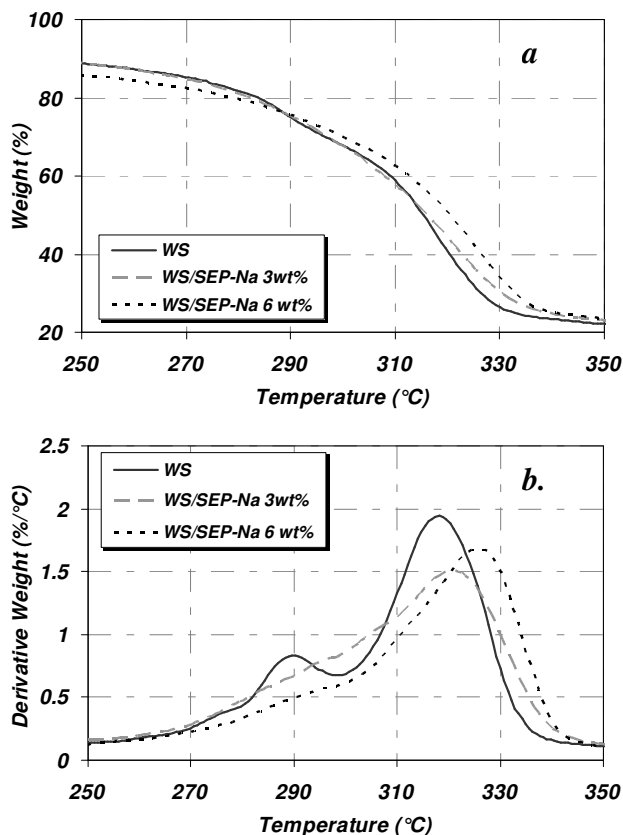
Figure V.10. (a.) TG and (b.) DTG curves recorded for WS, WS/SEP-Na 3 wt% and 6 wt%.

Figure V.11 displays the thermograms recorded for the pristine plasticized wheat starch matrix and the nano-biocomposites filled with 6 wt% of OSEP-1CS, OSEP-2CS, OSEP-4CS and OSEP-6CS. Contrary to the SEP-Na nano-biocomposites, a decrease in the starch maximum degradation temperature (319,316, 312 and 309°C, respectively) is observed. This decrease is correlated with the cationic starch content (1, 2, 4 and 6 CS equivalent, respectively). Thus, the cationic starch organo-modifier likely accelerates the mechanisms of the plasticized starch degradation. To highlight its influence, blends of plasticized starch and cationic starch have been elaborated with a ratio of 97 wt%/3 wt% and 94 wt%/6 wt% and then have been analyzed by TGA. In addition, pure cationic starch has also been studied. The different thermograms are presented in Figure V.12. The cationic starch main degradation occurs at 284 °C, this temperature being lower than the main degradation temperature of starch. Moreover, a clear link between the cationic starch content and the blend degradation temperature is observed. The blends elaborated with 3 and 6 wt% of cationic starch content

present respectively a maximum degradation temperature located at 311 and 306 °C. According to Torre et al. (Torre, L., 1998), if the degradations of each compound of a blend are independent, the weight loss obtained by TGA is given by Equation V.5, where W is the residual weight fraction of the blend. W_{CS} and W_{starch} are the residual weight fractions of the cationic starch and the plasticized starch, respectively, and x_{CS} and x_{starch} are the original weight fractions of the cationic starch and the plasticized starch in the blend, respectively.

$$W = W_{CS} x_{CS} + W_{starch} x_{starch} \qquad\qquad (V.5)$$

Thus, starting from the experimental TGA of the plasticized starch and the cationic starch, one can build up the calculated TG curve for all respective blends. For the plasticized starch/cationic starch systems, the calculated and the experimental curves are not superposed, the experimental curve displaying a lower degradation temperature than the calculated one (not shown here). We can conclude that, in such blends, the degradation of the plasticized starch and the degradation of the cationic starch are interdependent. Thus, one may suppose, that the by-products generated during the cationic starch degradation favor the plasticized starch thermal degradation. Further experiments have to be carried out to better understand the degradation reaction mechanisms and to verify a hypothetical degradation catalytic effect linked to the cationic starch.
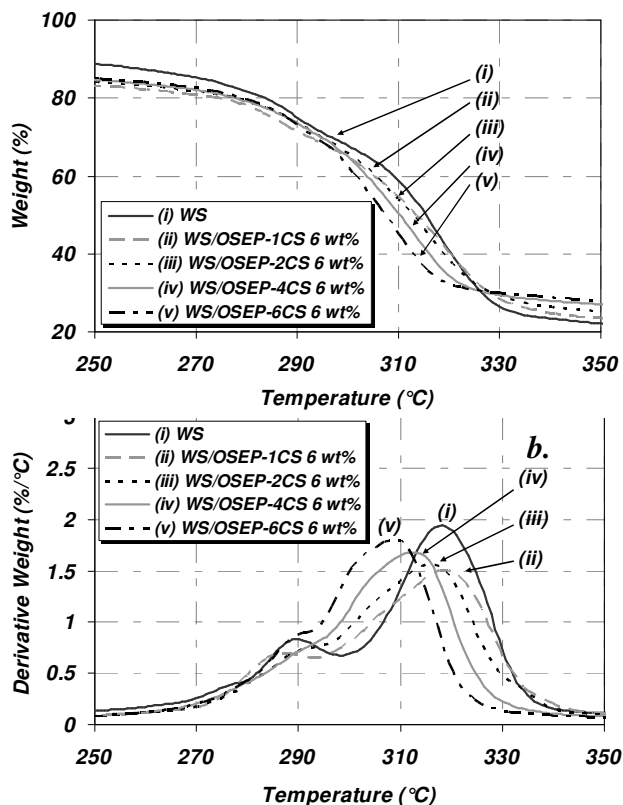
Figure V.11. (a.) TG and (b.) DTG curves recorded for WS, WS/OSEP-1CS 6 wt%, WS/OSEP-2CS 6 wt%, WS/OSEP-4CS 6 wt% and WS/OSEP-6CS 6 wt%.
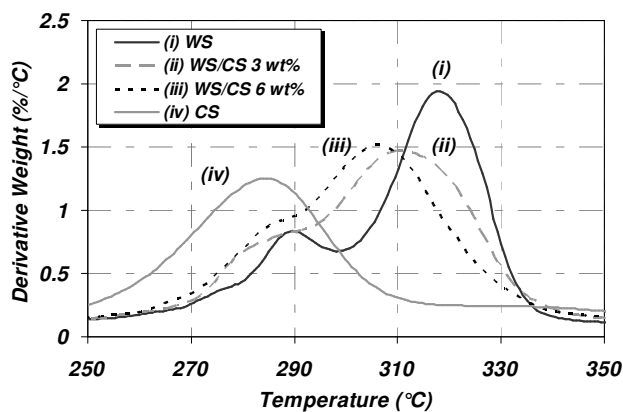
Figure V.12. DTG curves recorded for WS, WS/CS 3 wt%, WS/CS 6 wt% and CS (cationic starch).

3. Mechanical properties

Figure V.13 displays the Young's modulus variations of plasticized starch and the nano-biocomposites filled with 6 wt% of (O)SEP. For the nanofillers with and without surfactant, an increase in the matrix stiffness is obtained with the clay incorporation. This stiffness increase is commonly observed in nano-biocomposite systems and is related to the

nanofiller dispersion state and to the nanofiller/matrix interface quality (Luo, J.J., 2003). Moreover, the transcrystallinity phenomenon, which occurs at the (O)SEP interface and which rises the overall material crystallinity, also explains the stiffness increase. For the OSEP hybrids, a relationship between the amount of cationic starch adsorbed on the SEP and the Young's modulus is observed, the highest modulus being obtained for the WS/OSEP-4CS samples. According to the presented results, it seems that further addition of cationic starch does not influence the final material stiffness. Moreover, the Young's modulus values are higher than those of the SEP-Na samples. This trend can be explained by the cationic starch affinity toward starch material which generates intense interactions between the nanofiller and the matrix and thus locally reduces the starch chains mobility.

The mechanical properties of the nano-biocomposites filled with 6 wt% of MMT-Na and OMMT-CS are listed in Table V.2 and are given for the sake of comparison (results presented in a previous article (Chivrac, F., 2008b). It is clearly seen from these values that the WS/(O)SEP stiffness values are higher than those of the corresponding MMT nano-biocomposites. For non-modified nanofillers, this trend is explained by the higher affinity of the starch macromolecules toward the SEP-Na than the MMT-Na. Indeed, MMT-Na leads to an aggregated structure. On the contrary, the higher affinity of SEP-Na with the starch matrix is linked to the numerous silanol groups located at the edge of the clay structure. The nanofillers organo-modified by cationic starch are well and homogeneously nanodispersed into the plasticized starch matrix. Such nanostructures lead to optimal interfaces with strong interactions between the nanofiller and the plasticized starch matrix. Thus, the stiffness differences recorded for the WS/OMMT-CS and WS/OSEP-4CS nano-biocomposites are linked to a combination of different factors that influence the plasticized starch rigidity, namely a transcrystallinity phenomenon, the sepiolite aspect ratio and a higher rigidity of the sepiolite strands compared to the more flexible montmorillonite platelets (Fornes, T.D., 2003, Gopakumar, T.G., 2002).
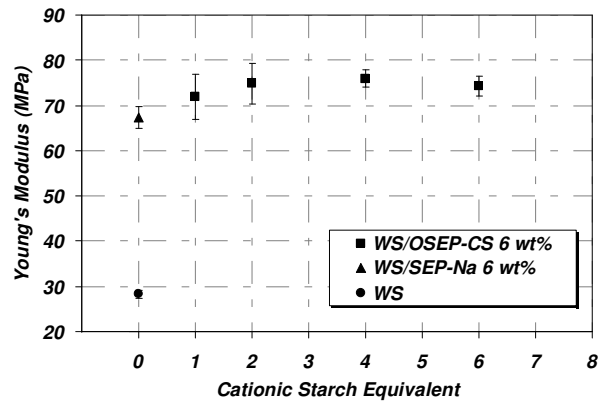
Figure V.13. Variations of the Young's modulus against cationic starch content for WS and WS/(O)SEP 6 wt% nano-biocomposites.

Table V.2. WS/(O)MMT mechanical properties.

	Young's Modulus (MPa)	Strain at break (%)	Energy at break (M J/m^3)
WS/MMT-Na 6 wt%	39.2 ± 1.4	21.0 ± 0.8	0.32 ± 0.02
WS/OMMT-CS 6 wt%	46.5 ± 1.2	33.3 ± 2.0	1.01 ± 0.07

Figure V.14 displays the values of the strain at break obtained for plasticized starch and the nano-biocomposites elaborated with 6 wt% of (O)SEP. Compared to the neat matrix, a small decrease in the strain at break is obtained with the incorporation of the SEP-Na nanofiller. This decrease is likely due to the global increase in the plasticized starch crystallinity, which is known to reduce the strain at break (Van Soest, J.J.G., 1997a). Regarding the WS/OSEP-1CS samples, a strong decrease in the strain at break value is observed. This decrease is a direct consequence of the large clay aggregates observed by optical microscopy which embrittle the materials. However, a relationship between the amount of cationic starch surfactant and the strain at break values is shown, the highest values being obtained for the nano-biocomposites elaborated with the highest surfactant contents (OSEP-4CS and OSEP-6CS). These remarkable values are even higher than the neat matrix one. This trend is a consequence of the cationic starch addition, which seems to induce a slightly better nano-scale dispersion of e.g., the OSEP-4CS strands compared to the SEP-Na. If we compare with WS/(O)MMT nano-biocomposites, it can be seen that in this case the strain at break of the WS/MMT-Na is lower than the neat matrix one. As for the Young's modulus evolution, this tendency is due to the MMT-Na aggregates, which embrittle the hybrids materials. On the contrary, WS/OMMT-CS nano-biocomposites present a constant strain at break, close to the value of the neat matrix and lower than the WS/OSEP-4CS one.
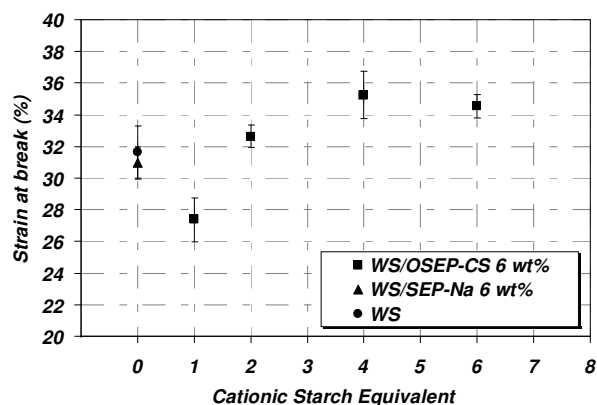
Figure V.14. Variations of the strain at break against cationic starch content for WS and WS/(O)SEP 6 wt% nano-biocomposites.

The energy at break values (Figure V.15) show for all the nano-biocomposite samples an increase when the SEP nanofiller is incorporated into the starchy matrix. These raises are due to the high stiffness increase induced by the SEP incorporation without decreasing the strain at break values (except for WS/OSEP-1CS). More surprisingly, even if a decrease in the strain at break properties of the samples with OSEP-1CS is observed, these materials present an increase in the energy at break values compared to the virgin matrix. This increase is related to the reinforcement effect of the organo-modified nanofiller, which induces a strong increase in the matrix stiffness properties and a higher stress transfer at the interface. Finally, in agreement with the previous results, the energy at break values of the (O)SEP nano-biocomposites are higher than those obtained for the (O)MMT nano-biocomposites. Thus, it has been demonstrated that the SEP needle-shaped nanofiller leads to a higher enhancement of mechanical properties compared to materials based on lamellar MMT.
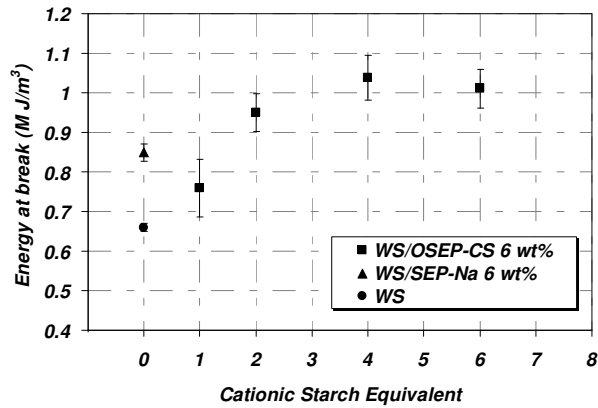
Figure V.15. Variations of the energy at break against cationic starch content for WS and WS/(O)SEP 6 wt% nano-biocomposites.

V. Conclusions

This paper reports the successful elaboration of high performance plasticized starch nano-biocomposites based on sepiolite clay with and without surfactant, natural sepiolite (SEP-Na) and sepiolite organo-modified with cationic starch (OSEP-CS). This innovative class of nano-hybrid materials has then been analyzed in terms of morphology, crystalline structure, thermal and mechanical properties to highlight the interest in using these needle-shaped nanofillers.

Morphological analyses have highlighted a nano-scale dispersion of SEP-Na. Surprisingly, the dispersion of OSEP-CS led to different micro/nano-structurations depending on the cationic starch content adsorbed on the clay surface. The incorporation of OSEP-1CS into plasticized starch generates large clay aggregates. At higher cationic starch content, this surfactant fully acts as a compatibilizer and greatly favors the clay nano-dispersion within the plasticized starch matrix. The TEM micrographs have also shown a phase separation between domains with and without SEP for the nano-biocomposites materials based on SEP-Na or OSEP-CS. We assume that this inhomogeneity is induced by the high glycerol content of the formulation, which leads to phase separation between domain rich in glycerol and domains with low glycerol content, the sepiolite being dispersed into the domain rich in glycerol. Besides, X-ray diffraction measurements have shown that transcrystallization phenomenon occurs at the SEP/matrix interface thanks to the hydrogen bonds established between the nanofiller and the starch chains.

Thermal analyses have demonstrated that the SEP-Na enhances the thermal stability of the starch matrix thanks to dehydration mechanism which locally reduces the sample

temperature. On the contrary, it has been pointed out that cationic starch thermal degradation by-products may favor the plasticized starch degradation mechanism. Finally, tensile tests have been performed and have demonstrated that the incorporation of well dispersed sepiolite nanofiller can increase the material rigidity without affecting its strain at break properties, the best results being obtained with the OSEP-4CS.

Thus, this study clearly highlights the great potential of the sepiolite nanofiller to elaborate plasticized starch nano-biocomposites materials with enhanced properties. Further studies have now to be focused on the use of this needle-shaped nanofiller in other matrices, such as polyhydroxyalkanoates or poylactides. In addition to its exceptional properties, the sepiolite nanofiller can also be used for enzymes immobilization or as a drug carrier thanks to its great adsorption capabilities. Indeed, functional molecules could be sequestrated within its structural cavities (Ruiz-Hitzky, E., 2005). Thus, with the combination of its porous structure and reinforcing properties, it would be possible to develop new functional and bioactive hybrid materials.

VI. Acknowledgment

Publication V : Discussion et commentaires

Cette étude a porté sur l'introduction d'une nanocharge argileuse peu utilisée, la sépiolite, au sein d'une matrice d'amidon plastifié. Deux types de sépiolite ont été incorporées par voie fondue : de la sépiolite sodique (SEP-Na) et de la sépiolite organo-modifiée par de l'amidon cationique (OSEP-CS). Les analyses morphologiques effectuées sur les nano-hybrides amidon/SEP-Na ont mis en évidence une dispersion/distribution à l'échelle nanométrique des aiguilles de sépiolite. De manière surprenante, la dispersion d'OSEP-CS conduit à différentes micro/nano-structurations en fonction de la quantité d'amidon cationique adsorbé à la surface de l'argile. L'incorporation d'OSEP-1CS, c'est-à-dire organo-modifiée avec un équivalent (1 fois la CEC) d'amidon cationique, génère de larges agrégats micrométriques de sépiolite. A cette concentration, l'amidon cationique agit comme un agent floculant créant des « ponts » entre les différentes aiguilles de sépiolite. Au-delà de cette concentration, l'amidon cationique joue pleinement son rôle de compatibilisant et favorise significativement la nano-dispersion de la sépiolite. Par ailleurs, les analyses de MET ont mis en lumière une séparation de phases entre des domaines riches et pauvres en nanocharges. A l'image des résultats obtenus sur des nano-biocomposites amidon/montmorillonite, cette disparité est probablement induite par le fort taux de glycérol de la formulation qui conduit à une dispersion hétérogène des aiguilles de sépiolite entre des domaines pauvres et riches en plastifiant. Les analyses de diffraction des rayons-X ont également mis à jour un phénomène de transcristallinité localisé à l'interface matrice/sépiolite probablement favorisé par les nombreuses liaisons hydrogènes établies entre les nanocharge et les chaînes d'amidon.

Les analyses thermo-gravimétriques effectuées sur ces nano-hybrides ont démontré que la SEP-Na augmentait la stabilité thermique des nano-biocomposites grâce à la déshydratation de la nanocharge qui réduit localement la température de l'échantillon. A l'inverse, dans le cas de l'incorporation de l'OSEP-CS, il semble que les sous-produits de la dégradation thermique de l'amidon cationique favorisent et augmentent la dégradation de l'amidon plastifié. Enfin, les tests de traction uniaxiale réalisés ont clairement démontré que la bonne dispersion de la sépiolite conduit à une rigidification de la matrice sans affecter ses propriétés d'élongation à la rupture. Ces améliorations des propriétés mécaniques sont nettement supérieures à celles observées pour les nano-hybrides amidon/montmorillonite. Par conséquent, cette étude a permis de mettre en évidence le fort potentiel de la sépiolite pour élaborer des nano-biocomposites d'amidon avec des propriétés largement améliorées.

Chapitre III : Conclusions et perspectives

Ce chapitre aura permis d'améliorer la compréhension de l'influence de l'amidon cationique sur la nano-dispersion des argiles dans les nano-biocomposites d'amidon. La première étude aura révélé l'effet de la nature du plastifiant sur le processus d'intercalation/exfoliation dans des matrices amidon plastifiées. Ainsi, il a été démontré que si l'amidon cationique est un compatibilisant efficace avec le glycérol, son efficacité est moindre avec le sorbitol.

L'étude de l'organo-modification de la sépiolite a aussi permis de mettre en lumière le comportement de l'amidon cationique qui dépend de la proportion adsorbée sur les aiguilles de sépiolite. Ce tensio-actif peut, suivant sa concentration, jouer le rôle de compatibilisant matrice/nanocharge ou au contraire d'agent floculant.

Références du chapitre III

Alexandre, M.; Dubois, P., Polymer-layered silicate nanocomposites: Preparation, properties and uses of a new class of materials. Mater. Sci. Eng. R-Rep. 2000, 28, 1-63.

Averous, L., Biodegradable multiphase systems based on plasticized starch: A review. J. Macromol. Sci. Part C-Polym. Rev. 2004b, 44, 231-274.

Bagdi, K.; Muller, P.; Pukanszky, B., Thermoplastic starch/layered silicate composites: Structure, interaction, properties. Compos. Interfaces 2006, 13, 1-17.

Bilotti, E.; Fischer, H. R.; Peijs, T., Polymer nanocomposites based on needle-like sepiolite clays: Effect of functionalized polymers on the dispersion of nanofiller, crystallinity, and mechanical properties. J. Appl. Polym. Sci. 2008, 107, 1116-1123.

Chen, H.; Zheng, M.; Sun, H.; Jia, Q., Characterization and properties of sepiolite/polyurethane nanocomposites. Mater. Sci. Eng. A-Struct. Mater. Prop. Microstruct. Process. 2007, 445-446, 725-730.

Chiou, B.-S.; Yee, E.; Wood, D.; Shey, J.; Glenn, G.; Orts, W., Effects of processing conditions on nanoclay dispersion in starch-clay nanocomposites. Cereal Chem. 2006, 83, 300-305.

Chiou, B. S.; Wood, D.; Yee, E.; Imam, S. H.; Glenn, G. M.; Orts, W. J., Extruded starch-nanoclay nanocomposites: Effects of glycerol and nanoclay concentration. Polym. Eng. Sci. 2007, 47, 1898-1904.

Chivrac, F.; Kadlecova, Z.; Pollet, E.; Averous, L., Aromatic copolyester-based nano-biocomposites: Elaboration, structural characterization and properties. J. Polym. Environ. 2006, 14, 393-401.

Chivrac, F.; Pollet, E.; Schmutz, M.; Averous, L., New Approach to Elaborate Exfoliated Starch-Based Nanobiocomposites. Biomacromolecules 2008, 9, 896-900.

Cyras, V. P.; Manfredi, L. B.; Ton-That, M. T.; Vazquez, A., Physical and mechanical properties of thermoplastic starch/montmorillonite nanocomposite films. Carbohydr. Polym. 2008a, 73, 55-63

Cyras, V. P.; Manfredi, L. B.; Ton-That, M. T.; Vazquez, A., Physical and mechanical properties of thermoplastic starch/montmorillonite nanocomposite films. Carbohydr. Polym. 2008b, 73, 55-63.

Darder, M.; Lopez-Blanco, M.; Aranda, P.; Aznar, A. J.; Bravo, J.; Ruiz-Hitzky, E., Microfibrous chitosan - Sepiolite nanocomposites. Chem. Mat. 2006, 18, 1602-1610.

Dean, K.; Yu, L.; Wu, D. Y., Preparation and characterization of melt-extruded thermoplastic starch/clay nanocomposites. Compos. Sci. Technol. 2007, 67, 413-421.

Dean, K. M.; Do, M. D.; Petinakis, E.; Yu, L., Key interactions in biodegradable thermoplastic starch/poly(vinyl alcohol)/montmorillonite micro- and nanocomposites. Compos. Sci. Technol. 2008, 68, 1453-1462.

Dennis, H. R.; Hunter, D. L.; Chang, D.; Kim, S.; White, J. L.; Cho, J. W.; Paul, D. R., Effect of melt processing conditions on the extent of exfoliation in organoclay-based nanocomposites. Polymer 2001, 42, 9513-9522.

Duquesne, E.; Moins, S.; Alexandre, M.; Dubois, P., How can nanohybrids enhance polyester/sepiolite nanocomposite properties? Macromol. Chem. Phys. 2007, 208, 2542-2550.

Fornes, T. D.; Paul, D. R., Modeling properties of nylon 6/clay nanocomposites using composite theories. Polymer 2003, 44, 4993-5013.

Gain, O.; Espuche, E.; Pollet, E.; Alexandre, M.; Dubois, P., Gas barrier properties of poly(ε-caprolactone)/clay nanocomposites: Influence of the morphology and polymer/clay interactions. J. Polym. Sci. Pt. B-Polym. Phys. 2005, 43, 205-214.

Gaudin, S.; Lourdin, D.; Le Botlan, D.; Ilari, J. L.; Colonna, P., Plasticisation and mobility in starch-sorbitol films. J. Cereal Sci. 1999, 29, 273-284.

Gopakumar, T. G.; Lee, J. A.; Kontopoulou, M.; Parent, J. S., Influence of clay exfoliation on the physical properties of montmorillonite/polyethylene composites. Polymer 2002, 43, 5483-5491.

Gorrasi, G.; Tortora, M.; Vittoria, V.; Pollet, E.; Lepoittevin, B.; Alexandre, M.; Dubois, P., Vapor barrier properties of polycaprolactone montmorillonite nanocomposites: Effect of clay dispersion. Polymer 2003, 44, 2271-2279.

Huang, M.; Yu, J.; Ma, X., High mechanical performance MMT-urea and formamide-plasticized thermoplastic cornstarch biodegradable nanocomposites. Carbohydr. Polym. 2006, 63, 393-399.

Huang, M. F.; Yu, J. G.; Ma, X. F., Studies on the properties of Montmorillonite-reinforced thermoplastic starch composites. Polymer 2004, 45, 7017-7023.

Kampeerapappun, P.; Aht-ong, D.; Pentrakoon, D.; Srikulkit, K., Preparation of cassava starch/montmorillonite composite film. Carbohydr. Polym. 2007, 67, 155-163.

Kuang, W.; Facey, G. A.; Detellier, C.; Casal, B.; Serratosa, J. M.; Ruiz-Hitzky, E., Nanostructured Hybrid Materials Formed by Sequestration of Pyridine Molecules in the Tunnels of Sepiolite. Chem. Mat. 2003, 15, 4956-4967.

Lilichenko, N.; Maksimov, R. D.; Zicans, J.; Merijs Meri, R.; Plume, E., A biodegradable polymer nanocomposite: Mechanical and barrier properties. Mech. Compos. Mater. 2008, 44, 45-56.

Lourdin, D.; Coignard, L.; Bizot, H.; Colonna, P., Influence of equilibrium relative humidity and plasticizer concentration on the water content and glass transition of starch materials. Polymer 1997, 38, 5401-5406.

Lourdin, D.; Ring, S. G.; Colonna, P., Study of plasticizer-oligomer and plasticizer-polymer interactions by dielectric analysis: maltose-glycerol and amylose-glycerol-water systems. Carbohydr. Res. 1998, 306, 551-558.

Lourdin, D.; Colonna, P.; Ring, S. G., Volumetric behaviour of maltose-water, maltose-glycerol and starch-sorbitol-water systems mixtures in relation to structural relaxation. Carbohydr. Res. 2003, 338, 2883-2887.

Luo, J. J.; Daniel, I. M., Characterization and modeling of mechanical behavior of polymer/clay nanocomposites. Compos. Sci. Technol. 2003, 63, 1607-16.

Ma, J.; Bilotti, E.; Peijs, T.; Darr, J. A., Preparation of polypropylene/sepiolite nanocomposites using supercritical CO2 assisted mixing. Eur. Polym. J. 2007, 43, 4931-4939.

Ma, X.; Yu, J.; Wang, N., Production of thermoplastic starch/ MMT-sorbitol nanocomposites by dual-melt extrusion processing. Macromol. Mater. Eng. 2007, 292, 723-728.

Mondragon, M.; Mancilla, J. E.; Rodriguez-Gonzalez, F. J., Nanocomposites from plasticized high-amylopectin, normal and high-amylose maize starches. Polym. Eng. Sci. 2008, 48, 1261-1267.

Neus Angles, M.; Dufresne, A., Plasticized starch/tuniein whiskers nanocomposites. 1. Structural analysis. Macromolecules 2000, 33, 8344-8353.

Pandey, J. K.; Singh, R. P., Green nanocomposites from renewable resources: Effect of plasticizer on the structure and material properties of clay-filled starch. Starch-Starke 2005, 57, 8-15.

Park, H. M.; Li, X.; Jin, C. Z.; Park, C. Y.; Cho, W. J.; Ha, C. S., Preparation and properties of biodegradable thermoplastic starch/clay hybrids. Macromol. Mater. Eng. 2002, 287, 553-558.

Park, H. M.; Lee, W. K.; Park, C. Y.; Cho, W. J.; Ha, C. S., Environmentally friendly polymer hybrids Part I mechanical, thermal, and barrier properties of thermoplastic starch/clay nanocomposites. J. Mater. Sci. 2003, 38, 909-915.

Ruiz-Hitzky, E.; Darder, M.; Aranda, P., Functional biopolymer nanocomposites based on layered solids. J. Mater. Chem. 2005, 15, 3650-3662.

Sandi, G.; Winans, R. E.; Seifert, S.; Carrado, K. A., In situ SAXS studies of the structural changes of sepiolite clay and sepiolite-carbon composites with temperature. Chem. Mat. 2002, 14, 739-742.

Sinha Ray, S.; Okamoto, M., Polymer/layered silicate nanocomposites: A review from preparation to processing. Prog. Polym. Sci. 2003, 28, 1539-1641.

Swanson, C. L.; Shogren, R. L.; Fanta, G. F.; Imam, S. H., Starch-plastic materials-Preparation, physical properties, and biodegradability (a review of recent USDA research). J. Environ. Polym. Deg. 1993, 1, 155-166.

Tang, X.; Alavi, S.; Herald, T. J., Effects of plasticizers on the structure and properties of starch-clay nanocomposite films. Carbohydr. Polym. 2008, 74, 552-558.

Tartaglione, G.; Tabuani, D.; Camino, G., Thermal and morphological characterisation of organically modified sepiolite. Micropor. Mesopor. Mat. 2008, 107, 161-168.

Tomka, I., Thermoplastic starch. Adv. Exp. Med. Biol. 1991, 302, 627-637.

Torre, L.; Kenny, J. M.; Maffezzoli, A. M., Degradation behaviour of a composite material for thermal protection systems Part I-Experimental characterization. J. Mater. Sci. 1998, 33, 3137-3143.

Van Soest, J. J. G.; Hulleman, S. H. D.; De Wit, D.; Vliegenthart, J. F. G., Changes in the mechanical properties of thermoplastic potato starch in relation with changes in B-type crystallinity. Carbohydr. Polym. 1996, 29, 225-232.

Van Soest, J. J. G.; Essers, P., Influence of amylose-amylopectin ratio on properties of extruded starch plastic sheets. J. Macromol. Sci. Part A-Pure Appl. Chem. 1997, 34, 1665-1689.

Weir, M. R.; Kuang, W.; Facey, G. A.; Detellier, C., Solid-state nuclear magnetic resonance study of sepiolite and partially dehydrated sepiolite. Clay Clay Min. 2002, 50, 240-247.

Wilhelm, H.-M.; Sierakowski, M.-R.; Souza, G. P.; Wypych, F., The influence of layered compounds on the properties of starch/layered compound composites. Polym. Int. 2003a, 52, 1035-1044.

Wilhelm, H.-M.; Sierakowski, M.-R.; Souza, G. P.; Wypych, F., Starch films reinforced with mineral clay. Carbohydr. Polym. 2003b, 52, 101-110.

Zhang, Q. X.; Yu, Z. Z.; Xie, X. L.; Naito, K.; Kagawa, Y., Preparation and crystalline morphology of biodegradable starch/clay nanocomposites. Polymer 2007, 48, 7193-7200.

Zhang, X.; Do, M. D.; Dean, K.; Hoobin, P.; Burgar, I. M., Wheat-gluten-based natural polymer nanoparticle composites. Biomacromolecules 2007, 8, 345-353.

Zheng, Y., Study on sepiolite-reinforced polymeric nanocomposites. J. Appl. Polym. Sci. 2006, 99, 2163-2166.

Chapitre IV

-

Modélisation des propriétés mécaniques des nano-biocomposites amidon/montmorillonite

Introduction

Les chapitres précédents ont mis en avant la forte influence de l'incorporation de nanocharges sur le comportement de l'amidon plastifié. Ce chapitre, qui se présente sous la forme de deux publications complémentaires, s'attachera plus particulièrement à la modélisation et à la compréhension de l'impact de l'état de dispersion de la montmorillonite sur les propriétés mécaniques. La première publication est dédiée à la modélisation des propriétés d'élasticité des nano-biocomposites amidon de blé/montmorillonite. La deuxième publication est plus particulièrement focalisée sur la modélisation des propriétés à la limite d'élasticité.

La **Publication VI** est axée sur l'application du modèle de Mori-Tanaka généralisé afin de modéliser, comprendre et donc prévoir le module d'Young de matériaux nano-biocomposites. Ce modèle classique est ici modifié afin de tenir compte de la concentration ainsi que de l'état de dispersion des nanocharges au sein de la matrice. Les modélisations effectuées sont ensuite confrontées aux valeurs expérimentales obtenues lors des tests de traction uniaxiale réalisés sur des nano-biocomposites d'amidon élaborés avec 3 ou 6 % en masse de MMT-Na ou d'OMMT-CS.

La **Publication VII** traite de la modélisation des propriétés à la limite d'élasticité de nano-biocomposites amidon/montmorillonite présentant différentes morphologies et différents taux d'inorganique. Ces modélisations ont été effectuées à partir d'un modèle micromécanique dit coopératif décrivant de manière adéquate le comportement de matériaux polymères semi-cristallins. Ce modèle est lui aussi modifié afin de tenir compte de l'état de dispersion des nanocharges au sein de la matrice. Les modélisations obtenues sont ensuite confrontées aux résultats expérimentaux obtenus sur les différents nano-biocomposites amidon/montmorillonite.

Micromechanical modeling and characterization of the effective properties in starch-based nano-biocomposites

Frédéric CHIVRAC, Olivier GUEGUEN, Éric POLLET, Said AHZI, Ahmed MAKRADI, Luc AVEROUS

Acta Biomaterialia, 2008, vol. 4, n° 6, pages 1707-1714

UNIVERSITÉ DE STRASBOURG

Publication VI : Discussion et commentaires

Cette étude a porté sur la modélisation des propriétés élastiques des nano-biocomposites à base d'amidon. Il a été montré que, comme les plastifiants de l'amidon (eau et glycérol) s'adsorbent à la surface des feuillets de montmorillonite, la rigidité de la nanocharge n'est pas totalement transmise à la matrice lors de la sollicitation en traction uniaxiale. Par conséquent, la notion de module effectif représentant la contribution réelle de la nanocharge aux propriétés élastiques des nano-biocomposites a été introduite. Les différentes modélisations effectuées ont permis de décrire le comportement des nano-biocomposites d'amidon en fonction du taux d'inorganique, de l'humidité relative de stockage et du vieillissement. Par ailleurs, la variation du rapport exfoliation/agrégation permet d'envisager la mise au point d'un outil indirect, mais global, de quantification de la qualité de la nano-dispersion des charges dans les matériaux nanocomposites. Il faut noter que le taux d'exfoliation déterminé avec la MMT-Na est probablement surestimé de part l'immobilisation d'une partie du plastifiant dans l'espace inter-feuillets de la montmorillonite. Cependant, grâce à ce modèle, il apparaît possible de prévoir les variations de propriétés élastiques en fonction de l'humidité, du temps de stockage, de la concentration en nanocharge et du taux d'exfoliation/agrégation de ces nano-biocomposites. Et à l'inverse, à partir de ce modèle et d'un simple test de traction uniaxiale, il est possible en connaissant les autres paramètres d'estimer le taux d'exfoliation/agrégation de ces nano-biocomposites. Ceci en fait donc un outil simple d'analyse de la nanostructuration de ces matériaux.

Toutefois, bien que ce modèle prévoit de manière adéquate les résultats expérimentaux, plusieurs phénomènes physiques influençant les propriétés élastiques finales de ces matériaux, tels que des interactions spécifiques charge/matrice, des effets d'échelle ou des orientations de charges sous contrainte sont encore négligés.

Afin de décrire plus globalement l'influence des nanocharges et de leur état de dispersion sur les propriétés mécaniques de nos nano-hybrides, nous nous sommes attaché dans la **Publication VII** à la description de leur comportement à la limite d'élasticité.

Publication VII – Micromechanically-based formulation of the cooperative model for the yield behavior of starch-based nano-biocomposites

Frédéric Chivrac[2], Olivier Gueguen[1], Eric Pollet[2], David Ruch[3], Said Ahzi[1]*, Luc Avérous[2]

I. Abstract

The tensile yield stress of plasticized starch filled with montmorillonite has been studied as a function of the temperature and the strain rate and has been compared to the yield behavior of the original matrix. Aggregated/intercalated and exfoliated nano-biocomposites, obtained from different nanofillers, have been produced and tested under uniaxial tension (tensile test). To describe the nanocomposite tensile yield stress behavior, a preexisting cooperative model, which describes properly the semi-crystalline polymer tensile yield stress, has been modified. According to our development, the yield behavior of nano-biocomposites is strongly dependant on the clay concentration and exfoliation ratio. Based on the thermodynamics properties, an effective activation volume and an effective activation energy are computed through the Takayanagi homogenization model. The predicted results at low strain rates and at different temperatures are in agreement with our experimental results.

Keywords: yield behavior, micromechanical modeling, nano-biocomposites, starch, cooperative model

[*] Corresponding author: Said Ahzi.

Tel.: +33-3-90-242-952 - Fax: +33-3-88-614-300 - Ahzi@imfs.u-strasbg.fr

[1] IMFS, UMR 7507, Université Louis Pasteur, 2 Rue Boussingault, 67000 Strasbourg, France

[2] LIPHT-ECPM, UMR 7165, Université Louis Pasteur, 25 rue Becquerel, 67087 Strasbourg Cedex 2, France

[3] LTI, Research Center Henry Tudor, 70 Rue de Luxembourg, L-4221 Esch-sur-Alzette, Luxembourg

II. Introduction

Nanocomposites are organic/inorganic hybrid materials composed of nanosized fillers (nanofillers) incorporated into a polymer matrix (Vaia, R.A., 1993). Depending on the chosen nanofillers and on the obtained nanostructure, the nanocomposite materials can exhibit drastic modifications in their properties, such as the mechanical properties, transparency, barrier properties, or change in their electrical and thermal conductivity (Alexandre, M., 2000, Gain, O., 2005, Gorrasi, G., 2004, Sinha Ray, S., 2003)… Such properties enhancements rely both on the nanofiller geometry and on its surface area (700 m^2/g for the montmorillonite when this nanofiller is exfoliated) (Sinha Ray, S., 2003). The interface created between the nanofiller and the matrix depends on the nanofiller dispersion state (Cho, J.W., 2001, Dennis, H.R., 2001). In the case of layered silicates, the nanofillers can either be intercalated by macromolecules and/or exfoliated, leading to strong differences in the behavior. Intercalated structures show regularly alternating layered silicates and polymer chains compared to exfoliated structures in which the clay platelets are individually delaminated and fully dispersed in the polymer matrix (Fornes, T.D., 2001, Sinha Ray, S., 2003). The best performances are commonly observed with the exfoliated structures (Lepoittevin, B., 2002a, Pollet, E., 2004). Up to now, most of the published work concerning nanocomposites has been focused on their preparation and resulting properties. However, only few studies have been carried out to investigate and model the montmorillonite morphology/dispersion. In the present study, we are interested in developing a micromechanically based model for yield behavior of polymer nanocomposites with particular application to plasticized starch/montmorillonite nano-biocomposites (biodegradable nanocomposite) (Chivrac, F., 2006).

The strain rate and temperature dependence of the yield stress of many polymers can be described by an Eyring formulation (Eyring, H., 1936) where it is assumed that polymer chain segments have to overcome an energy barrier at the yield point. Accordingly, the reduced yield stress is given by Equation VII.1 (Brooks, N.W.J., 1995):

$$\frac{\sigma_y}{T} = \frac{k}{V} \sinh^{-1}\left(\frac{\dot{\varepsilon}}{\dot{\varepsilon}_0 \exp\left(-\dfrac{\Delta H}{kT}\right)}\right) \qquad (VII.1)$$

where σ_y is the yield stress, T refers to the absolute temperature, k is the Boltzmann's constant, V is the activation volume, ΔH is the activation energy, $\dot{\varepsilon}$ is the strain rate and $\dot{\varepsilon}_0$ is a pre-exponential factor (or reference strain rate). Many authors (Brooks, N.W.J., 1995, Eyring, H., 1936, Fotheringham, D.G., 1978, Truss, R.W., 1984, Ward, I.M., 1984) indicated that the yield behavior of both amorphous and semi-crystalline polymers could not be represented by a single molecular process, but rather by at least two activated processes acting in parallel. Recently, Richeton et al. (Richeton, J., 2005) developed a new formulation of the cooperative model of Fotheringham and Cherry (Fotheringham, D.G., 1978) starting from a strain rate/temperature superposition principle for the yield stress. Gueguen et al. (Gueguen, O., 2008a) extended the cooperative model to semi-crystalline polymers through a multiscale development of an effective activation energy, ΔH_{eff}, and an effective activation volume, V_{eff}, as follows:

$$\Delta H_{eff} = \frac{\varphi \cdot \Delta H_2 \cdot \Delta H_1}{\Omega \cdot \Delta H_1 + (1-\Omega) \cdot \Delta H_2} + (1-\varphi) \cdot \Delta H_1$$

$$V_{eff} = \frac{\varphi \cdot V_2 \cdot V_1}{\Omega \cdot V_1 + (1-\Omega) \cdot V_2} + (1-\varphi) \cdot V_1$$

(VII.2)

where φ and Ω are parameters relating the crystalline (f_c) and amorphous (f_a) volume fractions (Equation VII.3):

$$\begin{cases} f_c = \varphi \cdot \Omega \\ f_a = 1 - \varphi \cdot \Omega \end{cases}$$

(VII.3)

The semi-crystalline polymer was considered as a two-phase material where the yield processes are described by the activation parameters in the amorphous phase, ΔH_1 and V_1, and in the crystalline phase, ΔH_2 and V_2. The resulted yield process is then expressed by (Gueguen, O., 2008a):

$$\frac{\sigma_y}{T} = \frac{\sigma_i(0) - m \cdot T}{T} + \frac{2k}{V_{eff}} \sinh^{-1} \left(\frac{\dot{\varepsilon}}{\dot{\varepsilon}_0 \exp\left(-\dfrac{\Delta H_{eff}}{kT}\right)} \right)^{1/n}$$

(VII.4)

where $\sigma_i(0)$ is the internal stress at 0 K; m is a material parameter equal to $\sigma_i(0)/T^*$, T^* being the compensation temperature (Gueguen, O., 2008a, Rault, J., 1998) and n describes the cooperative character of the yield process.

In the present study, we propose to adapt the previous model, which describes properly the yield stress of semi-crystalline polymer materials, to predict the yield stress of plasticized starch and those of two nano-biocomposite families based on starch with two different dispersion states (Chivrac, F., 2008a, Chivrac, F., 2008b). To test this developed model, we have conducted tensile tests to characterize the yield behavior as function of temperature and strain rate. The predicted results are compared to our experiments for different nanoclay concentrations and exfoliation ratios, at different temperatures and strain rates. These two morphologies present different yield behaviors, which constitute a good starting point towards the understanding of the deformation mechanisms in nanocomposite materials.

III. Experimental

1. Materials and preparation protocol

Wheat starch (WS) was supplied by Roquette (France). The amylose and amylopectin contents are 23 and 77 %, respectively. Residual protein content is less than 1 %. The glycerol, a non volatile plasticizer, was supplied by the Société Française des Savons (France) and is a 99.5 % purity product. The cationic starch (CS), a modified polysaccharide, has been supplied by Roquette (France). Its charge density is 944 µequiv.g^{-1}. The Dellite$^®$ LVF sodium montmorillonite (MMT-Na) was supplied by Laviosa Chimica Mineraria S.p.A. (Italy) and has a cationic exchange capacity (CEC) of 1050 µequiv.g^{-1}. The MMT-Na organo-modification has been carried out by exfoliation/adsorption technique with CS leading to the formation of OMMT-CS as described elsewhere (Chivrac, F., 2008b). Two nano-biocomposites with different dispersion state have been elaborated with MMT-Na and OMMT-CS, respectively, according to the following protocol.

First, wheat starch granules and glycerol are both introduced into a turbo-mixer and mixed at high speed (3000 rpm) to obtain a homogeneous dispersion. The mixture is then placed in a ventilated oven at 170 °C for 40 min and occasionally stirred, allowing vaporization of water and diffusion of glycerol into the starch granules. The obtained powder is called "dry-blend". In parallel, the adequate amount of MMT (organo-modified or not) is dispersed in water for 4 h into an ultra-sonic bath at 60 °C to obtain a swollen clay. Then, the dry blend and the swollen clay are pooled together in a mixing chamber (Counter-rotating mixer Rheocord 9000 - Haake, USA) at 70 °C for 20 min with a rotor speed of 150 rpm. The plasticized starch formulation used contains 23 wt% of glycerol, 23 wt% of water and 54 wt% of native starch. The nano-biocomposites have an inorganic fraction of 3 and 6 wt% compared

to the weight of starch and glycerol. After melt processing, the molten materials were compression-molded, to obtain films or plates, with a hot press at 110 °C applying 20 MPa pressure for 15 min. The molded specimens were quenched between two steel plates for 15 min. After elaboration, the samples were equilibrated for 1 month at 57 %RH and 23 °C before characterization. All along this paper, the obtained samples are named WS/XXX y % where WS stands for wheat starch, XXX for the type of (organo)clay and y for the weight percentage of clay inorganic fraction.

2. Morphological Characterization

For TEM observation, the samples were microtomed at low temperature (-80 °C) using a Leica Ultracut S cryo-microtome (Japan) equipped with a diamond knife. The ultra thin sections (ca. 60 nm, prepared from 3mm thick plates) were examined using a Philips CM 12 (Netherland) transmission electron microscope using an acceleration voltage of 120 kV.

Figure VII.1 displays typical TEM micrographs of WS/OMMT-CS 3 wt% nano-biocomposites. A heterogeneous dispersion between rich MMT-domains and region without clay has been observed. This heterogeneity could be explained by the high glycerol content of the plasticized starch formulation which is known to induce a phase separation between low and high glycerol content domains (Averous, L., 2004a). The montmorillonite platelets are probably dispersed into the rich glycerol domains thanks to the good affinity between glycerol and montmorillonite (Chivrac, F., 2008b). In the MMT-rich domains, the TEM pictures show almost individually dispersed layers (~5 platelets per tactoïds) attesting an exfoliated morphology. The clay inter-layer spacing of these small tactoïds estimated from these TEM picture is ~25 Å. Moreover, it is seen that the nanofillers are dispersed into the matrix with no preferential orientation. Thus, according to these results, the WS/OMMT-CS nano-biocomposites are considered as fully exfoliated with an exfoliated ratio $r_e = 1$. Then, the mechanical properties of these nano-biocomposites have been used as a reference to quantify the dispersion state of the WS/MMT-Na samples. This quantification has been carried out thanks to micromechanical models based on the Mori-Tanaka approach (Chivrac, F., 2008a). From this computation, it has been demonstrated that WS/MMT-Na nano-biocomposites present an intercalated structure with the presence of aggregates leading to an exfoliation ratio $r_e = 0.5$.
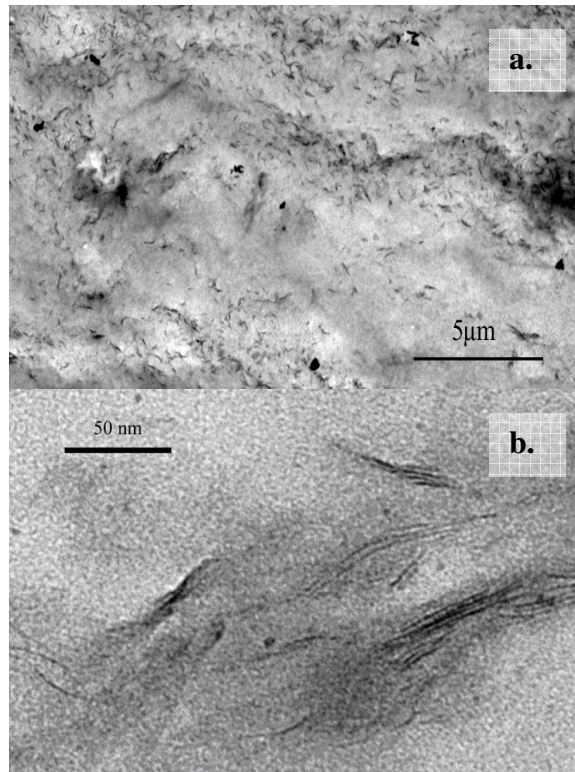
Figure VII.1. TEM pictures of WS/OMMT-CS 3 wt% nano-biocomposites at (a) low magnification and (b) high magnification level.

3. Tensile tests

Tensile tests were carried out with an Instron tensile testing machine (model 4204, USA), at temperatures from 20 to 50 °C and at constant strain rates from 10^{-3} to 10^{-1} s^{-1}. The selected range of temperatures is limited by the water volatilization temperature (100 °C). Before testing, the samples (dumbbell-shaped specimens prepared by compression molding) are stabilized 30 min at the desired temperature. The yield stress values (σ_y) are determined as described in Figure VII.2 (Meijer, H.E.H., 2003, Oleinik, E.F., 2003, Ward, I.M., 1971). For each formulation five samples were tested.
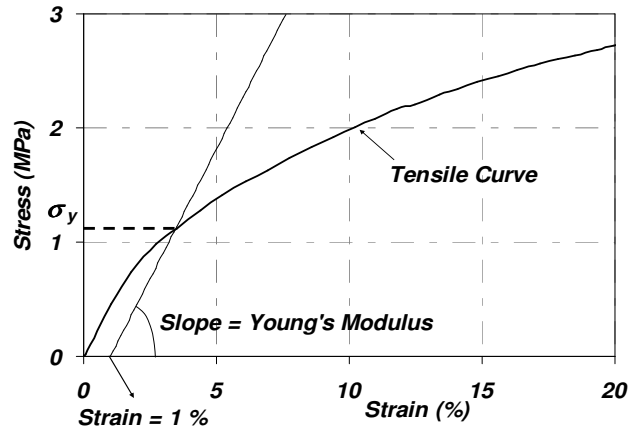
Figure VII.2. Yield stress (σ_y) determination from the tensile curve.

Figure VII.3 displays the WS typical tensile curves obtained at 293 K for different strain rates. In the same way, Figure VII.4 shows the tensile curves recorded at 293 K for WS, WS/OMMT-CS 3 and 6 wt% and WS/MMT-Na 6 wt% for a given strain rate. The tensile yield stress values of the plasticized starch and its nano-biocomposites estimated from these curves are given in Table VII.1. It is clearly seen from these data that, the higher the strain rate, the higher the yield stress. Moreover, the higher the inorganic content, the higher the yield stress. This behavior is commonly observed in nanocomposite materials and is induced by the montmorillonite platelets reinforcing effect (Alexandre, M., 2000, Sinha Ray, S., 2003, Vaia, R.A., 1997). Moreover, a clear link between the yield stress and the dispersion state is observed, the yield stress obtained for exfoliated samples (OMMT-CS) being higher than those of aggregated samples (MMT-Na). This trend is directly linked with the montmorillonite dispersion state into the nano-biocomposite material. Indeed, the better the dispersion state, the higher the interfaces created between the nanofiller and the matrix and thus, the higher the reinforcing efficiency (Chivrac, F., 2008a).
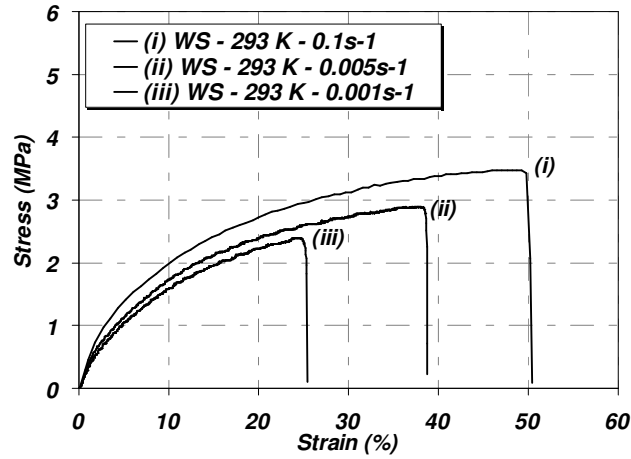
Figure VII.3. Plasticized starch typical tensile curves obtained at 293 K at different strain rates
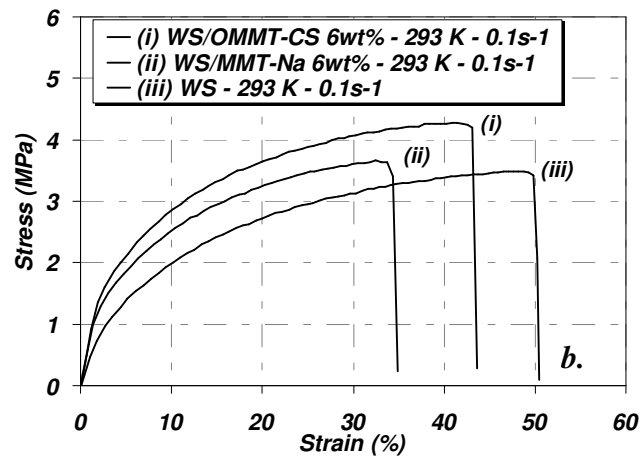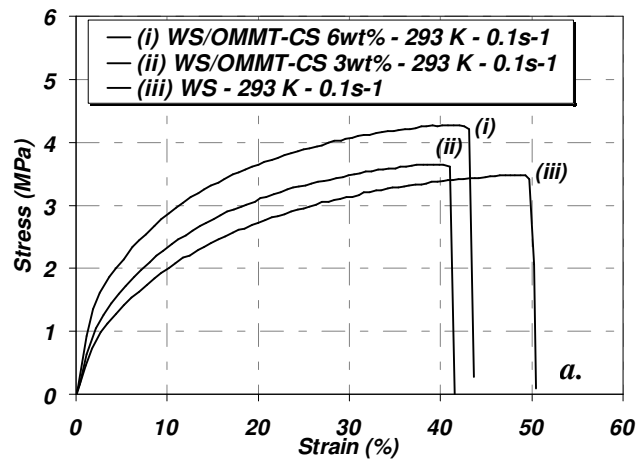
Figure VII.4. Typical tensile curves obtained at 293 K for (*a.*) WS, WS/OMMT-CS 3 and 6 wt% at a given strain rate and for (*b.*) WS, WS/(O)MMT 6 wt% at a given strain rate.

Table VII.1. Tensile yield stress obtained at different $\dot{\varepsilon}$ for WS and its nano-biocomposites at different temperature.

	T (K)	$\dot{\varepsilon} = 0.1$ s^{-1}	$\dot{\varepsilon} = 0.01$ s^{-1}	$\dot{\varepsilon} = 0.005$ s^{-1}	$\dot{\varepsilon} = 0.001$ s^{-1}
	293	1.12	/	0.89	0.80
WS	308	1.06	0.84	/	0.72
	323	0.96	0.78	/	0.65
	293	1.42	1.09	/	0.87
WS/OMMT-CS 3 wt%	308	1.24	0.90	/	0.70
	323	1.00	0.76	/	0.54
	293	1.80	1.26	/	0.79
WS/OMMT-CS 6wt%	308	1.40	1.01	/	0.67
	323	1.12	0.75	/	0.57
WS/MMT-Na 3 wt%	293	1.16	0.90	/	0.72
	323	1.04	0.80	/	0.65
WS/MMT-Na 6 wt%	293	1.50	1.02	/	0.71

IV. Modeling, Results and discussion

1. Identification and discussion on the model parameters

The cooperative model, given by Equation VII.4, has been used to predict the plasticized starch and the corresponding nano-biocomposites yield stress dependence versus strain rate and temperature.

For the model parameters determination, the experimental data have to be superposed horizontally and vertically in an Eyring plot graphic (σ_y / T vs. $\log \dot{\varepsilon}$) to create a master curve at a reference temperature (T_{ref}) (Bauwens-Crowet, C., 1969). The horizontal and vertical shifts are given respectively by the following expressions (Gueguen, O., 2008a, Richeton, J., 2005):

$$\begin{cases} \Delta\left(\log \dot{\varepsilon}\right) = \dfrac{\Delta\mathrm{H}_{eff}}{k \ln 10}\left(\dfrac{1}{\mathrm{T}} - \dfrac{1}{\mathrm{T}_{ref}}\right) \\[3mm] \Delta\left(\dfrac{\sigma_y}{\mathrm{T}}\right) = -\sigma_i\left(0\right)\left(\dfrac{1}{\mathrm{T}} - \dfrac{1}{\mathrm{T}_{ref}}\right) \end{cases} \qquad (VII.5)$$

Once the master curve is built, the parameters ΔH_{eff} and $\sigma_i\left(0\right)$ could be determined with Equation VII.5. From the ΔH_{eff} value, the parameters ΔH_1 and ΔH_2 could be estimated through Equation VII.2 for a given clay inorganic content. The remaining cooperative model

parameters (V_{eff}, n, $\dot{\varepsilon}_0$) are then calculated with a fit of the master curve. Finally, the parameters V_1 and V_2 are also derived from Equation VII.2.

To take into account the montmorillonite dispersion state, the volume fraction f_c used in Equation VII.3 is replaced by the clay inorganic content, y_{clay}, which is equal to:

$$y_{clay} = y \times r_e = \varphi \cdot \Omega \qquad (VII.6)$$

where r_e is the exfoliation ratio. The parameter Ω is determined using Equation VII.6 for each specific exfoliation ratio, r_e, and clay content, y. As explained above, according to our previous work based on the starch nano-biocomposites, the WS/OMMT-CS nano-biocomposites present a good nano-dispersion with a high extent of exfoliation ($r_e = 1$). In contrast, the WS/MMT-Na nano-biocomposite presents an intercalated structure with the presence of aggregates leading to $r_e = 0.5$ (Chivrac, F., 2008a).

2. Strain rate and temperature dependence

To determine the cooperative model parameters, the experimental tensile yield stress values recorded for the plasticized starch matrix and the nano-biocomposites have been shifted using Equation VII.5 at T_{ref} = 293 K. The master curves obtained are presented into an Eyring plot shown in Figure VII.5 and the cooperative model parameters obtained from theses curves are given in Table VII.2.

Table VII.2. Parameters for the cooperative model.

Parameters	Value
N	1.4
Φ	0.65
V_M (m^3)	$8.00 \ 10^{-26}$
V_{clay} (m^3)	$1.30 \ 10^{-27}$
$\sigma_i(0)$ (MPa)	0.8
ΔH_M (kJ/mol)	80
ΔH_{clay} (kJ/mol)	454
T^* (K)	273
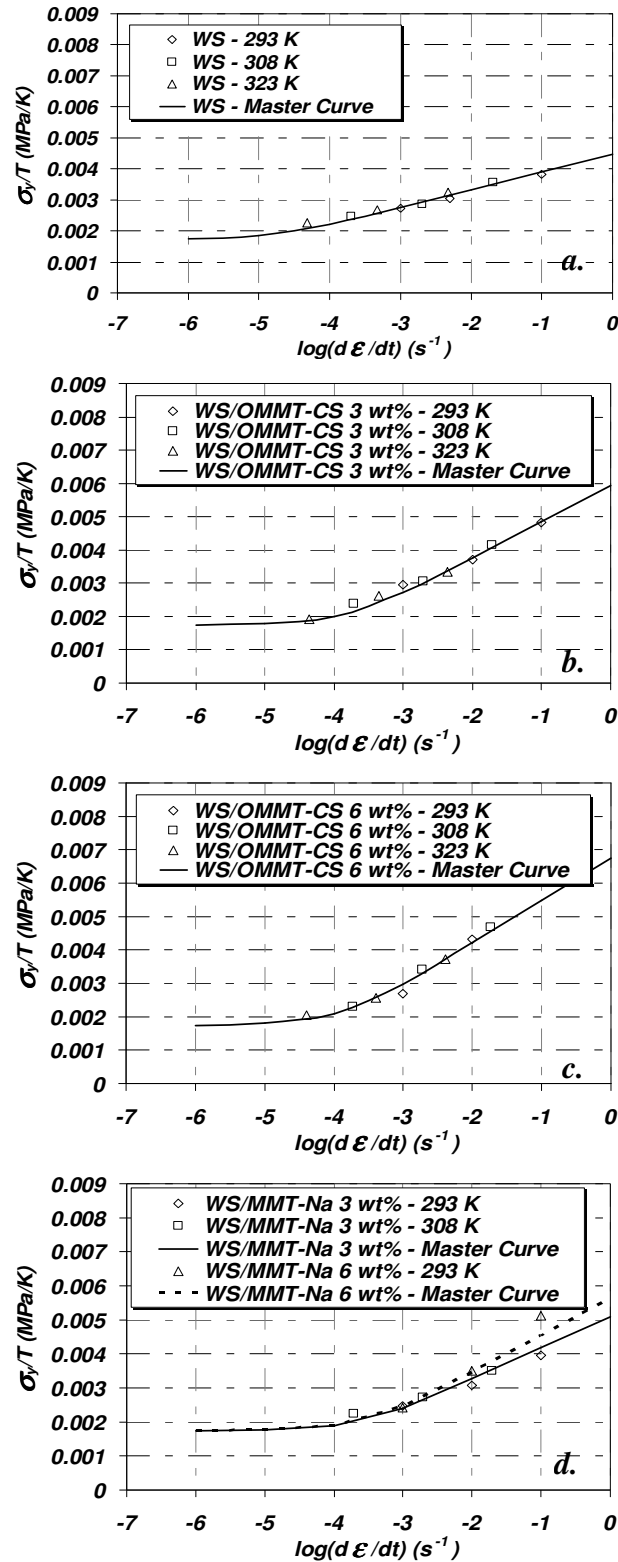
Figure VII.5. Master curves build at 293 K for (*a.*) WS, (*b.*) WS/OMMT-CS 3 wt%, (*c.*) WS/OMMT-CS 6 wt% and (*d.*) WS/MMT-Na 3 and 6 wt% samples tested under uniaxial tension.

As the plasticized starch is mainly amorphous (less than 10 % of crystallinity), the compensation temperature T^* is assumed equal to the starch glass transition temperature (273 K) (Richeton, J., 2005). Therefore, the material parameter m is given by: $m = \sigma_i(0)/T^* \approx 1.10^{-3}$. The pre-exponential parameter values ($\dot{\varepsilon}_0$) variations, listed in Table VII.3, highlight a dependence on the nanoclays concentration. The $\dot{\varepsilon}_0$ values obtained with the two nano-biocomposite families (not shown here), namely WS/OMMT-CS and WS/MMT-Na, are equivalents. Thus, this parameter does not depend on the nanofiller nature. The value of the parameter φ used in Equation VII.6 is fitted for 3% of WS/OMMT-CS and its influence is illustrated in Figure VII.6. At low strain rates, its effect can be neglected but a discrepancy is observed on the predicted results by increasing the strain rates.

Table VII.3. $\dot{\varepsilon}_0$ (s^{-1}) values for the different clay inorganic contents.

Clay inorganic content	$\dot{\varepsilon}_0$ (s^{-1})
0.00	7.30 10^9
0.03	1.53 10^{11}
0.06	3.00 10^{11}
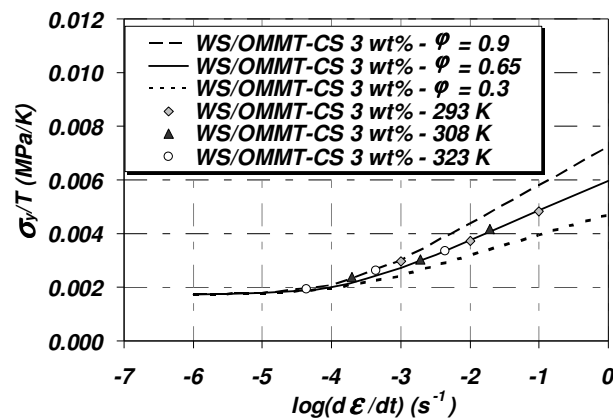
Figure VII.6. Influence of the parameter φ.

From these parameters, the yield stress experimental values are compared to the predicted values using the cooperative model and are represented in Figure VII.7. It is seen from these results that the cooperative model is in fair agreement with the yield properties of plasticized starch materials and its nano-biocomposites, whatever the dispersion state (50 or 100 % exfoliated samples). Nevertheless, for a strain rate $\dot{\varepsilon} = 0.1$ s^{-1} and a montmorillonite concentration of 6 wt%, the cooperative model underestimates the experimental data for both types of nano-biocomposites, WS/OMMT-CS and WS/MMT-Na. Additional experiments need to be conducted to verify the results for higher strain rates as well as a microscopic

analysis of the deform samples at different strains to check a possible evolution of the microstructure.
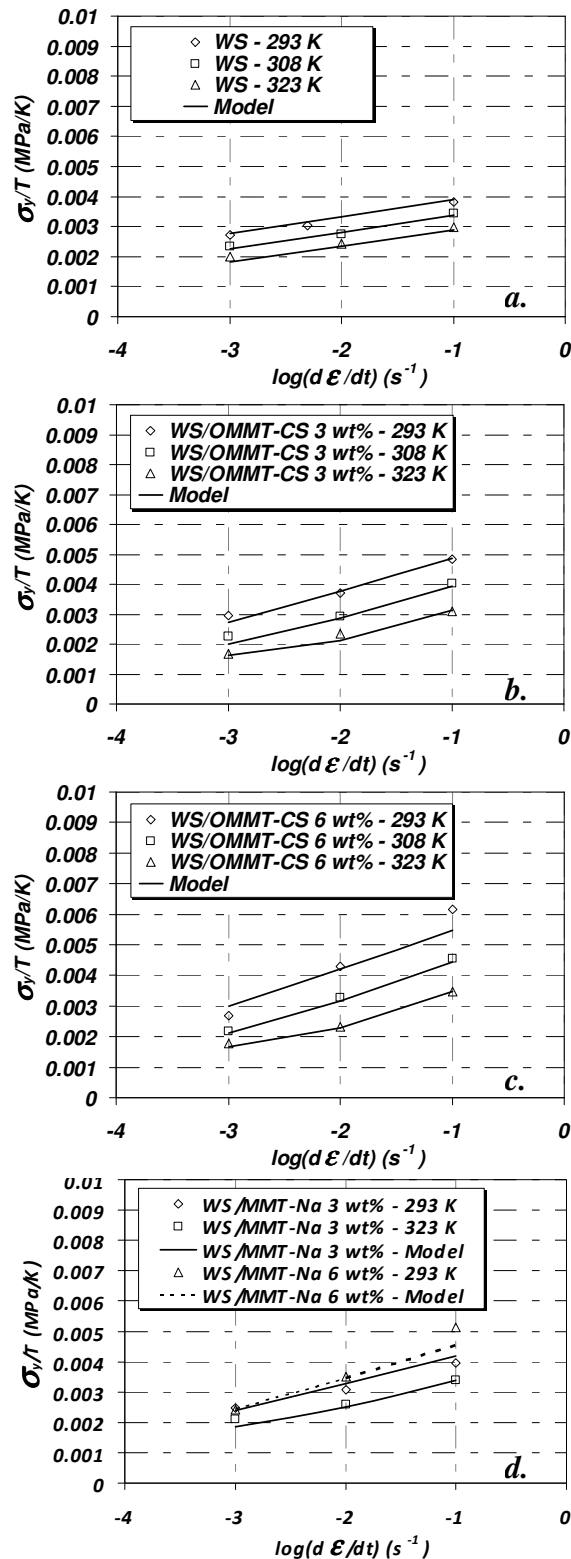
Figure VII.7. Tensile yield stress/temperature variation with strain rate obtained for (a.) WS, (b.) WS/OMMT-CS 3 wt%, (c.) WS/OMMT-CS 6 wt% and (d.) WS/MMT-Na 3 and 6 wt%.

3. Discussion

We have seen from the experimental and modeling analyses that the cooperative model predicts correctly the yield stress of the nano-biocomposites for different clay concentrations and different exfoliation ratios at different strain rates and temperatures. The activation parameters, ΔH_1 and V_1, are associated to the glass transition of the plasticized starch matrix and are experimentally determined. These results are in agreement with the observations of Truss and Lee (Truss, R.W., 2003) and Truss and Yeow (Truss, R.W., 2006) who observed that the yield behavior of the melt-mixed polyethylene-modified montmorillonite nanocomposites depends completely on the yield stress of the virgin matrix, the polyethylene. Besides, the activation parameters (ΔH_2, V_2) in nanocomposite systems are connected to the considered nanoclays. In semi-crystalline materials, such as polyethylene, ΔH_2 is associated to the melting energy of the crystalline phase. Since the montmorillonite platelets are a mineral compound, this explanation can not be used. The ΔH_2 value is likely linked with a structure modification of the montmorillonite tactoïds, such as dislocation mechanisms.

V. Conclusion

This study was focused on the characterization and the modeling of the plasticized starch based nano-biocomposites yield behavior. To model these properties, the preexisting cooperative model developed by Richeton et al. (Richeton, J., 2005) and Gueguen et al. (Gueguen, O., 2008a) has been modified to take into account the montmorillonite inorganic content and its dispersion state into the matrix. A micromechanical development with two rate activation processes, associated to the glass transition of the matrix and to the structure modification of the nanofillers, was considered. The simulations have been performed on different strain rates and temperatures and a good correlation between the experimental data and the predicted results was achieved. However, for high strain rate, it has been demonstrated that the cooperative model underestimate the experimental yield stress values. Nevertheless, experiments have to be carried out to support our proposed modeling of the yield behavior and to shed light on the interactions between the matrix and the nanoclays. Consequently, this work remains a first step to understand the yield behavior in such nanomaterials. The proposed modeling is also valid for other polymer nanocomposites and can be extended over a wider range of temperatures and strain rates, the range of temperature

that can be considered being limited by the degradation temperature of the considered material.

VI. Acknowledgments

Publication VII : Discussion et commentaires

Cette étude était centrée sur la compréhension et la modélisation du comportement à la limite élastique des nano-biocomposites d'amidon. Cette modélisation s'est basée sur un modèle préexistant, nommé modèle coopératif, qui a été modifié afin de tenir compte de la concentration et de l'état de dispersion de la montmorillonite dans la matrice. Les modélisations ont été effectuées pour différentes températures et pour différents taux d'élongation afin d'étudier le comportement de ces matériaux dans la gamme la plus large possible.

Une bonne corrélation entre données calculées et expérimentales est obtenue. Cependant pour des taux d'élongation importants, le modèle coopératif sous-estime les valeurs expérimentales. Par conséquent, ce modèle doit encore être affiné afin de mieux représenter le comportement de ces matériaux nanocomposites dans une gamme de sollicitations plus étendue. Afin d'affiner ce modèle, il faudra notamment tenir compte des interactions matrice/nanocharge et de l'orientation possible des feuillets de montmorillonite sous contrainte. En conclusion, ce modèle reste une première approche permettant de mieux appréhender l'influence des nanocharges sur le comportement à la limite d'élasticité des nano-biocomposites.

Chapitre IV : Conclusions et perspectives

Ce chapitre nous aura permis de présenter des approches de modélisation des propriétés mécaniques des nano-biocomposites d'amidon en fonction de la concentration et du degré d'exfoliation de la montmorillonite.

Nous avons, en outre, clairement mis en évidence l'impact du plastifiant sur les propriétés élastiques de ces nano-hybrides, la rigidité des feuillets de montmorillonite n'étant pas intégralement transmise à la matrice amidon plastifiée. Au dela de la prédiction des propriétés mécaniques, ces modèles constituent un outil complémentaire indirect de caractérisation et de quantification de la nano-dispersion de la montmorillonite. Cet outil permettra en effet à partir d'un simple test de traction uniaxiale d'estimer la qualité de dispersion des feuillets de montmorillonite et sera donc complémentaire aux techniques d'analyses plus traditionnelles que sont la DRXPA et la MET. Enfin, une approche permettant de modéliser la limite d'élasticité de matériaux nano-biocomposites en fonction de la température et de l'intensité de la sollicitation a été développée. Néanmoins, cette étude reste une pemière approche qu'il conviendra d'élargir au travers d'une étude sur une plus large gamme de sollicitations.

Dans ces différents modèles, un certain nombre de phénomènes physiques, tels que des interactions préférentielles matrice/nanocharge ou des orientations possibles des nanocharges n'ont pas été pris en compte dans ces modélisations. Par conséquent, ils devront être étoffés afin de modéliser au mieux le comportement mécanique des matériaux nano-biocomposites.

Par ailleurs, il a clairement été montré dans les précédents chapitres que les nanocharges et leur qualité de dispersion modifient de manière très significative les propriétés à la rupture de ces nano-biocomposites. Ces propriétés devront être modélisées dans de futures études afin de représenter de manière satisfaisante l'ensemble des propriétés mécaniques de ces matériaux. De plus, afin de prouver la robustesse des prédictions effectuées avec ces modèles micromécaniques, des travaux analogues devront être effectués sur des systèmes nanocomposites basés sur d'autres matrices polymères. Enfin, ces modélisations ont pour l'instant été uniquement effectuées sur des nano-biocomposites à base de montmorillonite. Il existe une large gamme de nanocharges disponibles (e.g. la sépiolite, la silice, les nanotubes de carbone) permettant l'élaboration de matériaux nano-biocomposites. La modélisation du comportement mécanique de ces différents matériaux hybrides devra être effectuée afin de développer des modèles les plus pertinents et versatiles possibles.

Références du Chapitre IV

Alexandre, M.; Dubois, P., Polymer-layered silicate nanocomposites: Preparation, properties and uses of a new class of materials. Mater. Sci. Eng. R-Rep. 2000, 28, 1-63.

Averous, L.; Boquillon, N., Biocomposites based on plasticized starch: Thermal and mechanical behaviours. Carbohydr. Polym. 2004a, 56, 111-122.

Averous, L., Biodegradable multiphase systems based on plasticized starch: A review. J. Macromol. Sci. Part C-Polym. Rev. 2004b, 44, 231-274.

Bauwens-Crowet, C.; Bauwens, J. C.; Homès, G., Tensile yield-stress behaviour of glassy polymers. J. Polym. Sci. Pt. A-Polym. Chem. 1969, 7, 735-742.

Benveniste, Y., A new approach to the application of Mori-Tanaka's theory in composite materials. Mech. Mater. 1987, 6, 147-57.

Brooks, N. W. J.; Duckett, R. A.; Ward, I. M., Modeling of double yield points in polyethylene: temperature and strain-rate dependence. J. Rheol. 1995, 39, 425-436.

Brune, D. A.; Bicerano, J., Micromechanics of nanocomposites: comparison of tensile and compressive elastic moduli, and prediction of effects of incomplete exfoliation and imperfect alignment on modulus. Polymer 2002, 43, 369-387.

Chivrac, F.; Kadlecova, Z.; Pollet, E.; Averous, L., Aromatic copolyester-based nano-biocomposites: Elaboration, structural characterization and properties. J. Polym. Environ. 2006, 14, 393-401.

Chivrac, F.; Pollet, E.; Averous, L., Nonisothermal crystallization behavior of poly(butylene adipate-co-terephthalate)/clay nano-biocomposites. J. Polym. Sci. Pt. B-Polym. Phys. 2007, 45, 1503-1510.

Chivrac, F.; Gueguen, O.; Pollet, E.; Ahzi, S.; Makradi, A.; Averous, L., Micromechanical Modeling and Characterization of the Effective Properties in Starch Based Nano-Biocomposites. Acta Biomater. 2008a, 2008, 4, 1707-1714.

Chivrac, F.; Pollet, E.; Schmutz, M.; Averous, L., New Approach to Elaborate Exfoliated Starch-Based Nanobiocomposites. Biomacromolecules 2008b, 9, 896-900.

Cho, J. W.; Paul, D. R., Nylon 6 nanocomposites by melt compounding. Polymer 2001, 42, 1083-1094.

Dennis, H. R.; Hunter, D. L.; Chang, D.; Kim, S.; White, J. L.; Cho, J. W.; Paul, D. R., Effect of melt processing conditions on the extent of exfoliation in organoclay-based nanocomposites. Polymer 2001, 42, 9513-9522.

Eshelby, J. D., The determination of the elastic field of an ellipsoidal inclusion and related problems. Proc. Roy. Soc. 1957, A241, 376-96.

Eyring, H., J. Chem. Phys. 1936, 4, 283-291.

Fornes, T. D.; Yoon, P. J.; Keskkula, H.; Paul, D. R., Nylon 6 nanocomposites: The effect of matrix molecular weight. Polymer 2001, 42, 9929-9940.

Fotheringham, D. G.; Cherry, B. W., J. Mater. Sci. 1978, 13, 951-964.

Gain, O.; Espuche, E.; Pollet, E.; Alexandre, M.; Dubois, P., Gas barrier properties of poly(ε-caprolactone)/clay nanocomposites: Influence of the morphology and polymer/clay interactions. J. Polym. Sci. Pt. B-Polym. Phys. 2005, 43, 205-214.

Gorrasi, G.; Tortora, M.; Vittoria, V.; Pollet, E.; Lepoittevin, B.; Alexandre, M.; Dubois, P., Vapor barrier properties of polycaprolactone montmorillonite nanocomposites: Effect of clay dispersion. Polymer 2003, 44, 2271-2279.

Gorrasi, G.; Tortora, M.; Vittoria, V.; Pollet, E.; Alexandre, M.; Dubois, P., Physical Properties of Poly(ε-caprolactone) Layered Silicate Nanocomposites Prepared by Controlled Grafting Polymerization. J. Polym. Sci. Pt. B-Polym. Phys. 2004, 42, 1466-1475.

Gueguen, O.; Ahzi, S.; Belouettar, S.; Makradi, A., Comparison of micromechanical models for the prediction of the effective elastic properties of semi-crystalline polymers: Application to Polyethylene. Polym. Sci. Ser. A 2008a, 50, 523-532.

Gueguen, O.; Ahzi, S.; Makradi, A.; Belouettar, S.; Etienne, S.; Ruch, D., New estimates of the effective elastic constants of semi-crystalline polymers. Comput. Mater. Sci. 2008b, Submitted.

Gueguen, O.; Richeton, J.; Ahzi, S.; Makradi, A., Micromechanically based formulation of the cooperative model for the yield behavior of semi-crystalline polymers. Acta Mater. 2008c, 56, 1650-1655.

Lepoittevin, B.; Devalckenaere, M.; Pantoustier, N.; Alexandre, M.; Kubies, D.; Calberg, C.; Jerome, R.; Dubois, P., Poly(ε-caprolactone)/clay nanocomposites prepared by melt intercalation: mechanical, thermal and rheological properties. Polymer 2002, 43, 4017-4023.

Luo, J. J.; Daniel, I. M., Characterization and modeling of mechanical behavior of polymer/clay nanocomposites. Compos. Sci. Technol. 2003, 63, 1607-16.

Meijer, H. E. H.; Govaert, L. E., Multi-scale analysis of mechanical properties of amorphous polymer systems. Macromol. Chem. Phys. 2003, 204, 274-288.

Mori, T.; Tanaka, K., Average stress in matrix and average elastic energy of materials with misfitting inclusions. Acta. Metall. Mater. 1973, 21, 571-4.

Oleinik, E. F., Plasticity of Semicrystalline Flexible-Chain Polymers at the Microscopic and Mesoscopic Levels. Polym. Sci. Ser. C 2003, 45, 17-117.

Park, H. M.; Li, X.; Jin, C. Z.; Park, C. Y.; Cho, W. J.; Ha, C. S., Preparation and properties of biodegradable thermoplastic starch/clay hybrids. Macromol. Mater. Eng. 2002, 287, 553-558.

Park, H. M.; Lee, W. K.; Park, C. Y.; Cho, W. J.; Ha, C. S., Environmentally friendly polymer hybrids Part I mechanical, thermal, and barrier properties of thermoplastic starch/clay nanocomposites. J. Mater. Sci. 2003, 38, 909-915.

Pollet, E.; Delcourt, C.; Alexandre, M.; Dubois, P., Organic-inorganic nanohybrids obtained by sequential copolymerization of ε-caprolactone and L,L-lactide from activated clay surface. Macromol. Chem. Phys. 2004, 205, 2235-2244.

Rault, J., Yielding in amorphous and semi-crystalline polymers: the compensation law. J. Non-Cryst. Solids 1998, 235-237, 737-741.

Reuss, A., Z. Angew. Math. Mech 1929, 9, 49.

Richeton, J.; Ahzi, S.; Daridon, L.; Rémond, Y., A Formulation of the cooperative model for the yield stress of amorphous polymers for a wide range of strain rates and temperature. Polymer 2005, 46, 6035-6043.

Sheng, N.; Boyce, M. C.; Parks, D. M.; Rutledge, G. C.; Abes, J. I.; Cohen, R. E., Multiscale micromechanical modeling of polymer/clay nanocomposites and the effective clay particle. Polymer 2004, 45, 487-506.

Sinha Ray, S.; Okamoto, M., Polymer/layered silicate nanocomposites: A review from preparation to processing. Prog. Polym. Sci. 2003, 28, 1539-1641.

Truss, R. W.; Clarke, P. L.; Duckett, R. A.; Ward, I. M., J. Polym. Sci. Pt. B-Polym. Phys. 1984, 22, 191-209.

Truss, R. W.; Lee, A. C., Yield behavior of a melt-compounnded polyethylene-intercalated montmorillonite nanocomposite. Polym. Int. 2003, 52, 1790-1794.

Truss, R. W.; Yeow, T. K., Effect of exfoliation and dispersion on the yield behavior of melt-compounded polyethylene-montmorillonite nanocomposites. J. Appl. Polym. Sci. 2006, 100, 3044-3049.

Tucker, C. L.; Liang, E., Stiffness predictions for unidirectional short-fiber composites: Review and evaluation. Compos. Sci. Technol. 1999, 59, 655-671.

Vaia, R. A.; Ishii, H.; Giannelis, E. P., Synthesis and properties of two-dimensional nanostructures by direct intercalation of polymer melts in layered silicates. Chem. Mat. 1993, 5, 1694-1696.

Vaia, R. A.; Giannelis, E. P., Polymer melt intercalation in organically-modified layered silicates: Model predictions and experiment. Macromolecules 1997, 30, 8000-8009.

Voigt, W., Lehrbuch des Krystalphysik 1928, 410.

Ward, I. M., Review: The yield behaviour of polymers. J. Mater. Sci. 1971, 6, 1397-1417.

Ward, I. M.; Wilding, M. A., J. Polym. Sci. Pt. B-Polym. Phys. 1984, 22, 561-575.

Wilhelm, H.-M.; Sierakowski, M.-R.; Souza, G. P.; Wypych, F., Starch films reinforced with mineral clay. Carbohydr. Polym. 2003, 52, 101-110.

Conclusion Générale et Perspectives

Conclusion générale

Ce travail, associant la physico-chimie et les procédés d'élaboration des polymères, avait notamment pour objectif l'élaboration et l'étude de nouveaux matériaux nano-structurés performants à base d'amidon plastifié. Le développement de cette matrice agro-sourcée, en tant que matériau de substitution ou complémentaire aux polymères synthétiques classiques, est aujourd'hui limité par certaines faiblesses intrinsèques (e.g. faibles propriétés mécaniques, forte sensibilité à l'eau). Par rapport aux approches conventionnelles de modification chimique des agro-polymères, la démarche retenue dans le cadre de cette thèse est principalement axée sur la formulation, et plus précisément sur l'élaboration de matériaux hybrides amidon plastifié/argile. Dans notre cas, les argiles nous sont apparues comme un choix judicieux en tant que nanocharge du fait de leurs caractéristiques intrinsèques (facteur de forme important, surface interfaciale très élevée, possibilités d'organo-modification, ressources naturelles…) et de leurs disponibilités.

Cette étude s'est structurée en trois parties distinctes et complémentaires :

(i)   Une partie axée sur l'organo-modification de la montmorillonite afin de changer la nature de l'interface matrice/nanocharge et d'obtenir une morphologie exfoliée.

(ii)   Une partie centrée sur l'analyse de différents paramètres et composants matériaux influençant la morphologie et les propriétés finales de ces nano-biocomposites.

(iii)   Enfin, une dernière partie dédiée la modélisation des propriétés mécaniques des nano-biocomposites d'amidon.

L'étude bibliographique réalisée en préambule à ce travail a clairement identifié le rôle majeur de la nature et du taux de plastifiant sur le processus d'intercalation/exfoliation de la montmorillonite au sein de matrices polysaccharides. Par exemple, l'incorporation de MMT-Na (montmorillonite sodique dite naturelle) au sein d'amidon plastifié ne permet l'obtention de morphologies exfoliées qu'à des taux de glycérol inférieurs à 10 % en masse.

La première partie de cette thèse avait pour objectif l'exfoliation des feuillets de montmorillonite au sein d'une matrice amidon surplastifiée par du glycérol. Pour cela, cette nanocharge a été organo-modifiée avec de l'amidon cationique suivant deux approches distinctes : une approche « voie solvant » et une approche « voie fondue » novatrice, plus directe et respectueuse de l'environnement. Les différentes analyses morphologiques

effectuées sur les nano-hybrides élaborés avec ces nanocharges ont révélé une structure exfoliée. Par conséquent, il a été démontré que le choix de l'amidon cationique comme compatibilisant matrice/nanocharge s'avère pertinent et que celui-ci limite l'effet du plastifiant sur la morphologie finale du matériau. Néanmoins, l'élaboration de nano-biocomposites à base d'amidon plastifié avec du sorbitol ou du Polysorb® (mélange de glycérol et sorbitol) a montré que l'efficacité de l'amidon cationique est moindre avec le sorbitol, des structures intermédiaires intercalées/exfoliées ayant été obtenues. Par conséquent, il a été conclu que le sorbitol perturbe le processus d'intercalation/exfoliation des feuillets de l'OMMT-CS sans toutefois connaître parfaitement, à ce stade, le mécanisme sous-jacent.

Ce travail de thèse s'est également focalisé sur la dispersion au sein d'une matrice amidon plastifié d'une nanocharge argileuse très peu étudiée dans ce contexte et qui présente une structure aciculaire, la sépiolite. Pour ce faire, de la sepiolite sodique et de la sépiolite organo-modifiée par de l'amidon cationique (SEP-Na et OSEP-CS) ont été testées. Les analyses morphologiques effectuées sur les nano-hybrides amidon/SEP-Na ont mis en évidence une dispersion/distribution nanométrique des aiguilles de sépiolite favorisée par l'établissement de liaisons hydrogènes entre les groupements silanols et hydroxyles de la nanocharge et des chaînes amylacées. L'effet de la concentration de l'amidon cationique a également été clairement montré. L'incorporation d'OSEP-1CS, c'est-à-dire la sépiolite organo-modifiée avec un équivalent d'amidon cationique, génère de larges agrégats micrométriques. A cette concentration précise, l'amidon cationique agit comme un agent floculant créant des « ponts » entre les différentes aiguilles de sepiolite. Au-delà de cette concentration, et à l'image des matériaux amidon/montmorillonite, l'amidon cationique joue pleinement son rôle de compatibilisant et favorise significativement la nano-dispersion de la charge.

Par ailleurs, il a été montré par analyse de MET qu'indépendamment du type d'argile utilisé (montmorillonite ou sépiolite), une séparation de phase entre des domaines riches et pauvres en nanocharges apparaît. Cette hétérogénéité est induite par le taux élevé de plastifiant dans la formulation qui engendre une démixtion entre des domaines riches et pauvres en plastifiant.

De plus, les différentes analyses effectuées sur ces nano-biocomposites ont montré l'influence significative de l'obtention d'une dispersion nanométrique des argiles (exfoliation) sur les propriétés du matériau. Ainsi, quelle que soit la nature des nanocharges, la nano-

dispersion obtenue entraîne une rigidification des matériaux, tout en conservant les propriétés d'élongation à la rupture de la matrice vierge.

La dernière partie de cette étude aura permis de modéliser, et aussi donc de mieux comprendre, l'influence des nanocharges, de leur concentration et de leur degré d'exfoliation sur les propriétés élastiques et les propriétés à la limite d'élasticité des nano-biocomposites d'amidon. L'étude basée sur le modèle de Mori-Tanaka, aura clairement démontré que la contribution effective des feuillets de montmorillonite à la rigidité était plus faible qu'escomptée. De même, une première approche décrivant l'impact des nanocharges sur les propriétés à la limite d'élasticité a également été formulée. Enfin, un nouvel outil indirect de caractérisation morphologique des nano-biocomposites, basé sur l'analyse de leurs propriétés élastiques, a été développé. Cet outil prometteur devrait permettre, à terme, une quantification de la qualité de dispersion de la nanocharge au sein de la matrice polymère.

.

Perspectives

Cette étude aura clairement mis en évidence l'influence prépondérante du plastifiant sur le processus d'intercalation-exfoliation de la montmorillonite, organo-modifiée ou non. Cependant, une étude plus fondamentale ayant pour objectif une meilleure compréhension des interactions polysaccharide/plastifiant/organo-modifiant/nanocharge devra être menée. Celle-ci pourrait notamment être réalisée au travers de l'analyse par RMN du solide de la mobilité des espèces dans des espaces plus ou moins confinés. De même, la séparation de phase entre des domaines riches et pauvres en nanocharges devra être étudiée plus en détail à l'aide de techniques de caractérisation avancées telles que la nanoindentation, des analyses diéléctriques ou des techniques spectroscopiques couplées à de la microscopie électronique pouvant éventuellement être basées sur un marquage du glycérol, par exemple.

L'ensemble de ces études devra aussi être effectué à différents taux de plastifiant sur différentes sources d'amidon présentant différents rapport amylose/amylopectine. La structure et la masse moléculaire de ces deux macromolécules étant très différentes (structure "en grappe" ou linéaire), la variation de leur ratio permettrait de mieux appréhender le rôle de chaque constituant et de leur structure sur le processus d'intercalation/exfoliation des nanocharges.

Le mécanisme de dégradation de l'amidon cationique ainsi que son impact sur la stabilité thermique des nano-biocomposites d'amidon devront être étudiés par ATG et éventuellement en analysant les gaz émis lors de la décomposition par spectroscopie de masse et/ou spectroscopie infra-rouge (ATG couplée IRTF – SM).

L'analyse, par des tests de perméabilité, de l'influence de la morphologie de ces matériaux nano-biocomposites sur les propriétés barrières aux gaz en termes de diffusion et de solubilité (vapeur d'eau, oxygène…) paraît également indispensable et est actuellement en cours.

Cette étude pourrait aussi être étendue à l'organo-modification d'argiles telles que la brucite, l'hectorite, la laponite… et avec d'autres organo-modifiants de type ammoniums ou phosphoniums en utilisant le procédé de « Shear Induced Clay Organo-modification » qui, de part son caractère direct et rapide, présente un intérêt considérable.

Les propriétés à la rupture de ces nano-biocomposites d'amidon à base de montmorillonite devront être modélisées et reliées à la concentration et à l'état de dispersion

des nanocharges. Par ailleurs, les modèles développés devront être adaptés afin de modéliser les propriétés mécaniques des nano-hybrides à base de sépiolite.

Enfin, l'OMMT-CS pourrait être dispersée dans différents plastiques biodégradables commerciaux à base d'amidon, tels que le Mater-Bi® de Novamont (mélange amidon/PCL), le Bioplast® de SPhere (amidon/Ecoflex®) ou les résines de Plantic (amidon/PVAL). Ces développements permettraient d'améliorer les propriétés d'usage de ces matériaux, notamment leurs propriétés mécaniques et barrières.

Bibliographie Générale

Alexandre, M.; Dubois, P., Polymer-layered silicate nanocomposites: Preparation, properties and uses of a new class of materials. Mater. Sci. Eng. R-Rep. 2000, 28, 1-63.

Appelqvist, I. A. M.; Cooke, D.; Gidley, M. J.; Lane, S. J., Thermal properties of polysaccharides at low moisture: 1 - An endothermic melting process and water-carbohydrate interactions. Carbohydr. Polym. 1993, 20, 291-299.

Atalla, R. H.; Van der Hart, D. L., Native cellulose: a composite of two distinct crystalline forms. Science 1984, 223, 283-285.

Atkins, E. D. T., Conformation in polysaccharides and complex carbohydrates. J. Biosci. 1985, 8, 375-387.

Avella, M.; De Vlieger, J. J.; Errico, M. E.; Fischer, S.; Vacca, P.; Volpe, M. G., Biodegradable starch/clay nanocomposite films for food packaging applications. Food Chem. 2005, 93, 467-474.

Averous, L.; Moro, L.; Dole, P.; Fringant, C., Properties of thermoplastic blends: Starch-polycaprolactone. Polymer 2000a, 41, 4157-4167.

Averous, L.; Fauconnier, N.; Moro, L.; Fringant, C., Blends of Thermoplastic Starch and Polyesteramide: Processing and Properties. J. Appl. Polym. Sci. 2000b, 76, 1117-1128.

Averous, L.; Fringant, C., Association between plasticized starch and polyesters: Processing and performances of injected biodegradable systems. Polym. Eng. Sci. 2001, 41, 727-734.

Averous, L., Biodegradable multiphase systems based on plasticized starch: A review. J. Macromol. Sci. Part C-Polym. Rev. 2004a, 44, 231-274.

Averous, L.; Boquillon, N., Biocomposites based on plasticized starch: Thermal and mechanical behaviours. Carbohydr. Polym. 2004b, 56, 111-122.

Bagdi, K.; Muller, P.; Pukanszky, B., Thermoplastic starch/layered silicate composites: Structure, interaction, properties. Compos. Interfaces 2006, 13, 1-17.

Baud, B.; Colonna, P.; Della Valle, G.; Roger, P., Macromolecular degradation of extruded starches measured by HPSEC-MALLS. . In *Biopolymer Science: Food and Non Food Applications/Les Colloques de l'INRA*, Colonna, P.; Guilbert, S., Eds. Paris, 1999; pp 217-221.

Bauwens-Crowet, C.; Bauwens, J. C.; Homès, G., Tensile yield-stress behaviour of glassy polymers. J. Polym. Sci. Pt. A-Polym. Chem. 1969, 7, 735-742.

Benveniste, Y., A new approach to the application of Mori-Tanaka's theory in composite materials. Mech. Mater. 1987, 6, 147-57.

Bilotti, E.; Fischer, H. R.; Peijs, T., Polymer nanocomposites based on needle-like sepiolite clays: Effect of functionalized polymers on the dispersion of nanofiller, crystallinity, and mechanical properties. J. Appl. Polym. Sci. 2008, 107, 1116-1123.

Bledzki, A. K.; Gassan, J., Composites reinforced with cellulose based fibres. Prog. Polym. Sci. 1999, 24, 221-274.

Bokobza, L.; Burr, A.; Garnaud, G.; Perrin, M. Y.; Pagnotta, S., Fibre reinforcement of elastomers: Nanocomposites based on sepiolite and poly(hydroxyethyl acrylate). Polym. Int. 2004, 53, 1060-1065.

Bordes, P.; Pollet, E.; Bourbigot, S.; Averous, L., Structure and properties of PHA/clay nano-biocomposites prepared by melt intercalation. Macromol. Chem. Phys. 2008, 209, 1473-1484.

Brooks, N. W. J.; Duckett, R. A.; Ward, I. M., Modeling of double yield points in polyethylene: temperature and strain-rate dependence. J. Rheol. 1995, 39, 425-436.

Brune, D. A.; Bicerano, J., Micromechanics of nanocomposites: comparison of tensile and compressive elastic moduli, and prediction of effects of incomplete exfoliation and imperfect alignment on modulus. Polymer 2002, 43, 369-387.

Buchanan, C. M.; Gedon, S. C.; White, A. W.; Wood, M. D., Cellulose acetate butyrate and poly(hydroxybutyrate-co-valerate) copolymer blends. Macromolecules 1992, 25, 7373-7381.

Campbell, N. A.; Reece, J. B.; Mitchell, L. G., Biology. 5th ed.; Menlo Park CA: New Work, 1999.

Cases, J. M.; Brend, I.; Besson, G.; François, M.; Uriot, J. P.; Thomas, F.; Poirier, J. E., Mechanism of adsorption and desorption of water vapor by homoionic montmorillonite. 1. The sodium-exchanged form. Langmuir 1992, 8, 2730-2739.

Chanzy, H., Aspects of Cellulose Structure. In *Cellulose Sources and Exploitation*, Kennedy, J. F.; Phillips, G. O.; Williams, P. A., Eds. Ellis Horwood Ltd.: New York, 1990; pp 3-12.

Chaudhary, D. S., Understanding amylose crystallinity in starch-clay nanocomposites. J. Polym. Sci. Pt. B-Polym. Phys. 2008, 46, 979-987.

Chen, B.; Evans, J. R. G., Thermoplastic starch-clay nanocomposites and their characteristics. Carbohydr. Polym. 2005, 61, 455-463.

Chen, H.; Zheng, M.; Sun, H.; Jia, Q., Characterization and properties of sepiolite/polyurethane nanocomposites. Mater. Sci. Eng. A-Struct. Mater. Prop. Microstruct. Process. 2007, 445-446, 725-730.

Chen, M.; Chen, B.; Evans, J. R. G., Novel thermoplastic starch-clay nanocomposite foams. Nanotechnology 2005, 16, 2334-2337.

Chiou, B.-S.; Yee, E.; Glenn, G. M.; Orts, W. J., Rheology of starch-clay nanocomposites. Carbohydr. Polym. 2005, 59, 467-475.

Chiou, B.-S.; Yee, E.; Wood, D.; Shey, J.; Glenn, G.; Orts, W., Effects of processing conditions on nanoclay dispersion in starch-clay nanocomposites. Cereal Chem. 2006, 83, 300-305.

Chiou, B. S.; Yee, E.; Glenn, G. M.; Orts, W. J.; Wood, D. F.; Imam, S. H. In *Biopolymer nanocomposites containing native wheat starch and nanoclays*, ACS National Meeting Book of Abstracts, 2004///, 2004; 2004.

Chiou, B. S.; Wood, D.; Yee, E.; Imam, S. H.; Glenn, G. M.; Orts, W. J., Extruded starch-nanoclay nanocomposites: Effects of glycerol and nanoclay concentration. Polym. Eng. Sci. 2007, 47, 1898-1904.

Chivrac, F.; Kadlecova, Z.; Pollet, E.; Averous, L., Aromatic copolyester-based nano-biocomposites: Elaboration, structural characterization and properties. J. Polym. Environ. 2006, 14, 393-401.

Chivrac, F.; Pollet, E.; Averous, L., Nonisothermal crystallization behavior of poly(butylene adipate-co-terephthalate)/clay nano-biocomposites. J. Polym. Sci. Pt. B-Polym. Phys. 2007, 45, 1503-1510.

Chivrac, F.; Gueguen, O.; Pollet, E.; Ahzi, S.; Makradi, A.; Averous, L., Micromechanical Modeling and Characterization of the Effective Properties in Starch Based Nano-Biocomposites. Acta Biomater. 2008a, doi: 10.1016/j.actbio.2008.05.002.

Chivrac, F.; Pollet, E.; Schmutz, M.; Averous, L., New Approach to Elaborate Exfoliated Starch-Based Nanobiocomposites. Biomacromolecules 2008b, 9, 896-900.

Cho, J. W.; Paul, D. R., Nylon 6 nanocomposites by melt compounding. Polymer 2001, 42, 1083-1094.

Colonna, P.; Mercier, C., Macromolecular structure of wrinkled- and smooth-pea starch components. Carbohydr. Res. 1984, 126, 233-247.

Cooke, D.; Gidley, M. J., Loss of crystalline and molecular order during starch gelatinisation: Origin of the enthalpic transition. Carbohydr. Res. 1992, 227, 103-112.

Cuq, B.; Gontard, N.; Guilbert, S., Proteins as agricultural polymers for packaging production. Cereal Chem. 1998, 75, 1-9.

Curvelo, A. A. S.; De Carvalho, A. J. F.; Agnelli, J. A. M., Thermoplastic starch-cellulosic fibers composites: Preliminary results. Carbohydr. Polym. 2001, 45, 183-188.

Cyras, V. P.; Manfredi, L. B.; Ton-That, M. T.; Vazquez, A., Physical and mechanical properties of thermoplastic starch/montmorillonite nanocomposite films. Carbohydr. Polym. 2008a, 73, 55-63.

Cyras, V. P.; Manfredi, L. B.; Ton-That, M. T.; Vazquez, A., Physical and mechanical properties of thermoplastic starch/montmorillonite nanocomposite films. Carbohydr. Polym. 2008b, 73, 55-63

Dai, J. C.; Huang, J. T., Surface modification of clays and clay-rubber composite. Appl. Clay Sci. 1999, 15, 51-65.

Darder, M.; Colilla, M.; Ruiz-Hitzky, E., Biopolymer-clay nanocomposites based on chitosan intercalated in montmorillonite. Chem. Mater. 2003, 15, 3774-3780.

Darder, M.; Colilla, M.; Ruiz-Hitzky, E., Chitosan-clay nanocomposites: Application as electrochemical sensors. Appl. Clay Sci. 2005, 28, 199-208.

Darder, M.; Lopez-Blanco, M.; Aranda, P.; Aznar, A. J.; Bravo, J.; Ruiz-Hitzky, E., Microfibrous chitosan - Sepiolite nanocomposites. Chem. Mat. 2006, 18, 1602-1610.

Davidson, V. J.; Parker, R.; Diosady, L. L.; Rubin, L. T., A Model for Mechanical Degradation of Wheat Starch in a Single-Screw Extruder J. Food Sci. 1984a, 49, 1154-1169.

Davidson, V. J.; Paton, D.; Diosady, L. L.; Larocque, G., Degradation of Wheat Starch in a Single Screw Extruder: Characteristics of Extruded Starch Polymers J. Food Sci. 1984b, 49, 453-458.

Dean, K.; Yu, L.; Wu, D. Y., Preparation and characterization of melt-extruded thermoplastic starch/clay nanocomposites. Compos. Sci. Technol. 2007, 67, 413-421.

Dean, K. M.; Do, M. D.; Petinakis, E.; Yu, L., Key interactions in biodegradable thermoplastic starch/poly(vinyl alcohol)/montmorillonite micro- and nanocomposites. Compos. Sci. Technol. 2008, 68, 1453-1462.

Della Valle, G.; Boche, Y.; Colonna, P.; Vergnes, B., The extrusion behaviour of potato starch. Carbohydr. Polym. 1995, 28, 255-264.

Della Valle, G.; Buleon, A.; Carreau, P. J.; Lavoie, P. A.; Vergnes, B., Relationship between structure and viscoelastic behavior of plasticized starch. J. Rheol. 1998, 42, 507-525.

Dennis, H. R.; Hunter, D. L.; Chang, D.; Kim, S.; White, J. L.; Cho, J. W.; Paul, D. R., Effect of melt processing conditions on the extent of exfoliation in organoclay-based nanocomposites. Polymer 2001, 42, 9513-9522.

Dufresne, A.; Vignon, M. R., Improvement of starch film performances using cellulose microfibrils. Macromolecules 1998, 31, 2693-2696.

Duquesne, E.; Moins, S.; Alexandre, M.; Dubois, P., How can nanohybrids enhance polyester/sepiolite nanocomposite properties? Macromol. Chem. Phys. 2007, 208, 2542-2550.

Edgar, K. J.; Buchanan, C. M.; Debenham, J. S.; Rundquist, P. A.; Seiler, B. D.; Shelton, M. C.; Tindall, D., Advances in cellulose ester performance and application. Prog. Polym. Sci. 2001, 26, 1605-1688.

Eshelby, J. D., The determination of the elastic field of an ellipsoidal inclusion and related problems. Proc. Roy. Soc. 1957, A241, 376-96.

Eyring, H., J. Chem. Phys. 1936, 4, 283-291.

Fischer, H. R.; Gielgens, L. H.; Koster, T. P. M., Nanocomposites from polymers and layered minerals. Acta polym. 1999, 50, 122-126.

Fischer, S.; De Vlieger, J.; Kock, T.; Batenburg, L.; Fischer, H. In *"Green" nano-composite materials - New possibilities for bioplastics*, Materials Research Society Symposium - Proceedings, 2001, 2001; 2001; pp 628-661.

Fornes, T. D.; Yoon, P. J.; Keskkula, H.; Paul, D. R., Nylon 6 nanocomposites: The effect of matrix molecular weight. Polymer 2001, 42, 9929-9940.

Fornes, T. D.; Paul, D. R., Modeling properties of nylon 6/clay nanocomposites using composite theories. Polymer 2003, 44, 4993-5013.

Forssell, P.; Mikkila, J.; Suortti, T.; Seppala, J.; Poutanen, K., Plasticization of barley starch with glycerol and water. J. Macromol. Sci. Part A-Pure Appl. Chem. 1996, 33, 703-715.

Fotheringham, D. G.; Cherry, B. W., J. Mater. Sci. 1978, 13, 951-964.

Fringant, C.; Desbrieres, J.; Rinaudo, M., Physical properties of acetylated starch-based materials: Relation with their molecular characteristics. Polymer 1996, 37, 2663-2673.

Gain, O.; Espuche, E.; Pollet, E.; Alexandre, M.; Dubois, P., Gas barrier properties of poly(ε-caprolactone)/clay nanocomposites: Influence of the morphology and polymer/clay interactions. J. Polym. Sci. Pt. B-Polym. Phys. 2005, 43, 205-214.

Gardner, K. H.; Blackwell, J., Refinement of the structure of β-chitin. Biopolymers 1975, 14, 1581-1595.

Gaudin, S.; Lourdin, D.; Le Botlan, D.; Ilari, J. L.; Colonna, P., Plasticisation and mobility in starch-sorbitol films. J. Cereal Sci. 1999, 29, 273-284.

Gaudin, S.; Lourdin, D.; Forssell, P. M.; Colonna, P., Antiplasticisation and oxygen permeability of starch-sorbitol films. Carbohydr. Polym. 2000, 43, 33-37.

Genkina, N. K.; Wikman, J.; Bertoft, E.; Yuryev, V. P., Effects of structural imperfection on gelatinization characteristics of amylopectin starches with A- and B-type crystallinity. Biomacromolecules 2007, 8, 2329-2335.

Giannelis, E. P., Polymer layered silicate nanocomposites. Adv. Mater. 1996, 8, 29-35.

Godbillot, L.; Dole, P.; Joly, C.; Roge, B.; Mathlouthi, M., Analysis of water binding in starch plasticized films. Food Chem. 2006, 96, 380-386.

Gomes, M. E.; Ribeiro, A. S.; Malafaya, P. B.; Reis, R. L.; Cunha, A. M., A new approach based on injection moulding to produce biodegradable starch-based polymeric scaffolds: Morphology, mechanical and degradation behaviour. Biomaterials 2001, 22, 883-889.

Gopakumar, T. G.; Lee, J. A.; Kontopoulou, M.; Parent, J. S., Influence of clay exfoliation on the physical properties of montmorillonite/polyethylene composites. Polymer 2002, 43, 5483-5491.

Gorrasi, G.; Tortora, M.; Vittoria, V.; Pollet, E.; Lepoittevin, B.; Alexandre, M.; Dubois, P., Vapor barrier properties of polycaprolactone montmorillonite nanocomposites: Effect of clay dispersion. Polymer 2003, 44, 2271-2279.

Gorrasi, G.; Tortora, M.; Vittoria, V.; Pollet, E.; Alexandre, M.; Dubois, P., Physical Properties of Poly(ε-caprolactone) Layered Silicate Nanocomposites Prepared by Controlled Grafting Polymerization. J. Polym. Sci. Pt. B-Polym. Phys. 2004, 42, 1466-1475.

Gross, R. A.; Kalra, B., Biodegradable polymers for the environment. Science 2002, 297, 803-807.

Gueguen, O.; Richeton, J.; Ahzi, S.; Makradi, A., Micromechanically based formulation of the cooperative model for the yield behavior of semi-crystalline polymers. Acta Mater. 2008a, 56, 1650-1655.

Gueguen, O.; Ahzi, S.; Belouettar, S.; Makradi, A., Comparison of micromechanical models for the prediction of the effective elastic properties of semi-crystalline polymers: Application to Polyethylene. Polym. Sci. Ser. A 2008b, 50, 523-532.

Gueguen, O.; Ahzi, S.; Makradi, A.; Belouettar, S.; Etienne, S.; Ruch, D., New estimates of the effective elastic constants of semi-crystalline polymers. Comput. Mater. Sci. 2008c, Submitted.

Günister, E.; Pestreli, D.; Unlu, C. H.; Atici, O.; Gungor, N., Synthesis and characterization of chitosan-MMT biocomposite systems. Carbohydr. Polym. 2007, 67, 358-365.

Guilbert, S.; Gontard, N.; Gorris, L. G. M., Prolongation of the shelf-life of perishable food products using biodegradable films and coatings. LWT-Food Sci. Technol. 1996, 29, 10-17.

Guilbot, A.; Mercier, C., The Polysaccharides. In *Molecular Biology*, Aspinall, G. O., Ed. Academic Press Incorporation: New-York, 1985; Vol. 3, pp 209-282.

Hayashi, A.; Kinoshita, K.; Miyake, Y.; Cho, C. H., Conformation of amylose in solution. Polym. J. 1981, 13, 537-541.

Heiner, A. P.; Teleman, O., Interface between monoclinic crystalline cellulose and water: Breakdown of the odd/even duplicity. Langmuir 1997, 13, 511-518.

Hendricks, S. B., Lattice Structure of Clay Minerals and Some Properties of Clay. J. Geol. 1942, 50, 276-293.

Hizukuri, S.; Takeda, Y.; Yasuda, M., Multibranched nature of amylose and the action of debranching enzymes. Carbohydr. Res. 1981, 94, 205-213.

Hizukuri, S., Polymodal distribution of the chain lengths of amylopectins, and its significance. Carbohydr. Res. 1986, 147, 342-347.

Huang, M.; Yu, J.; Ma, X., Studies on properties of the thermoplastic starch/montmorillonite composites. Acta Polym. Sin. 2005, 862-867.

Huang, M.; Yu, J.; Ma, X., High mechanical performance MMT-urea and formamide-plasticized thermoplastic cornstarch biodegradable nanocomposites. Carbohydr. Polym. 2006a, 63, 393-399.

Huang, M.; Yu, J., Structure and properties of thermoplastic corn starch/montmorillonite biodegradable composites. J. Appl. Polym. Sci. 2006b, 99, 170-176.

Huang, M. F.; Yu, J. G.; Ma, X. F., Studies on the properties of Montmorillonite-reinforced thermoplastic starch composites. Polymer 2004, 45, 7017-7023.

Huang, M. F.; Yu, J. G.; Ma, X. F.; Jin, P., High performance biodegradable thermoplastic starch - EMMT nanoplastics. Polymer 2005a, 46, 3157-3162.

Huang, M. F.; Yu, J. G.; Ma, X. F., Preparation of the thermoplastic starch/montmorillonite nanocomposites by melt-intercalation. Chin. Chem. Lett. 2005b, 16, 561-564.

Hulleman, S. H. D.; Kalisvaart, M. G.; Janssen, F. H. P.; Feil, H.; Vliegenthart, J. F. G., Origins of B-type crystallinity in glycerol-plasticised, compression-moulded potato starches. Carbohydr. Polym. 1999, 39, 351-360.

Jang, J. K.; Pyun, Y. R., Effect of Moisture Content on the Melting of Wheat Starch. Starch-Starke 1986, 48, 48-51.

Jenkins, P. J.; Donald, A. M., The influence of amylose on starch granule structure. Int. J. Biol. Macromol. 1995, 17, 315-321.

Jimenez, G.; Ogata, N.; Kawai, H.; Ogihara, T., Structure and thermal/mechanical properties of poly(ε-caprolactone)-clay blend. J. Appl. Polym. Sci. 1997, 64, 2211-2220.

Jin, Y. H.; Park, H. J.; Im, S. S.; Kwak, S. Y.; Kwak, S., Polyethylene/clay nanocomposite by in-situ exfoliation of montmorillonite during Ziegler-Natta polymerization of ethylene. Macromol. Rapid Commun. 2002, 23, 135-140.

Jozja, N. Étude de matériaux argileux Albanais. Caractérisation "multi-échelle" d'une bentonite magnésienne. Impact de l'interaction avec le nitrate de plomb sur la perméabilité. Université d'Orléans, Orléans, 2003.

Kalambur, S.; Rizvi, S. S. H., Biodegradable and functionally superior starch-polyester nanocomposites from reactive extrusion. J. Appl. Polym. Sci. 2005, 96, 1072-1082.

Kalambur, S. B.; Rizvi, S. S., Starch-based nanocomposites by reactive extrusion processing. Polym. Int. 2004, 53, 1413-1416.

Kalichevsky, M. T.; Jaroszkiewicz, E. M.; Ablett, S.; Blanshard, J. M. V.; Lillford, P. J., The glass transition of amylopectin measured by DSC, DMTA and NMR. Carbohydr. Polym. 1992, 18, 77-88.

Kalichevsky, M. T.; Blanshard, J. M. V., The effect of fructose and water on the glass transition of amylopectin. Carbohydr. Polym. 1993, 20, 107-113.

Kampeerapappun, P.; Aht-ong, D.; Pentrakoon, D.; Srikulkit, K., Preparation of cassava starch/montmorillonite composite film. Carbohydr. Polym. 2007, 67, 155-163.

Ke, Y.; Lü, J.; Yi, X.; Zhao, J.; Qi, Z., The effects of promoter and curing process on exfoliation behavior of epoxy/clay nanocomposites. J. Appl. Polym. Sci. 2000, 78, 808-815.

Krishnamoorti, R.; Vaia, R. A.; Giannelis, E. P., Structure and dynamics of polymer-layered silicate nanocomposites. Chem. Mater. 1996, 8, 1728-1734.

Kuang, W.; Facey, G. A.; Detellier, C.; Casal, B.; Serratosa, J. M.; Ruiz-Hitzky, E., Nanostructured Hybrid Materials Formed by Sequestration of Pyridine Molecules in the Tunnels of Sepiolite. Chem. Mat. 2003, 15, 4956-4967.

Lagaly, G., Interaction of alkylamines with different types of layered compounds. Solid State Ion. 1986, 22, 43-51.

Lagaly, G., Introduction: from clay mineral-polymer interactions to clay mineral-polymer nanocomposites. Appl. Clay Sci. 1999, 15, 1-9.

Lebaron, P. C.; Wang, Z.; Pinnavaia, T. J., Polymer-layered silicate nanocomposites: An overview. Appl. Clay Sci. 1999, 15, 11-29.

Lee, S. Y.; Xu, Y. X.; Hanna, M. A., Tapioca starch-poly (lactic acid)-based nanocomposite foams as affected by type of nanoclay. Int. Polym. Process. 2007, 22, 429-435.

Lee, S. Y.; Chen, H.; Hanna, M. A., Preparation and characterization of tapioca starch-poly(lactic acid) nanocomposite foams by melt intercalation based on clay type. Ind. Crop. Prod. 2008a, 28, 95-106.

Lee, S. Y.; Hanna, M. A., Preparation and characterization of tapioca starch-poly(lactic acid)-Cloisite NA$^+$ nanocomposite foams. J. Appl. Polym. Sci. 2008b, 110, 2337-2344.

Lee, S. Y.; Hanna, M. A.; Jones, D. D., An adaptive neuro-fuzzy inference system for modeling mechanical properties of tapioca starch-poly(lactic acid) nanocomposite foams. Starch/Staerke 2008c, 60, 159-164.

Lepoittevin, B.; Devalckenaere, M.; Pantoustier, N.; Alexandre, M.; Kubies, D.; Calberg, C.; Jerome, R.; Dubois, P., Poly (ε-caprolactone)/clay nanocomposites prepared by melt intercalation: mechanical, thermal and rheological properties. Polymer 2002a, 43, 4017-4023.

Lepoittevin, B.; Pantoustier, N.; Devalckenaere, M.; Alexandre, M.; Kubies, D.; Calberg, C.; Jerome, R.; Dubois, P., Poly(ε-caprolactone)/clay nanocomposites by in-situ intercalative polymerization catalyzed by dibutyltin dimethoxide. Macromolecules 2002b, 35, 8385-8390.

Lepoittevin, B.; Pantoustier, N.; Devalckenaere, M.; Alexandre, M.; Calberg, C.; Jerome, R.; Henrist, C.; Rulmont, A.; Dubois, P., Polymer/layered silicate nanocomposites by combined intercalative polymerization and melt intercalation: A masterbatch process. Polymer 2003, 44, 2033-2040.

Lilholt, H.; Lawther, J. M., Natural organic fibres. In *Comprehensive composite materials*, Kelly, A.; Zweben, C., Eds. Elsevier: 2000; Vol. 1, pp 303-325.

Lilichenko, N.; Maksimov, R. D.; Zicans, J.; Merijs Meri, R.; Plume, E., A biodegradable polymer nanocomposite: Mechanical and barrier properties. Mech. Compos. Mater. 2008, 44, 45-56.

Lin, K.-F.; Hsu, C.-Y.; Huang, T.-S.; Chiu, W.-Y.; Lee, Y.-H.; Young, T.-H., A novel method to prepare chitosan/montmorillonite nanocomposites. J. Appl. Polym. Sci. 2005, 98, 2042-2047.

Lourdin, D.; Della Valle, G.; Colonna, P., Influence of amylose content on starch films and foams. Carbohydr. Polym. 1995, 27, 261-270.

Lourdin, D.; Bizot, H.; Colonna, P., Correlation between static mechanical properties of starch-glycerol materials and low-temperature relaxation. Macromol. Symp. 1997a, 114, 179-185.

Lourdin, D.; Bizot, H.; Colonna, P., "Antiplasticization" in starch-glycerol films? J. Appl. Polym. Sci. 1997b, 63, 1047-1053.

Lourdin, D.; Coignard, L.; Bizot, H.; Colonna, P., Influence of equilibrium relative humidity and plasticizer concentration on the water content and glass transition of starch materials. Polymer 1997c, 38, 5401-5406.

Lourdin, D.; Ring, S. G.; Colonna, P., Study of plasticizer-oligomer and plasticizer-polymer interactions by dielectric analysis: maltose-glycerol and amylose-glycerol-water systems. Carbohydr. Res. 1998, 306, 551-558.

Lourdin, D.; Colonna, P.; Ring, S. G., Volumetric behaviour of maltose-water, maltose-glycerol and starch-sorbitol-water systems mixtures in relation to structural relaxation. Carbohydr. Res. 2003, 338, 2883-2887.

Lu, T. J.; Jane, J. L.; Keeling, P. L., Temperature effect on retrogradation rate and crystalline structure of amylose. Carbohydr. Polym. 1997, 33, 19-26.

Lu, Y.; Weng, L.; Zhang, L., Morphology and properties of soy protein isolate thermoplastics reinforced with chitin whiskers. Biomacromolecules 2004, 5, 1046-1051.

Luckham, P. F.; Rossi, S., The colloid and rhelogical properties of bentonite suspensions, Advances in Colloid and Interface Science. Adv. Colloid Interface Sci. 1999, 82, 43-92.

Luo, J. J.; Daniel, I. M., Characterization and modeling of mechanical behavior of polymer/clay nanocomposites. Compos. Sci. Technol. 2003, 63, 1607-16.

Ma, J.; Bilotti, E.; Peijs, T.; Darr, J. A., Preparation of polypropylene/sepiolite nanocomposites using supercritical CO_2 assisted mixing. Eur. Polym. J. 2007, 43, 4931-4939.

Ma, X.; Yu, J.; Wang, N., Production of thermoplastic starch/ MMT-sorbitol nanocomposites by dual-melt extrusion processing. Macromol. Mater. Eng. 2007, 292, 723-728.

Magini, M.; Colella, C.; Iasonna, A.; Padella, F., Power measurements during mechanical milling - II. The case of "single path cumulative" solid state reaction. Acta Mater. 1998, 46, 2841-2850.

Maiti, P.; Yamada, K.; Okamoto, M.; Ueda, K.; Okamoto, K., New polylactide/layered silicate nanocomposites: Role of organoclays. Chem. Mater. 2002, 14, 4654-4661.

Maiti, P.; Batt, C. A.; Giannelis, E. P., New biodegradable polyhydroxybutyrate/layered silicate nanocomposites. Biomacromolecules 2007, 8, 3393-3400.

Mangiacapra, P.; Gorrasi, G.; Sorrentino, A.; Vittoria, V., Biodegradable nanocomposites obtained by ball milling of pectin and montmorillonites. Carbohydr. Polym. 2006, 64, 516-523.

Martin, O.; Averous, L., Poly(lactic acid): Plasticization and properties of biodegradable multiphase systems. Polymer 2001, 42, 6209-6219.

Martin, O.; Averous, L.; Della Valle, G., In-line determination of plasticized wheat starch viscoelastic behavior: Impact of processing. Carbohydr. Polym. 2003, 53, 169-182.

May, C. D., Industrial pectins: Sources, production and applications. Carbohydr. Polym. 1990, 12, 79-99.

McGlashan, S. A.; Halley, P. J., Preparation and characterisation of biodegradable starch-based nanocomposite materials. Polym. Int. 2003, 52, 1767-1773.

Meijer, H. E. H.; Govaert, L. E., Multi-scale analysis of mechanical properties of amorphous polymer systems. Macromol. Chem. Phys. 2003, 204, 274-288.

Méring, J., The hydration of montmorillonite. Trans. Faraday Soc. 1946, 42B, 205-219.

Messersmith, P. B.; Giannelis, E. P., Polymer-layered silicate nanocomposites: In situ intercalative polymerization of ε-Caprolactone in layered silicates. Chem. Mat. 1993, 5, 1064-1066.

Minke, R.; Blackwell, J., The structure of α-chitin. J. Mol. Biol. 1978, 120, 167-181.

Mohanty, A. K.; Misra, M.; Drzal, L. T., Sustainable Bio-Composites from renewable resources: Opportunities and challenges in the green materials world. J. Polym. Environ. 2002, 10, 19-26.

Mondragon, M.; Mancilla, J. E.; Rodriguez-Gonzalez, F. J., Nanocomposites from plasticized high-amylopectin, normal and high-amylose maize starches. Polym. Eng. Sci. 2008, 48, 1261-1267.

Mori, T.; Tanaka, K., Average stress in matrix and average elastic energy of materials with misfitting inclusions. Acta. Metall. Mater. 1973, 21, 571-4.

Neus Angles, M.; Dufresne, A., Plasticized starch/tuniein whiskers nanocomposites. 1. Structural analysis. Macromolecules 2000, 33, 8344-8353.

Nishiyama, Y.; Langan, P.; Chanzy, H., Crystal structure and hydrogen-bonding system in cellulose 1 beta from synchrotron X-ray and neutron fiber diffraction. J. Am. Chem. Soc. 2002, 124, 9074-9082.

Ogata, N.; Jimenez, G.; Kawai, H.; Ogihara, T., Structure and thermal/mechanical properties of poly(L-lactide)-clay blend. J. Polym. Sci. Pt. B-Polym. Phys. 1997, 35, 389-396.

Ogawa, K., Effect of heating an aqueous suspension of chitosan on the crystalliity and polymorph. Agric. Biol. Chem. 1991, 55, 2375-2379.

Ogawa, K.; Yui, T.; Miya, M., Dependence on the preparation procedure of the polymorphism and crystallinity of chitosan membranes. Biosci. Biotech. Biochem. 1992, 56, 858-862.

Oleinik, E. F., Plasticity of Semicrystalline Flexible-Chain Polymers at the Microscopic and Mesoscopic Levels. Polym. Sci. Ser. C 2003, 45, 17-117.

Ollett, A. L.; Parker, R.; Smith, A. C.; Miles, M. J.; Morris, V. J., Microstructural changes during the twin-screw extrusion cooking of maize grits. Carbohydr. Polym. 1990, 13, 69-84.

Ollett, A. L.; Parker, R.; Smith, A. C., Deformation and fracture behaviour of wheat starch plasticized with glucose and water. J. Mater.Sci. 1991, 26, 1351-1356.

Orford, P. D.; Parker, R.; Ring, S. G., The Functional Properties of Extrusion-cooked Waxy-maize Starch. J. Cereal Sci. 1993, 18, 277-286.

Paillet, M.; Dufresne, A., Chitin whisker reinforced thermoplastic nanocomposites [1]. Macromolecules 2001, 34, 6527-6530.

Pandey, J. K.; Singh, R. P., Green nanocomposites from renewable resources: Effect of plasticizer on the structure and material properties of clay-filled starch. Starch-Starke 2005, 57, 8-15.

Park, H. M.; Li, X.; Jin, C. Z.; Park, C. Y.; Cho, W. J.; Ha, C. S., Preparation and properties of biodegradable thermoplastic starch/clay hybrids. Macromol. Mater. Eng. 2002, 287, 553-558.

Park, H. M.; Lee, W. K.; Park, C. Y.; Cho, W. J.; Ha, C. S., Environmentally friendly polymer hybrids Part I mechanical, thermal, and barrier properties of thermoplastic starch/clay nanocomposites. J. Mater. Sci. 2003, 38, 909-915.

Park, H. M.; Misra, M.; Drzal, L. T.; Mohanty, A. K., "Green" nanocomposites from cellulose acetate bioplastic and clay: Effect of eco-friendly triethyl citrate plasticizer. Biomacromolecules 2004a, 5, 2281-2288.

Park, H. M.; Liang, X.; Mohanty, A. K.; Misra, M.; Drzal, L. T., Effect of compatibilizer on nanostructure of the biodegradable cellulose acetate/organoclay nanocomposites. Macromolecules 2004b, 37, 9076-9082.

Park, H. M.; Mohanty, A. K.; Drzal, L. T.; Lee, E.; Mielewski, D. F.; Misra, M., Effect of sequential mixing and compounding conditions on cellulose acetate/layered silicate nanocomposites. J. Polym. Environ. 2006, 14, 27-35.

Paul, M. A.; Alexandre, M.; Degee, P.; Henrist, C.; Rulmont, A.; Dubois, P., New nanocomposite materials based on plasticized poly(L-lactide) and organo-modified montmorillonites: Thermal and morphological study. Polymer 2002, 44, 443-450.

Paul, M. A.; Alexandre, M.; Degee, P.; Calberg, C.; Jerome, R.; Dubois, P., Exfoliated polylactide/clay nanocomposites by in-situ coordination-insertion polymerization. Macromol. Rapid Commun. 2003, 24, 561-566.

Paul, M. A.; Delcourt, C.; Alexandre, M.; Degee, P.; Monteverde, F.; Rulmont, A.; Dubois, P., (Plasticized) polylactide/(organo-)clay nanocomposites by in situ intercalative polymerization. Macromol. Chem. Phys. 2005, 206, 484-498.

Peprnicek, T.; Kalendova, A.; Pavlova, E.; Simonik, J.; Duchet, J.; Gerard, J. F., Poly(vinyl chloride)-paste/clay nanocomposites: Investigation of thermal and morphological characteristics. Polym. Degrad. Stabil. 2006, 91, 3322-3329.

Perez, C. J.; Alvarez, V. A.; Stefani, P. M.; Vazquez, A., Non-isothermal crystallization of MaterBi-Z/clay nanocomposites. J. Therm. Anal. Calorim. 2007a, 88, 825-832.

Perez, C. J.; Alvarez, V. A.; Mondragon, I.; Vazquez, A., Mechanical properties of layered silicate/starch polycaprolactone blend nanocomposites. Polym. Int. 2007b, 56, 686-693.

Perez, C. J.; Alvarez, V. A.; Mondragon, I.; Vazquez, A., Water uptake behavior of layered silicate/starch-polycaprolactone blend nanocomposites. Polym. Int. 2008a, 57, 247-253.

Perez, C. J.; Alvarez, V. A.; Vazquez, A., Creep behaviour of layered silicate/starch-polycaprolactone blends nanocomposites. Mater. Sci. Eng. A-Struct. 2008b, 480, 259-265.

Perez, C. J.; Vazquez, A.; Alvarez, V. A., Isothermal crystallization of layered silicate/starch-polycaprolactone blend nanocomposites. J. Therm. Anal. Calorim. 2008c, 91, 749-757.

Peter, M. G. P. I., Chitin and Chitosan from Fungi. In *Biopolymers, Vol. 6: Polysaccharides II*, Steinbüchel, A., Ed. Wiley-VCH: Weinheim, 2002; pp 123 - 157.

Picard, E.; Vermogen, A.; Gerard, J. F.; Espuche, E., Barrier properties of nylon 6-montmorillonite nanocomposite membranes prepared by melt blending: Influence of the clay content and dispersion state. Consequences on modelling. J. Membr. Sci. 2007, 292, 133-144.

Picard, E.; Gerard, J. F.; Espuche, E., Water transport properties of polyamide 6 based nanocomposites prepared by melt blending: On the importance of the clay dispersion state on the water transport properties at high water activity. J. Membr. Sci. 2008, 313, 284-295.

Pluta, M.; Galeski, A.; Alexandre, M.; Paul, M. A.; Dubois, P., Polylactide/montmorillonite nanocomposites and microcomposites prepared by melt blending: Structure and some physical properties. J. Appl. Polym. Sci. 2002, 86, 1497-1506.

Pogodina, N. V.; Cerclé, C.; Averous, L.; Thomann, R.; Bouquey, M.; Muller, R., Processing and characterization of biodegradable polymer nanocomposites: detection of dispersion state. Rheol. Acta 2008, 47, 543-553.

Pollet, E.; Delcourt, C.; Alexandre, M.; Dubois, P., Organic-inorganic nanohybrids obtained by sequential copolymerization of ε-caprolactone and L,L-lactide from activated clay surface. Macromol. Chem. Phys. 2004, 205, 2235-2244.

Powell, D. H.; Fischer, H. E.; Skipper, N. T., The structure of interlayer water in Li-montmorillonite studied by neutron diffraction with isotopic substitution. J. Phys. Chem. B 1998a, 102, 10899-10905.

Powell, D. H.; Tongkhao, K.; Kennedy, S. J.; Slade, P. G., Interlayer water structure in Na- and Li-montmorillonite clays. Physica B 1998b, 241-243, 387-389.

Qiao, X.; Jiang, W.; Sun, K., Reinforced thermoplastic acetylated starch with layered silicates. Starch-Starke 2005, 57, 581-586.

Rault, J., Yielding in amorphous and semi-crystalline polymers: the compensation law. J. Non-Cryst. Solids 1998, 235-237, 737-741.

Reddy, C. S. K.; Ghai, R.; Rashmi; Kalia, V. C., Polyhydroxyalkanoates: An overview. Bioresour. Technol. 2003, 87, 137-146.

Redl, A.; Morel, M. H.; Bonicel, J.; Vergnes, B.; Guilbert, S., Extrusion of wheat gluten plasticized with glycerol: Influence of process conditions on flow behavior, rheological properties, and molecular size distribution. Cereal Chem. 1999, 76, 361-370.

Reuss, A., Z. Angew. Math. Mech 1929, 9, 49.

Revol, J. F., Change of the d spacing in cellulose crystals during lattice imaging. J. Mat. Sci. Letters 1985, 4, 1347-1349.

Richeton, J.; Ahzi, S.; Daridon, L.; Rémond, Y., A Formulation of the cooperative model for the yield stress of amorphous polymers for a wide range of strain rates and temperature. Polymer 2005, 46, 6035-6043.

Rinaudo, M., Chitin and chitosan: Properties and applications. Prog. Polym. Sci. 2006, 31, 603-632.

Rudall, K. M.; Kenchington, W., The chitin system. Biol. Rev. 1973, 40, 597-636.

Ruiz-Hitzky, E.; Darder, M.; Aranda, P., Functional biopolymer nanocomposites based on layered solids. J. Mater. Chem. 2005, 15, 3650-3662.

Sagar, A. D.; Merrill, E. W., Starch fragmentation during extrusion processing. Polymer 1995, 36, 1883-1886.

Sakurada, L.; Nukushina, Y.; Ito, T., Experimental determination of the elastic modulus of crystalline regions in oriented polymers. J. Polym. Sci. 1962, 57, 651-660.

Sanchez-Garcia, M. D.; Gimenez, E.; Lagaron, J. M., Morphology and barrier properties of nanobiocomposites of poly(3-hydroxybutyrate) and layered silicates. J. Appl. Polym. Sci. 2008, 108, 2787-2801.

Sandi, G.; Winans, R. E.; Seifert, S.; Carrado, K. A., In situ SAXS studies of the structural changes of sepiolite clay and sepiolite-carbon composites with temperature. Chem. Mat. 2002, 14, 739-742.

Shahidi, F.; Arachchi, J. K. V.; Jeon, Y. J., Food applications of chitin and chitosan. Trends Food Sci. Technol. 1999, 10, 37-51.

Shen, Z.; Simon, G. P.; Cheng, Y. B., Comparison of solution intercalation and melt intercalation of polymer-clay nanocomposites. Polymer 2002, 43, 4251-4260.

Sheng, N.; Boyce, M. C.; Parks, D. M.; Rutledge, G. C.; Abes, J. I.; Cohen, R. E., Multiscale micromechanical modeling of polymer/clay nanocomposites and the effective clay particle. Polymer 2004, 45, 487-506.

Shogren, R. L., Effect of moisture content on the melting and subsequent physical aging of cornstarch. Carbohydr. Polym. 1992a, 19, 83-90.

Shogren, R. L.; Swanson, C. L.; Thompson, A. R., Extrudates of Cornstarch with Urea and Glycols: Structure/Mechanical Property Relations. Starch-Starke 1992b, 44, 335-338.

Sinclair, R. G., The case for polylactic acid as a commodity packaging plastic. J. Macromol. Sci. Part A-Pure Appl. Chem. 1996, 33, 585-597.

Sinha Ray, S.; Maiti, P.; Okamoto, M.; Yamada, K.; Ueda, K., New polylactide/layered silicate nanocomposites. 1. Preparation, characterization, and properties. Macromolecules 2002, 35, 3104-3110.

Sinha Ray, S.; Okamoto, M., Polymer/layered silicate nanocomposites: A review from preparation to processing. Prog. Polym. Sci. 2003, 28, 1539-1641.

Sposito, G.; Grasso, D., Electrical Double Layer Structure, Forces, and Fields at the Clay Water Interface. Surfactant Sci. Ser. 1999, 85, 107-249.

Stevens, D. J.; Elton, G. A. H., Thermal Properties of the Starch/Water System Part I. Measurement of Heat of Gelatinisation by Differential Scanning Calorimetry. Starch-Starke 1971, 23, 8-11.

Swanson, C. L.; Shogren, R. L.; Fanta, G. F.; Imam, S. H., Starch-plastic materials-Preparation, physical properties, and biodegradability (a review of recent USDA research). J. Environ. Polym. Deg. 1993, 1, 155-166.

Tang, X.; Alavi, S.; Herald, T. J., Barrier and mechanical properties of starch-clay nanocomposite films. Cereal Chem. 2008a, 85, 433-439.

Tang, X.; Alavi, S.; Herald, T. J., Effects of plasticizers on the structure and properties of starch-clay nanocomposite films. Carbohydr. Polym. 2008b, 74, 552-558.

Tartaglione, G.; Tabuani, D.; Camino, G., Thermal and morphological characterisation of organically modified sepiolite. Micropor. Mesopor. Mat. 2008, 107, 161-168.

Tettenhorst, R., Cation migration in montmorillonites. Am. Miner. 1962, 47, 769-773.

Thakur, B. R.; Singh, R. K.; Handa, A. K., Chemistry and uses of pectin--a review. Crit. Rev. Food Sci. Nutr. 1997, 37, 47-73.

Thiewes, H. J.; Steeneken, P. A. M., The glass transition and the sub-Tg endotherm of amorphous and native potato starch at low moisture content. Carbohydr. Polym. 1997, 32, 123-130.

Thomas, F.; Michot, L. J.; Vantelon, D.; Montarges, E.; Prelot, B.; Cruchaudet, M.; Delon, J. F., Layer charge and electrophoretic mobility of smectites. Colloid Surf. A-Physicochem. Eng. Asp. 1999, 159, 351-358.

Thostenson, E. T.; Ren, Z.; Chou, T. W., Advances in the science and technology of carbon nanotubes and their composites: A review. Compos. Sci. Technol. 2001, 61, 1899-1912.

Tomka, I., Thermoplastic starch. Adv. Exp. Med. Biol. 1991, 302, 627-637.

Torre, L.; Kenny, J. M.; Maffezzoli, A. M., Degradation behaviour of a composite material for thermal protection systems Part I-Experimental characterization. J. Mater. Sci. 1998, 33, 3137-3143.

Truss, R. W.; Clarke, P. L.; Duckett, R. A.; Ward, I. M., J. Polym. Sci. Pt. B-Polym. Phys. 1984, 22, 191-209.

Truss, R. W.; Lee, A. C., Yield behavior of a melt-compounnded polyethylene-intercalated montmorillonite nanocomposite. Polym. Int. 2003, 52, 1790-1794.

Truss, R. W.; Yeow, T. K., Effect of exfoliation and dispersion on the yield behavior of melt-compounded polyethylene-montmorillonite nanocomposites. J. Appl. Polym. Sci. 2006, 100, 3044-3049.

Tsuji, H.; Ikada, Y., Blends of aliphatic polyesters. II. Hydrolysis of solution-cast blends from poly(L-lactide) and poly (ε-caprolactone) in phosphate-buffered solution. J. Appl. Polym. Sci. 1998, 67, 405-415.

Tucker, C. L.; Liang, E., Stiffness predictions for unidirectional short-fiber composites: Review and evaluation. Compos. Sci. Technol. 1999, 59, 655-671.

Vaia, R. A.; Ishii, H.; Giannelis, E. P., Synthesis and properties of two-dimensional nanostructures by direct intercalation of polymer melts in layered silicates. Chem. Mat. 1993, 5, 1694-1696.

Vaia, R. A.; Giannelis, E. P., Polymer melt intercalation in organically-modified layered silicates: Model predictions and experiment. Macromolecules 1997, 30, 8000-8009.

Van der Hart, D. L.; Atalla, R. H., Studies of microstructure in native celluloses using solid state 13C NMR. Macromolecules 1984, 17, 1465-1472.

Van Soest, J. J. G.; De Wit, D.; Tournois, H.; Vliegenthart, J. F. G., The influence of glycerol on structural changes in waxy maize starch as studied by Fourier transform infra-red spectroscopy. Polymer 1994, 35, 4722-4727.

Van Soest, J. J. G.; Hulleman, S. H. D.; De Wit, D.; Vliegenthart, J. F. G., Crystallinity in starch bioplastics. Ind. Crop. Prod. 1996a, 5, 11-22.

Van Soest, J. J. G.; Benes, K.; De Wit, D.; Vliegenthart, J. F. G., The influence of starch molecular mass on the properties of extruded thermoplastic starch. Polymer 1996b, 37, 3543-3552.

Van Soest, J. J. G.; De Wit, D.; Vliegenthart, J. F. G., Mechanical properties of thermoplastic waxy maize starch. J. Appl. Polym. Sci. 1996c, 61, 1927-1937.

Van Soest, J. J. G.; Hulleman, S. H. D.; De Wit, D.; Vliegenthart, J. F. G., Changes in the mechanical properties of thermoplastic potato starch in relation with changes in B-type crystallinity. Carbohydr. Polym. 1996d, 29, 225-232.

Van Soest, J. J. G.; Essers, P., Influence of amylose-amylopectin ratio on properties of extruded starch plastic sheets. J. Macromol. Sci. Part A-Pure Appl. Chem. 1997a, 34, 1665-1689.

Van Soest, J. J. G.; Borger, D. B., Structure and properties of compression-molded thermoplastic starch materials from normal and high-amylose maize starches. J. Appl. Polym. Sci. 1997b, 64, 631-644.

Van Soest, J. J. G.; Knooren, N., Influence of glycerol and water content on the structure and properties of extruded starch plastic sheets during aging. J. Appl. Polym. Sci. 1997c, 64, 1411-1422.

Vergnes, B.; Villemaire, J. P.; Colonna, P.; Tayeb, J., Interrelationships between thermomechanical treatment and macromolecular degradation of maize starch in a novel rheometer with preshearing. J. Cereal Sci. 1987, 5, 189.

Voigt, W., Lehrbuch des Krystalphysik 1928, 410.

Wang, S.; Chen, L.; Tong, Y., Structure-property relationship in chitosan-based biopolymer/montmorillonite nanocomposites. J. Polym. Sci. Pt. A-Polym. Chem. 2006, 44, 686-696.

Wang, S. F.; Shen, L.; Tong, Y. J.; Chen, L.; Phang, I. Y.; Lim, P. Q.; Liu, T. X., Biopolymer chitosan/montmorillonite nanocomposites: Preparation and characterization. Polym. Degrad. Stabil. 2005, 90, 123-131.

Wang, S. S.; Chiang, W. C.; Yeh, A. I.; Zhao, B.; KIM, I. H., Kinetics of Phase Transition of Waxy Corn Starch at Extrusion Temperatures and Moisture Contents. J. Food Sci. 1989, 54, 1298–1301.

Wang, X.; Du, Y.; Yang, J.; X., W.; Shi, X.; Hu, Y., Preparation, characterization and antimicrobial activity of chitosan/layered silicate nanocomposites. Polymer 2006, 47, 6738-6744.

Ward, I. M., Review: The yield behaviour of polymers. J. Mater. Sci. 1971, 6, 1397-1417.

Ward, I. M.; Wilding, M. A., J. Polym. Sci. Pt. B-Polym. Phys. 1984, 22, 561-575.

Weir, M. R.; Kuang, W.; Facey, G. A.; Detellier, C., Solid-state nuclear magnetic resonance study of sepiolite and partially dehydrated sepiolite. Clay Clay Min. 2002, 50, 240-247.

Wibowo, A. C.; Misra, M.; Park, H. M.; Drzal, L. T.; Schalek, R.; Mohanty, A. K., Biodegradable nanocomposites from cellulose acetate: Mechanical, morphological, and thermal properties. Compos. Pt. A-Appl. Sci. Manuf. 2006, 37, 1428-1433.

Wilhelm, H.-M.; Sierakowski, M.-R.; Souza, G. P.; Wypych, F., The influence of layered compounds on the properties of starch/layered compound composites. Polym. Int. 2003a, 52, 1035-1044.

Wilhelm, H.-M.; Sierakowski, M.-R.; Souza, G. P.; Wypych, F., Starch films reinforced with mineral clay. Carbohydr. Polym. 2003b, 52, 101-110.

Wilkie, C. A.; Zhu, J.; Uhl, F., How Do Nanocomposites Enhance the Thermal. Stability of Polymers? Polymer Preprints 2001, 42, 392.

Wollerdorfer, M.; Bader, H., Influence of natural fibres on the mechanical properties of biodegradable polymers. Ind. Crop. Prod. 1998, 8, 105-112.

Xu, W.; Ge, M.; He, P., Nonisothermal crystallization kinetics of polypropylene/montmorillonite nanocomposites. J. Polym. Sci. Pt. B-Polym. Phys. 2002, 40, 408-414.

Xu, Y.; Zhou, J.; Hanna, M. A., Melt-intercalated starch acetate nanocomposite foams as affected by type of organoclay. Cereal Chem. 2005, 82, 105-110.

Xu, Y.; Ren, X.; Hanna, M. A., Chitosan/clay nanocomposite film preparation and characterization. J. Appl. Polym. Sci. 2006, 99, 1684-1691.

Yoshioka, M.; Takabe, K.; Sugiyama, J.; Nishio, Y., Newly developed nanocomposites from cellulose acetate/layered silicate/poly(ε-caprolactone): Synthesis and morphological characterization. J. Wood Sci. 2006, 52, 121-127.

Zeleznak, K. J.; Hoseney, R. C., The glass transition in starch. Cereal Chem. 1987, 64, 121-124.

Zhang, Q. X.; Yu, Z. Z.; Xie, X. L.; Naito, K.; Kagawa, Y., Preparation and crystalline morphology of biodegradable starch/clay nanocomposites. Polymer 2007, 48, 7193-7200.

Zhang, X.; Do, M. D.; Dean, K.; Hoobin, P.; Burgar, I. M., Wheat-gluten-based natural polymer nanoparticle composites. Biomacromolecules 2007, 8, 345-353.

Zheng, Y., Study on sepiolite-reinforced polymeric nanocomposites. J. Appl. Polym. Sci. 2006, 99, 2163-2166.

Zobel, H. F., Molecules to granules: a comprehensive starch review. Starch-Starke 1988, 40, 44-50.